INVESTIGATIONS AND MODELING ON ADVANCEMENT IN MAGNETORHEOLOGICAL FLUID BASED HONING PROCESS

A Thesis submitted in fulfillment of the requirement for the award of the degree of

DOCTOR OF PHILOSOPHY

IN

MECHANICAL ENGINEERING

Submitted by

VISHWAS GROVER

Roll No. 901508006

Under the supervision of

Dr. ANANT KUMAR SINGH

Associate Professor, MED

Department of Mechanical Engineering,

Thapar Institute of Engineering and Technology, Patiala-147004, INDIA

(Deemed to be University)

February 2019

CONTENTS

CERTIFICATE

I, **Vishwas Grover**, Roll No. 901508006, hereby declared that the thesis entitled **"Investigations and Modeling on Advancement in Magnetorheological Fluid Based Honing Process"** submitted to the Department of Mechanical Engineering at Thapar Institute of Engineering and Technology, Patiala, Punjab (India) is an authenticated record of my own work for the award of the degree "Doctor of Philosophy" under the supervision of **Dr. Anant Kumar Singh**. This report has not been submitted to any other institute for the award of any other degree.

Vishwas Grover

Vishwas Grover

Roll No. 901508006

Place: Patiala

Date: 22/Feb/2019

This is to certify that the above statement my by the candidate is correct to the best of my knowledge.

Verified by:

22/02/2019

Dr. Anant Kumar Singh
(Supervisor)
Associate Professor
Department of Mechanical Engineering
Thapar Institute of Engineering and Technology, Patiala- 147004 (Punjab)
India

ACKNOWLEDGEMENT

First and the foremost, I wish to thank my supervisor **Dr. Anant Kumar Singh** for his valuable support and guidance. I am sincerely gratitude to him for judging my potential and providing me an interesting topic according to my capability. I am thankful for his positive suggestions, and meticulous guidance that helped me to improve my talent to write scientific research papers and carry out the new research. His patience and motivation enhanced me up to achieve my goal. I feel really honoured to have worked under his mentorship throughout my entire PhD work.

I thank the doctoral committee members **Dr. T.P. Singh** (Chairman, Board of Studies), **Dr. Puneet Sharma**, **Dr. Vinod Kumar Singla** and **Dr. Vivek Jain** for the feedback and reviews that were given on my research proposal and progress monitoring presentations. Their guidance was beneficial for me to improve my research work. I am also thankful to **Dr. Tarun Nanda** and **Dr. Gagandeep Bhardwaj**, our PhD coordinators for their approachability and keeping me informed with all the relevant communication throughout E-mails.

I gratefully acknowledge Science and Engineering Research Board "Department of Science and Technology" for providing the financial support for this research project.

I am thankful to my parents, my family and specially my cousin sister who motivated me throughout my entire research work. I was also encouraged by my research team members Dr. Talwinder Singh Bedi, Mr. Manpreet Singh, Mr. Sunil Kumar Paswan and Mr. Ankit Aggarwal. I am also so much thankful to my friends cum brothers Mr. Kulwinder Singh Chani, Mr. Ankit Sharma and Mr. Prakhar Jain who motivated and gave me support throughout my entire research work. From the core of my heart, I thank to my entire family members for their never-ending love, encouragement and support.

I thank to "**Almighty God**" for giving me the strength and patience for successfully completing my goal.

Vishwas Grover

ABSTRACT

The internal surface finishing of cylindrical components at nano-meter level with good surface characteristics is highly demanded in today's industries for improving their operative functionalities. There are various cylindrical components which require internal surface finishing at high precision level with good surface integrity. These cylindrical components are used for cylindrical molds and dies, hydraulic cylinders, cylindrical barrels for injection molding, air bearings and cylindrical tubes for the flow of high purity liquids etc. The highly finished internal surface of cylindrical components also results in resistance to wear, corrosion, pitting and oxidation. In industries, mostly traditional finishing processes like grinding or honing are used to finish the internal surface of the various cylindrical components because of their easy accessibility and low making cost. These traditional finishing processes make use of rigid tools and when the rigid tools perform surface finishing, they do not have control over the finishing forces. Owing to this, sometimes the defects get produced like pit holes, sharp edges, torn and folded metals etc. on the final finished surface. Moreover, the traditional finishing processes can finish the surface up to a certain level because of the use of the rigid abrasive tools and further to achieve a very fine level of surface finishing may not be possible. Therefore, there is a mandatory requirement of the advanced finishing processes to finish the internal surface of the cylindrical components for enhancing their operational life in real applications. The finished surface using the advanced finishing processes has several benefits like close tolerance design, reduction in wear, friction losses and increase in product service life etc.

To attain the finishing over the inner surface of the cylindrical workpieces, the advanced finishing processes like magnetorheological abrasive flow finishing (MRAFF) and rotational-magnetorheological abrasive flow finishing (R-MRAFF) are developed which make use of magnetorheological polishing fluid for finishing the surface. But, these processes are found more significant to finish the internal surface of the non-ferromagnetic cylindrical workpieces. Recently, another advanced finishing process named as magnetorheological honing (MRH) process is developed for the internal surface finishing of the both ferromagnetic as well as non-ferromagnetic cylindrical workpieces. This existing MRH process makes use of an electromagnet finishing tool whose electromagnetic cores are fixed to its central rotating shaft. Therefore, the single electromagnetic MRH tool can likely able to finish a particular inner surface diameter only

at a time of the cylindrical workpiece with keeping a working gap for the magnetorheological polishing fluid.

In the present research work, to overcome the challenges of the existing electromagnet based MR honing process for finishing the different sizes of the internal surface of the different cylindrical workpieces with a single tool, further a novel magnetorheological (MR) honing tool is designed and fabricated. This new designed MR honing tool is found to be capable of nano-finishing the different sizes of the internal surface of the different cylindrical workpieces. The present design of the magnetorheological (MR) honing tool constitutes of four permanent magnet strips on its outer periphery. The present MR honing tool is made flexible to move its outer magnetic surface (permanent magnet strips) radially inwards or outwards about the central axis of the tool. Since the tool's end surface of the permanent magnet strips can be adjusted either radially inwards or outwards as per the requirement of the internal surface diameter of the cylindrical workpiece to be finished, therefore the present designed MR honing tool is found to be capable for nano-finishing the inner surface of the cylindrical workpieces with different internal diameters. The present designed MR honing tool with stiffened MR polishing fluid over its magnetic surface rotates as well as reciprocates inside the cylindrical workpiece to finish its internal surface. The finishing tool moves inside the cylindrical workpiece, and the retained MR polishing fluid over the tool's magnetic surface interacts with the inner surface of the cylindrical workpiece in working gap and performs the finishing.

The present design of MR honing tool always possesses the higher magnitude of magnetic flux density on its outer magnetic surface as compared to the inner surface of the ferromagnetic cylindrical workpiece and there exists a gradient of magnetic flux density in the working gap. Due to the presence of a gradient of magnetic flux density in the working gap, the magnetic carbonyl iron particles move towards the tool's outer magnetic surface (higher magnetic flux density) and non-magnetic abrasives move towards the inner surface (lower magnetic flux density) of the ferromagnetic cylindrical workpiece. This is the foremost requirement of any finishing process based on magnetorheological (MR) fluid to finish the ferromagnetic material surfaces. Due to the magnetic field induced by the tool's permanent magnet strips, the carbonyl iron (CI) particles as present in the MR polishing fluid make chains in the working gap and grip the abrasives in between the chains of CI particles. Due to the relative motion between the active abrasives (gripped by the chains of CI particles) and the inner surface of the ferromagnetic

cylindrical workpiece, the surface gets finished by the present MR honing tool. Thus, the developed finishing tool is found to be effective of nano-finish the inner surface of ferromagnetic cylindrical workpieces with different internal diameters.

The magnetostatic finite element analysis for studying the distribution of magnetic flux density over the tool's magnetic end surface helped to fulfill the design requirement of MR honing tool for finishing the internal surface of the different ferromagnetic cylindrical workpieces. Initially, the MR honing tool is designed with the four flat end magnetic strips. In this design, a non-uniform working gap existed for the MR polishing fluid between the tool's flat end magnetic surface and the inner surface of the cylindrical workpiece. This non-uniform working gap resulted in the non-uniform distribution of magnetic flux density in between the tool outer flat end magnetic surface and the inner surface of the cylindrical workpiece. This may result in non-uniformly strength of MR polishing fluid over the tool magnetic end surface due to the non-uniformly distribution of magnetic flux density over its magnetic end surface. This may further result in slow down the performance of the finishing process. Therefore, to further enhance the performance of the present finishing process, the limitations of the initially designed MR honing tool with the flat end magnetic surface have been removed by the redesigning of the MR honing tool with the four curved end magnetic strips. This redesign of the tool with the curved end magnetic surface has improved the uniformity in distribution of magnetic flux density over the tool's magnetic end surface due to the accomplishment of the uniform working gap between the tool curved end magnetic surface and the inner surface of the cylindrical workpiece. This improved design of MR honing tool with curved end magnetic surface resulted in better finishing performance over the inner surface of the cylindrical workpieces as compared to the initial design of MR honing tool with the flat magnetic end surface.

To examine the validity of the finishing performance of the initial and improved design of MR honing tool, the preliminary experimentations have been performed by both the designed tools over the inner surface of the ferromagnetic cylindrical mild steel workpieces. Experimental results with the MR honing tool having curved end magnetic surface has demonstrated better surface finishing over the inner surface of ferromagnetic cylindrical mild steel workpiece as compared to the MR honing tool with the flat end magnetic surface. The surface roughness parameters R_a, R_q and R_z get decreased to 0.08 μm, 0.12 μm and 0.63 μm from 0.37 μm, 0.49 μm and 2.53 μm respectively in 60 minutes of finishing with an MR honing tool having curved end

magnetic surfaces. On the other hand, these parameters get reduced to 0.19 μm, 0.26 μm and 1.34 μm with MR honing tool having the flat end magnetic surface from the same initial surface roughness values in the same finishing time of 60 minutes. Thus, the improved MR honing tool design with the curved end magnetic surface is found more capable to nano-finish the inner surface of cylindrical workpieces as compared to the initially designed MR honing tool with the flat end magnetic surface.

A comprehensive study using statistical design (plan of experiments) has been performed for finishing the internal cylindrical surfaces of EN-31 steel material by the present developed magnetorheological honing (MRH) tool with the curved end magnetic surface. The EN-31 steel is commonly used for manufacturing the punches and dies. The response surface methodology (RSM) has been used in "Design expert 10" software to plan and analyze the effects of the different process parameters on the percentage change in surface roughness (R_a) value. As present MR honing tool has been made flexible to move its outer magnetic finishing surface radially inward or outward to finish the different internal cylindrical diameters, therefore variation in working gap is also considered as one of the important process parameters. This validates the present design of the MR honing tool can be used for finishing the different internal cylindrical diameters. The analysis of experimental data showed that the percentage change in surface roughness value is mostly contributed by the working gap (between tool's end surface and inner surface of the cylindrical workpiece) followed by the tool rotating speed, the percentage concentration of silicon carbide (SiC) abrasive particles, the tool reciprocating speed and the percentage concentration of carbonyl iron (CI) particles. Based on the results obtained from response surface methodology after regression analysis, the optimum process parameters for better process performance to finish the inner surface of the cylindrical EN-31 workpiece are found as 20 % volume concentration of SiC abrasive particles, 20 % volume concentration of carbonyl iron particles, the working gap of 2 mm, the tool rotating speed of 500 rpm and the tool reciprocating speed of 70 cm/min. At optimum process parameters, the least value of surface roughness of 95 nm is found from the initial value of 476 nm after 120 minutes of finishing over the inner surface of the cylindrical EN-31 workpiece.

Further, a mathematical model for the change in surface roughness (R_a) value during the present MR honing process has also been developed. The developed mathematical model demonstrates the distribution of the induced magnetic flux density in the working gap included the

contribution of the magnetic effect of iron particles as present in MR polishing fluid and the ferromagnetic cylindrical workpiece. From the evaluated magnitude of magnetic flux density at different points in the working gap, the indentation force acting on the actual tetrahedron shaped SiC abrasive particles has been evaluated mathematically. A theoretical expression is derived which predicts the change in surface roughness (R_a) value for the different number of finishing cycles during the present MR honing process. The developed mathematical model has been validated experimentally for the different number of finishing cycles. Results obtained from the theoretical mathematical model are found in close relation with the results obtained from the experimentations with an error in the range of 8.06 % to 1.03 %. This signifies the consistency of the developed mathematical model to predict the change in surface roughness R_a value while performed finishing with the present developed magnetorheological honing process. The developed mathematical model for the present MR honing process can be used to predict the change in surface roughness (R_a) value for finishing the different industrial cylindrical components and is further helpful in enhancing their operative functionality.

LIST OF FIGURES

LIST OF TABLES

LIST OF ABBREVIATIONS

AFF	Abrasive flow finishing
ANOVA	Analysis of variance
BEMRF	Ball end magnetorheological finishing
CAD	Computer aided design
CCD	Central composite design
CIPs	Carbonyl iron particles
CMP	Chemo-mechanical polishing
DC	Direct current
DOE	Design of experiments
EEM	Elastic emission machining
EIPs	Electrolytic iron particles
FEA	Finite element analysis
FMAB	Flexible magnetic abrasive brush
MFP	Magnetic float polishing
MAF	Magnetic abrasive finishing
MR	Magnetorheological
MRAFF	Magnetorheological abrasive flow finishing
MRAH	Magnetorheological abrasive honing
MRF	Magnetorheological finishing
MRH	Magnetorheological honing
MRJF	Magnetorheological jet finishing
NaOH	Sodium hydroxide
ND: YLF	Neodymium-doped yttrium lithium fluoride
NdFeB	Neodymium iron boron
PLC	Programmable logic controller
R-MRAFF	Rotational magnetorheological abrasive flow finishing
RSM	Response surface methodology
RMS	Root mean square
RPM	Rotations per minute
SEM	Scanning electron microscopy
SiC	Silicon carbide
VAC-MAF	Vibration assisted cylindrical magnetic abrasive finishing
VIF	Variance inflation factor
WA	White alumina

LIST OF NOMENCLATURES

A_p	projected area of penetration of single silicon carbide abrasive, mm^2
A_{inner_single}	internal surface area of cylindrical workpiece covered by the MR polishing fluid covering a particular strip of curved permanent magnet and taking part in the finishing, mm^2
A_{inner_total}	total internal surface area of cylindrical workpiece covered by the MR polishing fluid, covering the four strips of curved permanent magnet, and taking part in finishing, mm^2
a	edge length of single tetrahedron shaped silicon carbide abrasive, μm
B	magnetic flux density, T
C	centre distance between two pulleys, mm
D	desirability function
D_1	pitch circle diameter of the driving pulley, mm
D_2	pitch circle diameter of the driven pulley, mm
d	diameter of MR honing tool in C-shaped aluminium bracket, mm
F_{ax}	axial force acting on spherical-shaped active abrasive particle, N
F_{CI}	force acting on single CI particle, N
F_{cu}	cutting force acting on spherical-shaped active abrasive particle, N
F_i	indentation force acting on single tetrahedron shaped active silicon carbide particle, N
F_I	magnetic normal force acting on the single iron particle, N
F_m	magnetic force acting between two carbonyl iron particles, N
F_{mn}	magnetic normal force acting on single active spherical-shaped active abrasive particle, N
F_{ta}	tangential force acting on spherical-shaped active abrasive particle, N
H	magnetic field intensity, A/m
H_d	hardness of ferromagnetic cylindrical workpiece, MPa
h_w	height of ferromagnetic cylindrical workpiece, mm
h_{SiC_tetra}	height of tetrahedron shaped single silicon carbide (SiC) abrasive, μm
L	Length of timing belt used for power transmission, mm
L_{act}	actual length of contact made by the single SiC particle with the inner surface of the cylindrical workpiece, mm

l_{hel}	length of helical path moved by single active SiC particle during a single cycle of MRH tool inside the cylindrical workpiece, mm
M	intensity of magnetization, A-m^2/kg
M_{IP}	magnetization of an iron particle corresponding to the different magnitude of magnetic flux density in the working gap, A-m^2/kg
M_{wrk}	magnetization of ferromagnetic cylindrical workpiece corresponding to the magnitude of magnetic flux density present at the position of ferromagnetic cylindrical workpiece, A-m^2/kg
m_a	mass of single spherical shaped active abrasive particle, kg
m_{CI}	mass of single magnetic carbonyl iron (CI) particle, kg
m_I	mass of the single iron particle, kg
N_a	number of active silicon carbide abrasives per unit area present over the inner surface of the cylindrical workpiece
N_{act}	rotating speed of active abrasive with which it is rotating on the cylindrical workpiece's internal surface, RPM
N_{AAP}	number of active silicon carbide particles present on the inner surface of the ferromagnetic cylindrical workpiece
N_s	number of active abrasive which perform finishing over the internal surface of the cylindrical workpiece
P_1	tension in the tight side of the timing belt, N
P_2	tension in the slack side of the timing belt, N
R'	distance between the centers of two carbonyl iron particles, μm
R	radius of driven pulley, mm
R_A	reaction force to the rotating shaft of MR honing tool by the upper plate of C-shaped aluminium bracket, N
R_B	reaction force to the rotating shaft of MR honing tool by the lower plate of C-shaped aluminium bracket, N
R_a^n	surface roughness value over the cylindrical workpiece's internal surface after n number of cycles, μm
R_a^{n-1}	surface roughness value on the cylindrical workpiece's internal surface after (n-1) number of cycles, μm
R_a^0	initial surface roughness value on the cylindrical workpiece's internal surface, μm
r	radius of driving pulley, mm

r_c	radius of carbonyl iron particle, μm
r_{act}	radial distance between the central axis of present magnetorheological honing process and center of active SiC particle, mm
r_1'	inner radius of permanent magnet strip from central axis of MRH process, mm
r_2'	outer radius of permanent magnet strip from central axis of MRH process, mm
r_3'	inner radius of the cylindrical workpiece over which finishing is performed, mm
S_{yt}	ultimate tensile strength of stainless steel, MPa
S_{ut}	ultimate yield strength of stainless steel, MPa
$\mathcal{T}_{motor}$	Maximum torque acting by the servomotor, N-m
t_s	time taken by the single active silicon carbide particle to cover the complete height of the cylindrical workpiece during one cycle of MRH process, min
V_a	reciprocating velocity of active abrasive, cm/min
V_n	volume of material removed from internal surface of the cylindrical ferromagnetic workpiece in n^{th} cycle, μm^3
V_{SiC_tetra}	volume of tetrahedron shaped single SiC particle, μm^3
v	linear velocity of spherical-shaped active abrasive particle, m/sec
w_c	total width of MR polishing fluid present over the single strip of curved permanent magnet tool outer surface, mm
z_1'	upper half height of the magnet strip from the origin, mm
z_2'	lower half height of the magnet strip from the origin, mm
χ_m	mass susceptibility of the iron particle, m^3/Kg
μ_0	magnetic permeability of free space, H/m
μ_{MR}	relative permeability of MR polishing fluid
μ_{wrk}	relative permeability of ferromagnetic cylindrical workpiece
θ_1'	start angle of curved permanent magnet strip, degrees
θ_2'	end angle of curved permanent magnet strip, degrees
$\emptyset$	helix angle made by the single tetrahedron shaped SiC abrasive during its movement inside the cylindrical workpiece, degrees
σ_s	surface charge density present in permanent magnet strip, $C.m^{-2}$
σ_v	volume charge density present in permanent magnet strip, $C.m^{-3}$

ω	angular velocity of spherical-shaped active abrasive particle, rad/sec
μ	coefficient of friction of leather belt

CHAPTER 1

INTRODUCTION

1.1 Introduction

Surface roughness solely means the deviation of the surface in a normal direction from the ideal flat surface. The roughness value of any surface may not be attained zero but it can only be reduced. The phenomenon of reducing the surface roughness of any component is called surface finishing. Today, surface finishing of components is a very important requirement in industries for their precise operative functionality (Balogun and Mativenga, 2017). Some industrial products require surface finishing just for having the good appearance or aesthetic look. But, many industrial components require a finished surface with good surface characteristics for having benefits such as dimensional accuracy, close tolerance fit or design, increased tool life and a decrease in wear and frictional losses etc (Mohanty *et* al., 2013). Various industries like electronics, optics, automotive and avionics require specific surface characteristics of micro products and components for their precise operational requirements (Rajurkar *et* al., 2006). But, to attain the required precise surface finish over the surface of industrial components, it is not an easy task. Finishing of components which needs higher accuracy is a very difficult and time taking task in manufacturing industries (Pattnaik *et* al., 2012). Almost 10 to 15 percent of the total production cost of a component is expended for its precise surface finishing (Verma *et* al., 2017). Different finishing processes with their mechanism of material removal result in finishing over the surface of the various components.

1.2 Conventional finishing processes

Several conventional finishing processes such as lapping, honing and grinding are available in industries for attaining the surface finish over the various components. But, these traditional finishing operations might sometime provide the finished surface with some defects such as cracks, residual stresses etc. (Benardos and Vosniakos, 2003). Various conventional finishing processes are explained as under.

1.2.1 Lapping

Lapping is the oldest finishing operation which is commonly used for finishing of flat surfaces. It is low speed, a low-pressure operation which results in marvellous accuracy and remarkably close fitted structure (Khanna and Lal, 2010). It generally works on the principle of three body

abrasive wear (Jha and Jain, 2005). It makes use of loose abrasive slurry-like silicon carbide and aluminium oxide etc. Loose abrasives are placed between the workpiece and the backup wheel commonly known as lap plate. Workpiece surface gets finished under the pressure making contact with abrasives. The schematic of the lapping process performs the finishing on the flat workpiece is shown in Fig. 1.1.

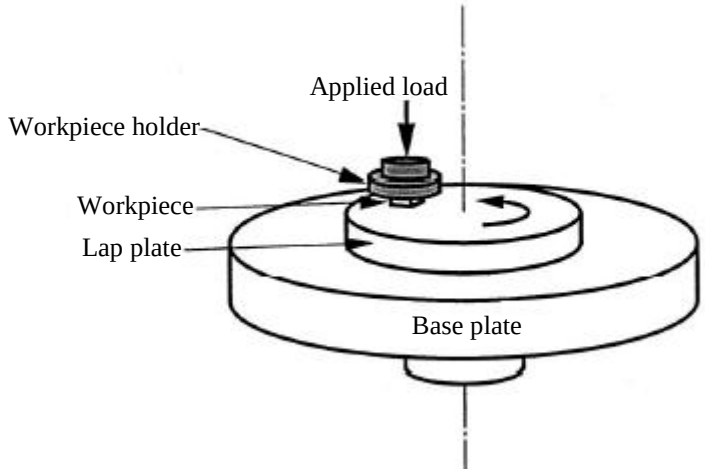

Fig. 1.1 Schematic of the lapping process performs the finishing on the flat workpiece (Chang *et* al., 2000)**.**

1.2.2 Honing

Honing is the foremost finishing process which is used to finish the inner surface of the cylindrical workpiece (Pawlus *et* al., 2009). It is the process which is generally used subsequently to boring or drilling operation to attain finishing over the inner surface of cylindrical components (Sabri *et* al., 2011). The schematic of honing process while it performs finishing of the inner surface of the cylindrical component is represented in Fig. 1.2. It consists of various honing stones having abrasives embedded in it. The honing tool is rotated as well as reciprocated simultaneously inside the cylindrical components. Due to the movement (rotation as well as reciprocation) of the embedded abrasives, surface roughness peaks present over the inner surface of cylindrical workpiece get slashed out and the finished surface is obtained. The process is used for the components which require precise geometric and form accuracy (Dimkovski *et* al., 2009; Sabri and Mansori, 2009; Spencer *et* al., 2011). It is also helpful in manufacturing the components where good dimensional tolerance is required.

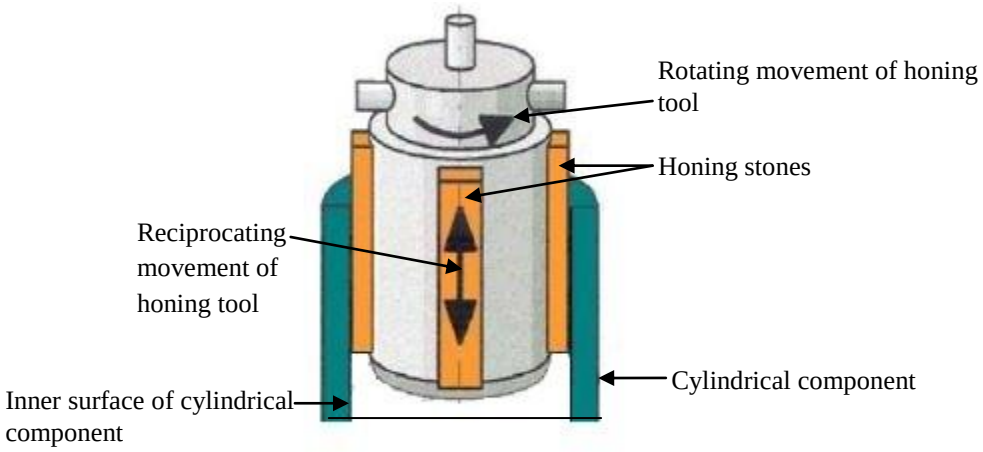

Fig. 1.2 Schematic of honing process while it performs finishing of the inner surface of the cylindrical component (Sabri and Mansori, 2009).

1.2.3 Grinding

Grinding is one of the commonly used processes which is utilized for surface finishing of different kinds of material. It is used for finishing the internal or external surfaces. It can be used for the soft material to the hardest material (Khanna and Lal, 2010). The photograph of the experimental setup of grinding process is represented in Fig. 1.3.

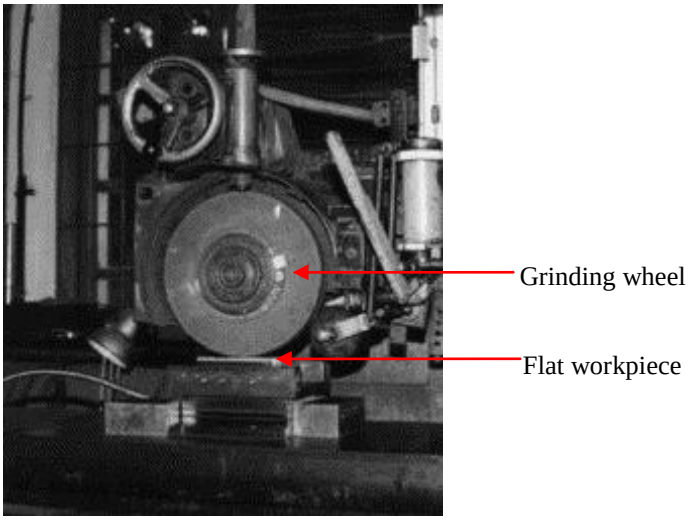

Fig. 1.3 Photograph of the experimental setup of grinding process (Shaji and Radhakrishnan, 2003).

Grinding process simply make use of a circular grinding wheel having abrasives like silicon carbide (SiC) embedded over its outer periphery. The grinding wheel is rotated over the surface to be finished. The relative movement between the workpiece surface and the abrasives removes the material in the form of microchips.

The above stated traditional finishing processes have various limitations due to which these processes cannot be opted for manufacturing the very high precise industrial components. These traditional finishing processes cannot be used to finish the complex surfaces and components which require a surface finish of very precise at nano-meter level. These processes make use of rigid tools for finishing due to which they do not have control over the finishing forces. Because of this, sometimes these processes may result in damaged surfaces or sub-surfaces (Lawrence and Ramamoorthy, 2011). In traditional finishing processes, certain problems like surface crack formation and residual stresses have been noticed due to the high quantity of heat generation during the surface finishing (Gupte *et* al., 2008). To overcome these limitations, various advanced finishing processes have been flourished to get better surface finish quality.

1.3 Advanced finishing processes without externally controlled forces

The advanced finishing processes have been developed to obtain the good surface integrity which is not possible with traditional finishing processes. Advanced finishing processes are suitable for finishing of optical, metallic and polymeric components etc. (Jain, 2009). The various advanced finishing processes are explained below.

1.3.1 Abrasive flow finishing (AFF) process

Abrasive flow finishing (AFF) process is an advanced finishing process which was basically invented for deburring and finishing the cylindrical internal intricate surfaces (Rhoades, 1988). The schematic of abrasive flow finishing setup and its components is shown in Fig. 1.4.

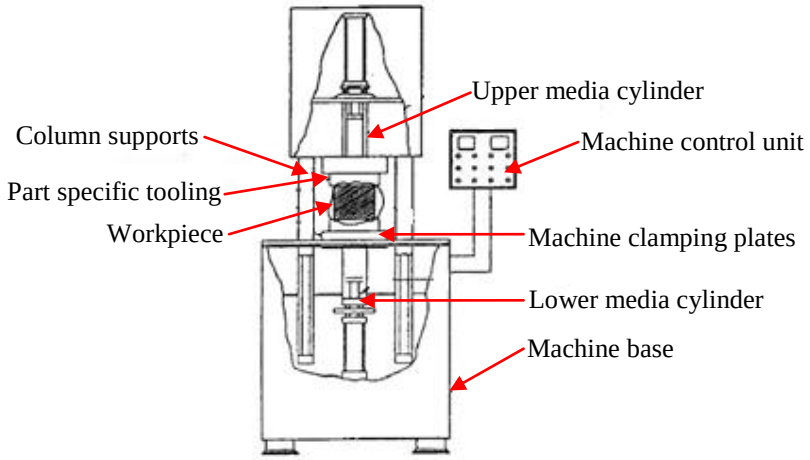

Fig. 1.4 Schematic of abrasive flow finishing setup and its components (Loveless *et* al., 1994).

This process is basically used for finishing of workpiece materials which are resistive to wear (Jain, 2009). AFF use the abrasive particles which are mixed in the carrier fluid for finishing the

internal cylindrical surfaces. Carrier fluid having abrasives mixed in it is allowed to flow through internal surfaces of cylindrical workpieces under an extrusion pressure. Under the action of extrusion pressure, abrasives erode out the surface roughness peaks in the form of microchips and result in cylindrical internal finishing. Rheological property of the fluid is responsible for the change in abrasive action performed by the abrasives into the restrictive passage (Genc and Phule, 2002). The viscosity of the fluid has a significant role in finishing action (Jha and Jain, 2006). The axial force acting on the abrasive particles is liable for the removal of material in form of chips, whereas the radial force is liable for the indentation of abrasives into the surface of the workpiece. The process is also used for finishing of hydraulic and fuel system components of aircraft which are non-ferromagnetic in nature (Lam and Smith, 1997). Components requiring uniform and repeatable outputs need this type of finishing processes. It can polish any surface through which fluid can flow. In this process, the abrading forces are not controllable during the finishing operation.

1.3.2 Elastic emission machining (EEM) process

Elastic emission machining (EEM) is another advanced finishing process in which small size abrasives strike the individual atom of the workpiece surface and split out the material from the surface of the workpiece as represented in Fig. 1.5.

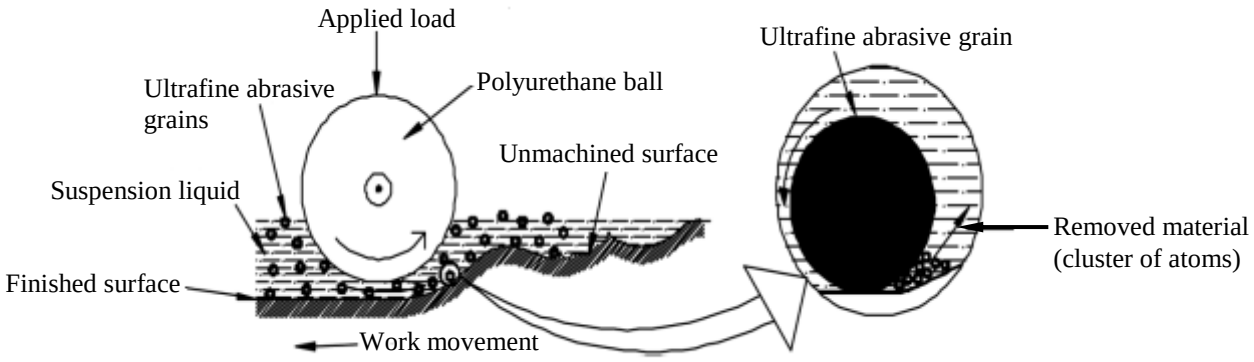

Fig. 1.5 Elastic emission machining process (Jain, 2009).

The process has the capability to extract the material from the surface of the workpiece at the atomic scale and produces the smooth surface (Kanaoka *et* al., 2007; Mori *et* al., 1990; Yamauchi *et* al., 2002). It is material removal process in which surface energy phenomenon is included for removal of atoms due to the contact made by the abrasives with the surface of the workpiece. In this process, the inclusion of atomic scale fracture elastically produces super

finished surface without any plastic deformation. It is used to finish the X-ray mirror optical surface (Yamauchi *et* al., 2002). In this process also, the abrading forces are not controllable during the surface finishing.

1.3.3 Chemo-mechanical polishing (CMP) process

Chemo-mechanical polishing (CMP) is an advanced finishing process in which chemical reaction takes place between the silica slurry and the workpiece (Larsen-Bassea, 1999). The process results in a surface that is free from surface defects (Komanduri *et* al., 1997). It is a finishing process which includes the combination of both chemical and mechanical actions and is useful for electronic industry. It gives the high average polishing rate i.e. 200nm/min and it gets change with polishing time (Jain, 2009). The workpiece is polished under an applied load over the rotating polishing pad. The schematic of the chemo-mechanical polishing process is shown in Fig. 1.6.

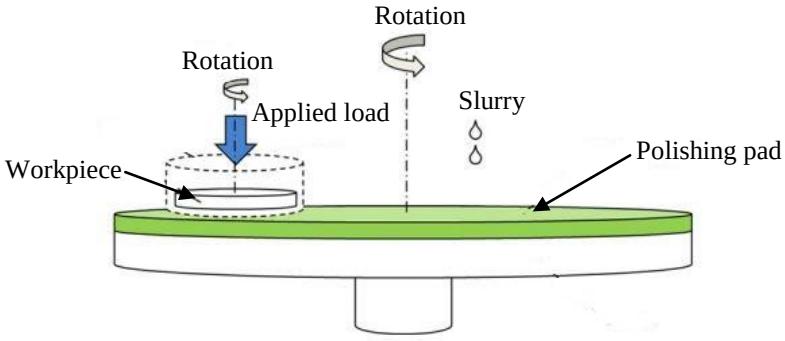

Fig. 1.6 Schematic of the chemo-mechanical polishing process (Oh and Seok, 2009).

The process is useful in semiconductor and electronic industries for polishing of silicon, optical and glass disc (Jain, 2009). It is used as surface finishing process that excludes the problem of surface damage, brittle fracture, and abrasion scratching etc. due to abrasives. This process is limited to the finishing of flat surfaces only.

The above-explained advanced finishing processes have the limitation that the finishing forces cannot be controlled externally during the finishing operation. Due to this, these advanced finishing processes may result in some defects such as surface or sub-surface damage and micro-cracks etc. To overcome the limitations of the above stated advanced finishing processes, various advanced finishing processes are developed in which finishing forces can be regulated externally by altering the strength of magnetic field.

1.4 Advanced finishing processes with externally controlled forces

Several advanced finishing processes are developed in which the finishing forces acting on the workpiece surface can be regulated by changing the magnitude of magnetic field in the working gap (region between the surface of the tool and the workpiece). With the change of the magnitude of current supplied to the electromagnet coil, the magnetic field strength in the working region get changed which consequently change the normal indenting force exerted by the magnetic particles over the workpiece surface (Jain, 2009). Different advance finishing processes with external control of finishing forces are discussed as under.

1.4.1 Magnetic abrasive finishing (MAF) process

Magnetic abrasive finishing (MAF) is an advanced finishing process in which either bonded or non-bonded particles are used in a magnetic field which acts like the self-deformable flexible magnetic abrasive brush (FMAB) (Shinmura *et* al., 1990). This process was first invented by the Soviet Union (Ruben, 1987) and later on the research was carried forward by Japan (Yamaguchi and Shinmura, 1999). The process was used to finish the internal or external surfaces of various components (Jayswal *et* al., 2005; Singh *et* al., 2004; Wang and Hu, 2005). Vibratory motion is performed in MAF to finish the edge and surface (Yamaguchi and Shinmura, 2004).

1.4.2 Magnetic float polishing (MFP) process

Magnetic float polishing (MFP) is another controllable process which is used to result in the ultrafine finishing of spherical parts like ball bearings and ceramic balls using fine abrasive particles (Umehara *et* al., 2006). The levitation force generated because of the hydrodynamic behaviour of magnetic fluid acts over the non-magnetic abrasives dispersed in it. The magnetic polishing fluid consists of fine abrasives and ferromagnetic particles suspended in carrier medium like kerosene oil or water.

The magnetic float polishing (MFP) and magnetic abrasive finishing (MAF) with regulated finishing forces are generally used for the finishing of materials which are very hard. These processes are used for finishing the materials like stainless steel, non-ferrous metals or ceramics. Since finishing medium in the MAF is mainly used as a dry powder consisting of iron and abrasive particles, the flow-ability of the brush of magnetic iron particles and abrasive particles on the surface of the workpiece is very less. So, MAF process with the dry magnetic brush may not be used for soft kind of materials. With the use of this process for soft materials, the

problems such as scratches, sub-surface damage or micro-cracks may pertain over the surface. To overcome these problems, further various other types of controllable advanced finishing processes are developed which make use of smart fluid called magnetorheological (MR) fluid.

1.5 Magnetorheological (MR) polishing fluid

The magnetorheological (MR) fluids are the smart controllable fluids whose rheological behavior can be controlled by the regulating the strength of magnetic fields. MR fluids are the suspension of micron sized magnetic particles such as carbonyl iron dispersed in a non-magnetic carrier medium like silicone oil, mineral oil or water (Jain, 2009; Sidpara *et* al., 2009). Stabilizers and surfactants are added to the MR fluids to prevent the corrosion and the wear (Genc and Phule, 2002). It is called as smart fluid because its rheological properties like yield strength and apparent viscosity can be altered in few milliseconds according to the requirement (Sidpara *et* al., 2009). When the magnetic field is "OFF", the MR fluids appear similar to liquid paints and exhibit comparable low levels of apparent viscosity. Under the action of the magnetic field, MR fluids get stiffen within the milliseconds due to the formation of carbonyl iron particles chains in the direction of magnetic lines of fields. The change in viscosity and shear strength of the MR fluid depends on the magnitude of the applied magnetic flux density. This smart rheological property of MR fluid makes it useful for different industrial operations.

The MR fluid gets stiff enough with the effect of the magnetic field. The schematic diagram representing the behaviour of magnetic particles in MR fluid without and with the influence of applied magnetic field is represented in Fig. 1.7 (a) and 1.7 (b) respectively.

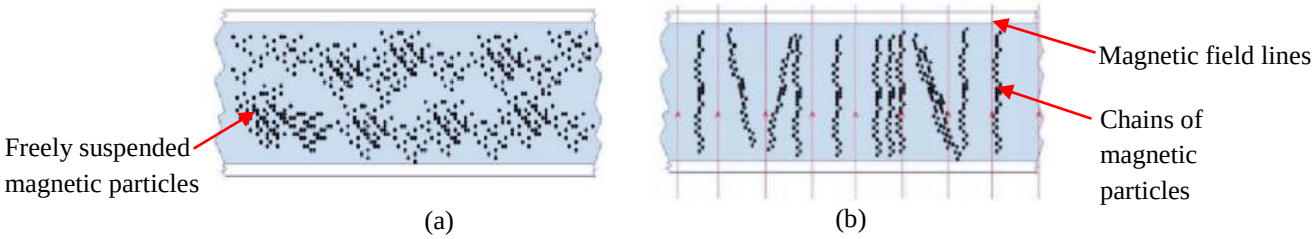

Fig. 1.7 Schematic diagram of magnetic particles present in MR fluid (a) in the absence of magnetic field and (b) in the presence of magnetic field (Mazurek *et* al., 2013).

Without a magnetic field, the magnetic particles in MR fluid get freely suspended in the base medium as shown in Fig. 1.7 (a). When MR fluid comes under the influence of magnetic field, the magnetic particles form chains in the direction of magnetic field lines as shown in Fig. 1.7 (b).

For finishing purposes, micro-sized abrasives are mixed in MR fluids which are called MR polishing fluids. In the influence of magnetic field, MR polishing fluids get stiffened and the abrasive particles get entangled between the carbonyl iron particles chains. When the magnetic finishing tool along with stiffened MR polishing fluid gets movement, the gripped abrasive particles make the relative motion with the roughness peaks of the workpiece surface. This results in finishing on the workpiece surface due to the abrasion action. The MR polishing fluid can be used to finish various kinds of materials varying from optical glass to the hardest materials (Kordonski and Jacobs, 1996). Under the effect of externally applied magnetic field, magnetic iron particles form chains which grip the abrasives strongly in between them. With the influence of the applied magnetic field, the viscosity of MR fluid get changed (Bossis *et* al., 2002; Jolly *et* al., 1999). Under the supremacy of the externally applied magnetic field, the MR polishing fluid behaves like Bingham plastic fluid (Sidpara *et* al., 2009). The rheological behaviour of the Bingham plastic model for magnetorheological fluid is shown in Fig. 1.8. The more is the strength of the externally applied magnetic field, stronger the chains of iron particles hold the abrasive particles. The stiffness of the MR polishing fluid is directly proportional to the externally applied magnetic field and also it controls the viscosity of the MR polishing fluid (Sidpara *et* al., 2009; Kordonski and Golini, 1999).

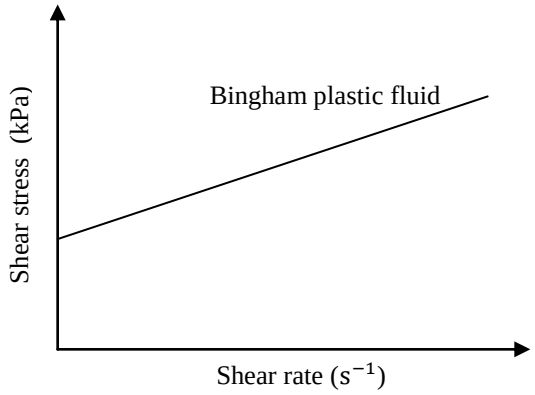

Fig. 1.8 Bingham plastic model of magnetorheological fluid (Mazurek *et* al., 2013).

Under the action of the magnetic field, magnetic iron particles get attracted towards the higher magnitude of magnetic field gradient (magnetic tool surface) which in turn exerts levitation force over the abrasives towards the lower magnitude of magnetic field gradient (workpiece surface). This levitation force makes the abrasives to indent into the workpiece's surface. The MR

polishing fluid also resists the sedimentation with the effect of the magnetic field (Jolly *et* al., 1999). The smart characteristics of MR polishing fluid of the different shear strengths make it more versatile for using it in surface finishing application also for various workpieces material (Ashtiani *et* al., 2015; Vicente *et* al., 2011; Premalatha *et* al., 2012). The constituents of MR polishing fluid are magnetic particles, abrasive particles, additives and carrier fluids.

The magnetic particles are micron-sized particles and are the main constituents of the MR fluid. With the effect of applied magnetic field, magnetic particles align in the direction of magnetic field lines, form the chains and grip the abrasive particles in between them (Vicente *et* al., 2011). Two commonly used magnetic particles for MR polishing fluid are carbonyl iron particles (CIPs) and electrolytic iron particles (EIPs). The carbonyl iron particles (CIPs) are highly purified iron manufactured by the chemical vapor deposition method. The electrolyte iron particles (EIPs) are manufactured by electro-deposition in the form of an amorphous, greyish and lusterless (Antony and Reddy, 2003). As the CIPs are the purer form of iron as compared to the EIPs so they get magnetized higher than EIPs. This in turn CIPs make chains with higher bonding strength than EIPs. The higher is the bonding strength between the iron particles, more strongly the abrasive particles can be gripped and perform better surface finishing.

The abrasive particles are non-magnetic in nature and are mixed in MR polishing fluid to perform finishing by the shearing action (Singh *et* al., 2011). There are various kinds of abrasives available which are used in MR polishing fluid such as cerium oxide (CeO_2) for finishing of optical glasses, aluminium oxide (Al_2O_3) for the materials having low hardness and diamond abrasives for high strength materials (Jain, 2009). The silicon carbide (SiC) abrasives are commonly used for finishing of metals. The kind of surface finishing required also depends on the shape and size of abrasives. Workpieces having high initial surface roughness are finished with abrasives of bigger size whereas abrasives of lower size are utilized for fine surface finishing.

Some additives are mixed with the carrier fluids for preventing sedimentation of particles in the MR polishing fluid. The additives are also used for maintaining the uniform scattering of particles in the fluid (Genc and Phule, 2002). There are various types of additives available which are used for the synthesis of MR polishing fluid such as grease, glycerol or oleic acid (Genc and Phule, 2002). Some special additives like polystyrene and gaur gum are coated over

the magnetic particle to prevent their oxidation in water-based carrier medium (Carlson and Jolly, 2000).

Fluids in which magnetic and abrasive particles are suspended are called carrier fluids (Haeri and Hashemabadi, 2008). There are varieties of carrier fluids available such as oil, synthetic hydrocarbon, esters, water and paraffin oil heavy etc. Carrier fluids like paraffin oil (heavy) are used in MR polishing for better flowability during the surface finishing of the metal workpieces. These fluids are being selected on the basis of various physical, chemical or thermal (boiling temperature) properties according to the requirement of the finishing processes. Carrier fluid must be non-reactive with magnetic particles (Carlson and Jolly, 2000).

1.6 Advanced finishing processes based on magnetorheological fluid with externally controlled forces

Various advanced finishing processes which make use of MR polishing fluid have been developed in the last two decades. In these processes, finishing forces which acts on the surface of the workpiece can be altered by changing the magnitude of current given to the electromagnetic coil or by changing the working gaps in the case for permanent magnets. These processes can finish the critical part at a slower rate so that there is no damage to the surface occurs. The surface accuracy obtained by these processes ranges from 10 nm to 100 nm. These processes have the capability to reduce the surface roughness value even less than 10 nm root mean square (RMS) value (Zantye *et* al., 2004). Different advanced finishing processes which make use of MR polishing fluid and having external control over finishing forces are given below.

1.6.1 Magnetorheological finishing (MRF) process

Magnetorheological finishing (MRF) is precise finishing process which depends on the magnetic field and is used for finishing the flat, convex, spherical, or concave shape of surfaces (Golini *et* al., 1999). Snapshot of the magnetorheological finishing setup is represented in Fig. 1.9. The process makes use of MR polishing fluid having ferromagnetic particles dispersed in a non-magnetic carrier medium (Kordonski and Jacobs, 1996). The process constitutes a rotating wheel to which MR polishing fluid is delivered through the nozzle as represented in Fig. 1.9. The magnetic field is applied across the wheel so that the fluid which comes in the magnetic line of forces gets stiffened and performs finishing. By using a computer controlled arm, the workpiece

(lens in this case) is brought in from the top as shown in Fig. 1.9. The workpiece makes contact with the stiffened fluid present on the rotating wheel and is kept in the area where the magnetic field is present. Under the action of the applied magnetic field, MR polishing fluid makes chains like structure for which energy is required to deform it.

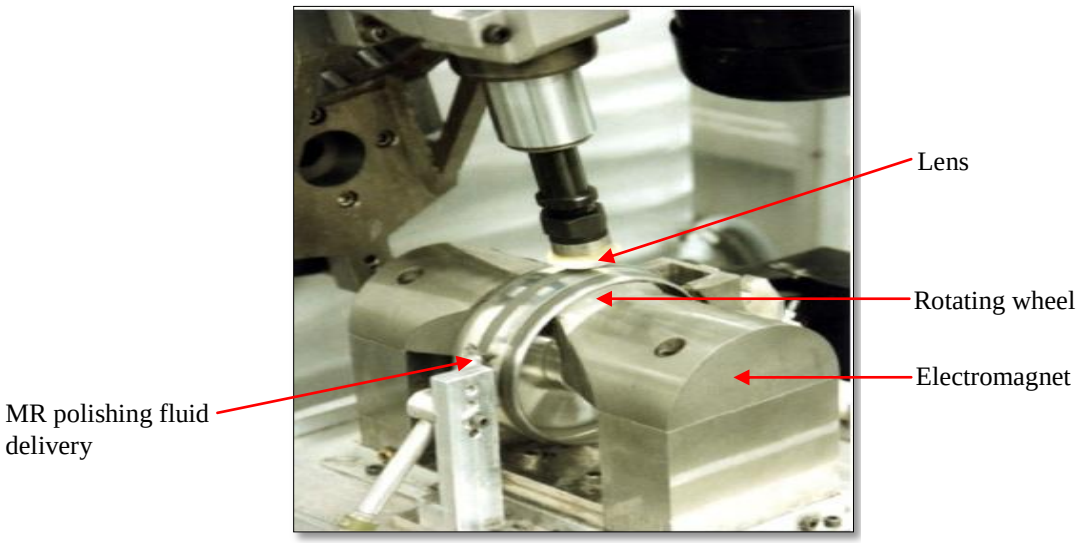

Fig. 1.9 A snapshot of the magnetorheological finishing setup (Shorey *et* al., 2001).

When the wheel rotates over the surface of the workpiece, then due to the relative motion between abrasives and the workpiece, the material gets eroded out and the nano-finished surface is obtained. Since the normal force applied by these particles is very small, therefore the material removal is very small and nano level of finishing is obtained. Material removal mechanism during the finishing of the lens by MRF process is represented in Fig. 1.10.

.

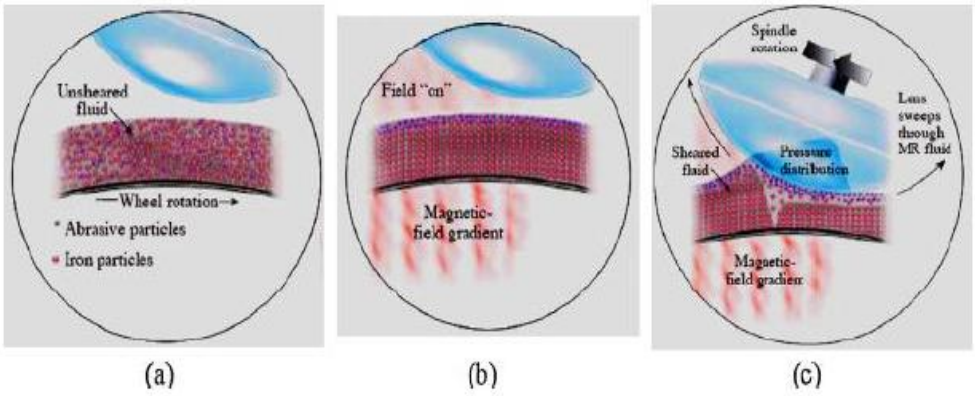

Fig. 1.10 Mechanism of material removal during the finishing of the lens by MRF process (Jain, 2009).

When the magnetic field is OFF, abrasive and iron particles are freely dispersed as shown in Fig. 1.10 (a).When the magnetic field is applied across the MR polishing fluid, the abrasives and the iron particles form chains in direction of magnetic field lines as represented in Fig. 1.10 (b). Workpiece (lens in the present case) surface interacts with the stiffened chains of particles under the influence of the applied magnetic field as represented in Fig. 1.10 (c) and results in surface finishing. The process is mainly used to finish the surfaces of optical glass and crystals (Lambropoulo *et* al., 1996) and produce surface accuracy in the order of 10 nm (Jain, 2008). It takes away heat and debris from the polishing zone and has low material removal rate. Despite being a complex nature of MR polishing fluid in the MRF process, it is greatly utilized for fine finishing of different types of workpieces without surface defects with deterministic control of finishing forces. These benefits of the MRF process compensate for the complexity and costs utilization for the process.

1.6.2 Magnetorheological jet finishing (MRJF) process

The magnetorheological jet finishing is the process which was developed for finishing of freeform dome optics, cavities and steep concave optics etc. (Kordonski *et* al., 2006). The photograph of the experimental setup of magnetorheological jet finishing is represented in Fig. 1.11 (a)

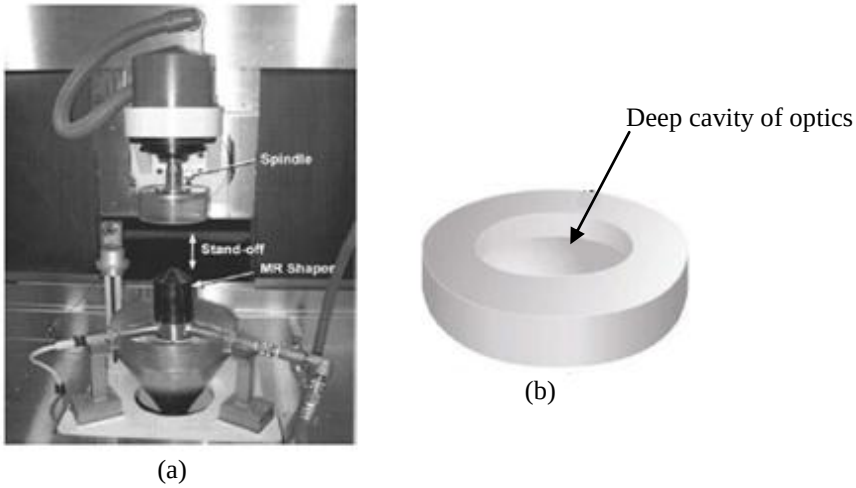

Fig. 1.11 (a) Photograph of the experimental setup of magnetorheological jet finishing and (b) CAD model of workpiece cavity finished with the MR jet (Tricard *et* al., 2006).

The finishing process was an improvement of MRF process. In the magnetorheological jet finishing process, a jet of MR polishing fluid is thrown into the internal surface or the geometry

of the workpiece. An axial magnetic field is applied to the jet of MR polishing fluid when the jet is out from the nozzle (Kordonski *et* al., 2006). The three-dimensional computer-aided design (CAD) model of the workpiece whose deep cavity is finished as shown in Fig. 1.11 (b).

The abrasive particles precisely finish the internal deep cavity of the workpiece. The surface roughness value is decreased from 0.54 µm to 0.04 µm (Kordonski and Shorey, 2007). The snapshot image of magnetic abrasive jet finishing (MRJF) is shown in Fig. 1.12.

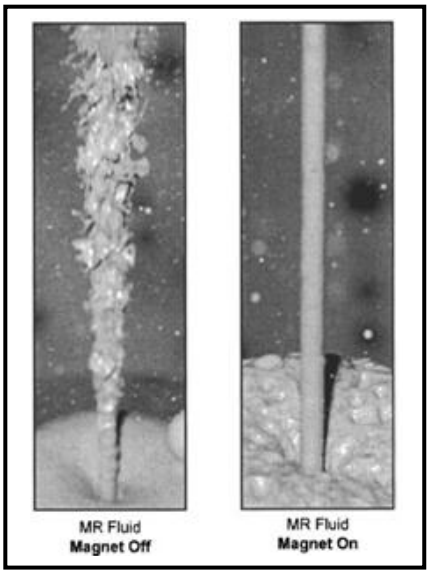

Fig. 1.12 A snapshot image of magnetic abrasive jet finishing (velocity of the jet as 30 m/s and nozzle tip diameter as 2 mm) (Tricard *et* al., 2006).

It polishes the surface where material removal is governed by impacting the abrasive particle's kinetic energy. As it can be observed from the Fig. 1.12, when the magnet is OFF, the jet of MR fluid loses its coherence coming out of the nozzle. When the magnet is ON, the stable jet of MR fluid comes out of the nozzle as shown in Fig. 1.12. This stable jet of MR fluid is used to finish the deep cavity surface of workpiece materials.

1.6.3 Magnetorheological abrasive flow finishing (MRAFF) process

Magnetorheological abrasive flow finishing (MRAFF) process is developed to fine finish the inner cylindrical surfaces having complex geometries (Jha and Jain, 2004). The limitation of the Abrasive Flow Machining (AFF) process was that it was an uncontrollable process i.e. the different forces exerted on the workpiece surface could not be controlled externally. Therefore, to increase the performance of the abrasive flow finishing process, a hybrid process termed as

MRAFF is developed. In MRAFF process, finishing forces can be regulated by regulating the induced magnetic field which was not possible in AFM process. However, in comparison with the AFF process, MRAFF process requires more precise control over the magnetic field and movement of stiffened MR polishing fluid. Also, finishing of very small internal surface of the longer cylindrical workpieces may difficult with MRAFF as the movement of stiffened MR polishing fluid could be difficult. As a source of the magnetic field was kept outside the cylindrical workpiece in MRAFF process and due to this effect, it was found more useful to finish only the non-ferromagnetic types of workpieces. The development of MRAFF process is represented in Fig. 1.13. The process comprises magnetorheological polishing fluid consisting of abrasives in it. As the magnetic field is applied, carbonyl iron particles (CIPs) make the columnar arrangement with abrasives entangled in between the chains (Furst and Gast, 2000).

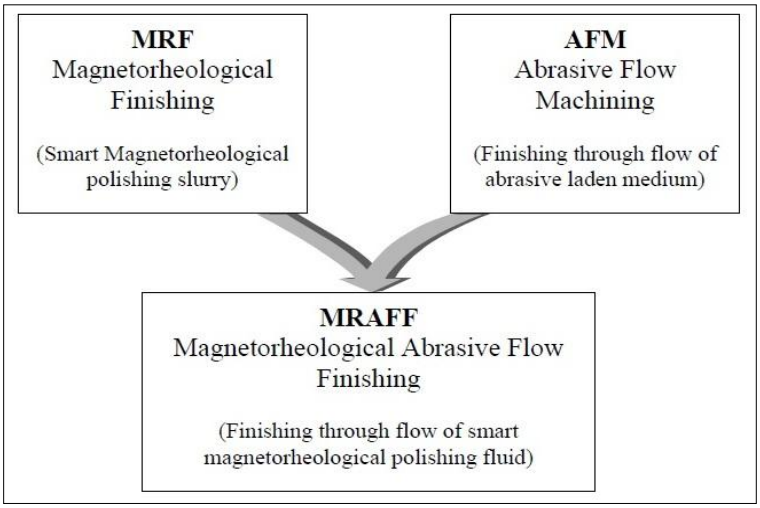

Fig. 1.13 Development of magnetorheological abrasive flow finishing process (Jha and Jain, 2004).

The CIP chains grip the abrasives on the surface of the workpiece and remove the peaks from workpiece surface as shown in Fig. 1.14. The abrasive slashes out the peak of surface roughness in three stages as shown in Fig. 1.14.

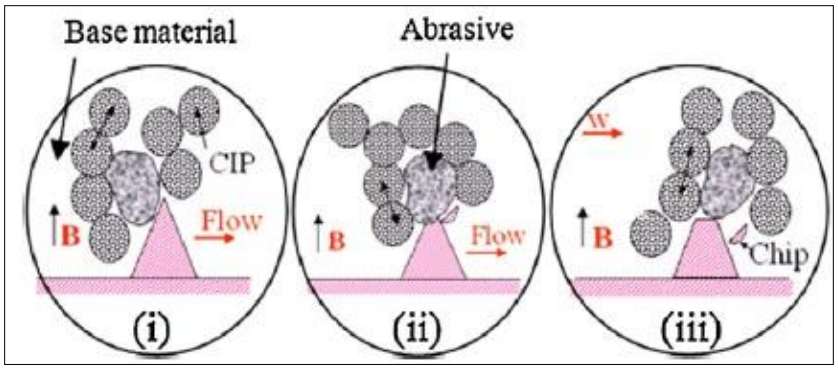

Fig. 1.14 Three stages (i-iii) of material elimination in case of MRAFF process (Jain, 2009).

In the first stage, the abrasives (held by the CIPs chains) approaches towards the peaks of the roughness. In the second stage, gripped abrasive slashes out the material and in the third stage the gripped abrasive proceed further. Due to the relative motion between the gripped abrasives and the workpiece surface, roughness peaks get slashed out by a shearing action as shown in Fig. 1.14. The process is used for finishing of complex internal geometries requiring nano-meter level surface roughness such as bushes and pipes which are made up of non-ferromagnetic materials (Jha and Jain, 2004).

1.6.4 Rotational magnetorheological abrasive flow finishing (R-MRAFF) process

The MRAFF process is later on updated with the rotating motion of the magnetic poles to raise the interaction between the abrasives and the surface of the workpiece by moving them in rotatory and reciprocatory motion. Schematic diagram showing the mechanism of rotational MRAFF is represented in Fig. 1.15.

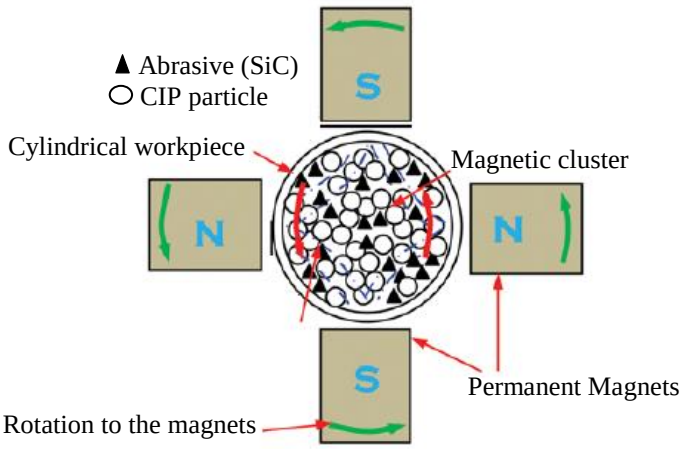

Fig. 1.15 Schematic of the mechanism of the rotational magnetorheological abrasive flow finishing (R-MRAFF) process (Das *et* al., 2011).

The additional rotational motion of magnetic poles is advantageous to have a better surface finish in less number of finishing cycles. The process is used for finishing of non-ferromagnetic hard material such as stainless steel (Das *et* al., 2010). It is an improved finishing process in comparison with MRAFF process due to the increased interaction of abrasives with workpiece surface because of the additional rotating motion applied to the magnetic field. Percentage change in surface roughness value in R-MRAFF process is found mostly contributed by the rotational speed of magnetic poles.

1.6.5 Magnetorheological abrasive honing (MRAH) process

The movement of the magnetorheological abrasive honing process is same as the conventional honing process. The process is used to finish the external curved surfaces of non-ferromagnetic materials (Sadiq and Shunmugam, 2009). Workpieces are placed over a spindle which rotates inside the cylinder. MR polishing fluid with abrasives is imparted into the cylinder and is allowed to move to and fro with the help of plunger as represented in Fig. 1.16. The magnetic field is induced by placing electromagnets outside the walls of the cylinder. Experiments were performed on both ferrous and non-ferrous material. It was found that process was good for finishing only non-ferrous materials. From the experiments, researchers found that the surface finishing was enhanced by increasing the magnitude of magnetic field intensity.

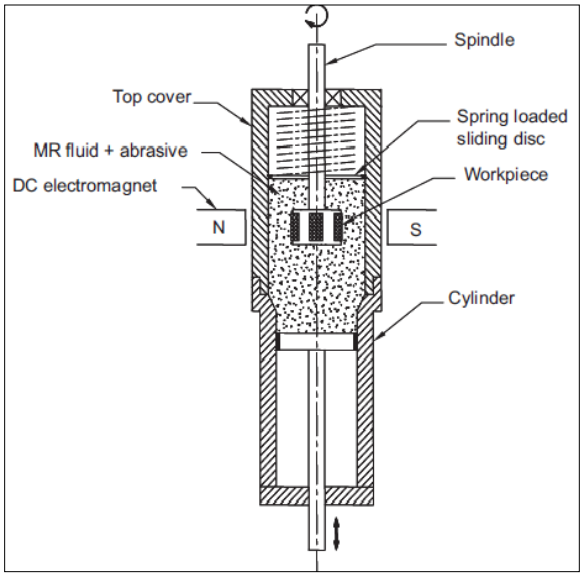

Fig. 1.16 Schematic of the magnetorheological abrasive honing process (Sadiq and Shunmugam, 2009).

Finishing forces on the abrasive particles can easily be controlled by varying the magnetic field strength generated by current given to the DC electromagnet in this process**.**

1.6.6 Ball end magnetorheological finishing (BEMRF) process

MRF and MR jet finishing processes are restricted to the particular geometries only because of the constraint on the relative motion of MR polishing fluid and the workpiece surfaces. Further, a novel finishing process is developed for finishing the three-dimensional surfaces through ball end MR finishing tool as shown in Fig. 1.17 (Singh *et* al., 2011). The process is named as ball end magnetorheological finishing process. In this process, MR polishing fluid enters from the top of the tool without applying the magnetic field. As soon as MR polishing fluid comes to the tip of the tool, the magnetic field is provided due to which MR polishing fluid get stiffened. In this process, the tool is rotated and the feed motion is provided to the workpiece surface.

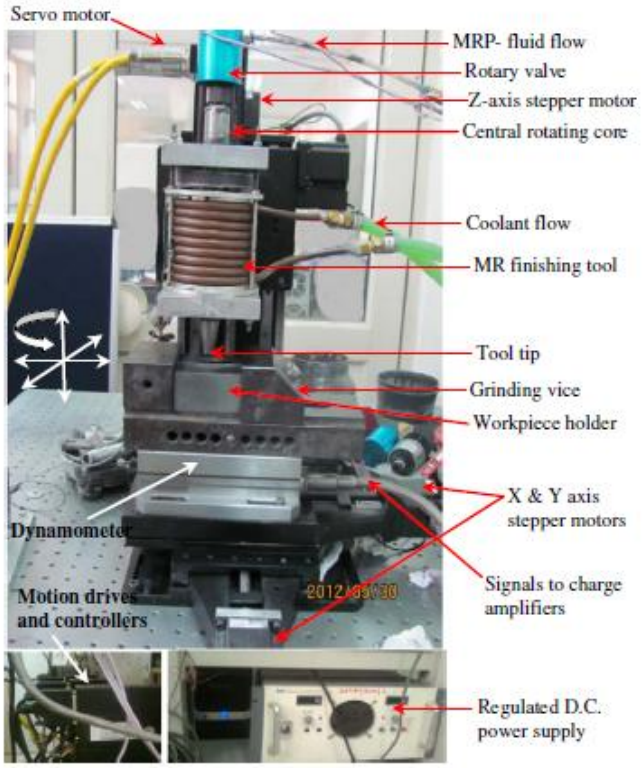

Fig. 1.17 Photograph of ball end magnetorheological finishing process (Singh *et* al., 2011).

The material removal mechanism in ball end magnetorheological finishing process is represented in Fig. 1.18. The abrasives get indent inside workpiece peaks because of the lower magnetic field at the surface of the workpiece as represented in Fig. 1.18 (a).

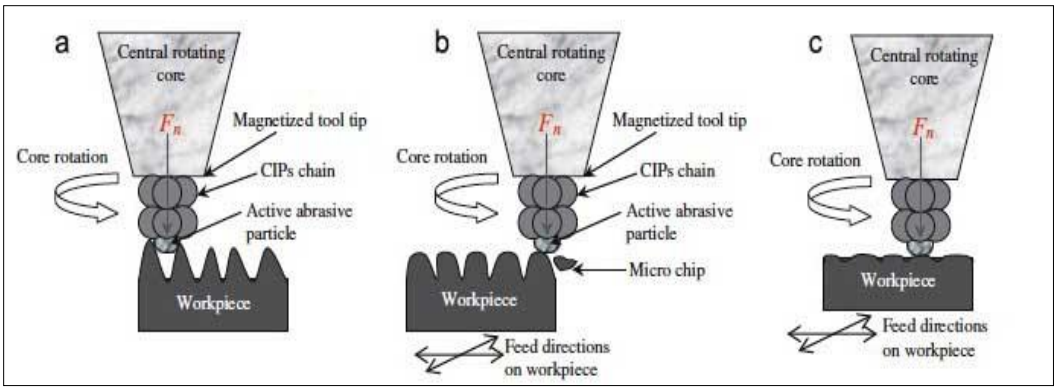

Fig. 1.18 Material removal mechanism in the ball end magnetorheological finishing process (Singh *et* al., 2013).

Due to rotation of the central rotating core and relative motion between the abrasives and the workpiece surface, indented abrasives break the roughness peaks into microchips as shown in Fig.1.18 (b). Due to a constant feed of workpiece, all the peaks get removed from the surface and better-finished surface is achieved as shown in Fig. 1.18 (c). By the action of shearing, gripped abrasives pluck out the workpiece material from its surface roughness (Brecker *et* al., 1969). It is used to finish flat and 3-D curved surfaces where fine finishing of the surface is of great concerned (Singh *et* al., 2013).

1.7 Advantages of magnetorheological fluid based finishing processes

- Close tolerance design can be achieved
- Capable to finish up to nanometer scale value
- Decreases the wear and friction losses
- Increases the life of work material
- Reduces the surface and subsurface defects
- Finishing forces exerted on the workpiece's surface can be regulated by controlling the magnetizing current as per the shear strength required for the workpiece surfaces. This is not possible in conventional finishing processes
- MR finishing processes are used to precisely finish the surfaces of any shapes of almost all type of materials.
- Due to the increase in the relative motion of the abrasive particles with the additional motion of magnetic poles as in R-MRAFF process, this results in the uniform smooth mirror like finish surface with improved material removal rate and finishing rate.

CHAPTER 2

LITERATURE REVIEW

The precise surface finishing of components with good surface integrity is a very important requirement in industries for improving the operative functionality (Bedi and Singh, 2016). Presently, there are many areas in an industry where nano-finishing (surface roughness value (R_a) less than 100 nanometers) of the workpiece surface is of great concern. The benefits of nano-finishing can be achieved like dimensional accuracy, close tolerance fit or design, enhancement in the life of the tool and reduced wear and frictional losses etc. The surface finishing of components with higher accuracy is a very difficult task and time taking in manufacturing industry (Gorana *et* al., 2004). Various traditional finishing processes such as honing and grinding are generally owned to attain finishing over the internal or external surfaces of various components. Honing is the finishing operation which uses a finishing tool called as honing tool. The honing tool consists of a number of honing stones on its outer surface. Honing tool has a unique property as its honing stones can move radially inwards or outwards as per the required inner diameter of the cylindrical workpiece to be finished. The honing stones consist of abrasives which make a relative movement with the inner surface of the cylindrical workpiece and finish the surface. Honing tool is moved with a simultaneous rotating and reciprocating motion into the cylindrical workpiece for its surface finishing. Grinding is a finishing process which is commonly used to finish the various internal or external surfaces. It consists of a circular wheel having abrasives, strongly bonded to its outer surface. The circular grinding wheel is made to rotate over the surface of the workpiece and the strongly bonded abrasives shear out the roughness peaks present over the surface. The traditional processes use a rigid type of tool for finishing the surfaces of the workpiece due to which the finishing forces cannot be controlled in these processes. Due to uncontrollable finishing forces, several surface defects like cavities, deeper grooves, grooves with sharper edges and ploughed materials remained over the finished surface (Gupte *et* al., 2008). To attain surface finish with good surface characteristics, various advanced finishing processes which make use of magnetorheological (MR) polishing fluid are developed. While performing finishing with these processes, finishing forces can easily be regulated by varying the magnitude of magnetic field in the working region (gap between the surface of finishing tool and the surface of the workpiece).

The detailed literature about the traditional and advanced finishing processes is discussed below. It details the limitations of various traditional finishing processes. Also, it covers the development of various advanced finishing processes, mechanism of material removal involved in that different advanced finishing processes and mathematical modeling of some advanced finishing processes to analyze their process mechanism.

2.1 Literature related to the traditional finishing processes

The detailed literature reviews regarding traditional finishing processes are discussed as follows.

Pei *et* al., (1999) analyzed the subsurface damage occurred on the flat surface of silicon wafer while performing the surface grinding process. The authors observed the several configurations of cracks formed over the surface of a silicon wafer with cross-sectional microscopy. The study has been performed for the design of experiments to analyze the effects of different grinding process parameters such as rotational speed of wheel and feed rate on the depth of the subsurface crack. Grinding wheels having diamond abrasives with different mesh size i.e. 360, 1200, 2000 and 4000 were used for experimentations. Experimental parameters i.e. grinding wheel speed, chuck speed and feed rate were ranged from 25-56.67 rev/sec, 0.33-1.33 rev/sec and 0.25-0.58 μm/sec respectively. It was concluded the depth of subsurface crack on the flat surface of the silicon wafer was approximately equal to half of the grit size of diamond abrasive used for grinding wheel.

Fergani *et* al., (2014) studied the effects of temperature on tensile residual stresses generated on the surface of a component while performing grinding. The authors developed a predictive model to evaluate the onset tensile temperature after which residual stresses start generating over the workpiece. The model relied on stresses and strains generated over the surface of the workpiece due to heat produced while grinding operation performed. The empirical relation was built between the stress profile generated over the surface of the component and the temperature attained over the component's surface. The results predicted from the model were experimentally validated with grinding of AISI52100 hardened steel. The author concluded that it is important to evaluate the onset tensile temperature after which residual stresses start generating because these are the major factor which may affect the precision and productive life of the final industrial product. The model built a scientific basis for the configuration of grinding process parameters to avoid the generation of stress over the surface of the component.

Obara *et* al., (2017) explained the harms of folded metals remained at the internal surface of cylinder liner by quantifying them through surface relocation. The authors explained that metal folds which remain on the internal surface of cylinder liner may cover up the grooves which are provided for lubrication. During the running of an engine, these folded metals may get erode from the surface of the cylinder liner and may produce axial scratches. Worn out debris of folded metals may create scuffing wear on the cylinder liner of automotive engines. These scuffing wear produce the scuffing marks on the surface of the cylinder liner and piston rings. The scuffing marks result with noise in the engine while running of the automobile engine.

Michalski and Pawlus, (1992) described the surface defects like torn and folded metals which remain on the internal surface of the cylinder liner of an automobile engine after finishing with the traditional honing operation. The honing operation is generally employed to finish the inner surface of the cylinder liner of an automobile engine. The traditional honing process may result in some surface defects like torn and folded metals which harm the functional performance of an engine. Torn and folded metals are the microscopic welds left over the inner surface of the cylinder liner. These defects get generated because of the heat produced over the internal surface of the cylinder liner and uncontrollable finishing forces of honing stones while performing honing operation. The microscopic torn and folded metals get erode while working of an engine and create the wear over the surface of the cylinder liner and piston rings. This may result in inducing of scuffing marks over the inner surface of cylinder liner which generates noise while the working of the engine. The authors described the torn and folded metal defects arise due to the uncontrollable finishing forces applied by the honing stones.

From the above-stated literature review, it is observed that traditional finishing processes are likely not suitable to result in the required surface finish with good surface integrity. The traditional finishing processes make use of rigid tools due to which finishing forces are uncontrollable in these processes. These traditional finishing processes may result in some surface defects such as pit holes or cavities and surface cracks etc. while finishing the surface of the components. These surface defects reduce the functional capability of the components for the various applications (Lim *et* al., 2002). So, to attain the desired defect-free surface for the longer functional applications of various industrial components, the advanced finishing processes need

to be employed, where the finishing forces can be regulated externally with the control of the magnitude of magnetic field.

2.2 Literature related to the advanced finishing processes with the external control of forces

To attain good surface integrity on the surface of various industrial components, the various advanced finishing processes are developed which have control over the finishing forces. By regulating the magnitude of magnetic flux density in the working gap, finishing forces are easily regulated in these processes. The advanced finishing processes having external control of finishing forces make use of magnetorheological (MR) polishing fluid. The MR polishing fluid gets stiffened in the presence of magnetic field and performs finishing action to attain the precise surface finish. The literature reviews detailing the advanced finishing processes relying on MR fluid having external control of finishing forces are discussed as under.

Kordonski and Jacobs, (1996) developed a magnetorheological finishing (MRF) process for finishing of high-quality lenses which generally tend to break while finishing by other traditional processes. The process made use of magnetorheological (MR) polishing fluid consisting of iron particles and cerium oxide dissolved in a non-magnetic carrier fluid such as water, silicon oil and mineral oil etc. for precise surface finishing of the lenses. The process finished the lenses by a non-contact method of finishing which results in no sub-surface damage while finishing. Under the action of magnetic field, carbonyl iron particles of the MR fluids get magnetized and formed dipoles with each other in the direction of magnetic lines of fields. Owing to this, MR fluids get stiffened. The magnetic dipoles lead to magnetic normal force. With the control of magnetizing current, precise finishing over the lens surface was achieved by regulated finishing forces.

Kim *et* al., (1997) performed fine finishing of the inner surface of the cylindrical workpieces made up of non-ferromagnetic material i.e. SUS-304 steel using magnetic abrasive jet machining. Combined mixture of particles such as aluminium oxide and pure iron was used with the working fluid of compressed air for finishing the cylindrical internal surface. The compressed air at the pressure of 4 to 5 atm was jetted at different angles into the internal surface of the SUS-304 steel cylindrical workpiece with the help of nozzle. Magnetic poles were placed outside the cylindrical workpiece surface to stiffen the MR polishing fluid. The results showed that

maximum material removal is obtained with the impact angle of 25^0-30^0, size of abrasive as 300-400 μm and the jet velocity of 40 m/sec.

Kordonski and Golini, (1999) utilized the rheological properties of MR polishing fluid to precisely finish the glass surface by making use of magnetorheological finishing (MRF) process. In MRF process, the MR polishing fluid is transported to the surface of the workpiece by making use of a rotating wheel rim and a nozzle on the rim. With the application of magnetic field, the magnetic particles form chains, due to which ribbon-like structure is formed which acts as the abrasives surface. The removal of material takes place due to the shear stress of the MR polishing fluid. Gripped abrasives in the stiffened MR polishing fluid erode the peaks of roughness from the workpiece surface.

Kordonski *et* al., (2004) performed the experiments on the developed magnetorheological jet finishing process to finish the fused silica glass. MR jet polishing system was mounted on 5-axis computer numeric control platform equipped with polishing control software. The MR polishing fluid was prepared with a mixture of water and abrasives. The experimentation was also performed on the small concave surface of fused silica glass with the initial surface roughness of 210 nm peak to valley and 50 nm RMS. The roughness profiles were measured with the help of the interferometer (NewView 500 white light). From the results, it is concluded that the surface roughness values of fused glass silica reduced to 13 nm peak to valley and 2 nm RMS whereas, it reduced to 44 nm peak to valley and 6 nm RMS for concave fused silica glass.

Yin and Shinmura, (2004) utilized vibration-assisted magnetic finishing process for evaluating the process performance, deburring and decrease in surface roughness. Authors used the mixer of iron particles, white alumina (WA) magnetic abrasives and straight oil type grinding fluid. They performed experimentations on different workpieces made up of different materials such as magnesium alloy (AZ31B), stainless steel (SUS304) and brass (C2680). Experimentations were performed by keeping the process parameters as workpiece feed rate of 17 mm/min, the magnetic flux density of 0.6 Tesla, working clearance of 3 mm and finishing time of 160 seconds. From the experimentations, it was concluded that better surface finishing and deburring was performed for magnesium alloy (AZ31B) as compared to other two materials.

Yamaguchi and Shinmura, (2004) made use of magnetic assisted finishing process to finish the internal surface of alumina ceramic tube. The experiments were performed using different sizes

of iron particles (i.e. 150 µm, 330 µm and 510 µm) and different sizes of diamond abrasives (i.e. 0-1 µm, 2-4 µm, 4-8 µm and 8-12 µm) with variable quantity of soluble type barrel finishing lubricants with quantity as 0.1 ml, 0.2, ml 0.25 ml, 0.3 ml and 0.35 ml. Results concluded that surface roughness (R_a) value reduced to a minimum value of 0.02 µm with workpiece rotation of 1800 rpm, working gap of 1 mm and magnetic flux density of 0.37 Tesla. For achieving this, the best combination of polishing fluid was found as iron particles of 330 µm, diamond abrasive of 0-1 µm and soluble type barrel finishing lubricant of 0.3 ml.

Singh *et* al., (2004) observed the effects of different process parameters on the percentage change in surface roughness using magnetic abrasive finishing (MAF) process. A mixture of 75% iron particles and 25% SiC abrasives was used for finishing of a flat surface. The percentage reduction in R_a value was found better in the case when the voltage of 11.5 V is applied to the electromagnet. Also, it was observed that with the rise in working gap, the change in surface roughness decreased because of the weaker bonding of carbonyl iron particles chains as less magnetization in the working gap.

Jha and Jain, (2004) developed a process named as magnetorheological abrasive flow finishing (MRAFF) for internal finishing of cylindrical workpieces. In this finishing process, the magnetic field was induced by the electromagnets which were placed outside the cylindrical workpiece. The MR polishing fluid consisted of a mixture of 20% carbonyl iron particles (CIPs), 20% silicon carbide (SiC) abrasive particles and 60% visco plastic base medium was used to finish the workpiece of stainless steel. Finishing cycles of 200 were performed with a magnetic flux density of 0.574 Tesla while performed experimentations. From the experimental results, it was concluded by the authors that better surface finishing can be obtained with the increased strength of magnetic field which results in improved gripping of abrasives.

Bagnoud *et* al., (2005) performed correction of neodymium-doped yttrium lithium fluoride (ND: YLF) rods (used in high power laser) by making use of magnetorheological finishing. Magnetorheological finishing (MRF) was used to correct the wavefront which is transmitted by the laser gain material. A drastic rise in energy and wave-front quality of CLARA laser amplifier was obtained by MR finishing. From the experimental results, it was found that average power of 9W laser got increased from 20 % to 30 % by performing the magnetorheological finishing.

Feng *et* al., (2005) developed a manufacturing system to finish the silicon carbide (SiC) aspheric mirrors using magnetorheological finishing (MRF) process. Authors carried out experiments for finishing a parabolic silicon carbide (SiC) aspheric mirror having a diameter of 100 mm aperture to study the features of MR polishing fluids. Experiments were performed to demonstrate the capability of developed manufacturing system by producing an ultra-smooth SiC aspheric mirror surface with high shape accuracy. Experiments were performed to study the effects of different constituents of MR polishing fluids and their concentration on material removal rate.

Jha and Jain, (2006) studied the effects of the use of different grades of carbonyl iron particles (CIPs) like CS grade having a diameter of 18 μm and HS grade having a diameter of 3.5 μm separately by using magnetorheological abrasive flow finishing (MRAFF) process. The authors developed a mathematical model for change in surface roughness in MRAFF process and validated it by experimentations. The authors concluded from the experimental results that the change in surface roughness value (R_a) decreased with the decrease in the size of abrasive particle for the same size of CIPs. Also, it was concluded that finishing forces acting over the abrasives is mainly dependent on the number of CIPs present in the MR polishing fluid.

Kordonski and Shorey, (2007) performed finishing on fused silica glass (having dome concave shape) by making use of magnetorheological jet finishing (MRJF) process. The authors utilized cerium oxide as abrasive particles along with liquid jet as the constituents of MR polishing fluid for obtaining precise surface finishing over the fused silica glass. Experimental results showed that the surface roughness (R_a) value get decreased from the initial of 50.3 nm to final of 6 nm with a velocity of MR jet as 30 m/sec. It was concluded that to obtain a stable polishing spot, a magnetically stable collimated jet of MR fluid is much required.

Jha *et* al., (2007) performed the finishing on stainless steel workpiece with the magnetorheological abrasive flow finishing (MRAFF) process. The authors observed the effects of process variables such as extrusion pressure and number of finishing cycles on the percentage change in surface roughness. At the extrusion pressure of 3.75 MPa, the highest reduction in surface roughness was observed. MR polishing fluid with the composition of 20 % of carbonyl iron particles, 20 % of silicon carbide abrasives and 60 % of the base medium was used for experimentations. Also, it was concluded that the real finishing gets performed after the erosion

of loosely held ploughed material remained after grinding. The effect of hydraulic extrusion pressure for change in surface roughness R_a value in MRAFF process is shown in Fig. 2.1.

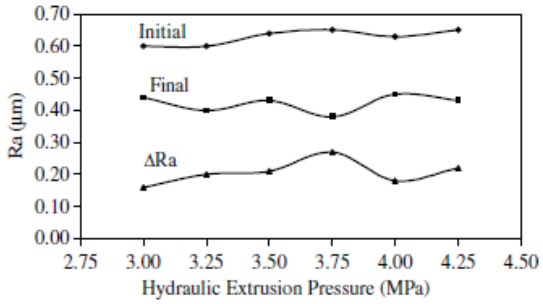

Fig. 2.1 Effect of hydraulic extrusion pressure on surface roughness R_a value.

Yamaguchi *et* al., (2007) performed experimentations on the inner cylindrical surface finishing of SUS 304 workpiece having an internal diameter of 800 µm using magnetic abrasive finishing (MAF) process. A mixer of 80% by weight of iron particles and 20% by weight of magnetic abrasives was used for performing the finishing. While performing the finishing, flexible magnetic abrasive brush (FMAB) get formed inside the cylindrical tube. With the reciprocating motion of external magnetic poles and rotating motion of cylindrical non-ferromagnetic austenite stainless steel tube workpiece, the magnetic abrasive brush performed the surface finishing of the internal surface of cylindrical tubes. With a rotational speed of 30,000 min^{-1} of the cylindrical workpiece, reduction of more than 80% in the surface roughness (R_a) value was observed within finishing time of 16 minutes. The process was not significantly suitable for internal finishing of ferromagnetic cylindrical workpieces. In case of internal finishing of ferromagnetic cylindrical workpieces, the maximum magnetic flux density is present on the inner surface of the ferromagnetic cylindrical workpiece due to the placement of magnetic poles outside the cylindrical workpiece. Because of the presence of maximum magnetic flux density on the inner surface of the ferromagnetic cylindrical workpiece, the mixer of magnetic particles and abrasive particles stuck to the inner cylindrical's surface. No relative motion becomes possible between the abrasives and ferromagnetic cylindrical workpiece's inner surface due to which significant finishing cannot take place.

Das *et* al., (2008) proposed a mathematical model for change in surface roughness in magnetorheological abrasive flow finishing (MRAFF) process. Experimentations were performed on the inner surface of the stainless steel to validate the developed mathematical

model. The finishing was performed with the help of MR polishing fluid consisted of 20% of carbonyl iron particles (CIPs), 20% of SiC abrasives with 60% visco plastic base medium by volume. Experimentations were performed for a different number of finishing cycles. It was concluded that the change in surface roughness gets rises with increasing the number of finishing cycles up to a limit of 350 cycles and after that, it started decreasing. Reduction in surface roughness value increased with increasing the current given to the electromagnet coils from both i.e. mathematical model and experimentations.

Seok *et* al., (2009) developed a model of material removal to illustrate the tribological behaviour of the MR polishing fluid while performing finishing. For analysis, the authors used a wheel-type MR finishing process and MR polishing fluid having 85% by weight of carbonyl iron (CI) particles and 15 % by weight of water and surfactants. To illustrate the tribological behaviour of MR polishing fluid, both solid and fluid-like characteristics were studied under the influence of magnetic field. Researchers found that material removal rate gets increased with the rise in rotating velocity of the magnetic tool due to the increased shear force acting by the abrasives.

Sadiq and Shunmugam, (2009) developed a process named as magnetorheological abrasive honing (MRAH) process for the finishing of the external curved surface. The effects of change in magnetic field on the change in the surface roughness were studied by performing experimentations on workpieces surface made up of aluminium alloy (AL 6063) and austenite stainless steel. MR polishing fluid used for the experimentations consisted of a mixture of 30% carbonyl iron particles (CIPs), 25% SiC abrasive particles and natural castor oil. It was concluded that with the increase of the magnetic field in the working gap resulted in enhancement of surface finish. The higher magnitude of magnetic field raises the yield strength of MR polishing fluid which results in the better surface finish. A threshold limit of 0.633 Tesla was observed after which further improvement in the surface finish was not possible. With the magnetic flux density of 0.633 Tesla and the workpiece rotating speed of 420 rpm, the surface roughness (R_a) value get decreased from 1.629 μm to 1.3 μm over the surface of aluminium alloy in the finishing time of 15 minutes. While with the same magnetic flux density of 0.633 Tesla and workpiece rotating speed of 450 rpm the surface roughness (R_a) value get decreased from 0.696 μm to 0.633 μm over the surface of austenite stainless steel in the same finishing time of 15 minutes.

Cheng *et* al., (2010) developed a dual axis magnetorheological finishing (MRF) wheel type tool for finishing of the BK7 mirror workpiece. The finishing was carried out with the help of MR polishing fluid (included 10% CeO_2 abrasive particles). The mathematical modeling was carried out to calculate the material removal rate. The process parameters were considered as magnetic field strength- 860 kA/m (1.08 Tesla) and polishing time of 1 min. The results obtained as the surface roughness value decreases from 328.42 nm to 42.93 nm and the shape accuracy gets changed from 0.519λ (RMS) to 0.067λ (RMS) in finishing time of 75 minutes.

Sadiq and Shunmugam, (2010) performed experiments for the finishing of external curved surfaces of mild steel (AISI 1020) and stainless steel (SS 316L) using magnetorheological abrasive honing (MRAH) process. It was concluded by the authors that there is a significant change in surface finishing of non-magnetic stainless steel workpiece (41.7%) as compared to little change in finishing for magnetic mild steel workpiece around 6% for the same finishing time of 10 minutes. The reason behind this difference in finishing performance is that accumulation of MR polishing fluid on the external curved surface of the mild steel workpiece takes place due to the existence of high magnetic field over that surface. While finishing the mild steel workpiece, high magnetic field gets accumulated on the external curved surface of mild steel workpiece, MR polishing fluid sticks on that surface and there is no relative movement between MR polishing fluid and the external curved surface of mild steel workpiece. So, the process was found likely not appropriate for finishing the workpieces made up of ferromagnetic materials.

Das *et* al., (2010) enhanced the performance of magnetorheological abrasive flow finishing (MRAFF) process by modifying it. The modification was made by adding an addition to the process i.e. providing rotational movement to the electromagnet and they named that process as rotational-magnetorheological abrasive flow finishing (R-MRAFF) process. Nano-finishing of the inner surface of the stainless steel tubes was performed using the developed process. To observe the effects of the process variables, the design of experiments was performed using response surface regression analysis. It was found that percentage change in surface roughness is mostly contributed by the rotational speed of the electromagnet. The optimum process parameters were found as the rotational speed of electromagnet as 149 RPM, extrusion pressure

40 bar, abrasive mesh size of 153 and number of finishing cycles 1200. Least surface roughness of 16 nm was obtained over the internal surface of stainless steel.

Sidpara and Jain, (2011) performed experiments to observe the effects of different process variables for forces acting over the flat workpiece while performing experiments with the magnetorheological (MR) fluid based finishing process. The process parameters were considered as working gap, percentage concentration of carbonyl iron particles (CIPs) and silicon carbide (SiC) abrasives, and the rotating speed of the wheel. To observe the normal and tangential forces acting over the surface of the workpiece while experimentation, the dynamometer was used. The authors used blend of CIPs, abrasive particles and glycerol as the constituents of MR polishing fluid. It was concluded that forces acting over the surface of the workpiece is majorly influenced by the working gap followed by the CIP concentration and least influenced by the wheel's rotational speed. From the results, it was concluded that the normal force as well as tangential forces decreased with increase in thickness of working gap but increased with increase in CIPs concentration. Also, normal and tangential forces increased with the increase in percentage concentration of SiC abrasives up to a level of 3.5 % but decreased with further increase in the concentration of SiC abrasives as shown in Fig. 2.2.

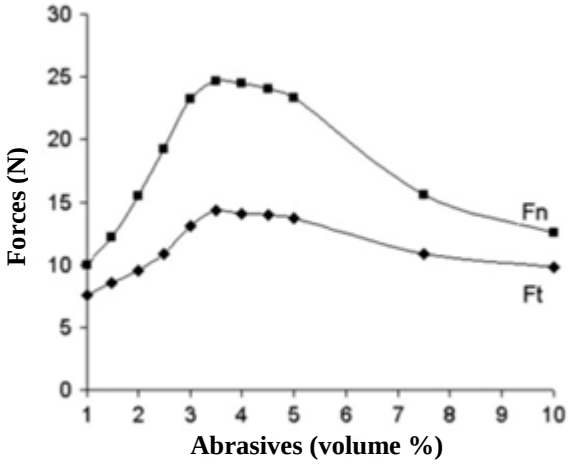

Fig. 2.2 Effect of concentration of abrasives on normal force (F_n) and tangential force (F_t).

Sidpara and Jain, (2012) developed two mathematical models to predict the forces (normal and tangential) acting over the flat workpiece surface in the magnetorheological fluid based finishing process. One mathematical model was developed by considering squeeze force and another mathematical model by omitting the same. Normal force acting over the workpiece surface was

calculated by summing up the magnetic normal force, centrifugal force and gravitational force acting over the abrasive particles. The tangential force was calculated by summing up the shear force and the coriolis force acting over the workpiece surface. In the second mathematical model, normal and tangential forces were evaluated by also accounting the respective normal and tangential component of squeezing force. Mathematical models were verified with the experimental results of forces (normal and tangential) which were measured with the help of dynamometer. Parameters considered for validating the mathematical models with the experimentations were working gap, percentage concentration of carbonyl iron particles (CIPs) and abrasives, and the rotational speed of the wheel. Mathematical models have been developed and verified with the experimental results with detailing the processing mechanism because of the consideration of squeezing factor.

Hong *et* al., (2012) performed experimentations for the precise nano-finishing of alumina reinforced zirconia ceramics by making use of magnetorheological (MR) polishing fluids. The MR polishing fluid used for experimentations constituted of magnetic carbonyl iron (CI) particles, diamond abrasives and de-ionized water. The process parameters considered for various experiments were rotational speed of magnetic poles as 200 and 300 RPM, the magnitude of the magnetic field as 3.8, 4.7, 5.5 and 6.1 kA/m and the polishing time as 10, 20, 40 and 60 minutes. The experimental results showed that for the polishing time of 60 minutes, least surface roughness of 1.96 nm was obtained with wheel's rotational speed of 300 RPM and magnetic field of 3.8 kA/m.

Singh *et* al., (2013) developed a theoretical mathematical model for calculating normal force acting over the flat ferromagnetic workpiece surface for different working gaps in ball end magnetorheological finishing process. The normal average force acting over the workpiece surface was computed with the developed mathematical model for different values of working gaps. Experimentations were also performed to validate the mathematical model. MR polishing fluid constituted of 20% by volume carbonyl iron particles (CIPs), 20% by volume SiC abrasive particles and 60% visco plastic base medium by volume was used for finishing. The experimental results concluded that with the working gap of 0.66 mm, magnetic normal force of 16.35 N was acting on the workpiece surface and surface roughness (R_a) value get decreased to the least value of 0.028 μm from an initial value of 0.143 μm. The percentage reduction of 80.42

in surface roughness value R_a was obtained after the finishing. The surface roughness profiles of initial and final finished surface processed by ball end magnetorheological finishing (BEMRF) process at working gap of 0.66 mm are represented in Fig. 2.3 (a) and (b) respectively.

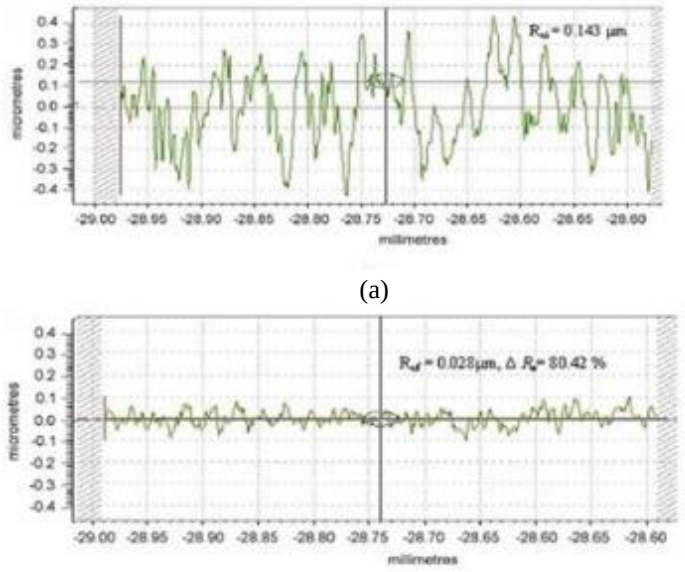

(a)

(b)

Fig. 2.3 Surface roughness profiles of (a) initial, and (b) after (BEMRF) at working gap of 0.66 mm.

Judal *et* al., (2013) developed a new vibration assisted cylindrical magnetic abrasive finishing (VAC-MAF) process for the finishing of the external cylindrical surface of the aluminium workpiece. The finishing was performed with the steel grit and aluminium oxide abrasives. The effects of various process variables such as rotating speed of workpiece, the frequency of vibration given to the tool, magnitude of magnetic flux density and size of abrasive particles on material removal rate were observed. Size of abrasive particles and frequency of vibration given to the finishing tool are the two key factors which contribute maximum to the change in surface roughness and material removal. It was concluded that more material gets removed from the surface of aluminium workpiece with the rise of the frequency of vibration provided to the finishing tool as shown in Fig. 2.4. It was scrutinized that the rate of material removal and change in surface roughness gets improved by almost 100 % and 150 % respectively with the use of VAC-MAF as compared to the conventional magnetorheological abrasive finishing (MAF) without vibrations.

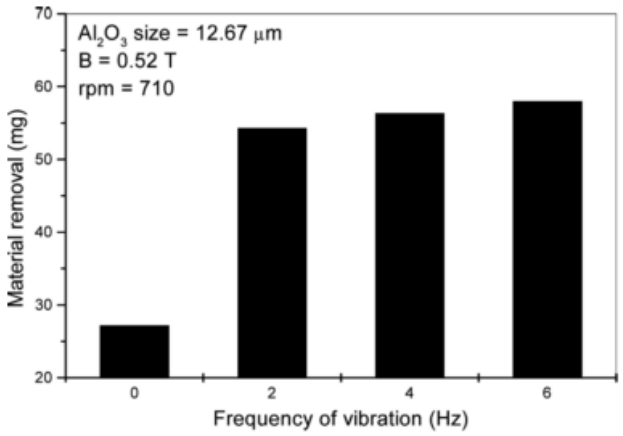

Fig. 2.4 Material removal variation with frequency of vibration provided to the finishing tool.

Saraswathamma *et* al., (2015) performed finishing on the flat silicon wafer workpiece using ball end magnetorheological finishing (BEMRF) process. Authors used MR polishing fluid that constituted of 25% by volume carbonyl iron particles (CIPs), 66.75% by volume deionized water, 6% by volume ceria abrasives, 2.5% by volume glycerol and 0.75% by volume sodium hydroxide (NaOH) for finishing. The effects of different process parameters i.e. the tool rotational speed, the magnetizing current given to the electromagnet coil, and the working gap on the percentage change in surface roughness R_a value were observed. The working gap was found the most influencing parameter for change in surface roughness R_a value. It was observed that with the increase of working gap, the percentage change in surface roughness R_a value decreases. The experimental results concluded that with the tool rotational speed of 30 rotations per second (rps), the magnetizing current of 3A and the working gap of 0.6 mm, surface roughness (R_a) value get decreased from the initial value of 457 nm to the final value of 89.8 nm.

Saraeian *et* al., (2016) performed finishing over the external surface of cylindrical AISI321 stainless steel using magnetic abrasive finishing. Experimentations were performed by designing a full factorial model for the influential parameters i.e. rotating speed of magnetic poles, working gap and abrasive particle size for obtaining optimum parameters for finishing of steel AISI321. The working gap was found the most influencing parameter followed by the rotating speed of magnetic poles and abrasive particle size. Working gap of 1 mm with the rotating speed of 500 rpm and abrasive particle size of 100 mesh was found best for achieving 50 % improvement in surface roughness. It was found that further rise in rotating speed of magnetic poles after 500 rpm leads to the dispersion of particles. Also, it was concluded that reduction in surface roughness with the optimum process parameters mainly rely on the initial surface roughness.

Bedi and Singh, (2017) performed the internal surface finishing of the ferromagnetic cylindrical workpiece using magnetorheological (MR) polishing fluid. The authors developed two finishing tools, one with electromagnetic I-shaped core and another with electromagnetic rectangular shaped cores. In both the cases, electromagnetic cores were placed inside the ferromagnetic cylindrical workpieces. Both the tools had maximum magnitude of magnetic flux density over its outer finishing surface as compared to the inner surface of the ferromagnetic cylindrical workpiece. The finishing tool with rectangular cores had a uniform magnetic flux density distribution over its outer surface. On the other hand, the finishing tool with I-shaped core had a non-uniform magnetic flux density distribution over its outer surface. The finishing tool with rectangular cores was found better in terms of uniform finishing and reduced finishing time as compared to the finishing tool with the I-shaped core. While performing experimentations, the finishing tool with I-shaped core reduced the surface roughness R_a value in the range of 65-78 % after 150 minutes of finishing. On the other hand, the finishing tool with rectangular cores reduced the surface roughness R_a value in the range of 78-81 % after 90 minutes of finishing.

2.3 Research gaps

- The traditional finishing processes like honing or grinding are available for the inner surface finishing of the cylindrical components but are not well suitable to obtain very fine precise surface finish with better surface characteristics. These processes make use of rigid tools in which finishing forces cannot be controlled or regulated. These processes may result in various surface defects like flakes, groove interrupt, folded metals, smudgy grooves etc. (Beyerer and Puente Leon, 1997). Also, the traditional finishing processes can finish the surface up to a certain level and due to the rigidness of their abrasive tool, these processes cannot perform further finishing achieving very fine precision surface.
- The advanced finishing processes like magnetorheological abrasive flow finishing (MRAFF) process and rotational magnetorheological abrasive flow finishing (R-MRAFF) process have been developed by researchers for the inner surface finishing of the cylindrical workpieces. These processes make use of MR polishing fluid. Finishing forces can be regulated in these processes. These advanced finishing processes are found more effective for further reduction in surface roughness values at the nano-meter range after the traditional grinding or honing process. This results in enhancing the functional applications of cylindrical components. But

these processes may not be well suitable for the internal finishing of the ferromagnetic cylindrical workpieces. In case of internal finishing of ferromagnetic cylindrical workpieces, the maximum magnetic flux density is obtained on the inner surface of the ferromagnetic cylindrical workpiece due to the placement of the magnetic poles outside the cylindrical workpiece. Due to the presence of maximum magnetic flux density on the inner surface of the ferromagnetic cylindrical workpiece, the MR polishing fluid gets stuck to the inner surface of the cylindrical workpiece. Due to this, no relative motion between the active abrasive particles and the inner surface of the ferromagnetic cylindrical workpiece is possible and finishing doesn't take place.

- Recently, limitations of these above-stated advanced finishing processes have been overcome by the development of the magnetorheological honing tool (MRH) by the authors (Bedi and Singh, 2017). In the developed finishing process, the finishing of the internal surface of the ferromagnetic cylindrical workpiece was performed by rotating and reciprocating the developed MR finishing tool inside the cylindrical workpiece keeping a working gap for the MR polishing fluid. The movements of the developed finishing tool were just like a conventional honing tool so the process was named as magnetorheological honing process. The developed MR finishing tool was made up of electromagnetic cores and was rotated and reciprocated inside the ferromagnetic cylindrical workpiece. Due to the placement of electromagnet cores of the developed MR finishing tool inside the ferromagnetic cylindrical workpiece, a higher magnitude of magnetic flux density was obtained on the finishing tool's outer surface as compared to the inner surface of the ferromagnetic cylindrical workpiece. Due to the magnetic field gradient in the working gap, the magnetic iron particles get attracted to the outer surface of the tool because of the presence of higher magnetic field at that surface. Also, magnetic iron particles push the non-magnetic abrasive particles with levitation force towards the inner surface of the ferromagnetic cylindrical workpiece having a lower magnetic field. Abrasive particles get indented into the inner surface of the ferromagnetic cylindrical workpiece due to levitation force and erode out the material in form of microchips during predefined movement of the tool. In this way, the developed finishing tool was made capable to finish the inner surface of the ferromagnetic cylindrical workpieces.

- But this already developed MR honing tool is limited to finish the inner surface of the cylindrical workpiece of a particular internal diameter only at a time. As the outer surface of the already developed MR honing tool is not flexible to move radially inwards or outwards, so it is capable to finish the internal surface of the cylindrical workpiece of a particular internal diameter only at a time. The outer diameter of the developed finishing tool is constant that is why it can finish the internal surface of the cylindrical workpiece of a particular internal diameter at a time by keeping the constant working gap for the MR polishing fluid.
- Also, the problem of heating arises while using the electromagnet type magnetorheological honing (MRH) tool. When the current is given to the electromagnet coils of the MR honing tool, the heat generation takes place in the coils. Due to the heating of electromagnet coils, the cores of the MR honing tool also get heated up. Heating up of the cores of MR honing tool results in reduced viscosity of the MR polishing fluid. MR polishing fluid can't perform its proper finishing action after the reduced viscosity.
- Detailed mathematical modeling for change in surface roughness in the magnetorheological honing process is also required to understand the in-depth mechanism of material removal during the finishing process.

In contrast with the above-said research gaps, there is a need for a development of a finishing tool based on MR fluid which can perform nano-finishing of the internal surfaces of different sizes (internal diameters) of cylindrical workpieces. Also, the finishing tool is required to work for long duration for performing nano-finishing of the internal surfaces of different sizes of cylindrical workpieces without getting heated up. Mathematical modeling for change in surface roughness in the magnetorheological honing process along with the experimental validation is required to be performed to analyze the process mechanism. Parametric analysis of the newly developed MR honing process is also required to obtain the optimum process parameters for the fine finishing of the internal surfaces of the ferromagnetic cylindrical workpieces such as EN-31 to make it useful for the industries. The newly developed MR honing process with the flexible magnetic tool can overcome the limitations of traditional and advanced finishing processes by providing flexibility to finish the internal surface of different sizes (internal diameters) of cylindrical workpieces. The developed finishing tool can be used in industries for finishing the

components like cylindrical molds and dies, hydraulic cylinder, cylindrical barrel for injection molding etc. for their better functional applications. The developed finishing tool can result in a reduction in wear between the mating parts which subsequently increase the service life and reduce the maintenance of cylindrical components.

2.4 Research Objectives

- Design and fabrication of modified magnetorheological honing tool to finish the internal surface of ferromagnetic as well as non-ferromagnetic cylindrical workpieces of different sizes.
- To study the effects of process parameters (% volume of carbonyl iron particles, % volume of abrasives, rotational speed of tool and reciprocating speed of tool) with EN-31 cylindrical material on the process response such as surface finish improvement using Response Surface Methodology (RSM) in order to optimize the developed finishing process for better performance.
- To understand the material removal mechanism and surface characteristics with the developed magnetorheological honing tool, the scanning electron microscopy (SEM) is to be carried out.
- Develop a mathematical model for mechanism of material removal and change in surface roughness value during the magnetorheological honing process.
- Experimentally validate the developed mathematical model with different process parameters like reciprocating and rotary motions of magnetorheological honing tool, and number of finishing cycles.

2.5 Organization of the thesis chapters

The thesis is organized into the following chapters including the references.

Chapter 1 gives the introduction of various traditional and advanced finishing processes and their applications for different materials. This chapter states the benefits of using advanced finishing processes making use of magnetorheological (MR) polishing fluid for achieving fine finishing over the traditional finishing processes.

Chapter 2 represents the reviews of literature available related to various traditional and advanced processes used for finishing of different kind of surfaces and materials. This chapter also states the needs of the present work in industries over the existing

finishing processes based on the MR polishing fluid. The chapter ends with the main objectives of the present research work and organization of the thesis chapters.

Chapter 3 reports the design and fabrication of present magnetorheological (MR) honing tool for nano-finishing of the internal surface of the different sizes of cylindrical workpieces. In this chapter, improvement in the design of MR honing tool has also been discussed and validated through finite element analysis (FEA) performed in Maxwell Ansoft V13 software.

Chapter 4 states the detailed study regarding the preliminary experimentations performed on mild steel workpiece and statistical design (plan of experiments) to obtain the optimum process parameters for better fine finishing of the internal ferromagnetic EN-31 cylindrical workpiece's surface using developed magnetorheological (MR) honing tool.

Chapter 5 states the in-sight mechanism of the present MR honing process by developing a mathematical model for change in surface roughness value while performing finishing with the present designed MR honing tool. The developed mathematical model for change in surface roughness in MR honing process is validated with the experimentally obtained results.

Chapter 6 reports the various conclusions and significant outcomes from the performed present research work and also tells the scope for the future work.

CHAPTER 3

DESIGN AND FABRICATION OF MAGNETORHEOLOGICAL HONING TOOL FOR NANO-FINISHING OF INNER SURFACE OF DIFFERENT INTERNAL DIAMETERS OF CYLINDRICAL WORKPIECES

As illustrated under research gaps (chapter 2), an electromagnet tool based magnetorheological honing (MRH) process was developed by the authors (Bedi and Singh, 2017) to overcome the limitations of the existing magnetorheological (MR) fluid-based finishing processes for the inner surface of the ferromagnetic cylindrical workpieces. But, in this developed MRH process, an electromagnet-based MR honing tool was capable to finish the inner surface of the ferromagnetic cylindrical workpiece of a particular internal diameter only with a constant working gap for MR polishing fluid between tool's surface and workpiece's inner surface. Also, the problem of heating arises while using the electromagnet type magnetorheological honing tool. If the different internal surfaces of the different ferromagnetic cylindrical workpieces are required to finish continuously for a longer duration, a single electromagnet-based MR honing tool in that developed process was likely not capable to perform finishing. It means that different sizes of tools are needed to finish the different internal surface diameters of the different cylindrical workpieces. So, to fulfill the requirements of nano-finishing the inner surface of different diameters of the cylindrical workpieces, a novel magnetorheological honing tool has been designed and fabricated in the present research work. The present designed finishing tool has the flexibility that its radial outer magnetic surface can move inwards or outwards just like a conventional honing tool. This can be useful to fulfill the following requirements in today's modern industries.

- To achieve the nano-finish surface with good surface characteristics over the inner surface of the different cylindrical workpieces.
- To remove the various surface defects such as pit holes, sharp edges and deep grooves left over the inner surface of cylindrical workpieces after finishing with traditional grinding or honing process.
- To fine finish the inner surface of the various high-performance industrial products such as cylindrical dies, moulds and hydraulic cylinders with different sizes (internal diameters) for their better operation functionality.

- Industrial components like cylindrical barrels (with different internal diameters) for plastic injection molding machine require the super-finished inner cylindrical surface to prevent the intermixing of different colours of molten plastic material (Martínez-Mateo, 2011). The requirements of such industrial components can be fulfilled with the development of the present magnetorheological honing tool.
- To finish the inner surface of the cylindrical components at a high precision level for reducing the resistance in the flow of high purity gases or liquids (Wang and Hu, 2005).
- To extend the functional application of the cylindrical ferromagnetic components after the conventional honing or grinding process in terms of close tolerance design and its longer service life.

Thus, to achieve the above stated industrial requirements, a novel magnetorheological (MR) honing tool is designed and developed in the present work. The newly developed MR honing tool makes use of permanent magnet strips for finishing the inner surface of the cylindrical workpieces. The development of the present novel MR honing tool for nano-finishing of the inner surface of the different diameters of the cylindrical workpieces has been performed in two stages. At first, a novel initial design of MR honing tool with the flat end surface of the permanent magnetic strips is developed. After that, to overcome the observed limitations of the initial design of the tool, an improvement in the design of MR honing tool has been performed by developing a MR honing tool with the curved end surface of the permanent magnet strips in place of the flat end surface of permanent magnet strips. However, the novel both the designs of MR honing tool consists of four permanent magnets make neodymium iron boron (NdFeB) strips on its outer surface and has the capability to move its outer magnetic surface (permanent magnet strips) radially inwards or outwards about the central axis of the finishing tool as per the requirement of the inner surface diameter of the cylindrical workpiece to be finished. The radial movement of the outer magnetic surface is adjusted before the start of the finishing as per the requirement of the inner surface diameter of the cylindrical workpiece to be finished and is locked with maintaining a proper working gap for MR polishing fluid while performing the finishing. The schematic diagram of the proposed novel design of magnetorheological (MR) honing tool is shown in Fig. 3.1. The proposed design of MR honing tool rotates as well as reciprocates inside the cylindrical workpiece just like a conventional honing tool and perform

finishing over its inner surface. The proposed MR honing tool moves inside the cylindrical workpiece keeping a gap called as working gap for MR polishing fluid.

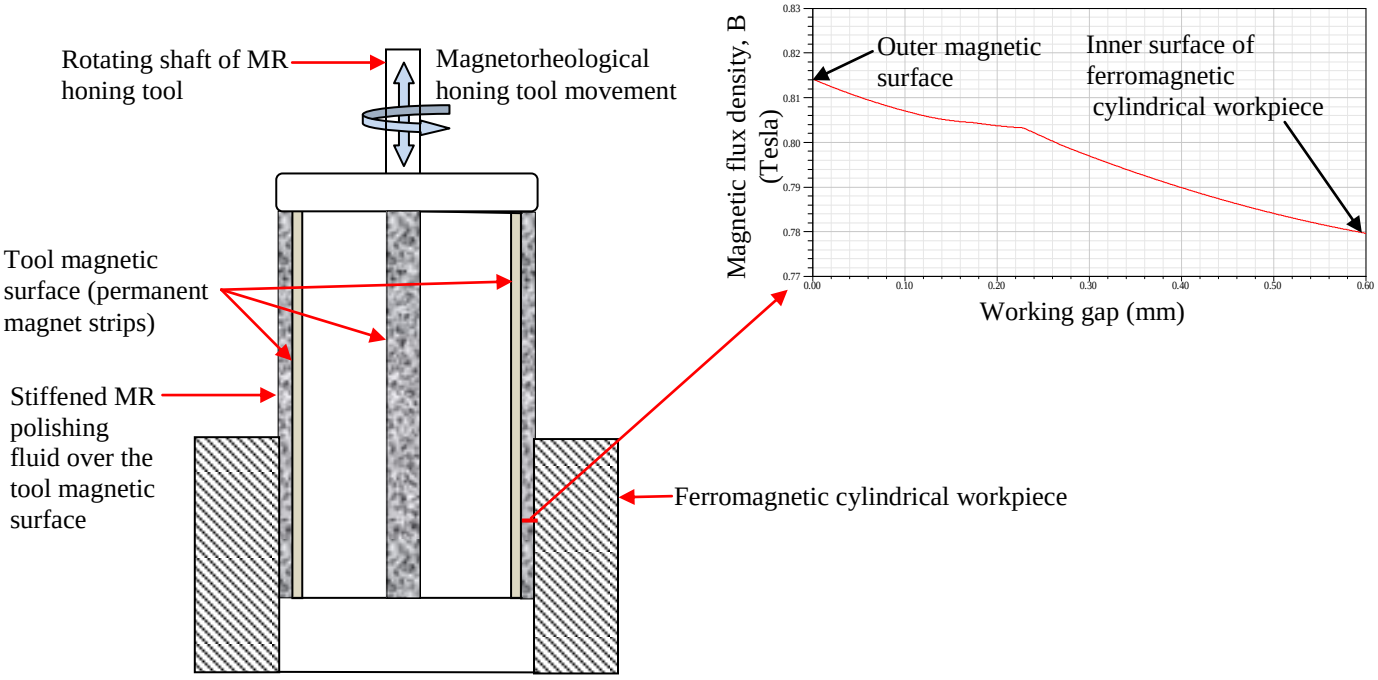

Fig. 3.1 Schematic diagram of the proposed magnetorheological honing tool to perform finishing on the inner surface of the ferromagnetic cylindrical workpiece.

MR polishing fluid is applied over the outer magnetic surface of the MR honing tool. Due to the presence of magnetic field (induced by the permanent magnet strips), MR polishing fluid becomes stiff over the tool's outer magnetic surface in the working gap and performs the finishing action by the predefined movement of the finishing tool as similar to the conventional honing tool. In the present proposed design of MR honing tool, permanent magnet strips are the source of inducing the magnetic field. The ferromagnetic cylindrical workpiece is at a certain gap from the magnetic strips, get magnetized due to the magnetic field induced by the permanent magnet strips and possesses lesser strength of magnetic field as compared to the permanent magnets. Due to this, a higher magnitude of magnetic flux density is present over the tool's surface as compared to the inner surface of the ferromagnetic cylindrical workpiece. This results in a magnetic field gradient between the tool's surface and workpiece's inner surface. In this way, the present proposed design of MR honing tool ensures the higher magnitude of magnetic flux density on its outer magnetic surface as compared to the inner surface of the cylindrical workpiece (ferromagnetic or non-ferromagnetic) in working gap as shown in Fig. 3.1.

For successful finishing in any MR fluid-based finishing processes, a higher magnitude of magnetic flux density must be obtained on the surface of the finishing tool as compared to the surface of the workpiece to be finished. The higher magnitude of magnetic flux density on the outer magnetic surface of the MR honing tool as compared to the inner surface of the ferromagnetic cylindrical workpiece as shown in Fig. 3.1 ensures the capability of the proposed tool to finish the inner surface of both ferromagnetic as well as non-ferromagnetic cylindrical workpieces. In case of the non-ferromagnetic cylindrical workpiece, a higher magnitude of magnetic flux density is surely present on the outer magnetic surface of MR honing tool as compared to the inner surface of the non-ferromagnetic cylindrical workpiece. The non-ferromagnetic material does not get magnetized in the presence of a magnetic field, so higher magnetic flux density is surely obtained on the magnetic surface of MR honing tool.

3.1 Initial design and fabrication of a novel magnetorheological honing tool for internal surface finishing of different diameters of cylindrical workpieces

To accomplish the requirement of nano-finishing the internal surface of different diameters of cylindrical ferromagnetic or non-ferromagnetic workpieces, a novel magnetorheological (MR) honing tool with four rectangular permanent magnet strips (having flat end surface) has been designed. The principal design requirement in the present MR honing process is that the MR polishing fluid should become stiff on the adjustable magnetic tool end surface for finishing the different sizes of the internal surface of the ferromagnetic or non-ferromagnetic cylindrical workpieces. Moreover, the magnetic finishing tool with the retained MR polishing fluid on its magnetic end surface should move inside the cylindrical workpiece with rotational as well as reciprocation movement simultaneously as similar to the movement of the conventional honing tool. The four rectangular strips of NdFeB are attached with the rotating variable opening finishing tool whose role is to retain the MR polishing fluid during the finishing of the internal cylindrical surface (Fig. 3.1). The novel MR honing tool has been designed in such a way that its magnetic strips can be adjusted to move radially inwards or outwards as per the required internal surface diameter of the cylindrical component to be finished. Before final fabrication of the finishing tool, a magnetostatic finite element (FE) analysis has been performed in Maxwell Ansoft V13 software for analyzing the distribution of the magnetic flux density in the proposed MR honing tool.

3.1.1 Magnetostatic finite element analysis of the initial design of MR honing tool

A magnetostatic finite element (FE) analysis has been performed in Maxwell Ansoft V13 software for the proposed MR honing tool with the MR polishing fluid and the ferromagnetic cylindrical workpiece to study the variation of magnetic flux density in the working gap. The magnetorheological (MR) honing tool constituting of four rectangular flat end permanent magnet strips (NdFeB) with end surface width of 23.2 mm and height 60 mm is modeled in Maxwell Ansoft V13 software. The four magnetic strips are symmetrically patterned at an angle of 90º from each other about the central axis of the finishing tool. The ferromagnetic cylindrical workpiece is modeled over the MR honing tool keeping a gap of 2.7 mm for MR polishing fluid as shown in Fig. 3.2. Magnetic model of the magnetorheological honing tool with the flat end magnetic surface with MR polishing fluid and the ferromagnetic cylindrical workpiece is shown in Fig. 3.2.

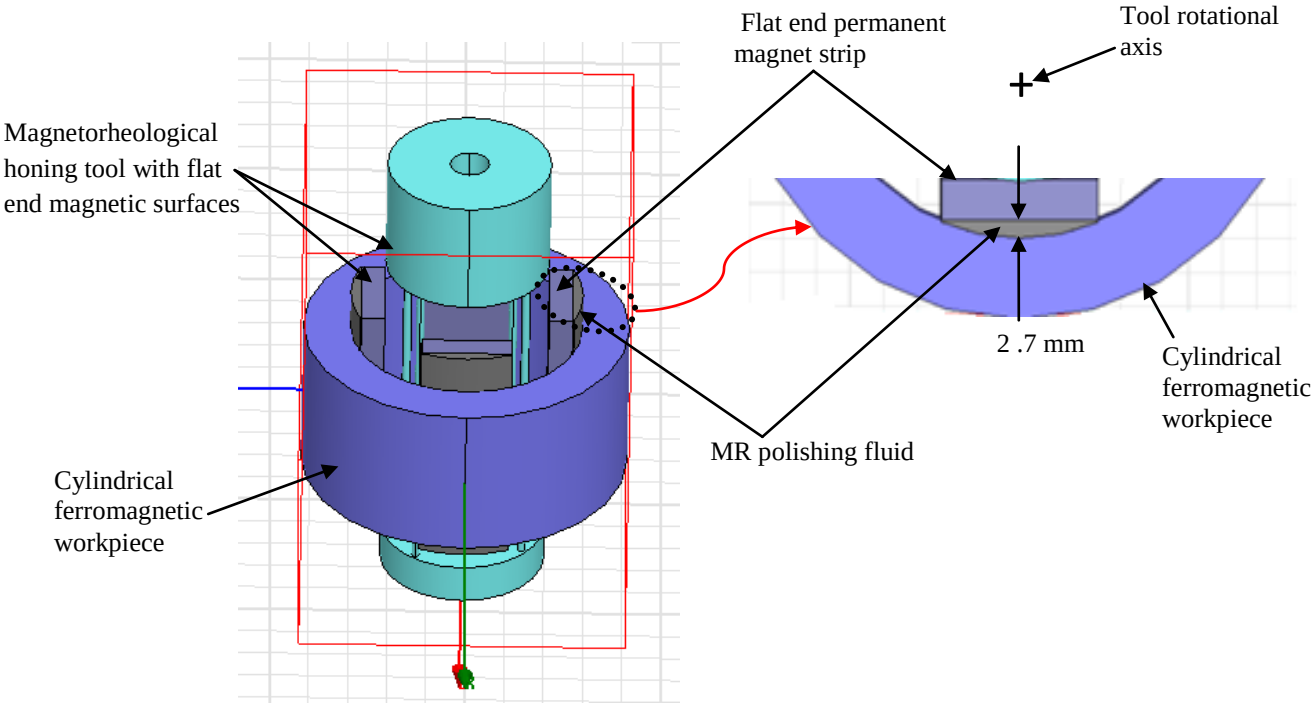

Fig. 3.2 Magnetic model of the magnetorheological honing tool with the flat end magnetic surface, MR polishing fluid and the ferromagnetic cylindrical workpiece.

For modeling of MR polishing fluid over the flat surface of the permanent magnet strip, the thickness of 2.7 mm is measured from the middle part of the magnet strip to the inner surface of the cylindrical ferromagnetic workpiece as shown in Fig. 3.2. To analyze the distribution of magnetic flux density on the outer end surface of the proposed MR honing tool having flat end

permanent magnets, the model has been magnetostatically analyzed through finite element (FE) analysis in Maxwell Ansoft V13 software. For magnetostatic finite element analysis, materials are assigned to the various parts of MR honing setup as specified in Table 3.1. Relative permeability for the different materials has been assigned using the library of Maxwell Ansoft V13 software or from the literature. The entire setup is insulated at the boundaries to avoid magnetic flux losses or leakages. The setup is simulated with a solution type of magnetostatics. Ignorance of maximum surface deviation has been placed for initial mesh settings. Simulation has been performed with default settings of maximum normal deviation and maximum aspect ratio. The analysis of setup has been performed by keeping auto mesh generation with a percentage error of 1 and 10 numbers of passes.

Table 3.1 Assigned parameters to the magnetic model of the proposed MR honing tool with the flat magnetic end surface

Parameters	**Materials**	**Relative Permeability**
Permanent magnet	NdFeB	1.04
Finishing medium	MR polishing fluid	5
Ferromagnetic cylindrical workpiece	Mild steel	600

Through magnetostatic finite element (FE) analysis, distribution of magnetic flux density across the cross-section of MR honing setup having flat permanent magnet strips is observed as shown in Fig. 3.3 (a). From FE analysis, the 2D plot of variation in the magnitude of magnetic flux density in the MR polishing fluid region (working gap) from the magnetic end surface to the inner surface of the ferromagnetic cylindrical workpiece is evaluated as shown in Fig. 3.3 (b). From Fig. 3.3 (b), it can be observed that higher magnitude of magnetic flux density is present on the flat end surface of the permanent magnet strip as compared to the inner surface of the ferromagnetic cylindrical workpiece. It ensures the sticking of MR polishing fluid on the outer magnetic surface of the MR honing tool while performing finishing on the inner surface of the either ferromagnetic or non-ferromagnetic cylindrical workpieces. From FE analysis, the 2D plot of variation in the magnitude of magnetic flux density over the flat end surface of the permanent magnet strip in the MR polishing fluid region is evaluated as shown in Fig. 3.3 (c). From Fig. 3.3 (c), it can be observed that there is enormous non-uniformity in magnetic flux density distribution over the tool's outer flat surface of magnet strip with the MR polishing fluid in

working gap. The magnitude of magnetic flux density is minimum over the middle part of the flat magnet strip and goes on increasing as moving toward its edges. This is because the distance from the outer flat surface of tool with the inner surface of the cylindrical workpiece gets decreasing in working gap as moving from middle part to the edges of flat magnet strips, and because of this, magnetic flux density goes on increasing as moving toward the edges of flat magnet strips as shown in Fig. 3.3 (c). It signifies that strong chains of carbonyl iron particles (CIPs) form over the tool edges of flat magnet strips due to the high magnetic field. The loose CIP chains are formed over the tool's middle part of the magnet strip due to the low magnetic field in that region. The variation of magnetic flux density (B) is evaluated in the working gap through FE analysis as shown in Fig. 3.3 (b). From FE analysis of the novel design of MR honing tool, it is observed that higher magnitude of magnetic flux density is obtained on the outer magnetic surface of MR honing tool as compared to the inner surface of the ferromagnetic cylindrical workpiece. This is an important requirement to finish the inner surface of ferromagnetic cylindrical components. It confirms the capability of the designed MR honing tool to nano-finish the inner surface of ferromagnetic as well as non- ferromagnetic cylindrical workpieces.

From Fig. 3.3 (a) and (c), it can be observed that there is non-uniform distribution of magnetic flux density over the flat outer surface of the two permanent magnet strips ($A'_1 - A'_2 - A'_1$). On the other hand, there is a more non-uniform distribution of magnetic flux density over the flat outer surface of other two permanent magnet strips ($A'_3 - A'_4 - A'_3$). The magnitude of magnetic flux density is maximum on the end edges of these two permanent magnet strips (A'_3) and is least over the surface of the middle part of the flat permanent magnet strips (A'_4). This higher variation in the distribution of magnetic flux density over the flat end surface of these two magnetic strips ($A'_3 - A'_4$) is occurring due to the interference of magnetic field in the working gap when the tool with four flat magnet strips are placed inside the ferromagnetic cylindrical workpiece. From Fig. 3.3 (a), it can be concluded that strongly bonded carbonyl iron particles (CIPs) chains get form over the edges area of these flat permanent magnets (A'_1 and A'_3) and weak chains of CIPs can form towards the middle surface area due to the interference of magnetic field (A'_2 and A'_4).

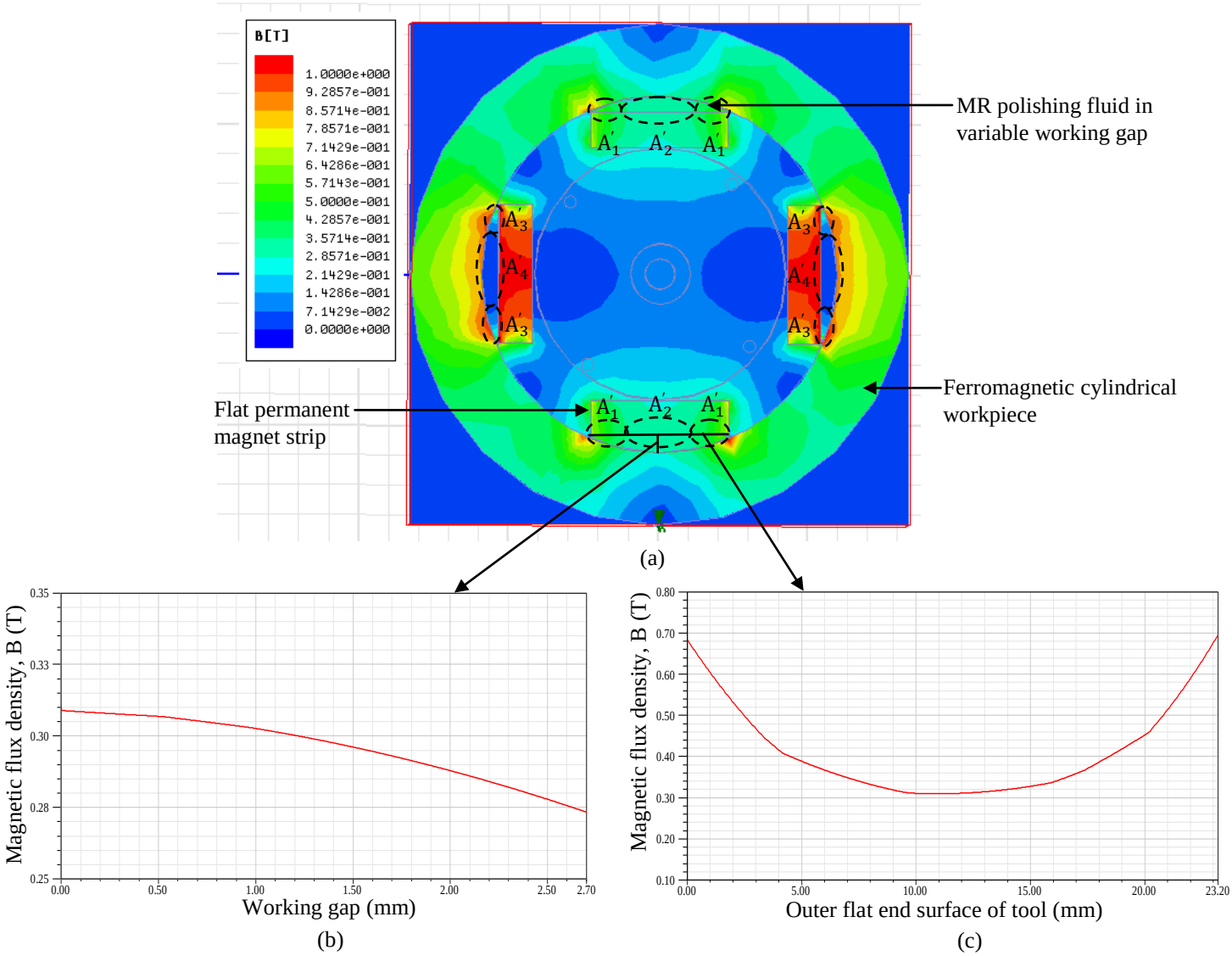

Fig. 3.3 Results obtained from the finite element analysis showing (a) magnetic flux density distribution through cross-section of MR honing setup having flat permanent magnet strips, (b) 2D plot of variation in magnitude of magnetic flux density in the MR polishing fluid region (working gap) from tool magnetic end surface to the inner surface of ferromagnetic cylindrical workpiece and (c) 2D plot of variation in magnitude of magnetic flux density over the flat end surface of the permanent magnet strip in the MR polishing fluid region.

Design of the MR honing tool with four flat rectangular permanent magnets has been finalized after the magnetostatic finite element (FE) analysis for the distribution of magnetic flux density. Before finalized design of the MR honing tool with the four flat rectangular permanent magnets, distribution of magnetic flux density in the MR honing tool with the two and three flat rectangular permanent magnet strips is also studied using magnetostatic finite element analysis. MR honing tool with two flat permanent magnet strips has the least interference of magnetic

field but has less finishing surface due to two flat permanent magnet strips. The MR honing tool with three flat permanent magnet strips has a more non-uniform distribution of magnetic flux density over the all three flat surface of the permanent magnet strips due to the interference of magnetic field and also has comparative less finishing surface area. Hence after various trials, the MR honing tool with four flat rectangular permanent magnet strips has been finalized for the present research work.

3.1.2 Design and fabrication of the magnetorheological honing tool structure and the associated components for finishing inner surface of cylindrical workpieces with different diameters

After performing finite element (FE) analysis of the novel design of magnetorheological (MR) honing tool for obtaining maximum magnetic flux density on the tool's end surface, the development and fabrication of feasible finishing tool structure have been performed. The three dimensional (3D) CAD model of the MR honing tool structure for finishing the inner surface of the cylindrical workpieces of different diameters is shown in Fig. 3.4 (a). The MR honing tool consists of four slots symmetrically patterned at 90^0 from each other about the central axis of the finishing tool. These four slots are used for inserting the magnetic strip holders as shown in Fig. 3.4 (a). The four magnetic strip holders as shown in Fig. 3.4 (b) are used to grip the flat permanent magnet strips. The magnetic strip holders have a unique taper shape at their back end as shown in Fig. 3.4 (b). The central part of MR honing tool has threads over it as shown in Fig. 3.4 (a). Two nuts with internal threads travel over the threaded central part of MR honing tool. A unique rotating grip is present on the upper part of the MR honing tool as shown in Fig. 3.4 (a). With the clockwise and anti-clockwise rotational movement of the rotating grip, the nuts come closer and move apart from each other, respectively. The four magnetic strip holders inserted into the slots of MR honing tool and are in contact with the nuts. With the axial movement of the nuts by the movement of a rotating grip, the magnetic strip holders move radially inwards or outwards simultaneously about the axis of the MR honing tool as shown in Fig. 3.4 (c) due to the taper shape present at the back of magnetic strip holder as shown in Fig. 3.4 (b). The positioning of the flat permanent magnets of the MR honing tool is adjusted with the movement of a rotating grip as per the requirement of the inner diameter of the cylindrical workpiece to be finished and is locked at a required particular position with the help of circlips.

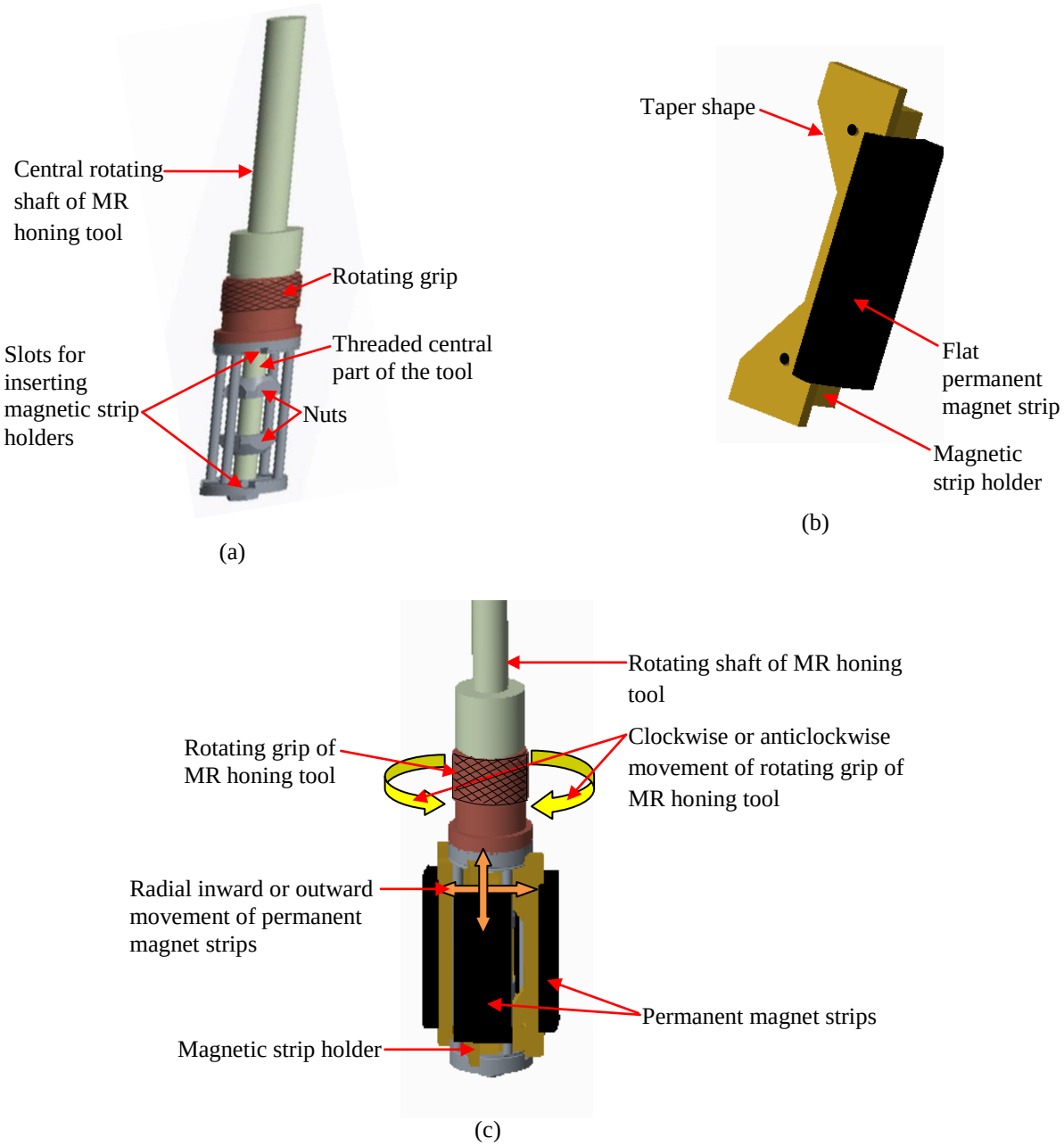

Fig. 3.4 Three dimensional computer-aided design model of (a) magnetorheological honing tool structure with the central rotating shaft, (b) magnetic strip holder for gripping the flat permanent magnet strip and (c) complete magnetorheological honing tool along with rotating shaft showing the movement of permanent magnet strips with the rotation of rotating grip in MR honing tool.

Further, after locking the radial movement for a particular internal diameter of the cylindrical component keeping the gap for MR polishing fluid, the finishing tool with retained MR polishing fluid performs finishing by its simultaneous rotational and reciprocation movement on the internal surface of the cylindrical component. The entire setup of developed MR honing process

is made to work on honeycomb breadboard. For precisely performing the experimentations in MR honing process, the entire work needs to be performed on breadboard. The three-dimensional (3D) computer-aided design (CAD) model of the complete MR honing setup is shown in Fig. 3.5. The cylindrical workpiece is required to be held rigidly while the experimentations for obtaining the precise results. So, the cylindrical workpiece is held tightly by clamping it to the breadboard with the help of fixture and grinding precision vice as shown in Fig. 3.5. Also, the MR honing tool requires precise movement in the cylindrical workpiece keeping the constant working gap.

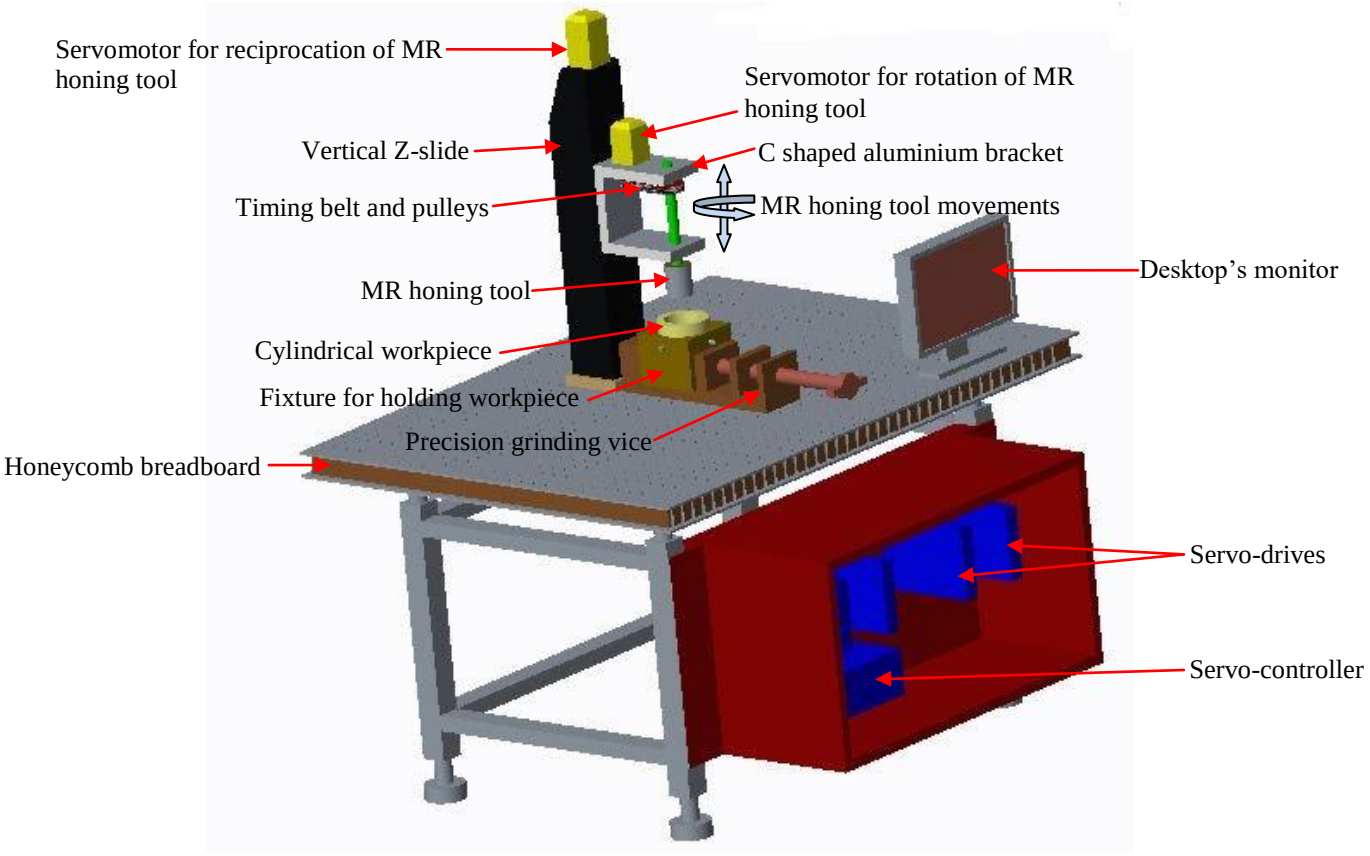

Fig. 3.5 Three-dimensional computer-aided design model of the complete magnetorheological honing setup.

Therefore, the MR honing tool is fastened with the vertical Z slide which is further clamped to the breadboard as shown in Fig. 3.5. The movements (rotating as well as reciprocating) to the MR honing tool are provided by clamping it to the vertical Z-slide with the help of C-shaped aluminium bracket as shown in Fig. 3.5. The finishing tool rotates as well as reciprocates inside the cylindrical workpiece with the help of two servomotors as shown in Fig. 3.5. These rotatory

and reciprocatory motions of MR honing tool are controlled by the servo-controller through programmable logic controllers (PLC). To hold the developed MR honing tool during its rotation and reciprocating movements, some important supporting parts have been designed and fabricated which are discussed below.

3.1.2.1 C- shaped aluminium bracket

In order to hold the magnetorheological honing tool during its rotation and reciprocating movements, a C-shaped bracket made up of aluminium is designed and fabricated whose three dimensional (3D) computer-aided design (CAD) model is shown in Fig. 3.6 (a). The material for the C-shaped bracket is selected as aluminium so that it remains light weighted and to prevent magnetic flux losses from the magnetic MR honing tool as aluminium is non-ferromagnetic in nature.

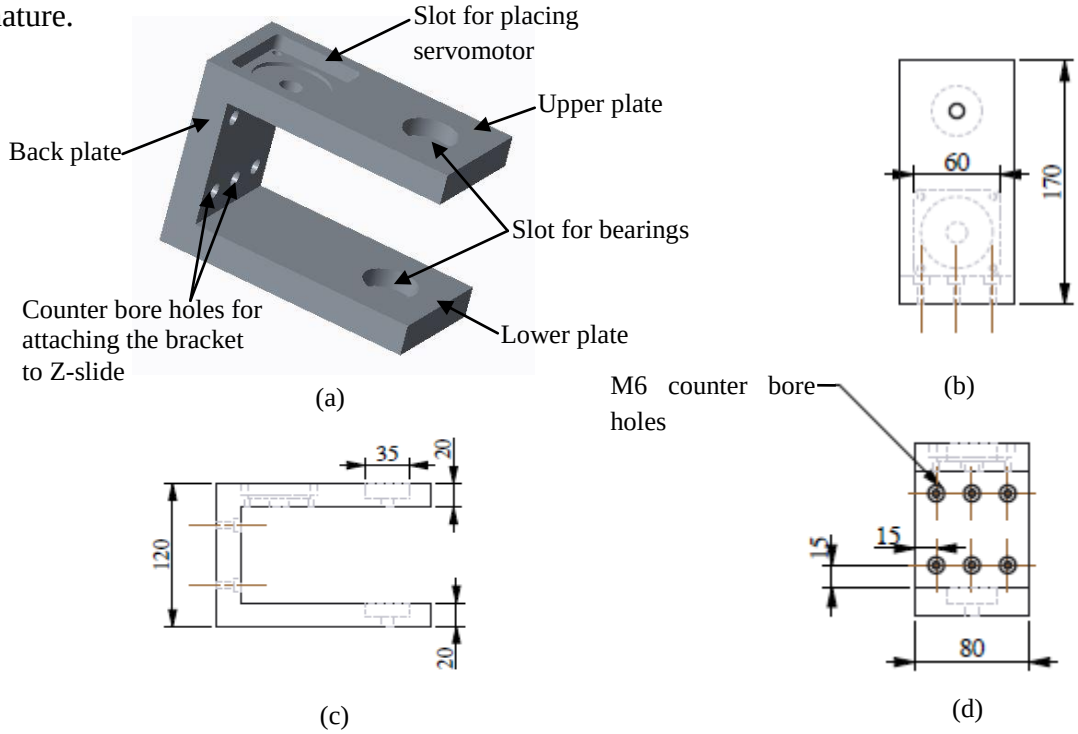

Fig. 3.6 (a) Three-dimensional computer-aided design model, (b) top view, (c) side view and (d) front view drawing of the C-shaped bracket used for holding the magnetorheological honing tool as well as a servomotor.

Counter-bore holes for M6 screws have been made at the back plate of the C-shaped bracket to hold the bracket over the base plate of the vertical Z-slide. The distance between the counter-bore holes has been kept according to the threaded holes available over the base plate of Z-slide. A slot for placing and holding the servomotor (used for rotating the MR honing tool) is made on the upper plate of the C-shaped bracket as shown in Fig. 3.6 (a). Two slots (as one in the upper

plate and another in the lower plate of the C-shaped bracket) have been made for placement of the bearings through which rotating shaft of the MR honing tool is rotated as shown in Fig. 3.6 (a). The top view, side view and front view drawings of the C-shaped bracket are shown in Figs. 3.6 (b), (c) and (d) respectively. The C-shaped aluminium bracket along with the MR honing tool and a servomotor together reciprocates up and down with the help of vertical Z-slide.

3.1.2.2 Timing pulleys and belt

Rotational motion is transmitted from the servomotor to the MR honing tool with the help of the timing belt and pulleys. Two timing pulleys have been fabricated as shown in Figs. 3.7 (a) and (b). Out of these two pulleys as shown in Fig. 3.7 (a) and (b), one is used as driving pulley which is attached to the shaft of the servo-motor having 24 number of teeth and another is used as the driven pulley which is attached to the rotating shaft of the magnetorheological honing tool having 48 number of teeth, respectively.

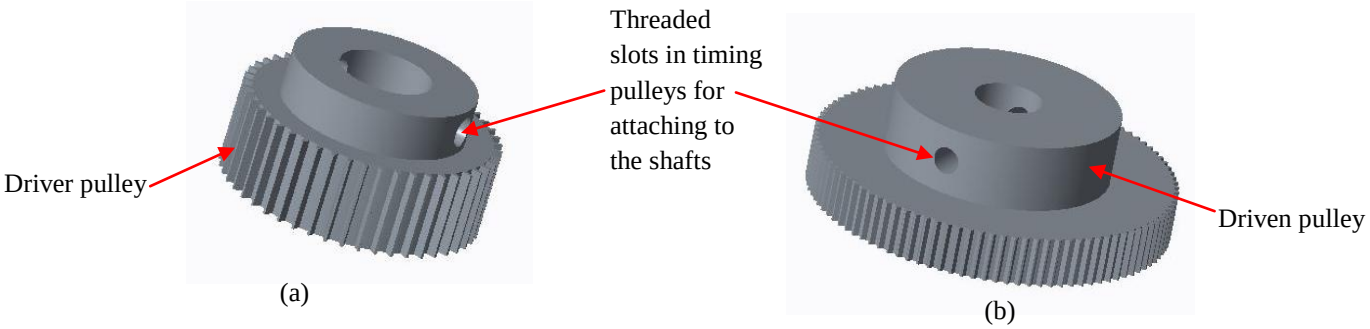

Fig. 3.7 Three-dimensional computer-aided design (CAD) model of (a) driver timing pulley and (b) driven timing pulley used for rotating the magnetorheological honing tool.

Following are the main benefits that can be obtained by selecting the timing pulleys and belt for transmission as stated below:

- No slippage
- High mechanical efficiency
- Minimum vibrations
- High drive ratio at a shorter distance

Both the pulleys are made up with aluminum to keep them light weighted and non-magnetic to avoid the magnetic flux losses from the present magnetic honing tool. A servomotor made of PARKER is used for the rotation of MR honing tool whose specifications are given in Table 3.2.

Table 3.2 Specification of servomotor used for rotating the MR honing tool.

Performance characteristics	Range
Maximum RPM	3000
Maximum torque	9.5 N-m
Weight	1.4 Kg

The maximum speed of the servomotor used is 3000 RPM. As per the literature, the rotational speed of the honing tool may not be more than 1500 RPM. So, to keep the maximum speed limit of MR honing tool as 1500 RPM, teeth ratio for the driver pulley to the driven pulley is kept as 1:2. Length of timing belt used for power transmission is calculated by using the Eq. (3.1).

$$L = \frac{\pi}{2}(D_1 + D_2) + 2C + \frac{(D_1 - D_2)^2}{4C} \quad (3.1)$$

where D_1 = Pitch circle diameter of the driver pulley equal to 39 mm.

D_2= Pitch circle diameter of the driven pulley equal to 78 mm.

C = Centre distance between two pulleys equal to 86 mm.

Centre distance between the two pulleys is kept on the basis of commercial availability of the size of the timing belt which is of the size 142XL (~360.68 mm) as used in the present work. Threaded slots are made over each of the pulleys to attach them to the shafts i.e. motor's shaft and the rotating shaft of the MR honing tool.

3.1.2.3 A rotating shaft of the magnetorheological honing tool

A circular rotating shaft for the rotation of the magnetorheological honing tool has been designed and fabricated whose 3D computer-aided design (CAD) model is shown in Fig. 3.8 (a). The material for the rotating shaft has been selected as stainless steel to have benefits like good strength and being non-ferromagnetic in nature (to avoid magnetic flux losses). The drawing of the circular rotating shaft in mm for the magnetorheological honing tool is shown in Fig. 3.8 (b). The length of the upper half of the rotating shaft has been designed according to the C-shaped aluminium bracket and the length of the lower half according to the MR honing tool. The diameter of the upper half of the rotating shaft which is held in C-shaped bracket has been evaluated on the basis of maximum torque applied by the servomotor.

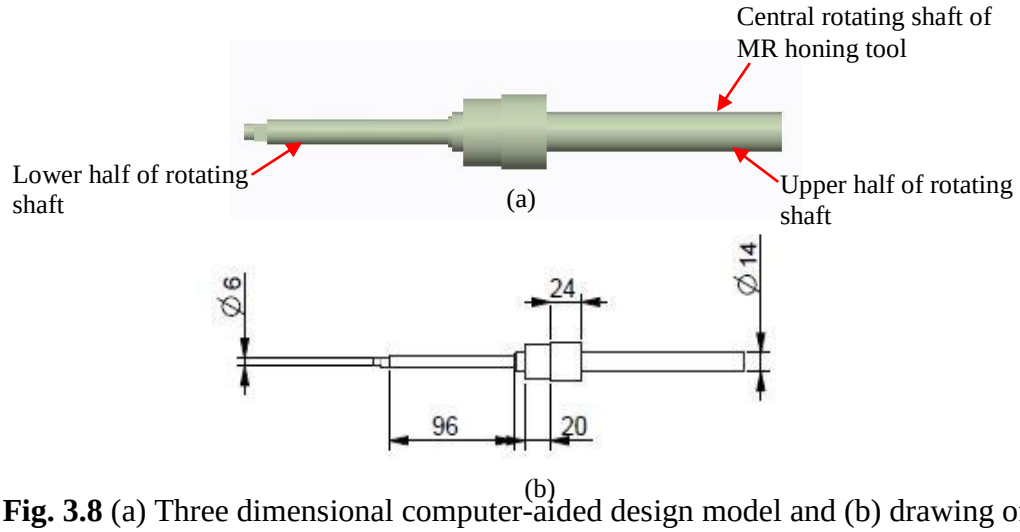

Fig. 3.8 (a) Three dimensional computer-aided design model and (b) drawing of the central rotating shaft of the magnetorheological honing tool.

The servomotor rotates the central shaft of MR honing tool with the help of a driven timing pulley which is positioned at a distance of 35 mm from the centre line of the upper plate of C-shaped aluminium bracket. The space diagram of upper half of rotating shaft of MR honing tool attached in the C-shaped aluminium bracket is shown in Fig. 3.9.

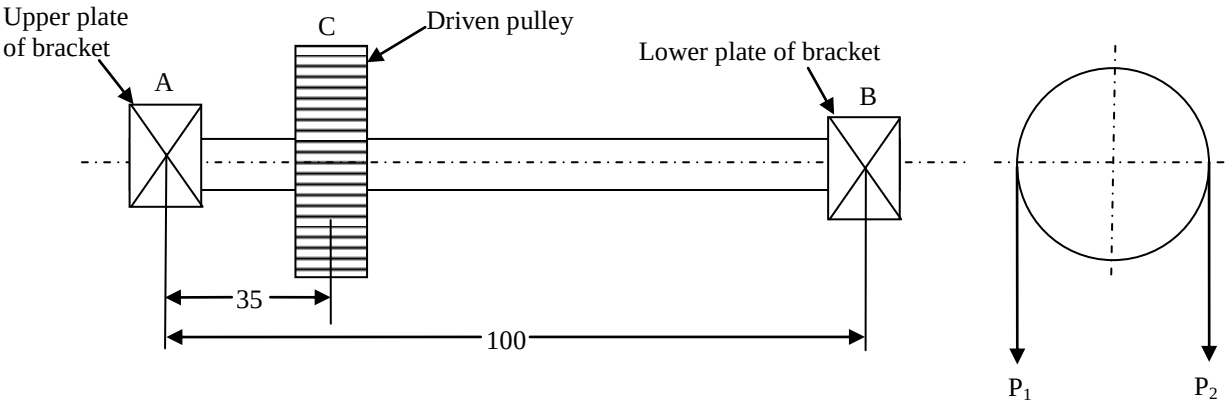

Fig. 3.9 Space diagram of the rotating shaft of the magnetorheological honing tool.

Maximum torque ($\mathcal{T}_{motor}$) in N-m acting by the servomotor can be written as in Eq. (3.2).

$$\mathcal{T}_{motor} = (P_1 - P_2) \times R \tag{3.2}$$

where P_1 is the tension in the tight side of the timing belt and P_2 is the tension in the slack side of the timing belt. R is the radius of the driven pulley which is equal to 39 mm in the present case. Putting the value of maximum torque ($\mathcal{T}_{motor}$) applied by the servomotor as specified in Table 3.2 and radius of the driven pulley in Eq. (3.2), the further relation is given in Eq. 3.3.

$$(P_1 - P_2) = 243.58 \tag{3.3}$$

The schematic diagram of timing belt and pulleys is shown in Fig. 3.10.

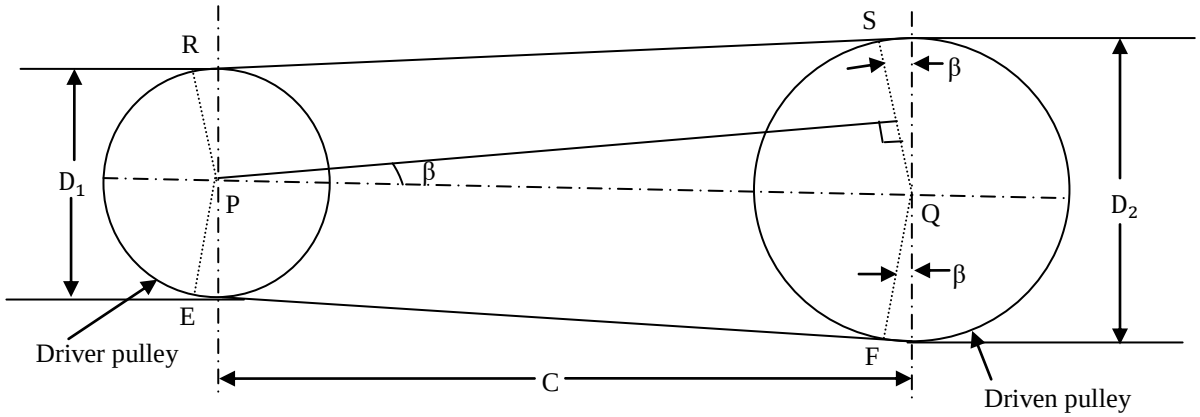

Fig. 3.10 Schematic diagram of timing belt and pulleys.

Another relation in P_1 and P_2 can also be written as Eq. 3.4.

$$\frac{P_1}{P_2} = e^{\mu\theta} \tag{3.4}$$

where μ is coefficient of friction of the leather belt which is equal to 0.3 and θ is the angle of wrap of timing belt with a driven pulley and is calculated by Eq. (3.5).

$$\theta = (180+2\beta)^0 \tag{3.5}$$

where β is the angle subtended by each common tangent (RS or EF) with PQ, the line of centers of two pulleys as shown in Fig. 3.10 and can be calculated by using Eq. (3.6).

$$\beta = sin^{-1}(\frac{R-r}{C}) \tag{3.6}$$

Here R is the radius of driven pulley, r is the radius of driving pulley and C is the centre distance between two pulleys. Putting all the values in Eq. (3.6), the value of β is obtained as follows:

$$\beta = sin^{-1}(\frac{39-19.5}{86}) \tag{3.7}$$

$$\beta = 13.10^0 \tag{3.8}$$

Putting the value of β in Eq. (3.5), the value of θ is obtained as follows:

$$\theta = 206.2^0 \tag{3.9}$$

$$= 3.59 \text{ radians} \tag{3.10}$$

Putting the value of μ and θ in Eq. (3.4), the relationship between P_1 and P_2 is obtained as follows:

$$\frac{P_1}{P_2} = e^{0.3\times3.59} \tag{3.11}$$

$$P_1 = 2.941\times P_2 \tag{3.12}$$

Solving Eq. (3.3) and Eq. (3.12), the value of P_1 and P_2 are obtained as follows:

$$P_1 = 369.07 \text{ N} \tag{3.13}$$

and $$P_2 = 125.49 \text{ N} \tag{3.14}$$

As these forces i.e. P_1 and P_2 are acting on the rotating shaft of MR honing tool, so the load diagram of the rotating shaft in the C-shaped aluminium bracket is shown in Fig. 3.11.

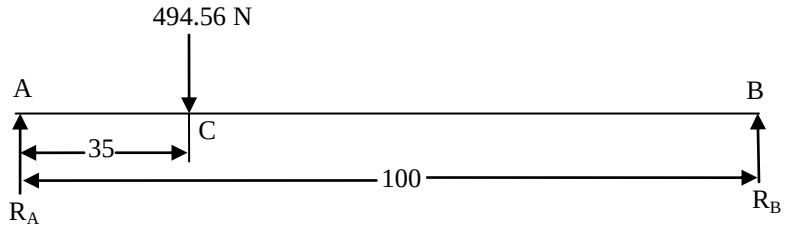

Fig. 3.11 Load diagram of rotating shaft of the magnetorheological honing tool.

Here R_A and R_B are the reaction forces to the rotating shaft of the MR honing tool by the respective upper and the lower plate of C-shaped aluminium bracket as shown in Fig. 3.11. Taking moment about point A as evaluated in Eq. 3.15

$$R_B \times 100 = 494.56 \times 35 \quad (3.15)$$

Also, from the load diagram as shown in Fig. 3.11

$$R_A + R_B = 494.56\ N \quad (3.16)$$

Solving the Eqs. (3.15) and (3.16), the values of reaction forces are obtained as R_A= 321.46 N and R_B = 173.09 N. The bending moment diagram for the rotating shaft of the MR honing tool is shown in Fig. 3.12.

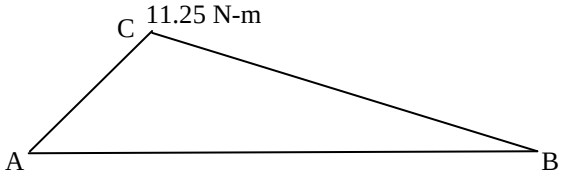

Fig. 3.12 Bending moment diagram for the rotating shaft of the magnetorheological honing tool.

Therefore, bending moment at point C, (M_b) = 11.25 N-m and twisting moment at point C, (M_t) = 9.50 N-m. As per the ASME code, the maximum shear stress (τ_{max}), a shaft can withstand is the lower of ($0.3\times S_{yt}$) or ($0.18\times S_{ut}$). Here S_{yt} is the ultimate tensile strength for shaft and is equal to 505 MPa for stainless steel and S_{ut} is the ultimate yield strength of shaft and is equal to 215 MPa for stainless steel in present case. Hence, considering the lower value of calculated shear stress for rotating shaft of MR honing tool as per the ASME code by considering the mechanical properties of stainless steel, τ_{max} is calculated as 38.7 N/mm^2. The maximum shear stress (τ_{max}) that rotating shaft of MR honing tool can withstand can be written as in Eq. 3.17.

$$\tau_{max} = \frac{16\sqrt{(M_b)^2+(M_t)^2}}{\pi d^3} \quad (3.17)$$

where d represents the diameter of the rotating shaft of the MR honing tool in C-shaped aluminium bracket. As per the ASME code, when the shaft is keyed, and then the value of maximum shear stress (τ_{max}) is further decreased by 25 %. Putting all the values in Eq. (3.17). Diameter (d) of the rotating shaft of the MR honing tool in C-shaped aluminium bracket is calculated as 13.72 mm. So, as per the standards, the diameter (d) of the rotating shaft of MR honing tool in C-shaped aluminium bracket is kept as 14 mm. By making use of these fabricated parts, MR honing tool is rotated as well as reciprocated inside the cylindrical workpiece.

After analyzing the design of MR honing tool with the four flat permanent magnet strips in Maxwell Ansoft V13 software for obtaining better magnitude and distribution of maximum magnetic flux density on the tool's end surface and also with designed supporting parts for its rotating and reciprocating movement, the proposed MR honing tool with flat end magnetic surface is fabricated. Photograph of fabricated MR honing tool with four flat permanent magnet strips is shown in Fig. 3.13 (a). Photograph of fabricated MR honing tool with retained MR polishing fluid over four flat permanent magnet strips is shown in Fig. 3.13 (b). From Fig. 3.13 (b), it can be observed that strongly bonded chains of carbonyl iron particles (CIPs) are formed over the edges area of the flat permanent magnet strips while weak bonded chains of CIPs are formed at the middle part of the permanent magnet strip with ferromagnetic cylindrical workpiece. Due to the presence of strong magnetic flux density over the edges area of the flat permanent magnet strips, CIPs present in this area gets strongly magnetized. Due to the magnetization of these CIPs, they also start inducing magnetic field in the edges area of flat permanent magnet strips. Because of the higher magnitude of magnetic flux density present over the edges area of flat permanent magnet strips, strong bonded chains of CIPs get formed in this area. While the CIPs present over the middle part of the tool's flat end magnetic surface get less magnetized due to the presence of weak magnet flux density in this area. This in turn results in less strong bonded CIPs chains in the area present over the middle part of the tool's flat end magnetic surface.

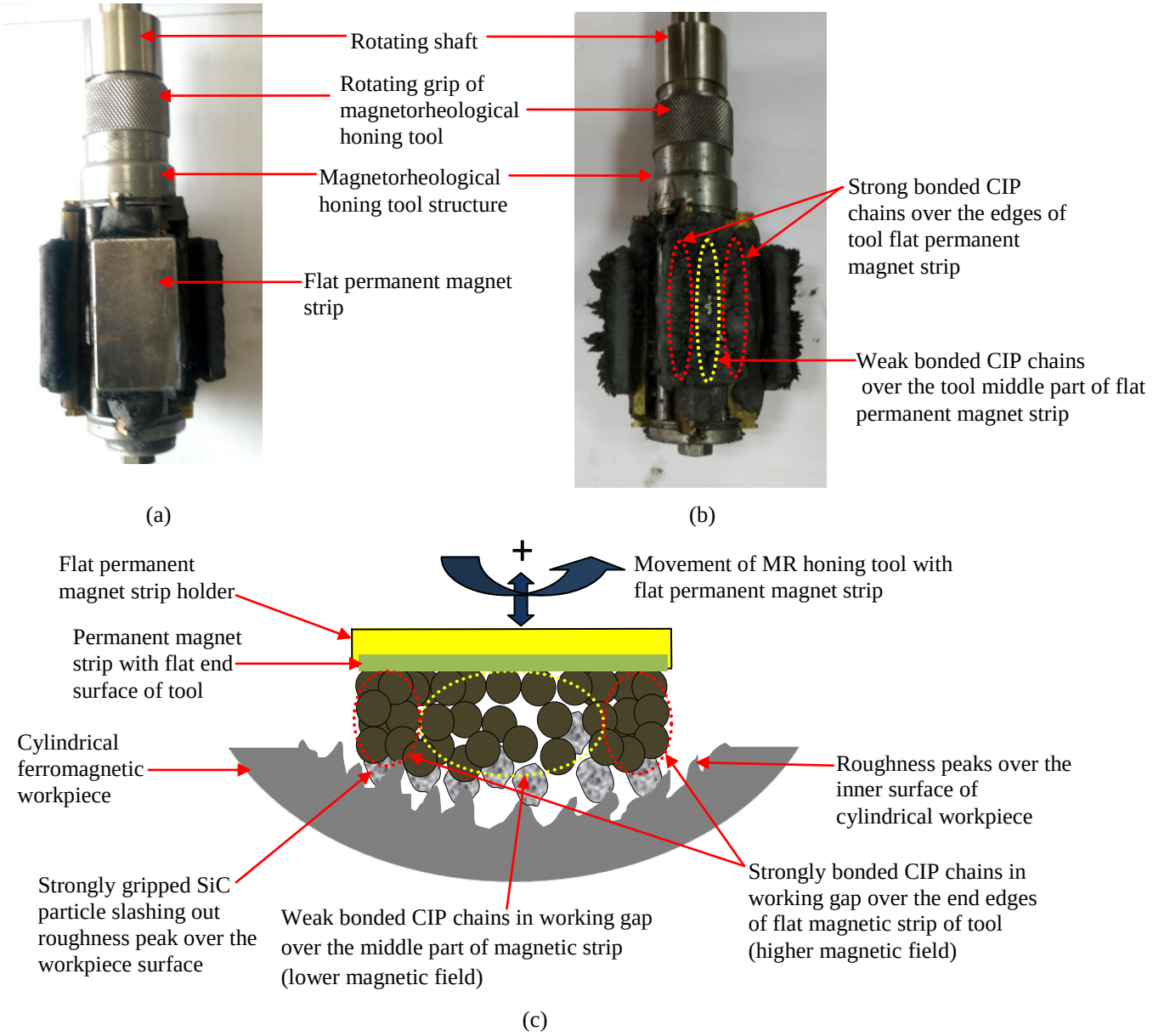

Fig. 3.13 (a) Photograph of fabricated initial design of MR honing tool with four flat permanent magnet strips, (b) photograph of fabricated initial design of MR honing tool with retained MR polishing fluid over the four flat permanent magnet strips and (c) mechanism of material removal with a magnetorheological honing tool having flat permanent magnet strip with ferromagnetic cylindrical workpiece.

While experimentation with MR honing tool having flat end magnetic surface, the strength of formed CIPs chains with abrasives go on decreasing as moving from the end edges area to the middle part over the tool's flat end magnetic surface as shown in Fig. 3.13 (c). The strength of

the formed CIPs chains over the middle part of the tool's flat end magnetic surface may be weak due to the low magnetic field in that region. These chains may not get sustain properly with the movement of the MR honing tool inside the cylindrical workpiece. The strongly bonded chains (due to the high magnetic field) formed in the region over the tool's flat end edges area (as shown in Fig. 3.13c) contribute more to the finishing of the inner surface of the cylindrical workpiece as compared to the weak chains formed at the middle part of the tool end surface. With the rotation and reciprocation movement of MR honing tool having flat end magnetic surface inside the cylindrical workpiece, the cylindrical internal surface gets finished mainly with the end magnetic surface area of tool where strongly bonded chains of CIPs are formed. However, the non-uniformity in the distribution of magnetic flux density over the flat magnetic end surface of this initially designed tool may slow down the finishing performance.

3.1.3 Limitations of the initial designed magnetorheological honing tool with the flat end magnetic surface

After analyzing the performance of initially designed MR honing tool with the flat end magnetic surface, the following limitations were observed.

- Non-uniform distribution of magnetic flux density over the end flat surface of the MR honing tool due to the variable working gap between the tool's flat end surface and the inner surface of the ferromagnetic cylindrical workpiece may slow down the finishing performance of the MR honing process. Weak carbonyl iron particles (CIPs) chains present over the middle part of the tool's flat end magnetic surface may get break down during the tool's movement inside the cylindrical workpiece which may reduce the process performance.
- Increasing the outer end surface width of the flat permanent magnet strips result in touching its flat edges with the inner surface of the cylindrical workpiece. So, the width of the flat end surface of the tool's magnetic strips cannot be extended after a certain limit. This further result in constraint in tool's finishing surface.
- Also, in the initially designed MR honing tool with flat end permanent magnets, the working gap for MR polishing fluid cannot be reduced after a certain limit. On further reducing the working gap, edges of flat permanent magnet strip get collide with the inner cylindrical surface of the workpiece.

The above mentioned few limitations in the initially designed MR honing tool with flat permanent magnet strips may hinder the process capability. These limitations directed that the initial design of the MR honing tool needs to be improved to overcome the above-stated limitations so that the finishing process capability can be better improved.

3.2 Improved design of MR honing tool with the curved end magnetic surface

After analyzing the limitations of the initial design of MR honing tool with flat permanent magnets, further modifications have been performed to enhance its finishing performance. The performance of MR fluid based finishing processes mainly depends on the distribution of magnetic flux density at the tool's outer end magnetic surface. The difference in the geometry of finishing tool's tip end surface in MR fluid based finishing process can create the difference in finishing performance of the entire process (Singh *et* al., 2017). In the context of this, the initial design of the MR honing tool with the flat end magnetic surface has been improved with the curved end magnetic surface. This improved design may result in uniform distribution of magnetic flux density over the magnetic end surface of the MR honing tool which can enhance the finishing performance. Before fabricating the improved design of MR honing tool with its curved end magnetic surface, a magnetostatic finite element analysis has been performed in Maxwell Ansoft V13 software for analyzing the distribution of magnetic flux density in the improved design of MR honing tool with the curved end magnetic surface.

3.2.1 Finite element analysis of the improved design of MR honing tool with the curved end magnetic surface

To study the distribution of magnetic flux density in the improved MR honing tool with curved permanent magnet strips, the magnetostatic finite element (FE) analysis is performed in Maxwell Ansoft V13 software. Magnetorheological honing tool constituting of four curved permanent magnet strips on its outer periphery is modeled and magnetostatically simulated in Maxwell Ansoft V13 software. Magnetic model of the magnetorheological honing tool having curved end magnetic surface along with the MR polishing fluid and the ferromagnetic cylindrical workpiece is shown in Fig. 3.14. The four curved magnetic strips are symmetrically patterned at an angle of 90º from each other about the central axis of the finishing tool. For magnetostatic FE analysis, materials assigned to the various parts of the improved MR honing tool are reported as in Table 3.1. MR polishing fluid with a uniform thickness of 2.7 mm is modeled in between the curved

end surface of permanent magnet strips and the inner surface of the ferromagnetic cylindrical workpiece as shown in Fig. 3.14. The end surface arc length and height of the curved permanent magnet strips are modeled as 23.2 mm and 60 mm respectively.

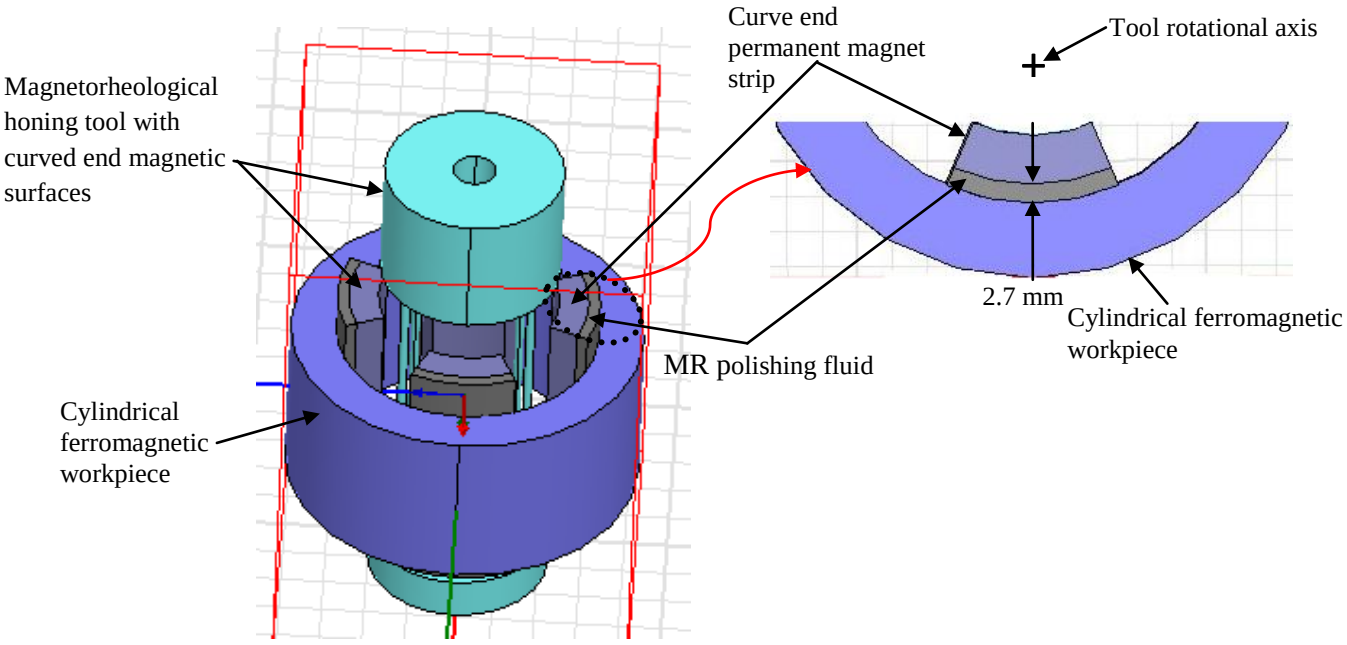

Fig. 3.14 Magnetic model of the magnetorheological honing tool with the curved end magnetic surface along with the MR polishing fluid and the ferromagnetic cylindrical workpiece.

The modeled MR honing setup along with the finishing tool is magnetostatically simulated with 10 numbers of passes in Maxwell Ansoft software and distribution of magnetic flux density in MR honing setup is observed as shown in Fig. 3.15. With magnetostatic finite element (FE) analysis, the result of the distribution of magnetic flux density through MR honing setup for improved MR honing tool with its curved magnetic end surface is shown in Fig. 3.15 (a). This shows the magnetic flux density distribution across the cross-section of MR honing setup having curved permanent magnet strips. From FE analysis, the 2D plot of variation in the magnitude of magnetic flux density in the MR polishing fluid region (working gap) from the tool magnetic end surface to the inner surface of the ferromagnetic cylindrical workpiece is evaluated as shown in Fig. 3.15 (b). From Fig. 3.15 (b), it can be observed that the higher magnitude of magnetic flux density is obtained on the tool outer curved end surface of permanent magnet strip as compared to the inner surface of the ferromagnetic cylindrical workpiece. It ensured that the MR polishing fluid is stuck on the tool's outer curved end surface of the MR honing tool while performed finishing on the inner surface of ferromagnetic workpieces. From FE analysis, the 2D plot of

variation in the magnitude of magnetic flux density over the curved end surface of permanent magnet strip in the presence of MR polishing fluid region is evaluated as shown in Fig. 3.15 (c). From Fig. 3.15 (c), it can be observed that there is the almost uniform distribution of magnetic flux density is obtained over the tool outer curved end surface of the permanent magnet strip.

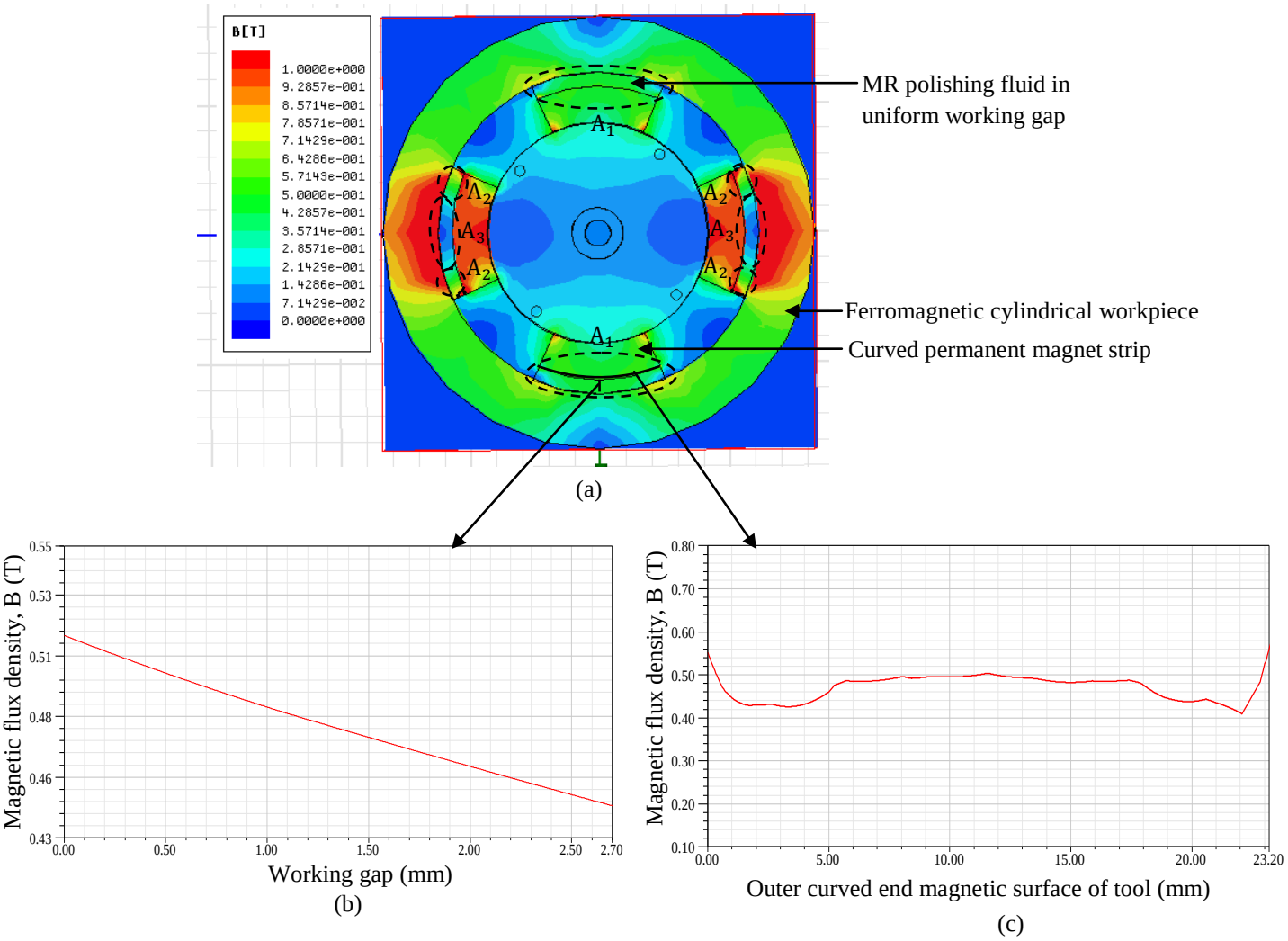

Fig. 3.15 Results obtained from the finite element analysis showing (a) magnetic flux density distribution across cross-section of MR honing setup having curved permanent magnet strips, (b) 2D plot of variation in magnitude of magnetic flux density in the MR polishing fluid region (working gap) from magnetic surface to the inner surface of the ferromagnetic cylindrical workpiece and (c) 2D plot of variation in magnitude of magnetic flux density over the curved end surface of a permanent magnet strip in presence of MR polishing fluid in working gap.

This is due to the uniform gap of 2.7 mm between the tool's outer curved end magnetic surface and the inner surface of the ferromagnetic cylindrical workpiece. Curved permanent magnetic strips induce magnetic field due to which cylindrical ferromagnetic workpiece get magnetized

and start inducing a magnetic field. As there is a uniform gap between the magnetic tool's surface and workpiece's surface, so this results in uniform magnetic flux density distribution over the outer curve end magnetic surface of MR honing tool. Due to uniformity in distribution of magnetic flux density over the tool's outer curved end surface of magnet strip, the uniformly strong bonded chains of carbonyl iron particles (CIPs) with silicon carbide (SiC) abrasive particles are formed in the working gap. Uniformly bonded CIPs chains may result in the better finishing of the inner surface of cylindrical workpieces. From the Fig. 3.15 (a), it can be observed that there is uniform distribution of magnetic flux density over the curved outer surface of the two permanent magnet strips as shown by the dotted line (A_1) in Fig. 3.15 (a). On the other hand, the magnitude of magnetic flux density decreased from the outer edges (A_2) to the middle over the curved surface (A_3) of the rest two magnetic strips as shown in Fig. 3.15 (a). This variation in magnetic flux density over the curved surface of the two magnetic strips is occurred due to the interference of magnetic field in the working gap when the tool's four curved magnet strips are placed inside the ferromagnetic cylindrical workpiece. From the Fig. 3.15 (a), it can be observed that over the outer curved surface of the two magnet strips having the interference of magnetic field lines, the higher magnetic flux density is present towards the start and end angle edges of the curved magnetic strips (A_2)and lower magnetic flux density towards the middle of the magnetic strips (A_3). On comparing Fig. 3.3 (a) and 3.15 (a), it can be observed that there is less effect of interference of magnetic field ($A_2 - A_3 - A_2$) in 3.15 (a) over the outer end magnetic surface in MR polishing fluid in case of MR honing tool with curved permanent magnetic surface as compared to the distribution of magnetic field ($A'_3 - A'_4 - A'_3$) in Fig. 3.3 (a) over the outer end flat magnetic surface in MR polishing fluid. There is lesser variation ($A_2 - A_3 - A_2$) in Fig. 3.15 (a) in the distribution of magnetic flux density over the tool curved end magnetic surface due to the interference of magnetic field as compared to the variation ($A'_3 - A'_4 - A'_3$) in Fig. 3.3 (a) over the flat end magnetic surface. This signifies the better finishing capability of MR honing tool with the curved magnetic surface as compared to the MR honing tool with the flat end magnetic surface.

3.2.2 Fabrication of improved design of MR honing tool with its curved end magnetic surface

After analyzing the distribution of magnetic flux density in MR honing tool with curved permanent magnet strips in Maxwell Ansoft software, the MR honing tool is fabricated as shown in Fig. 3.16 (a).

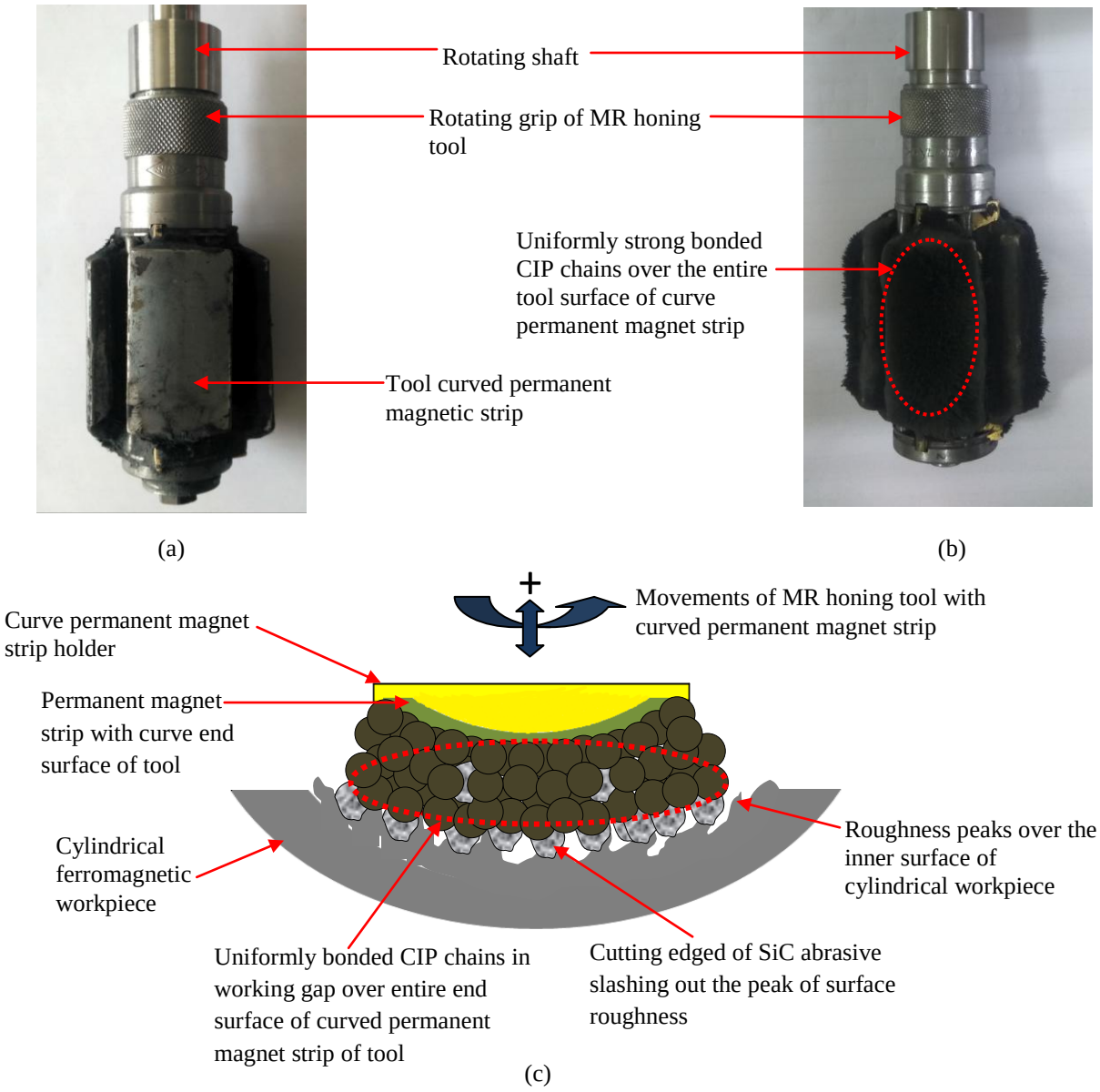

Fig. 3.16 (a) Photograph of fabricated improved MR honing tool with four curved permanent magnet strips, (b) photograph of fabricated improved MR honing tool with retained MR polishing fluid over four curved permanent magnet strips and (c) mechanism of material removal with a magnetorheological honing tool having four curved permanent magnet strips with ferromagnetic cylindrical workpiece.

The fabricated MR honing tool also has the ability to move its curved permanent magnet strips radially inwards or outwards about the central axis of the tool for finishing the inner surface of different diameters of cylindrical workpieces. The construction of MR honing tool structure with curved permanent end magnet strips is exactly same as that of MR honing tool with flat permanent magnet strips with the change of the magnetic strip holders. The fabricated MR honing tool with retained MR polishing fluid over the curved permanent magnet strips is shown in Fig. 3.16 (b). From Fig. 3.16 (c), it can be observed that uniformly strong bonded chains of carbonyl iron particles (CIPs) are formed over the entire magnetic curved end surface of MR honing tool with ferromagnetic cylindrical workpiece. The effects of the dissimilarity in the magnetic flux density distribution over the outer end surface of both the tools affect their mechanism of material removal as shown in Fig. 3.13 (c) and 3.16 (c). In case of MR honing tool having curved end magnetic surface, the equally strong bonded chains of CIPs are formed over the tool's outer end curved magnetic surface to grip the abrasives with uniform strength as shown in Fig. 3.16 (c). These equally strong bonded CIP chains give support to each other and have enough strength to sustain the movement (rotation and reciprocation) of MR honing tool inside the cylindrical workpiece. While finishing, the magnetic force acts on the carbonyl iron (CI) particles due to the induced magnetic field in the working gap which in turn exert a normal force on active silicon carbide (SiC) particles to indent them into the inner surface of the cylindrical workpiece. With the movement (rotation and reciprocation) of finishing tool inside the cylindrical workpiece, the indented sharp-edged SiC particles slash out the roughness peaks and result in surface finishing. The uniformly strong bonded chains of CIPs formed over the outer curved end magnetic surface grip more number of abrasives and with more bonding strength as compared to the chains formed over the flat end magnetic surface. This results in more efficiently slashing out the roughness peaks from the inner surface of the cylindrical workpiece. In this way, the improved design of the MR honing tool having curved end magnetic surface is found likely more suitable to finish the internal surface of the cylindrical workpiece as compared to the initial design of the MR honing tool having flat end magnetic surface. The photograph of the experimental setup of MR honing process with the improved design of tool with curved end magnetic surfaces for nano-finishing the inner surface of the cylindrical workpieces with different diameters is shown in Fig. 3.17.

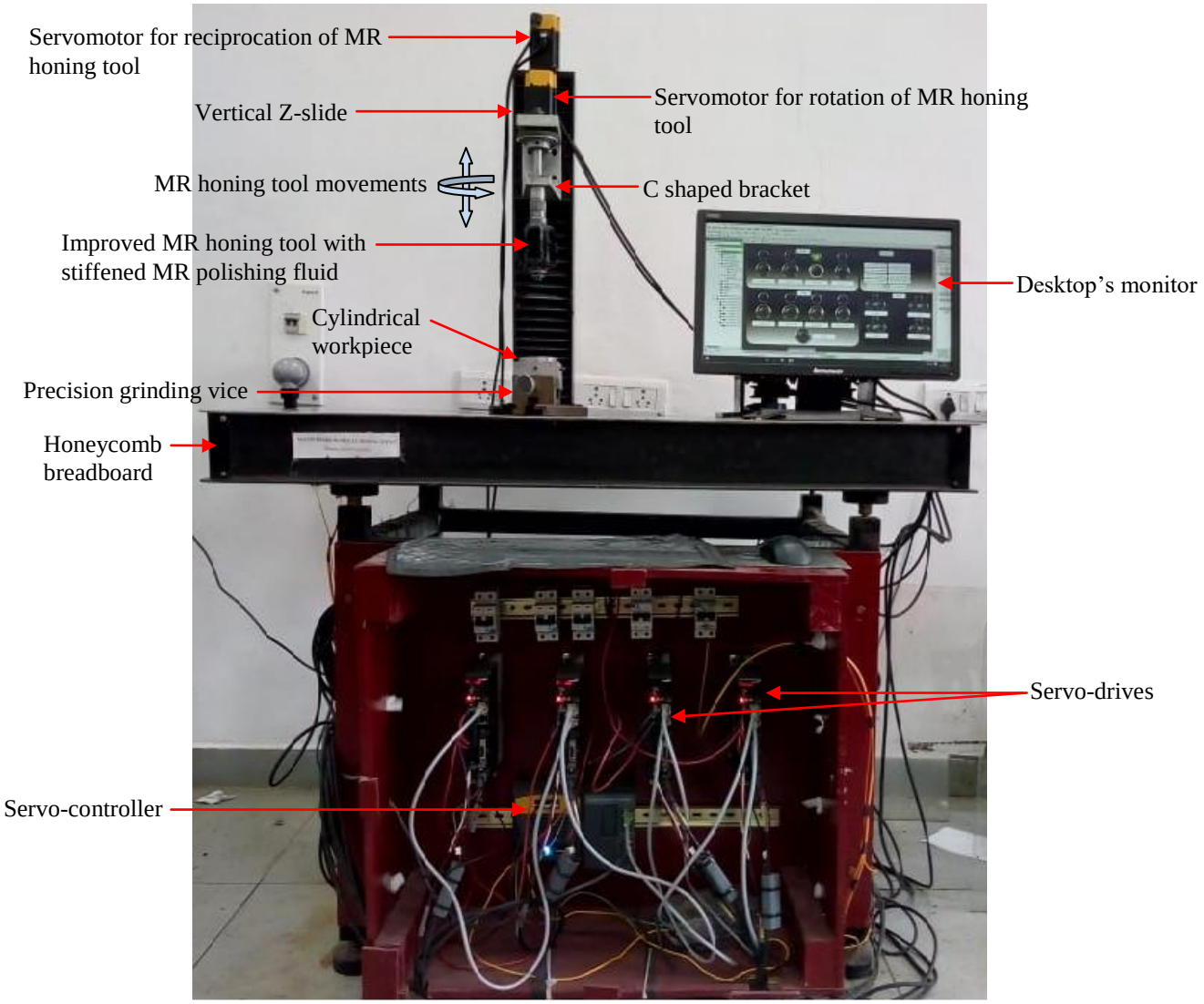

Fig. 3.17 Photograph of the experimental setup of MR honing process with the improved design of tool with curved end magnetic surfaces for nano-finishing the inner surface of the cylindrical workpieces with different diameters.

The fabricated MR honing tool having curved end magnetic surface is more useful in industries which require nano-finished internal cylindrical surface.

3.2.3 Advantages of the improved MR honing tool with the curved end magnetic surface over the MR honing tool with flat end magnetic surface

After developing both designed of the MR honing tools, the following advantages have been observed of the designed MR honing tool with the curved magnetic end surface as compared to the initial designed MR honing tool with flat magnetic end surface which can enhance the finishing process performance.

- Uniform distribution of magnetic flux density over the outer end curved surface of MR honing tool due to the uniform gap between tool's end surface and the inner surface of the ferromagnetic cylindrical workpiece help in forming uniformly bonded CIPs chains which enhance the finishing performance of the MR honing process as illustrated in Fig. 3.16 (c).
- Increasing the curved end magnetic surface of curved permanent magnet strip does not result in touching the edges of magnet strips with the inner surface of the cylindrical workpiece and even provide the uniform distribution of magnetic flux density over its surface.
- In case of MR honing tool with curve permanent magnets, the working gap for MR polishing fluid can be reduced to get less working gap which enhances the finishing performance of the MR honing process.
- The present improved design of MR honing tool with the curved end magnetic surface can finish the internal surface of cylindrical workpiece with internal diameter ranges from 50 mm to 70 mm. On the other hand, the initial design of MR honing tool with the flat end magnetic surface can finish the internal surface of cylindrical workpiece with internal diameter ranges from 55 mm to 70 mm due to its flat end magnetic surface. It signifies the better finishing capability of the improved design of MR honing tool in terms of wider ranges of the internal diameters of the cylindrical workpieces as compared to the initial designed MR honing tool.

Thus, the above-mentioned advantages of MR honing tool with the curved end permanent magnet strips proved its better capability to nano-finish the inner surface of cylindrical workpieces for the different internal diameters.

3.3 Mechanism of material removal in finishing with the developed MR honing process

The MR polishing fluid is applied over the outer tool magnetic surface of the developed MR honing tool and inserted into the cylindrical workpiece. Due to the higher magnitude of magnetic flux density present on the outer magnetic surface of the developed MR honing tool as shown in Fig. 3.3 (b) and 3.15 (b), the magnetic carbonyl iron (CI) particles stick over the tool's outer magnetic surface of the developed MR honing tool. The magnetic CI particles form chains in the working gap and grip the abrasives in between them as shown in Fig. 3.18 (a). The magnetic CI particles get attracted towards the tool's surface due to the magnetic field and push the abrasive particles with levitation force towards the inner surface of the cylindrical workpiece which indents them into the workpiece surface.

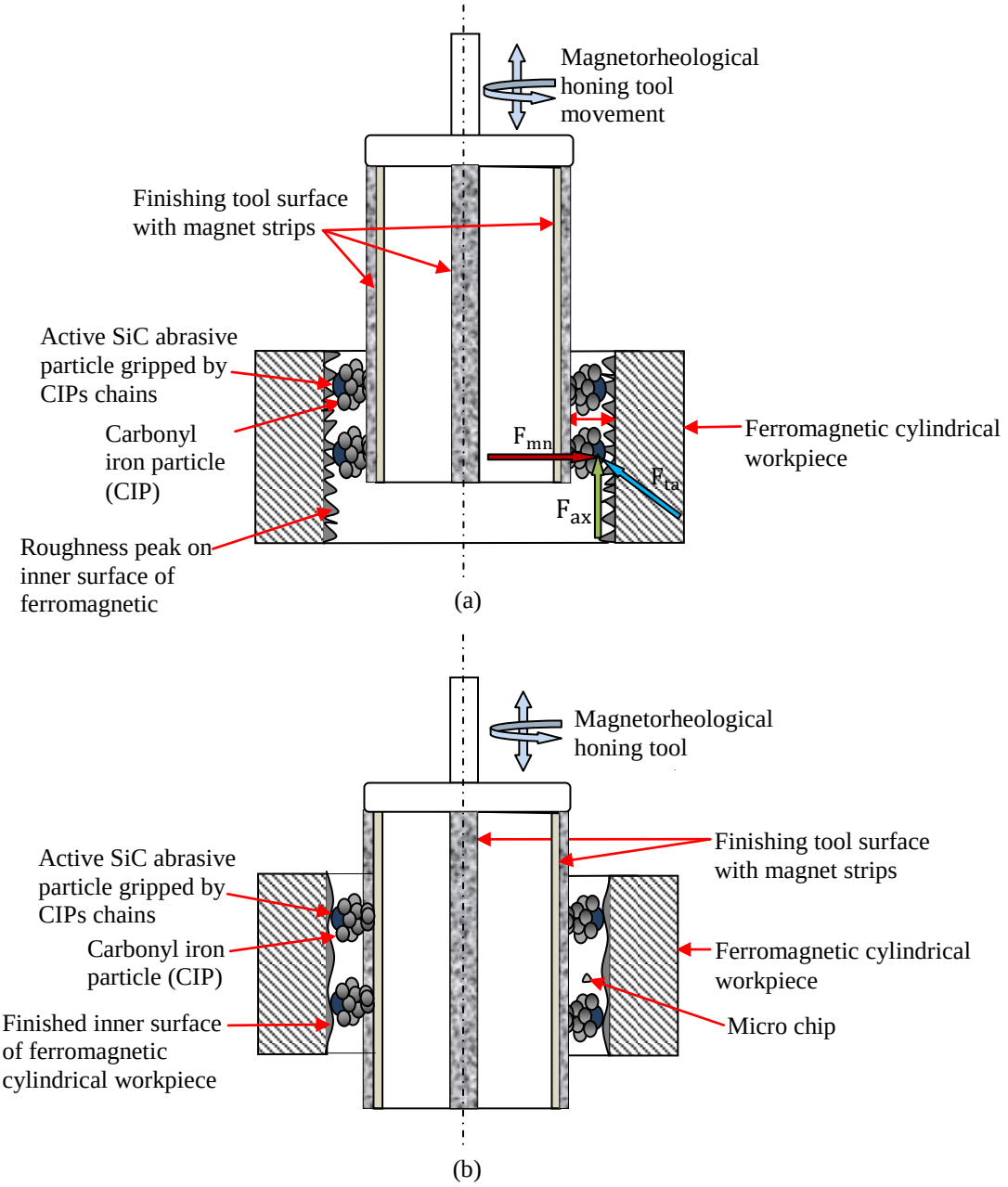

Fig. 3.18 Schematic of (a) active abrasives gripped by CIPs (carbonyl iron particles) chains removing roughness peaks of the internal surface of the ferromagnetic cylindrical workpiece and (b) updated roughness of cylindrical workpiece surface after removal of roughness peaks.

With the rotating and reciprocating movement of the MR honing tool, the gripped indent abrasive particles also move over the inner surface of the cylindrical workpiece. The sharp-edges of indented abrasive particles slash out the protrusions of the surface roughness from the cylindrical workpiece's inner surface as shown in Fig. 3.18 (a). With the repetitive movement of MR honing tool inside the cylindrical workpiece, the active abrasives erode out all the roughness peaks from the inner surface of the cylindrical workpiece and this result in surface finishing as

shown in Fig. 3.18 (b). While finishing, a magnetic normal force acts on carbonyl iron (CI) particles in working gap which can be calculated by using Eq. (3.18) (Stradling, 1993).

$$F_{CI} = m_{CI}\mu_0\chi_m H \nabla H \quad (3.18)$$

where F_{CI} is a force acting on single CI particle in Newton, μ_0 is magnetic permeability of free space in $^{H}/_{m}$, χ_m is magnetic susceptibility of CIPs in $^{m^3}/_{kg}$, m_{CI} is mass of a single magnetic carbonyl iron (CI) particle in kg and H is magnetic field strength in A/m. CI particles move towards the end surface of the magnetic strips of the finishing tool and push non-magnetic spherical-shaped active abrasives with magnetic normal force (F_{mn}) towards the inner surface of the ferromagnetic cylindrical workpiece as shown in Fig. 3.18 (a). Due to the reciprocating motion of gripped spherical-shaped active abrasives on the cylindrical workpiece's inner surface, an axial force (F_{ax}) acts on them in the direction parallel to the axis of the finishing tool (Das *et* al., 2008) as shown in Fig. 3.18 (a). Also, due to the rotating movement of gripped spherical-shaped active abrasives on the workpiece surface, the tangential force (F_{ta}) acts in the direction of the tangent to the circular motion of gripped abrasives as shown in Fig. 3.18 (a) and can be calculated by Eq. (3.19) (Gregory, 2006).

$$F_{ta} = 2\, m_a(\omega \times v) \quad (3.19)$$

where m_a is mass in kg, ω is angular velocity in rad/sec and v is linear velocity in m/sec of the spherical-shaped active abrasives. The magnetic normal force (F_{mn}) is accountable to indent an active abrasive on the inner surface of cylindrical workpiece, and axial force (F_{ax}) and tangential force (F_{ta}) are responsible for cutting the roughness peaks of inner surface of the cylindrical workpiece. Therefore, cutting force (F_{cu}) acts on spherical-shaped active abrasive particle which is the sum of axial force (F_{ax}) and tangential force (F_{ta}) and can be calculated by Eq. (3.20) (Das *et* al., 2011).

$$F_{cu} = F_{ax} + F_{ta} \quad (3.20)$$

In this way, the developed MR honing tool erodes out the roughness peaks from the inner surface of the cylindrical workpiece and performs the finishing.

3.4 Conclusions

The following conclusions have been drawn after the design and fabrication of two designs of the magnetorheological (MR) honing tool for nano-finishing of the inner surface of the different diameters of cylindrical workpieces.

- With the help of the magnetostatic finite element analysis, the uniform magnetic flux density distribution was obtained over the outer curved end magnetic surface of the MR honing tool as compared to the non-uniform magnetic flux density distribution over the flat end magnetic surface of the MR honing tool.
- Results of non-uniform distribution of magnetic flux density over the flat end surface of the MR honing tool due to the variable working gap between the tool's flat end surface and the inner surface of the ferromagnetic cylindrical workpiece may slow down the finishing performance of the MR honing process.
- The MR honing tool having flat end magnetic surfaces reveal the constraint in increasing the width of the flat permanent magnetic strips and also maintain the least working gap.
- The obtained uniform magnetic flux density over the outer curved end magnetic surface of MR honing tool helps in uniform gripping of abrasive particles by the uniformly bonded carbonyl iron (CI) particles chains which further facilitate better finishing over the internal surface of cylindrical workpieces with better surface integrity.
- The improved design of magnetorheological (MR) honing tool with the curved end magnetic surface was found to be more capable for finishing the inner surface of cylindrical workpieces as compared to the initial design of MR honing tool with the flat end magnetic surface in terms of uniform distribution of magnetic flux density over the tool end surface, capability of increasing the width of magnet end surface due to the uniform working gap.
- The present designed and fabricated magnetorheological honing tools with curved end magnets reveal its capability of finishing the inner surface of the different diameters of cylindrical workpieces. This is possible because the tool's outer magnetic surface is made flexible to move radially inwards or outwards as per the requirement of the internal diameter of the cylindrical workpiece to be finished.

CHAPTER 4

PRELIMINARY EXPERIMENTATION AND PARAMETRIC ANALYSIS OF MAGNETORHEOLOGICAL HONING PROCESS

4.1 Preliminary experimentations with the initial and improved design of magnetorheological honing tool

To analyze the finishing performance of the initially designed magnetorheological (MR) honing tool with the flat end magnetic surface and improved MR honing tool with the curved end magnetic surface, the preliminary experimentations were performed one after another. The experimentations were performed on the inner surface of the ferromagnetic cylindrical workpiece (made of mild steel) for investigating the change in surface roughness (R_a) values with finishing time. For experimentations, the MR polishing fluid was prepared by thoroughly mixing its ingredients as reported in Table 4.1 in the DC controlled mixing chamber. The MR polishing fluid was applied manually over the outer magnetic surface of the MR honing tool. Due to the induced magnetic field by permanent magnet strips, MR polishing fluid became stiff over the end magnetic surface of the MR honing tool and performed finishing over the inner surface of ferromagnetic mild steel workpiece by its predefined movements. The developed MR honing tool was rotated as well as reciprocated up and down inside the cylindrical mild steel workpiece with the help of two servo motors. These rotatory and reciprocatory motions of the MR honing tool were controlled by the servo controller through the programmable logic controllers (PLC). The experiments were conducted using the developed MR honing experimental setup as shown in Fig. 3.17 (chapter-3). Cylindrical mild steel workpiece was held in a fixture that was gripped by grinding precision vice which was further clamped to the honeycomb breadboard.

When MR polishing fluid was applied to the outer magnetic surface of the MR honing tool, it sticks on its magnetic end surface due to the magnetic field induced by the permanent magnet strips. The finishing was performed over the inner surface of the ferromagnetic cylindrical workpiece when the stiffened MR polishing fluid rotates and reciprocates there. For both the MR honing tools, experimentations were performed for 60 minutes, in three finishing sets each of 20 minutes. Experimentations with both the MR honing tools, that is, tool having flat and curved

permanent magnet strips, were performed using process parameters and conditions as reported in Table 4.1.

Table 4.1 Experimental process parameters and conditions for preliminary experimentations for both the MR honing tools having flat and curved magnetic end surface.

Experimental process parameters	Conditions
Rotating speed of MR honing tools having flat and curved magnetic end surface	400 RPM
Reciprocating speed of MR honing tools having flat and curved magnetic end surface	70 cm/min
Working gap	2.7 mm
SiC abrasives powder	20 % volume of particle size 19μm
Carbonyl iron powder	20 % volume of particle size 18μm
Base fluid medium	60 % volume
Workpiece material	Ferromagnetic cylindrical mild steel
Each finishing set time	20 minutes
Total finishing time	60 minutes

These process parameters were selected on the basis of initial trial experiments and available literature review for various MR fluid based finishing processes. Thoroughly mixed fresh MR polishing fluid was applied and replaced after every 20 minutes. Surface roughness parameters (R_a, R_q, and R_z) were measured after every 20 minutes with Mitutoyo surface roughness tester (model: SJ 400) with the cut-off length of 0.25 mm. The surface roughness parameters on the inner surface of ground cylindrical ferromagnetic workpieces before finishing were found as R_a = 0.37 μm, R_q = 0.49 μm, and R_z = 2.53 μm whose roughness profile is shown in Fig. 4.1 (a). Initially, the ground inner surface of the cylindrical workpiece has higher roughness peaks as shown in Fig. 4.1 (a). After three sets of finishing, that is, total 60 minutes with MR honing tool with the flat end magnetic surface, the surface roughness parameters were reduced as R_a = 0.19 μm, R_q = 0.26 μm, and R_z = 1.34 μm whose surface roughness profile is shown in Fig. 4.1 (b). Then experimentation with MR honing tool having curved end magnetic surface, the surface roughness parameters get decreased to R_a = 0.08 μm, R_q = 0.12 μm, and R_z = 0.63 μm in same 60 minutes of finishing whose surface roughness profile is shown in Fig. 4.1 (c). From Fig. 4.1 (a), (b), and (c), it can be observed that surface roughness values R_a, R_q, and R_z got decreased by

76.28%, 76.67%, and 75.20%, respectively, with a magnetorheological honing tool with the curved end magnetic surface in finishing time of 60 minutes. While in case of MR honing tool with the flat end magnetic surface, these parameters got reduced by 47.97%, 46.24%, and 47.08% in the same finishing time of 60 minutes.

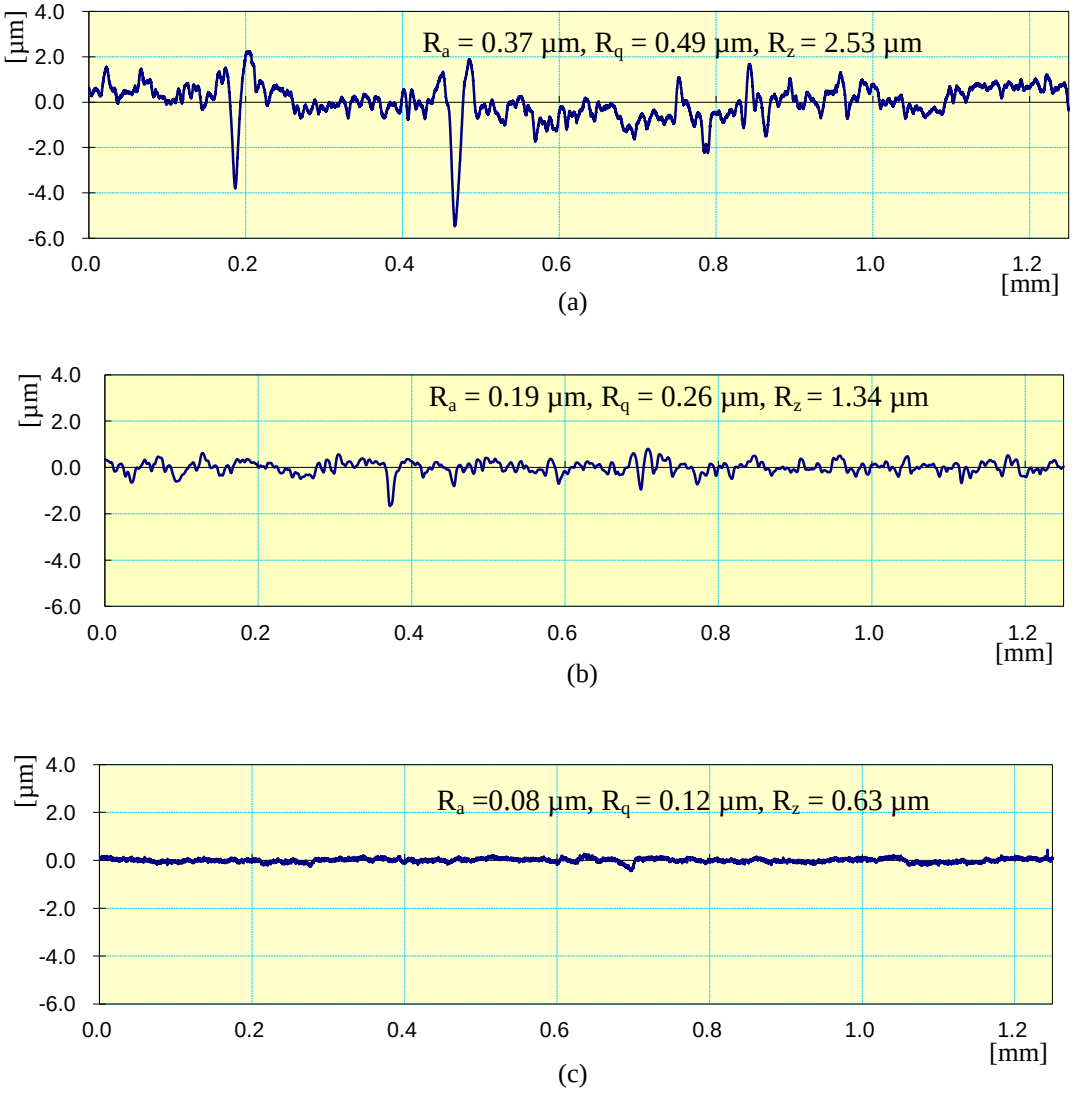

Fig. 4.1 Surface roughness profiles of the inner surface of ferromagnetic cylindrical mild steel workpiece (a) initial ground surface, (b) after 60 minutes of finishing using MR honing tool with flat end magnetic surface and (c) after 60 minutes of finishing using MR honing tool with the curved end magnetic surface.

Surface roughness parameter R_a got decreased with every set of finishing time while experimenting with both MR honing tools as shown in Fig. 4.2. The main reason for the difference in process performance is the dissimilarity in the distribution of magnetic flux density

over the magnetic end surface of both the tools. In the first set of finishing, R_a value gets decreased by 26.41% and 45.55% by MR honing tool with flat and curved permanent magnet strips, respectively. In this first set of finishing, the cutting-edged of the SiC abrasives slash out the sharp peaks of roughness present over the inner surface of cylindrical mild steel workpiece.

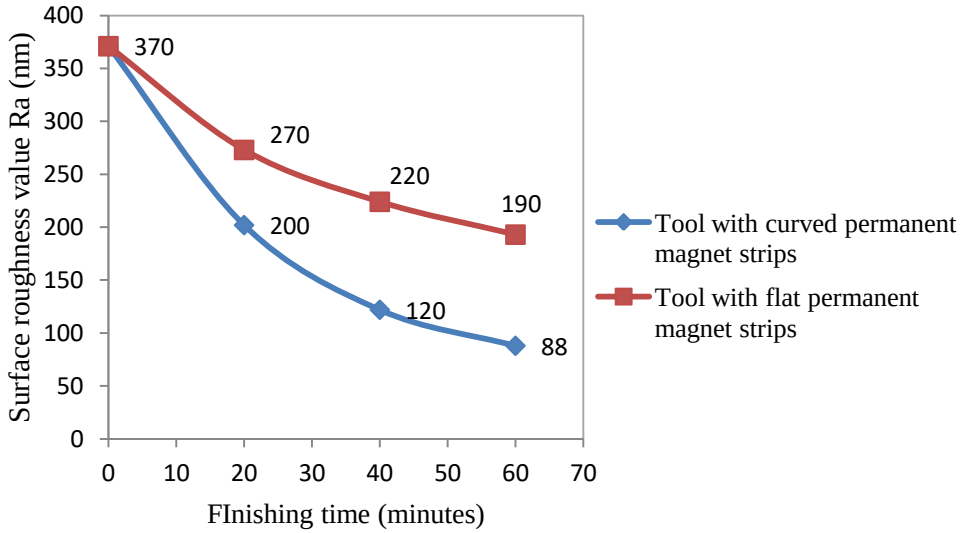

Fig. 4.2 Decrease in surface roughness R_a values with finishing time while performed finishing with MR honing tool having flat and curved permanent magnet strips.

After cutting the peaks of roughness over the surface, the distance between two peaks got decreased. Because of this, indentation of abrasives into the roughness peaks of workpiece became a little difficult after the first set of finishing. The material gets removed in the second set, and R_a value gets decreased by 17.94% and 39.60% by MR honing tool with flat and curved permanent magnet strips, respectively. After the second set of finishing, sharp roughness peaks get turned into flattened peaks, and it became difficult for the same size of abrasives to enter into the peaks. Because of this, material removal rate gets slower in the third set, and R_a value reduced by 13.83% and 27.86% by MR honing tool with flat and curved magnetic surface, respectively. Also, the rate of percentage reduction in R_a value got reduced in the third set because of the increased shear area of the flattened peaks at the base of the material (Martínez-Mateo, 2011). After 60 minutes of finishing by the MR honing tool with flat end magnetic surface, the final finish surface roughness value gets reduced to 190 nm from 370 nm as shown in Fig. 4.1(b). While after 60 minutes of finishing by MR honing tool with curved end magnetic surface, the final finish surface roughness value gets reduced to 88 nm from 370 nm as shown in Fig. 4.1(c). To visualize the finishing performed by both designs of MR honing tools, the scanning electron microscopy (SEM) test of the initial ground surface before experimentation

and final finished surface after 60 minutes of finishing was performed as shown in Fig. 4.3. Scanning electron microscopy (SEM) image at 1000X of the initial ground surface before experimentation is shown in Fig. 4.3 (a). The SEM image of the finished surface after 60 minutes of finishing by the MR honing tool having flat and curved permanent magnetic strips are shown in Fig. 4.3 (b) and (c), respectively.

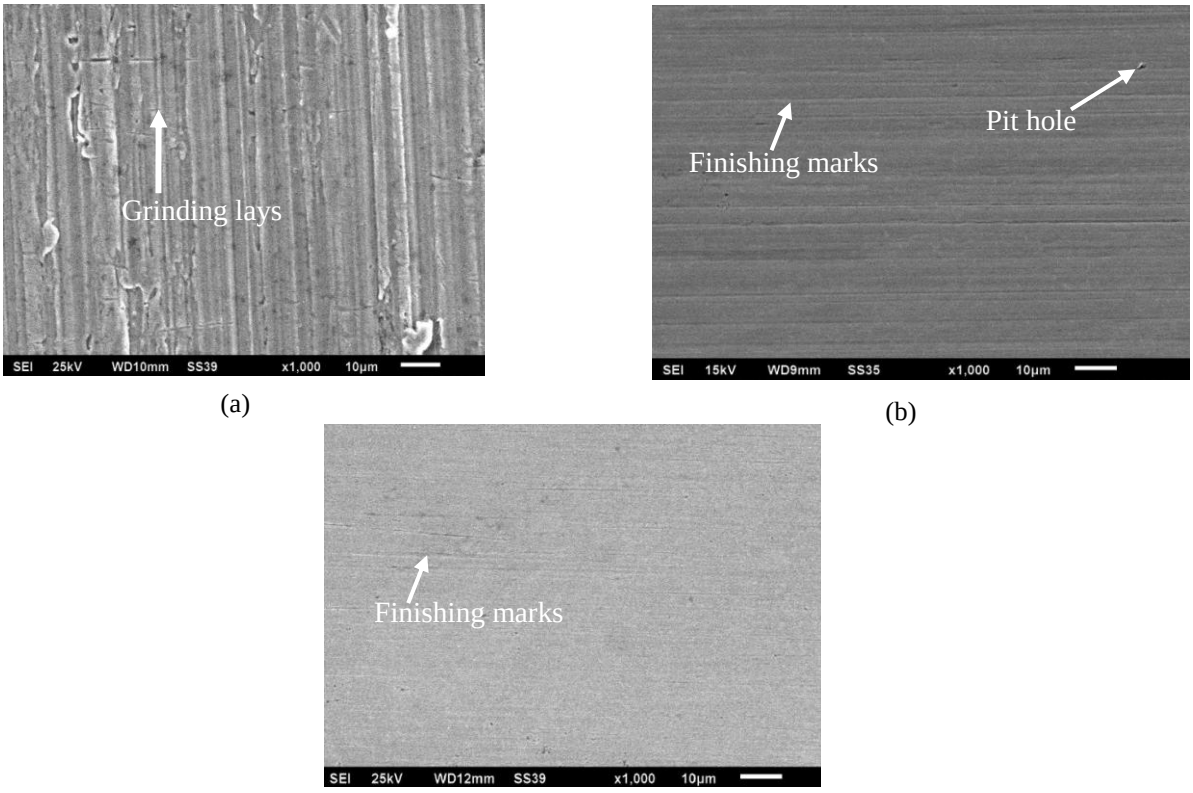

Fig. 4.3 Scanning electron microscopy (SEM) images at 1000x of the inner surface of cylindrical mild steel workpiece (a) initial ground surface, (b) finished surface after 60 minutes of finishing with MR honing tool having flat end permanent magnetic strips, and (c) finished surface after 60 minutes of finishing with MR honing tool having curved end permanent magnet strips.

It can be observed from the Fig. 4.3 (b) and (c) that MR honing tool with curved end permanent magnet strips resulted in better surface characteristics as compared to the surface obtained by finishing performed by the MR honing tool with flat permanent magnet strips. The MR honing tool with flat end magnetic surface resulted in the surface with some defects like pit holes as shown in Fig. 4.3 (b). On the other hand, MR honing tool with curved end magnetic surface resulted in the defect-free surface with the removal of all the grinding marks as shown in Fig. 4.3 (c). Thus, the preliminary experimental results showed that the finishing performance of the present designed MR honing tool with curved permanent magnet strips was better as compared

to the MR honing tool with flat permanent magnet strips. Thus, improved design of the MR honing tool with the curved end permanent magnet strips was found with better process capability to finish the inner surface of the ferromagnetic cylindrical workpieces as compared to the initial design of the MR honing tool with flat end permanent magnet strips.

4.2 Parametric analysis of the developed magnetorheological honing process

The developed magnetorheological (MR) honing tool with curved end magnetic surface was found most capable to result in nano-finishing on the inner surface of cylindrical workpieces with different internal diameters. So, parametric analysis of the developed magnetorheological honing process using MR honing tool having curved end magnetic surface was performed to obtain the optimum process parameters for better fine finishing of the internal ferromagnetic EN-31 cylindrical workpiece's surface. Response surface methodology (RSM) was utilized to plan and evaluate the effects of various process variables like rotating speed of the MR honing tool, reciprocating speed of the MR honing tool, percentage concentration of silicon carbide (SiC) abrasives, percentage concentration of carbonyl iron (CI) particles and working gap variation on percentage change in surface roughness R_a value. As present MR honing tool has been made flexible to move its outer magnetic finishing surface radially inward or outward to finish the different internal cylindrical diameters, therefore variation in working gap is also considered as one of the important process parameters. The optimum finishing parameters were identified for the given range of process parameters. The analysis of experimentations were conducted to study the percentage change in surface roughness R_a value with the working gap, the MR honing tool rotating speed, the percentage concentration of SiC particles, the MR honing tool reciprocating speed and the percentage concentration of CI particles. Further to observe the finishing performed by the MR honing tool over the inner cylindrical surface, the scanning electron microscopy (SEM) test was performed.

4.2.1 Magnetorheological (MR) honing process variables

The present developed magnetorheological honing process is a super finishing process that can be utilized for nano-finishing of cylindrical workpiece's inner surface of different internal diameter. The excellence of MR honing process depends on the various process variables (both controllable and uncontrollable) which are mentioned in Table 4.2.

Table 4.2 MR honing process variables for parametric analysis.

Independent controlled variables	Dependent uncontrolled variable
Percentage concentration of silicon carbide (SiC) abrasives	Ambient temperature
Percentage concentration of carbonyl iron particles (CIPs)	
Working gap	
MR honing tool rotating speed	
MR honing tool reciprocating speed	
Initial values of surface roughness	
Material properties of cylindrical workpiece	

For the parametric study, controlled variables (independent in nature) were considered which are discussed below.

4.2.1.1 Percentage volume concentration of silicon carbide (SiC) abrasive particles (S)

Silicon carbide abrasives are added in MR polishing fluid to shear out the roughness peaks from the cylindrical workpiece's inner surface in the terms of microchips. Abrasives are gripped by the chains formed by the carbonyl iron particles (CIPs) in the existence of magnetic field. With the induction of the magnetic field, the carbonyl iron particles get magnetized and formed dipoles with each other due to the magnetic force, and align themselves in the direction of magnetic field lines. Due to the strong bonding strength and alignment of carbonyl iron particles, the MR fluid polishing fluid gets stiffened. As the MR polishing fluid is composed of CIPs and abrasives, so during the formation of chains of CIPs, abrasives get entangled in between the CIPs chains. Abrasives present on the surface of the workpiece are called active abrasives and are strongly held by the CIPs chains. The abrasives present in the MR polishing fluid have a vital contribution in shearing of roughness peaks from the cylindrical workpiece's inner surface. The concentration of SiC abrasives governs the increasing or decreasing the percentage alteration (change) in surface roughness R_a value as changing the SiC abrasives concentration, the numbers of cutting edges get increased or decreased. In the present study, the range of percentage concentration of SiC abrasive particles has been taken from 15% to 25% as per the design levels. These ranges have been selected on the basis of previous literature available.

4.2.1.2 Percentage volume concentration of carbonyl iron (CI) particles (C)

Carbonyl iron particles (CIPs) are the important constituents of MR polishing fluid. CIPs are responsible for holding the abrasives within the chains formed in the presence of magnetic field.

The strength of CIP chains is proportional to the magnetic field intensity in which CIPs are present. For the particular amount of abrasives, there must be an adequate concentration of CIPs. If the CIPs concentration is too low, then they would not be able to hold the abrasives properly. If the CIPs concentration is too high then this can lead to the comparatively very less number of abrasives which ultimately results in a reduction in cutting action. In the present study, the percentage concentration of CIPs has been taken from 15 % to 25 % as per the design levels. These ranges have been selected on the basis of previous literature available.

4.2.1.3 Rotating speed of the MR honing tool (R)

The rotating speed of the present MR honing tool plays a vital role in finishing the internal cylindrical surfaces. The rotating speed of MR honing tool helps in providing tangential cutting force to the gripped active abrasives which help in performing finishing on the cylindrical workpiece's inner surface. It also helps in indenting the active abrasives into the roughness peaks of the surface by providing centrifugal force to them. In the current observation, the rotating speed of the MR honing tool has been varied from 300 RPM to 700 RPM as per the design levels. These ranges are being selected from the preliminary experimental trials.

4.2.1.4 Reciprocating speed of the MR honing tool (Z)

The continuous up and down movement of the abrasives along with its rotating movement onto the workpiece surface is required to shear out the peaks and obtain surface finish over the inner surface of the cylindrical workpiece. Due to the reciprocating speed of the MR honing tool, the abrasives are acted by axial cutting force which helps to erode out the roughness peaks from the cylindrical workpiece's surface. In the present study, reciprocating speed of MR honing tool has been varied from 50 cm/min to 90 cm/min as per the design levels. The range has been selected on the basis of preliminary trial experiments.

4.2.1.5 Working gap between the outer surface of MR honing tool and cylindrical workpiece's inner surface (W)

The working gap is kept in between the outer surface of the MR honing tool and the cylindrical workpiece's inner surface for MR polishing fluid. The decrease in thickness of working gap leads to increase in the magnitude of magnetic flux density (B) in working gap. The change in the strength of magnetic field in the working gap has a great influence on the rheological characteristics of MR polishing fluid. The bonding strength of CIPs chains gets increased with the increase of magnetic field in the working gap. Stronger bonded CIPs chains can grip the

abrasives more strongly which lead to enough shear strength to erode out the material even from the component having high shear strength. The developed MR honing tool with curved end magnetic surface is capable to nano-finish the different internal diameter of different cylindrical workpieces. In the present study, the working gap for MR polishing fluid has been varied from 1.5 mm to 3.5 mm. This range for working gap has been selected as per design of the MR honing tool.

4.2.2 Design of Experiments

To investigate the influence of various process variables on the percentage alteration (change) in surface roughness value ($\%\Delta R_a$), a set of the design of experiments (DOE) was performed. The experiments were conducted on cylindrical EN-31 workpieces using the developed magnetorheological (MR) honing setup as shown in Fig. 4.4.

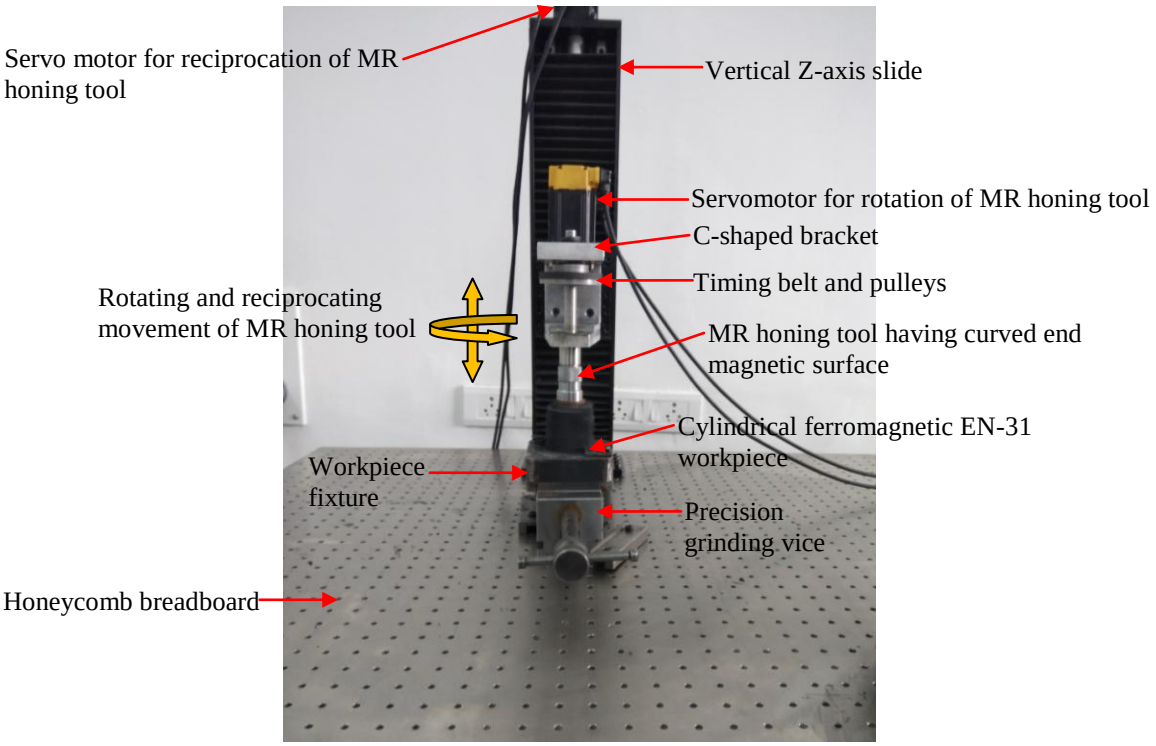

Fig. 4.4 Photograph of the developed magnetorheological honing setup during internal surface finishing of ferromagnetic EN-31 cylindrical workpieces.

The workpiece material used for cylindrical internal finishing was EN-31 (ferromagnetic in nature) having the hardness of 63 HRC and is used for manufacturing cylindrical dies and moulds for various cylindrical plastic products (Martinez-mateo, 2011). The experiments were performed on the cylindrical EN-31 workpiece which consists of two key type slots arrangement as shown in Fig. 4.5 (a). For measuring the surface roughness as well as better observations of

surface morphology under scanning electron microscopy (SEM), cylindrical key type workpieces of EN-31 were made in such a way that it can be attached or removed from the cylindrical EN-31 workpiece surface by means of an interference fit. The photograph of cylindrical ferromagnetic EN-31 steel workpiece having two small key slots along with its fixture is shown in Fig. 4.5 (a). Cylindrical key type workpieces made up of EN-31 steel as shown in Fig. 4.5 (b) were inserted in the cylindrical EN-31 workpiece, and experimentations were performed over them.

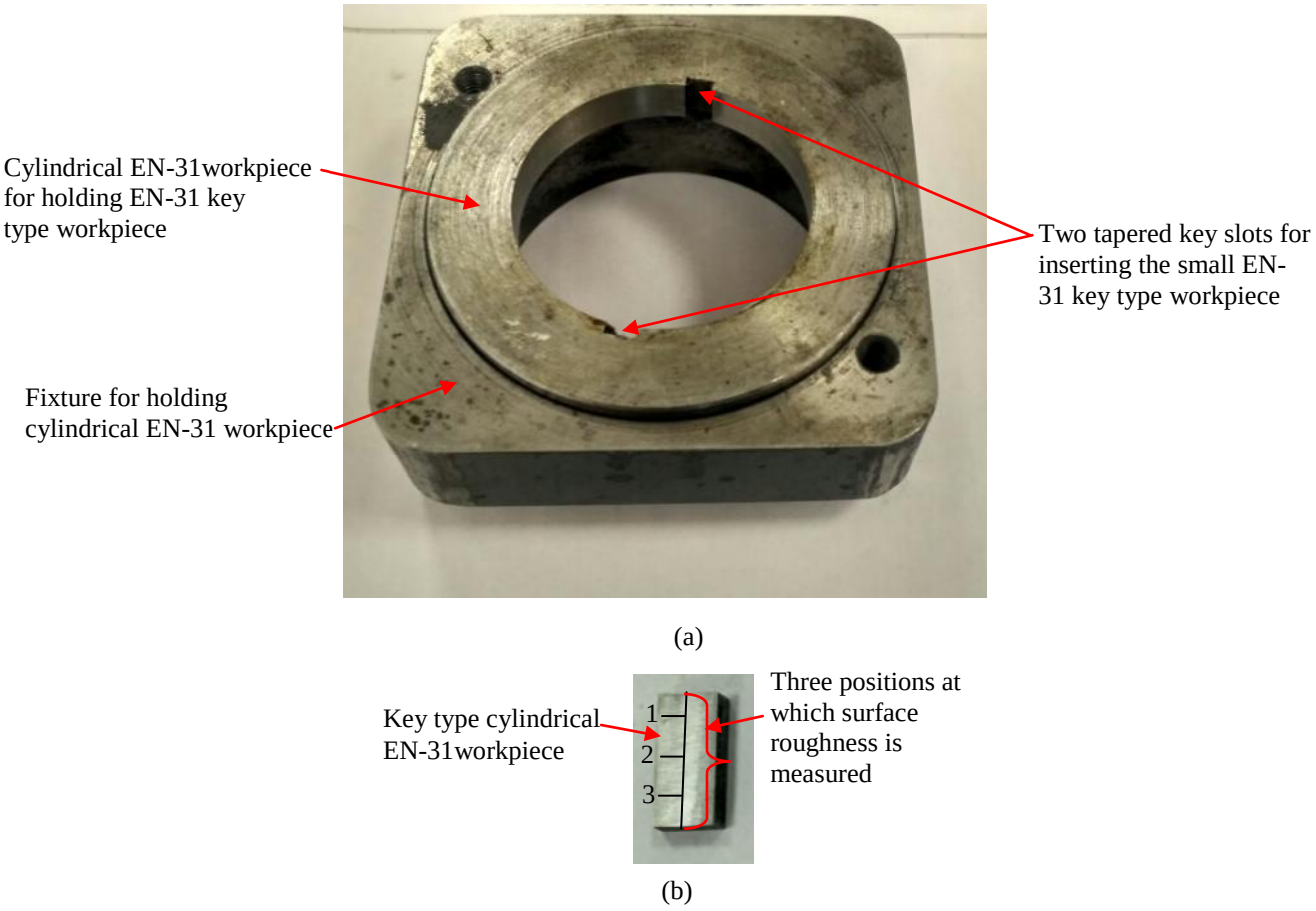

Fig. 4.5 Photograph of (a) cylindrical ferromagnetic EN-31 steel workpiece having two key slots along with its fixture and (b) cylindrical key type EN-31 workpiece.

The cylindrical EN-31 workpiece along with its fixture as shown in Fig. 4.5 (a) is further gripped by grinding precision vice clamped over the honeycomb breadboard as shown in Fig. 4.4. The initial ground surface of all key type workpieces was prepared by the internal cylindrical grinding process and measured using surface roughness tester named Mitutoyo SJ- 400. The initial and final measurement of surface roughness (i.e. before and after finishing) was performed at three different stages (1, 2 and 3) over a straight line on cylindrical key type EN-31 workpiece as shown in Fig. 4.5 (b) on the cylindrical key type workpiece. The average of three

measurements was calculated and taken as initial and final surface roughness value. The cut-off length for measuring the surface roughness was kept as 0.25 mm. Thoroughly mixed MR polishing fluid constituting of carbonyl iron (CI) particles, silicon carbide (SiC) abrasives, heavy paraffin oil and AP3 grease was used for experimentations. The initial values of surface roughness were not same for all the workpieces that is why the percentage change in surface roughness ($\%\Delta R_a$) value was considered as the final response which was calculated by using the Eq. 4.1.

$$\% \text{ change in } R_a = \frac{Initial\ surface\ roughness\ value - Final\ surface\ roughness\ value}{Initial\ surface\ roughness\ value} \times 100 \quad (4.1)$$

Response surface methodology (RSM) is made up of a collection of statistical and mathematical methods used for the advancement of a useful correlation between the inputs and the outputs. RSM determines the relation between the independently controlled variables and the final response. The experimental conditions decide the combinations of factor levels in the design. Five levels, central composite design with six central runs was utilized to perform the experiments. 'F' test via analysis of variance (ANOVA) was performed in order to analyze the importance of regression equation in detailing the connections between the response outputs and the control variables. RSM was utilized to monitor the effects of five process parameters on the percentage alteration in surface roughness value (% ΔR_a). The process parameters represented by its coded levels and along with its actual values used for finishing of the internal ferromagnetic surface of the EN-31 workpiece by using the developed MR honing tool are given in Table 4.3.

Table 4.3 Actual values of MR honing process parameters along with its coded levels.

Sr. No.	Process parameter	Units	Coded levels				
			-2	-1	0	1	2
1.	Percentage concentration of silicon carbide (SiC) abrasives (S)	%	15	17.5	20	22.5	25
2.	Percentage concentration of carbonyl iron particles (C)	%	15	17.5	20	22.5	25
3.	MR honing tool rotating speed (R)	rpm	300	400	500	600	700
4.	MR honing tool reciprocating speed (Z)	cm/min	50	60	70	80	90
5.	Working gap (W)	mm	1.5	2.0	2.5	3.0	3.5

The carbonyl iron particles of 400 mesh size, silicon carbide (SiC) abrasives of 600 mesh size were used for the complete design of experimentations. Each set of finishing experiments was

performed for 40 minutes. The cylindrical ferromagnetic workpiece made up of EN-31 die steel material was utilized for experimentations. The mixing chamber was used for preparing the MR polishing fluid indigenously. The experimentations were performed for finishing of the internal ferromagnetic cylindrical surface of EN-31 material according to the design of experiments as given in Table 4.4.

Table 4.4 Design of experiments and **s**ummary of responses obtained by performing design of experiments.

Std order	**Factors**					**Initial R_a value (µm)**	**Final R_a value (µm)**	**Response (% ΔR_a)**
	(S)	**(C)**	**(R)**	**(Z)**	**(W)**			
1	22.5	22.5	400	60	2	0.48	0.27	44
2	17.5	17.5	400	60	2	0.49	0.28	42
3	22.5	17.5	600	60	2	0.50	0.20	59
4	20	20	500	90	2.5	0.48	0.24	51
5	17.5	22.5	600	80	3	0.50	0.26	48
6	17.5	17.5	400	80	2	0.48	0.26	45
7	20	20	500	70	3.5	0.48	0.30	37
8	17.5	22.5	400	60	2	0.48	0.30	35
9	17.5	17.5	600	60	2	0.49	0.25	50
10	20	20	500	70	2.5	0.48	0.23	53
11	17.5	22.5	400	80	2	0.48	0.25	48
12	17.5	17.5	600	80	2	0.48	0.26	46
13	17.5	22.5	600	60	2	0.47	0.22	52
14	20	20	500	70	2.5	0.48	0.20	59
15	22.5	17.5	600	80	2	0.49	0.24	51
16	22.5	17.5	400	60	2	0.50	0.23	53
17	17.5	22.5	600	80	2	0.48	0.21	56
18	22.5	22.5	600	80	2	0.49	0.22	55
19	20	15	500	70	2.5	0.49	0.25	50
20	17.5	17.5	400	60	3	0.48	0.31	35
21	20	20	500	50	2.5	0.47	0.25	48
22	22.5	17.5	400	60	3	0.49	0.25	49
23	17.5	22.5	400	60	3	0.49	0.33	33
24	20	20	500	70	2.5	0.49	0.21	57
25	22.5	22.5	400	60	3	0.48	0.33	31
26	17.5	17.5	600	60	3	0.48	0.27	44
27	20	20	500	70	2.5	0.48	0.22	54
28	22.5	17.5	600	60	3	0.49	0.25	49
29	17.5	22.5	600	60	3	0.48	0.27	45
30	20	20	700	70	2.5	0.48	0.21	57
31	22.5	22.5	600	60	3	0.49	0.28	42
32	17.5	17.5	400	80	3	0.47	0.27	44

33	20	20	500	70	2.5	0.49	0.23	54
34	22.5	17.5	400	80	3	0.49	0.26	47
35	20	20	300	70	2.5	0.49	0.29	42
36	20	20	500	70	2.5	0.48	0.20	57
37	17.5	22.5	400	80	3	0.48	0.27	45
38	22.5	22.5	400	80	3	0.49	0.28	43
39	22.5	17.5	600	80	3	0.49	0.26	47
40	22.5	22.5	600	80	3	0.49	0.27	44
41	15	20	500	70	2.5	0.48	0.31	36
42	25	20	500	70	2.5	0.49	0.28	42
43	22.5	17.5	400	80	2	0.50	0.24	51
44	22.5	22.5	600	60	2	0.49	0.23	52
45	20	25	500	70	2.5	0.48	0.26	46
46	22.5	22.5	400	80	2	0.49	0.23	52
47	20	20	500	70	1.5	0.50	0.21	57
48	20	20	500	70	2.5	0.50	0.21	56
49	17.5	17.5	600	80	3	0.50	0.29	42
50	20	20	500	70	2.5	0.48	0.21	55

4.2.2.1 Response surface regression analysis

The responses in terms of percentage alteration in surface roughness R_a value (% ΔR_a) during each set of experimentation are reported in Table 4.4. The responses in terms of % ΔR_a values were analyzed using Eq. (4.1). The ANOVA for the entire model is given in Table 4.5.

Table 4.5 ANOVA for % ΔR_a value and percentage contribution of each process parameter.

Source	**Sum of squares**	**Degree of freedom**	**Mean square**	***F*-value**	**P-value**	**Remarks**	**Percentage contribution**
Model	2253.35	17	132.55	25.45	< 0.0001	significant	
S	126.02	1	126.02	24.19	< 0.0001		5.59
C	34.22	1	34.22	6.57	0.0153		1.51
R	330.62	1	330.62	63.48	< 0.0001		14.67
Z	75.62	1	75.62	14.52	0.0006		3.35
W	511.22	1	511.22	98.16	< 0.0001		22.68
S^2	457.53	1	457.53	87.85	< 0.0001		20.30
C^2	75.03	1	75.03	14.40	0.0006		3.32
R^2	42.78	1	42.78	8.21	0.0073		1.89
Z^2	42.78	1	42.78	8.21	0.0073		1.89
W^2	101.53	1	101.53	19.49	0.0001		4.50
SC	101.53	1	101.53	19.49	0.0001		4.50

SR	22.78	1	22.78	4.37	0.0445		1.01
SZ	22.78	1	22.78	4.37	0.0445		1.01
SW	22.78	1	22.78	4.37	0.0445		1.01
CR	52.53	1	52.53	10.08	0.0033		2.33
CZ	132.03	1	132.03	25.35	< 0.0001		5.85
RZ	101.53	1	101.53	19.49	0.0001		4.50
Residual	166.65	32	5.20				
Lack of Fit	138.77	25	5.55	1.39	0.3418	not significant	
Pure Error	27.87	7	3.98				0.09
Cor Total	2420	49					

In the present work, the significant level i.e. α= 0.05 was taken for the given hypothesis for which p-value ≤ 0.05 was considered as significant. The terms such as S, C, R, Z, W, S^2, C^2, R^2, Z^2, W^2, SC, SR, SZ, SW, CR, CZ and RZ were significant. If the p-value is > 0.05 then the terms were considered as insignificant. If insignificant terms exist in the model, then the model can further be improved by eliminating the insignificant terms. The R^2 value determines the closeness of experimental data points with the regression fit line. The R^2 for the given model is 0.93. This means that the model determines a good response input.

The confidence interval of 95% low values and 95% high values were the lower and the upper bound of 95% confidence interval that enclosed the coefficient approximate for the factor. The variance inflation factor (VIF) of the model quantifies how the variance is magnified by the need of orthogonality in the design. If the value of VIF is 1.00, then the factor was orthogonal to other factors within the model. If the value of VIF is >10, then the factors are not independent of each other. If the p-value is > 0.05, then the model is regarded as not significant. The factor coefficient represents a span that the accurate coefficient must be initiated 95% of the time. Following Eqs. (4.2) and (4.3) represents the quadratic equations which define the empirical relations between the process parameters. The final equation as per coded factors is represented in Eq. (4.2)

$$\%\,\Delta R_a = +55.32 + 1.78A - 0.92B + 2.88C + 1.38D - 3.57E - 3.78A^2 - 1.53B^2 - 1.16C^2 - 1.16D^2 - 1.78E^2 - 1.78AB - 0.84AC - 0.84AD - 0.84AE + 1.28BC + 2.03BD - 1.78CD \quad (4.2)$$

The final equation as per the actual factors is represented in Eq. (4.3).

$$\%\,\Delta R_a = -553.79 + 36.35S + 6.88C + 0.23R + 1.70Z + 41.98W - 0.61S^2 - 0.25C^2 - 1.16 \times 10^{-4}R^2 - 1.16 \times 10^{-2}Z^2 - 7.13W^2 - 0.29SC - 3.38 \times 10^{-3}SR - 3.38 \times 10^{-2}SZ - 0.68SW + 5.13 \times 10^{-3}CR + 0.08CZ - 1.78 \times 10^{-3}RZ \quad (4.3)$$

The contributions of each process parameters on % ΔR_a value are given in Table 4.5. The relation between the actual percentage change in surface roughness R_a value and predicted percentage alteration in surface roughness R_a value evaluated from the response surface regression analysis is shown in Fig. 4.6.

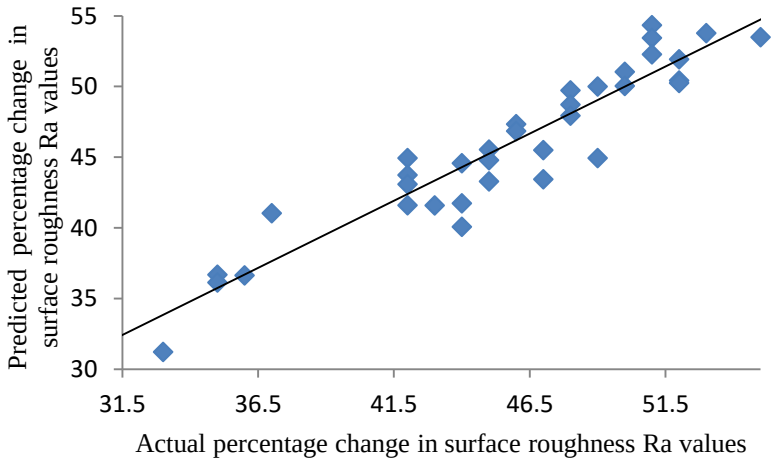

Fig. 4.6 Graph showing the relation between the actual percentage change in surface roughness R_a value and predicted percentage change in surface roughness (R_a) value.

From Fig. 4.6, it can be observed that predicted values of percentage alteration in surface roughness parameter R_a are in close relation to the actual obtained experimental percentage change in surface roughness parameter R_a.

4.2.3 Results and discussion

The results are observed after the regression analysis of the responses. The effect of percentage concentration of the abrasive particles, percentage concentration of carbonyl iron particles, the rotating speed of finishing tool, the reciprocating speed of finishing tool and variation of working gap on the percentage alteration of roughness value (% ΔR_a) of the surface have been observed and computed. The effects of these independent controllable variables on the % ΔR_a value have been discussed as follows:

4.2.3.1 Effect of percentage concentration of silicon carbide abrasive particles

The concentration of silicon carbide abrasive particles present in the MR polishing fluid has a significant role in finishing the internal cylindrical surfaces while performing experimentation with the developed MR honing process. The sharp edges of abrasive particles erode out the material from the cylindrical workpiece's inner surface. When the abrasives concentration is very less, then there remain insufficient numbers of abrasives to shear out the material. Strongly bonded chains of the carbonyl iron particles (CIPs) get formed with less number of SiC abrasive particles which results in reduced surface finishing. When the abrasive concentration is too high, the count of CIPs chains becomes less to grip the increased number of abrasive particles and therefore superfluous abrasives are free to move. With a higher percentage concentration of SiC abrasives, CIPs can't make strong bonds due to the abundance number of abrasives entangled in between the chains. For a particular percentage concentration of CI particles, too low or too high concentration of abrasives results in the less reduction in surface roughness value. There is a particular percentage concentration of abrasives for a particular concentration of carbonyl iron (CI) particles which makes most favorable MR polishing fluid. The effect of the concentration of SiC abrasives on the percentage change in the value of surface roughness (%ΔR_a) at tool rotating speed of 500 RPM, tool reciprocating speed as 70 cm/min, carbonyl iron particles concentration as 20% and a working gap of 2 mm was observed as shown in Fig. 4.7.

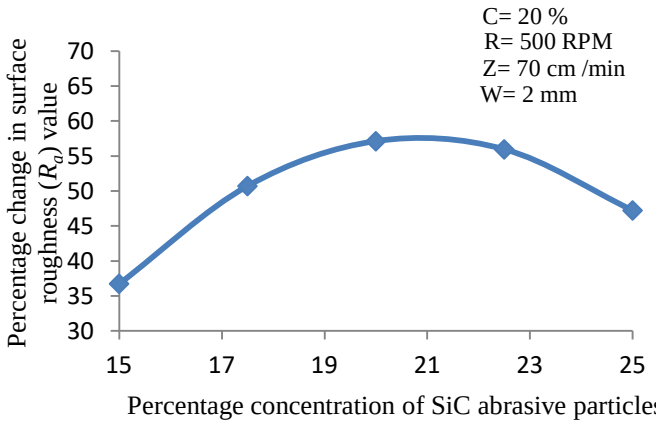

Fig. 4.7 Effect of percentage concentration of silicon carbide (SiC) abrasive particles on the percentage change in surface roughness (R_a) value.

For a particular percentage concentration of CI particles i.e. 20% in this case, when the SiC abrasive concentration is low i.e. below 20%, then it results with the low percentage alteration in the value of surface roughness (% ΔR_a). The reason behind this is that in these cases, not sufficient amount of abrasives were present in MR polishing fluid to erode the material. The rise

in percentage concentration of SiC abrasives (up to 20%) boosts the percentage alteration in surface roughness values (% ΔR_a) due to the rise in a number of cutting edges of abrasives to erode out more material from the workpiece surface. But after certain limit i.e. 20% in present work, the increase in percentage concentration of abrasives results in a decrease in percentage alteration in surface roughness values (% ΔR_a). As in this case, there becomes so much number of SiC abrasives which can't be properly gripped by the CI particles chains. The SiC abrasives remain loose within the MR polishing fluid which rolls over the workpiece's surface and may even damage the surface while finishing. So it has been concluded from Fig. 4.7 that optimum percentage concentration of abrasives required for maximum material removal is 20% for a particular CIP concentration of 20%.

4.2.3.2 Effect of percentage concentration of carbonyl iron particles

The carbonyl iron particles present in the MR polishing fluid helps in gripping of abrasives by making chains. For a particular concentration of SiC abrasives in the MR polishing fluid, the rise in percentage concentration of carbonyl iron (CI) particles after certain limit leads to decrease in value of surface roughness. As the concentration of CI particles gets increased, the formed CI particles chains get denser which lead to the stronger gripping of abrasives over the surface of the workpiece.

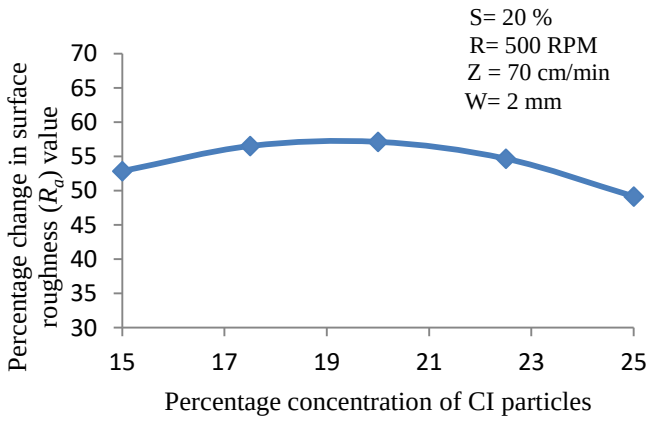

Fig. 4.8 Effect of percentage concentration of carbonyl iron (CI) particles on the percentage change in surface roughness (R_a) value.

The effect of CI particles concentration present in the MR polishing fluid on percentage alteration in surface roughness value (ΔR_a) with MR honing tool rotating speed of 500 RPM, tool reciprocating speed of 70 cm/min, SiC particles concentration as 20% and a working gap of 2 mm was observed as shown in Fig. 4.8. It is observed from Fig. 4.8 that for a particular

percentage concentration of SiC abrasives i.e. 20% in this case, the percentage alteration in surface roughness values (% ΔR_a) gets increased with the increase of CI particles concentration up to a level i.e. 20% in this case. After 20% increase in CI particles concentration, the percentage alteration in surface roughness value (% ΔR_a) starts decreasing. The reason behind this is that after 20% rise in CI particles concentration, the corresponding concentration of abrasives becomes less which is sufficiently required for the material removal in the present process (Das *et* al., 2012). Thus, it has been concluded that optimum percentage concentration of CI particles required for maximum material removal is 20 % for a particular SiC concentration of 20 %.

4.2.3.3 Effect of rotating speed of MR honing tool

The rotating speed of MR honing tool also plays a significant contribution in finishing the cylindrical workpiece's internal surface in the present MR honing process. The rotating speed of MR honing tool provides the tangential cutting force to the active abrasives which help in shearing out of roughness peaks from the cylindrical workpiece's internal surface. The effect of MR honing tool's rotating speed on percentage alteration in surface roughness value (*%* ΔR_a) at tool reciprocating speed of 70 cm/min, SiC abrasive particles concentration as 20%, CI particles concentration as 20% and a working gap of 2 mm was observed as represented in Fig. 4.9.

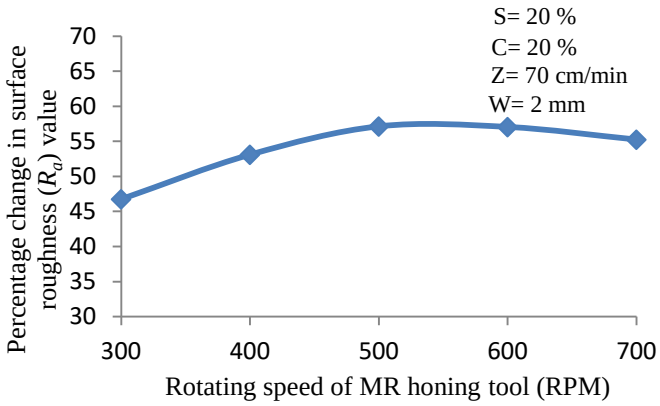

Fig. 4.9 Effect of rotating speed of MR honing tool on the percentage change in surface roughness (R_a) value.

It was perceived from the Fig. 4.9 that at a low value of tool rotating speed i.e. 300 RPM, the percentage variation in surface roughness value (% ΔR_a) is low and it gets increased with the rise in tool's rotating speed. The percentage variation in surface roughness value (% ΔR_a) increase with the rise in MR honing tool's rotating speed up to 500 RPM. After 500 RPM speed of tool

rotation, the percentage alteration in the value of surface roughness (% ΔR_a) starts decreasing. The reason behind this is that after 500 RPM speed of tool rotation, the bonding strength of MR polishing fluid does not remain sufficient enough to shear out the material from the cylindrical workpiece's inner surface. The centrifugal force (due to rotation of finishing tool) exerting over the CI particles weakens the magnetic normal force acting between the magnetic particles after 500 RPM of tool rotation. Therefore, at high tool rotating speed, the abrasives are not properly gripped by the CI particles chains and start rolling over the cylindrical workpiece's inner surface which results in less reduction in surface roughness values.

4.2.3.4 Effect of reciprocating speed of MR honing tool

The reciprocating speed of MR honing tool helps in eroding out of material from the workpiece surface by providing an axial force to the abrasives. The increase in reciprocating speed of MR honing tool leads to the rise in axial force acting over the abrasives to shear out the workpiece material. The effect of MR honing tool's reciprocating speed on percentage alteration in the value of surface roughness (% ΔR_a) at tool rotating speed of 500 RPM, SiC abrasive particles concentration as 20%, CI particles concentration as 20% and working gap of 2 mm was examined as represented in Fig. 4.10.

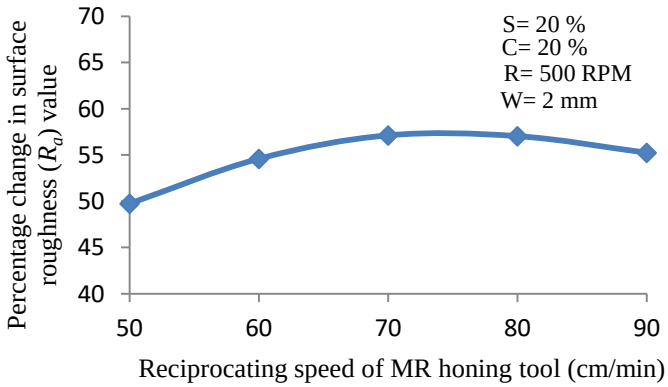

Fig. 4.10 Effect of reciprocating speed of MR honing tool on the percentage change in surface roughness (R_a) value.

It is observed from the Fig. 4.10 that at lower tool reciprocating speed of 50 cm/min, the percentage variation in surface roughness is low. The percentage alteration in surface roughness value (% ΔR_a) increases with increasing reciprocating speed of MR honing tool and is maximum at 70 cm/min. After further increasing the MR honing tool reciprocating speed beyond 70 cm/min, the percentage alteration in surface roughness value (% ΔR_a) start decreasing. This is due to the reason that, after this limit i.e. 70 cm/min, the SiC abrasive particles present over the

workpiece surface become unstable due to the high axial force acting over the CI particles chains. At high reciprocating speed i.e. 80 cm/min or 90 cm/min, the CI particles chains start breaking due to the high axial force acting over them and cannot grip the abrasives properly. So, the abrasives cannot perform the finishing properly and start rolling over the inner surface of the cylindrical workpiece. Due to this, the percentage variation in surface roughness value starts decreasing after MR honing tool reciprocating speed of 70 cm/min.

4.2.3.5 Effect of working gap variation between the MR honing tool's outer surface and the inner surface of a cylindrical workpiece

Working gap between the MR honing tool's outer surface and the inner surface of the cylindrical workpiece has a strong impact on the percentage alteration in surface roughness value *(%* ΔR_a). The effect of variation of working gap on percentage alteration in surface roughness value (% ΔR_a) at MR honing tool reciprocating speed of 70 cm/min, tool rotating speed of 500 RPM, SiC abrasive particles concentration as 20% and CIPs concentration as 20% was observed as represented in Fig. 4.11.

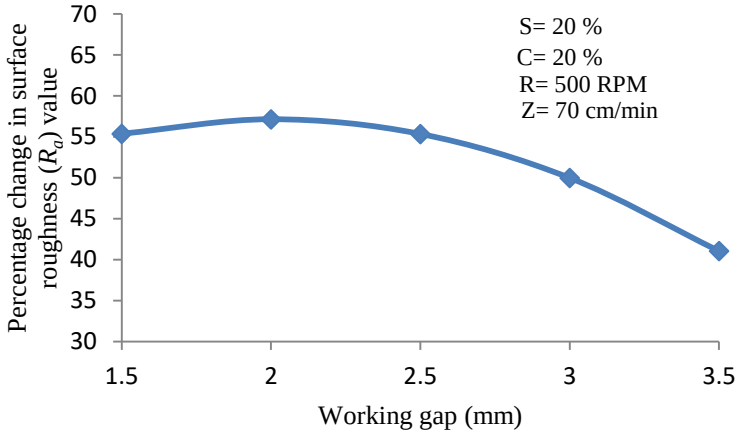

Fig. 4.11 Effect of variation of working gap on the percentage change in surface roughness (R_a) value.

From the Fig. 4.11, it can be observed that on increasing the working gap from 2 mm to 3.5 mm, the percentage alteration in surface roughness value (% ΔR_a) gets decreased. The reason behind this is that magnitude of magnetic flux density within the working gap decreases with the increase of working gap (Sidpara and Jain, 2013). At the higher working gap, magnetic force, F_m (which help CI particles to bind) acting between the two carbonyl iron (CI) particles gets decrease due to the decrease in intensity of magnetization (M) as illustrated by Eq. (4.4) (Huang *et* al., 2005).

$$F_m = \frac{\mu_0 \pi}{9} \left(\frac{r_c^2 CM}{R'}\right)^2 \quad (4.4)$$

Here r_c represents the radius of carbonyl iron particle, R' represents the distance between the centers of two carbonyl iron particles and C represents the collect coefficient (a function of H). In this way, with the increased working gap, the bonding strength between the CI particles gets decreased and they cannot perform the proper finishing. Due to this, the percentage alteration in surface roughness (% ΔR_a) value decreases on increasing the working gap. When the working gap is 2 mm, there is an adequate magnetic flux density present within the working gap which is sufficiently required for the eroding of roughness peaks in the shape of microchips to result in the finished surface as shown in Fig. 4.12 (a).

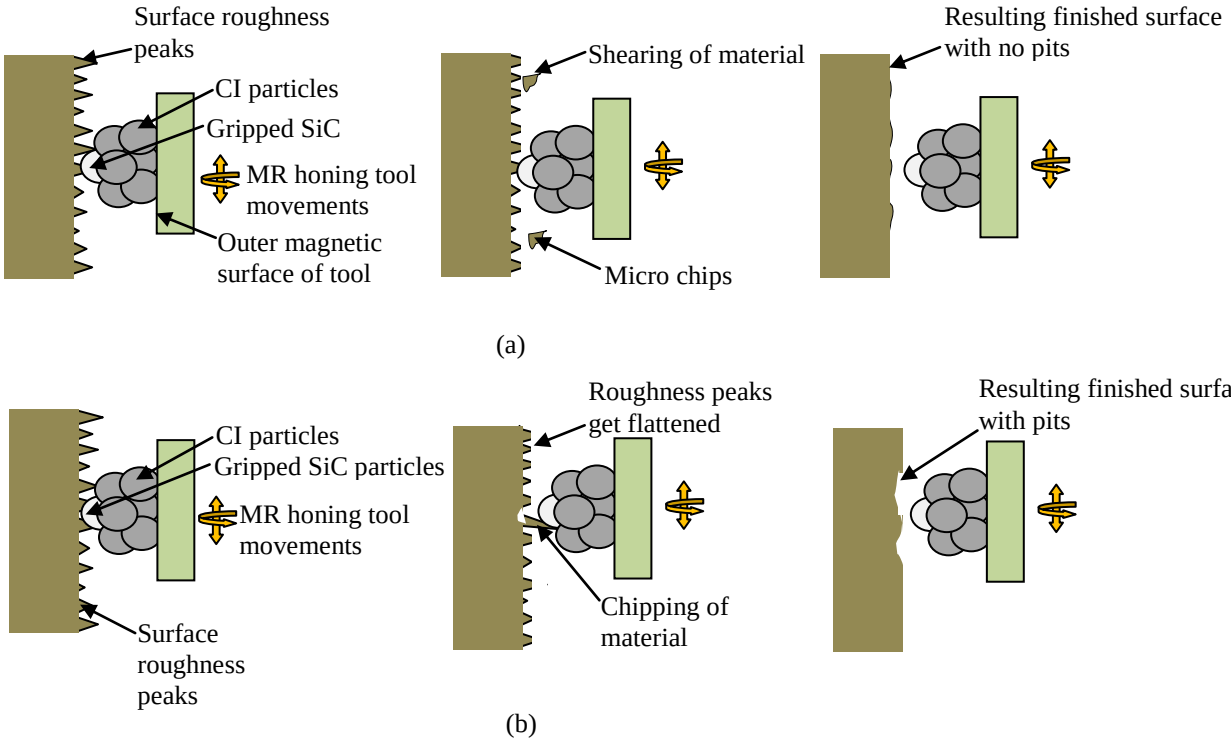

Fig. 4.12 Mechanism of material removal by MR honing tool with working gap of (a) 2 mm and (b) 1.5 mm.

When the working gap is 2 mm, initially, the abrasives slash out the peaks of roughness to make them flat. Then, with successive finishing cycles, abrasives erode out the all surface roughness peaks to result in the finished surface as shown in Fig. 4.12 (a). For the working gap of 1.5 mm, the percentage alteration in surface roughness value (% ΔR_a) was less than that at working gap of 2 mm. This is due to the fact that for these particular parameters, high indentation force is applied by the abrasives of rigidly stiffened (Eq. 4.4) MR polishing fluid onto the inner surface

of the cylindrical workpiece due to high magnetization within the working gap of 1.5 mm. Due to this high indentation force within the working gap of 1.5 mm, abrasives not only slash out the peaks but also strongly pluck out the material from its base surface as shown in Fig. 4.12 (b). This generates the pit holes in the resulting finished surface and results in higher surface roughness value R_a. Due to this, for the working gap of 1.5 mm, percentage alteration in surface roughness value (% ΔR_a) is less than that at working gap of 2 mm.

4.2.3.6 Effect of interaction of different concentration of SiC abrasives with different concentration of carbonyl iron particles

The effect of the interaction of different concentration of SiC abrasives with different concentration of carbonyl iron particles on percentage alteration in surface roughness R_a value at the reciprocating speed of 70 cm/min, rotating speed of 500 RPM and a working gap of 2 mm was observed as shown in Fig. 4.13.

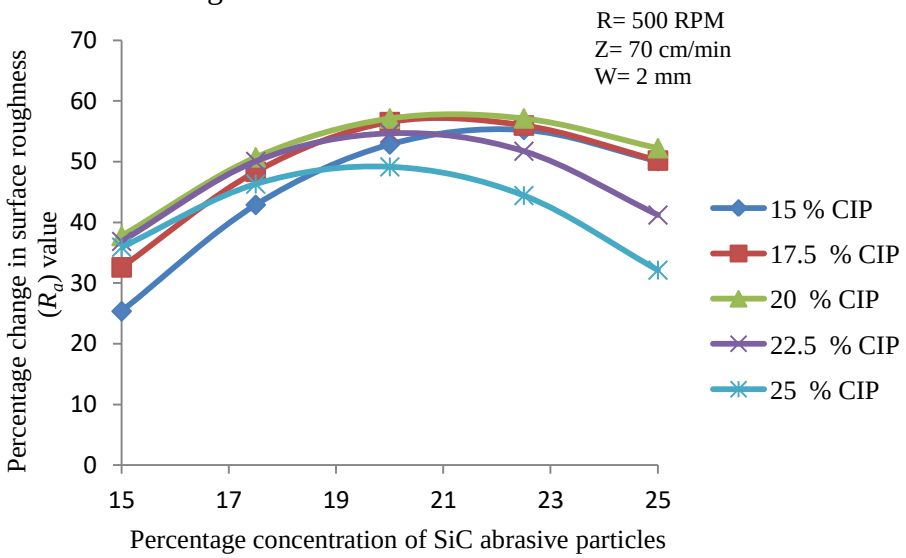

Fig. 4.13 Effect of interaction of different concentration of silicon carbide abrasive particles with carbonyl iron particles concentration on the percentage change in surface roughness (R_a) value.

For achieving significant surface finishing, the adequate concentration of SiC abrasive particles must be present in the MR polishing fluid with respect to the concentration of carbonyl iron (CI) particles. CI particles form chains to grip the abrasive particles. For a particular concentration of CI particles, if the percentage concentration of SiC abrasives is too low, then it would result in less variation in surface roughness value because of few numbers of available cutting edges. With the low concentration of abrasives, count of active abrasives present over the workpiece's surface remains less to perform adequate finishing. Also, for the same concentration of CI

particles, if the percentage concentration of SiC abrasives is too high, then it would also result in less change in surface roughness value. As in this case, there are so many numbers of SiC abrasives which can't be properly held by the CI particles chains. The SiC abrasives remain loose in the MR polishing fluid which even makes scratched marks on the inner cylindrical surface while finishing. It can be observed from the Fig. 4.13 that maximum percentage change in surface roughness value is obtained with 20% concentration of CI particles and is adequate to grip the 20% concentration of SiC abrasive particles properly at tool rotation of 500 RPM, reciprocating speed of 70 cm/min and a working gap of 2 mm. The maximum surface roughness reduction is obtained with a combination of 20% concentration of CI particles and 20% concentration of SiC abrasives.

4.2.3.7 Effect of interaction of different rotating speed of MR honing tool with different concentration of silicon carbide abrasive particles

The effect of the interaction of different rotating speed of MR honing tool with different concentration of silicon carbide (SiC) abrasive particles on percentage alteration in R_a value at reciprocating speed of 70 cm/min, CI particles concentration of 20% and a working gap of 2 mm was observed as represented in Fig. 4.14.

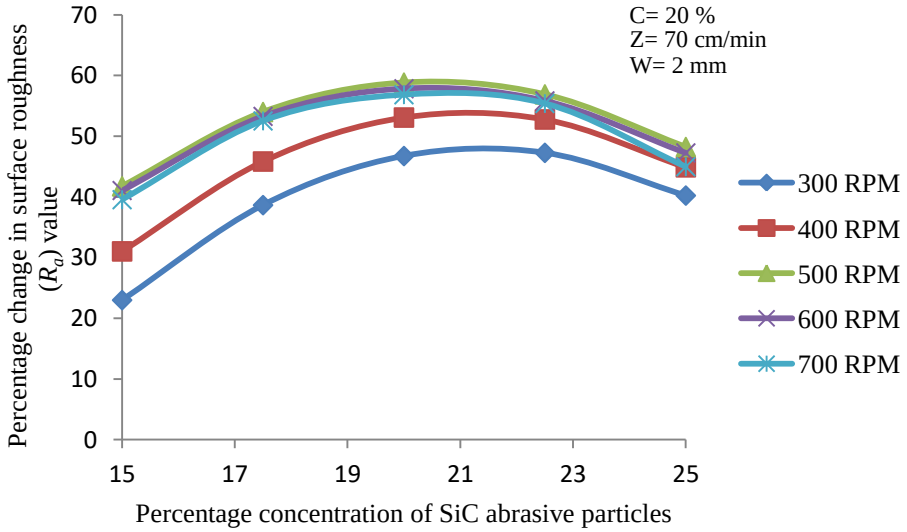

Fig. 4.14 Effect of interaction of different rotating speed of MR honing tool with percentage concentration of silicon carbide abrasive particles on the percentage change in surface roughness (R_a) value.

It can be observed from Fig. 4.14 that for a particular concentration of SiC abrasive particles, the rise in the tool rotating speed results in the increase in percentage alteration in surface roughness value. This is due to the increase in the magnitude of the tangential cutting force acting over the

active abrasives as the rotating speed of the MR honing tool increases. But for a particular concentration of SiC abrasives, the increase in percentage variation in surface roughness value limits to a particular value of tool rotating speed which is 500 RPM for this particular observation. After 500 RPM speed of tool rotation, the percentage alteration in the value of surface roughness (% ΔR_a) starts decreasing. This is due to the fact that after 500 RPM speed of tool rotation, the bonding strength of MR polishing fluid does not remain sufficient enough to hold the abrasive particles and erode out the material from the workpiece's surface. The centrifugal force (due to rotation of finishing tool) exerting over the CI particles weakens the magnetic normal force acting between the magnetic CI particles after 500 RPM of tool rotation. In the present observation, the further increase in the concentration of SiC abrasive particles beyond 20%, it becomes difficult for CI particles chains to properly grip the abrasive particles. Because of this reason, the percentage alteration in surface roughness R_a value decreases for the higher percentage concentration of SiC abrasives i.e. 22.5% or 25%. The maximum percentage alteration in surface roughness R_a value was obtained with an optimum combination of 20% concentration of SiC abrasive particles with 500 RPM rotating speed of the MR honing tool.

4.2.3.8 Effect of interaction of rotating speed of MR honing tool with working gap variation

The effect of interaction of different rotating speed of MR honing tool with the variation in working gap on percentage change in R_a value at 20% carbonyl iron (CI) particles concentration and 20% silicon carbide (SiC) abrasive particles concentration and 70 cm/min reciprocating speed of MR honing tool is observed as shown in Fig. 4.15. It can be observed from Fig. 4.15 that for every particular rotational speed of the MR honing tool, a higher working gap results in less percentage alteration in surface roughness R_a value. This is due to the proportionate decrease in magnetic flux density when the working gap increases (Sidpara and Jain, 2013). With the decreased magnitude of magnetic flux density within the increased working gap, the bonding strength of CI particles chains gets decreased (Eq. 4.4) due to which the CI particles chains cannot hold the abrasives tightly and subsequently cannot perform the adequate finishing action. This results in lesser percentage alteration in surface roughness R_a value. For a particular value of the working gap, the percentage alteration in surface roughness R_a value rise with increasing the rotating speed of the MR honing tool because of the rise in the tangential cutting force exerted by the active abrasives. After the certain limit of rotating speed of MR honing tool i.e. 500 RPM in the present case, the percentage alteration in surface roughness R_a value starts

decreasing because of the shear thinning effect of MR polishing fluid (Sidpara and Jain, 2013). SiC abrasives start loosely gripped by the CIPs chains with the shear thinning effect of MR polishing fluid.

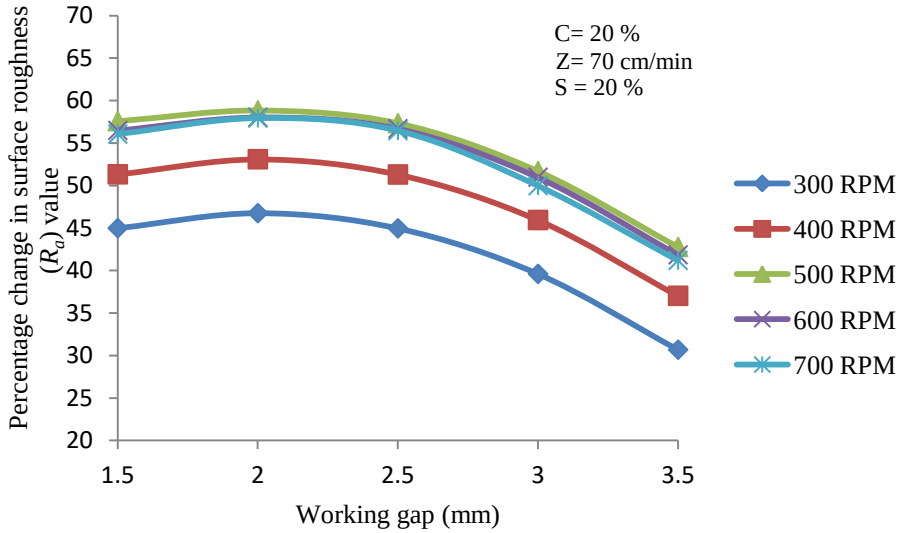

Fig. 4.15 Effect of interaction of different rotating speed of MR honing tool with working gap variation on the percentage change in surface roughness (R_a) value.

For the working gap of 1.5 mm in the present case, percentage alteration in surface roughness (R_a) value is lesser than that of the working gap of 2 mm. This is due to the high indentation force (due to high magnetization) exerted by the CI particles of the MR polishing fluid onto the inner surface of the cylindrical workpiece which creates small pit holes (Fig. 4.12b) and results in higher surface roughness R_a value. The maximum percentage alteration in surface roughness R_a value was obtained with an optimum combination of working gap as 2 mm with 500 RPM rotating speed of MR honing tool.

4.2.3.9 Effect of interaction of different concentration of silicon carbide abrasive particles with variation in working gap

The effect of interaction of different concentration of silicon carbide (SiC) abrasive particles with different working gap on percentage alteration in surface roughness R_a value with 20% carbonyl iron (CI) particles concentration, 500 RPM rotating speed of MR honing tool and 70 cm/min reciprocating speed of MR honing tool is observed as shown in Fig. 4.16. For individual working gap, the percentage alteration in surface roughness R_a value rises with increasing the percentage concentration of SiC abrasive particles due to the increase in the count of cutting edges. After further increasing the concentration of SiC abrasives beyond a particular level i.e.

20% for the present observation, results in lower percentage alteration in surface roughness R_a value.

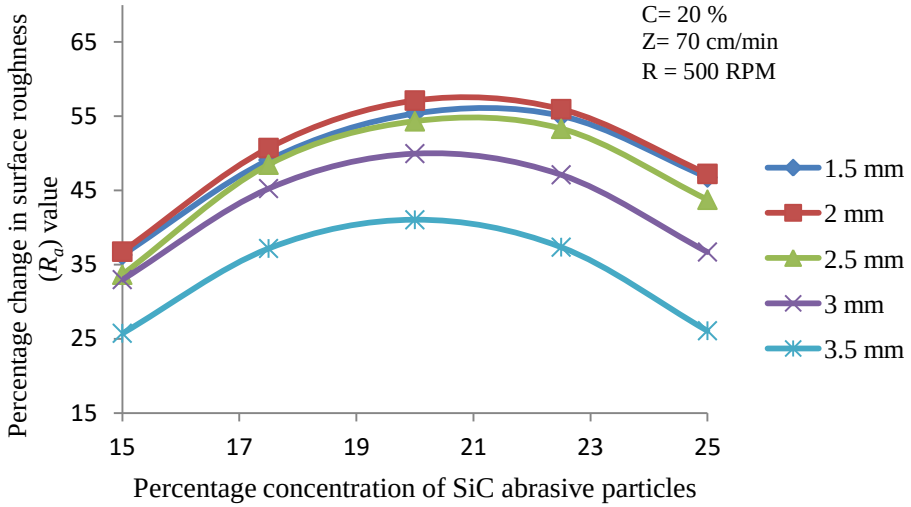

Fig. 4.16 Effect of interaction of different concentration of silicon carbide abrasive particles with different working gap on the percentage change in surface roughness (R_a) value.

The reason behind this is that after level of 20 % concentration of SiC abrasives, gripping of more number of abrasives by the same concentration of CI particles becomes difficult due to which abrasives rolls over the workpiece's surface. Percentage alteration in surface roughness R_a value rises with a reduction in the working gap (Fig. 4.16) due to increased magnetization within the working gap. Percentage alteration in surface roughness R_a value for the working gap of 1.5 mm is slightly less as compared to the gap of 2 mm due to the formation of pit holes by the more rigidly (due to high magnetization) gripped abrasives as shown in Fig. 4.12 (b). Therefore, the maximum percentage alteration in surface roughness R_a value was obtained with an optimum combination of 20% concentration of SiC abrasive particles with working gap of 2 mm.

4.2.3.10 Effect of interaction of different concentration of silicon carbide abrasive particles with reciprocating speed of MR honing tool

The effect of the interaction of different concentration of silicon carbide (SiC) abrasives with reciprocating speed of MR honing tool on percentage alteration in surface roughness R_a value with 20% carbonyl iron particle concentration, 500 RPM rotating speed of MR honing tool and a working gap of 2 mm is observed as shown in Fig. 4.17. With increasing the reciprocating speed of MR honing tool, axial force acting over the abrasives get increased due to which they erode out more material and results in increased percentage alteration in surface roughness R_a value. For a particular reciprocating speed of MR honing tool, the percentage alteration in surface

roughness R_a value rises with the rise of abrasives percentage concentration up to 20% by volume as shown in Fig. 4.17.

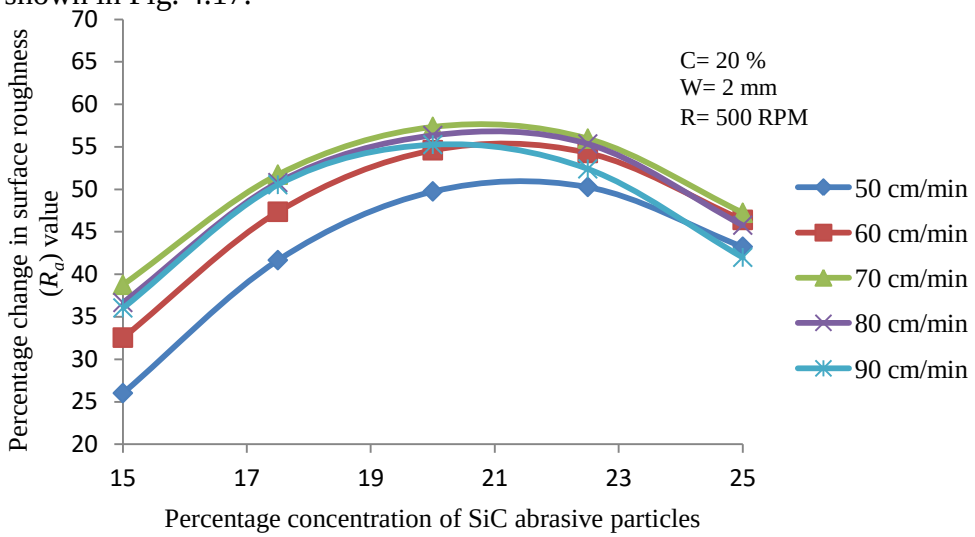

Fig. 4.17 Effect of interaction of different concentration of silicon carbide abrasive particles with different reciprocating speed of MR honing tool on the percentage change in surface roughness (R_a) value.

This is due to the increase in the count of cutting edges with the rise in percentage concentration of SiC abrasives. But after a certain limit i.e. 20% in the present observation, the rise in percentage concentration of SiC abrasives leads to the lower percentage alteration in surface roughness R_a value. The reason behind this is the accumulation of more number of abrasives on the cylindrical workpiece's inner surface which cannot be properly held by the chains of CI particles. Freely dispersed abrasives roll over the cylindrical workpiece's inner surface and are unable to carry out the finishing. The percentage alteration in surface roughness R_a value increases with the reciprocating speed of MR honing tool but limit up to the speed of 70 cm/min. After a further increase in reciprocating speed of MR honing tool, abrasives become unstable and cannot perform the adequate finishing. The maximum percentage alteration in surface roughness R_a value is obtained with a combination of 20% concentration of SiC abrasive particles with 70 cm/min reciprocating speed of MR honing tool.

4.2.4 Confirmatory experiments for validation of the regression model

To confirm the regression model obtained in Eq. (4.3) with the experimental results in terms of $\%\,\Delta R_a$ value, five different experiments have been performed. The confirmatory experiments and their similarity with the predicted designed for $\%\,\Delta R_a$ values are given in Table 4.6.

Table 4.6 Confirmatory experiments to validate the results obtained from the regression model.

Sr No.	Process parameters					Experimental (% ΔR_a) value	Predicted (% ΔR_a) value	Error (%)
	S	C	W	R	Z			
1	17.5	15	2	600	50	43.20	45.50	-5.32
2	15	20	2.5	600	70	37.11	40.05	-7.92
3	22.5	22.5	2	700	50	49.57	51.09	-3.06
4	20	22.5	2.5	300	70	38.83	39.92	-2.80
5	17.5	20	3	500	80	46.97	46.31	1.40

From the confirmatory analysis, the percentage (%) error among the experimental and predicted data lies within the range of -7.92 % to 1.40 %. The results are found to be in good agreement with each other.

4.2.5 Optimization of process parameters for better finishing performance

As the least value (R_a) of surface roughness is required for the final finished surface, therefore, to attain the highest percentage change in R_a value, the optimization of the quadratic model can be predicted from the results obtained. The optimum process parameters have been predicted on the basis of the effect of each process variable on % ΔR_a value. Optimization of process parameters has been performed in Design-Expert making use of Derringer and Suich (1980) algorithm (Derringer and Suich, 1980). For each response Y_i, a desirability function d_i (Y_i) has been assigned ranging from 0 to 1. Here 0 means completely undesirable response and 1 represent completely required response or ideal response. The individual desirabilities are then merged to obtain the overall desirability function (D) which can be calculated by Eq. (4.5).

$$D = (d_1 \times d_2 \times d_{3\ldots\ldots} d_j)^{1/j} \quad (4.5)$$

Here j represents the number of response variables. Design expert software finds out the best optimum combination of parameters having the maximum value of desirability function (D) (Montgomery, 2001). After analyzing the effect of process parameters for the higher percentage change in R_a value, the optimum process parameters have been found as mentioned in Table 4.7.

Table 4.7 Optimum process parameters.

Process parameters	Values
Percentage concentration of SiC abrasive particles (S)	20 %
Percentage concentration of CIPs (C)	20 %
MR honing tool rotating speed (R)	500 RPM
MR honing tool reciprocating speed (Z)	70 cm/min
Working gap (W)	2 mm

Feasibility of optimum process parameters of MR honing process was confirmed by performing the experimentations on the internal cylindrical workpiece's surface of EN-31 (as similar to those used in the plan of experiments) by using optimum process parameters (Table 4.7). The initial surface roughness R_a value of EN-31 cylindrical workpiece was measured as 476 nm. The experimentation was performed for 120 minutes of finishing. The MR polishing fluid was renewed after 20 minutes of finishing on the outer surface of finishing tool for maintaining the same quality of polishing fluid in each finishing cycle. The smallest value of surface roughness of 95 nm was achieved from the initial of 476 nm after 120 minutes of finishing. During the first two sets of finishing i.e. up to 40 minutes of finishing, the value of surface roughness parameter R_a decreases very quickly as it can be observed in Fig. 4.18. This is due to shearing of surface roughness peaks having sharp peaks. Change in surface roughness (R_a) value gets decreased during the successive finishing cycles.

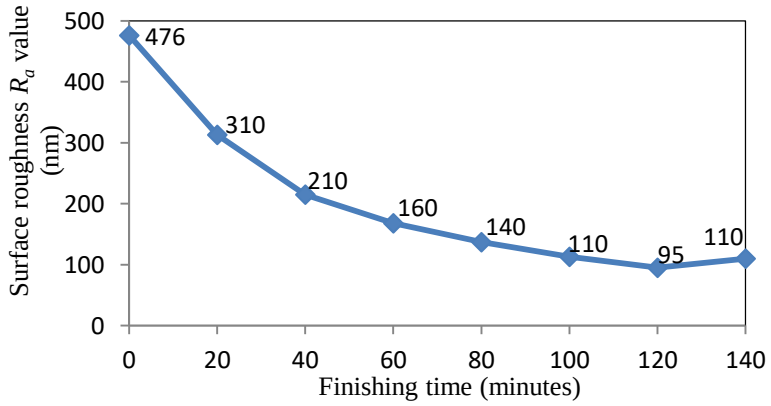

Fig. 4.18 Surface roughness R_a values with respect to finishing time with optimum process parameters.

As the finishing cycles proceed, the surface area of roughness peaks material gets increased due to which it becomes difficult to shear out the increased flattened roughness peaks having more

shear strength. After 120 minutes of finishing, roughness peaks became almost flat due to which least value of 95 nm of surface roughness parameter R_a was obtained. When one more set of 20 minutes finishing was performed, abrasives may pluck out the material from the base surface due to which at some places cavity get formed. Due to these formed cavities, the surface roughness parameter R_a get increased to 110 nm from the 95 nm of the finished surface as it can be seen in Fig. 4.18.

Percentage reduction in surface roughness parameter ($\%\Delta R_a$) obtained from both i.e. experimentally and the regression model with optimum process parameters was observed and represented in Table 4.8. Percentage error between these two values has also been evaluated as represented in Table 4.8.

Table 4.8 Comparison of the percentage change in surface roughness parameter (*Ra*) obtained from experimentation and regression model.

Optimum process parameters	**% ΔR_a (From experimentation)**	**% ΔR_a (From regression model) Eq. 4.3**	**% Error**
S= 20 % C= 20 % R= 500 rpm Z = 70 cm/min W = 2 mm	54.83	57.11	-4.15

Evaluated value from the regression model as represented in Table 4.8 signifies that the predicted value of the percentage change in surface roughness parameter (R_a) is in close agreement with the experimentally obtained value. The profiles of surface roughness of the initial ground and final finished surface after 120 minutes of finishing are represented in Figs. 4.19 (a) and (b), respectively. Scanning electron microscopy (SEM) test was also performed to inspect the performed finishing textures as shown in Figs. 4.20. Scanning electron microscopy images at 500X of initial ground surface and final finished surface after 120 minutes of finishing performed at optimum process parameters are shown in Figs. 4.20 (a) and (b) respectively.

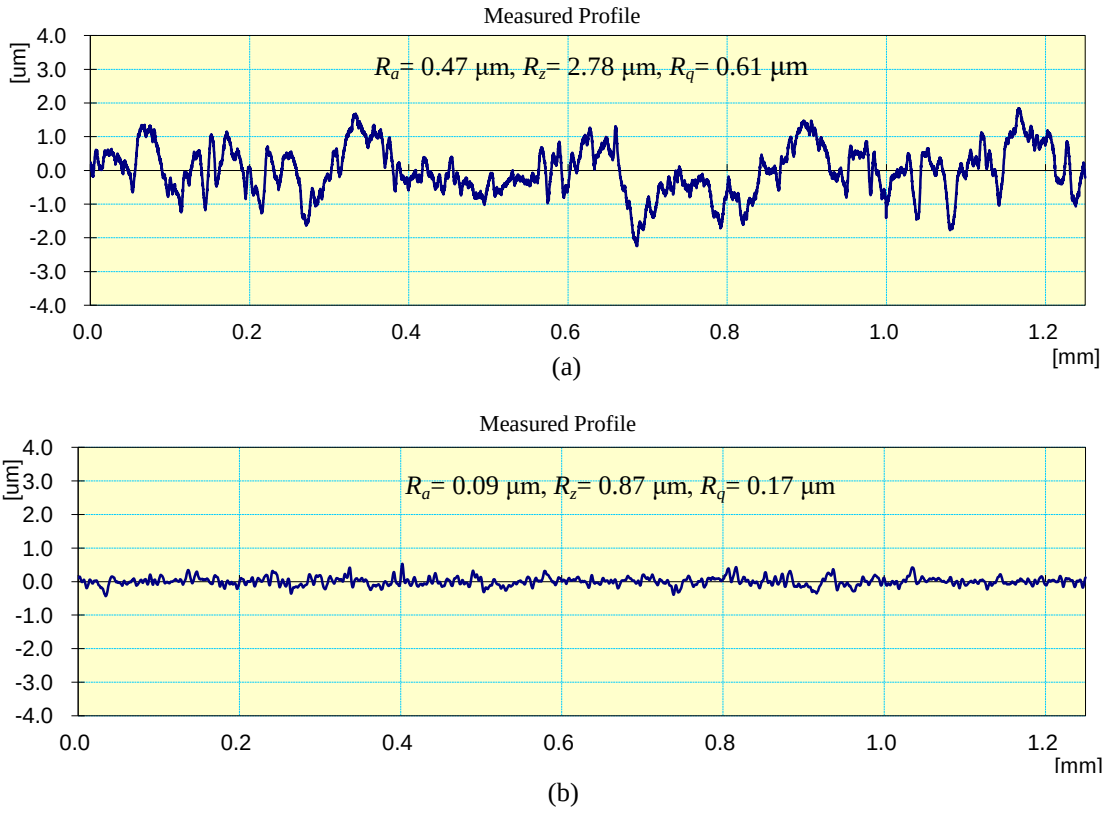

Fig. 4.19 Surface roughness profiles of (a) initial ground surface and (b) final finished surface after 120 minutes of finishing (at S= 20%, C= 20%, W= 2 mm, R= 500 RPM and Z= 70 cm/min).

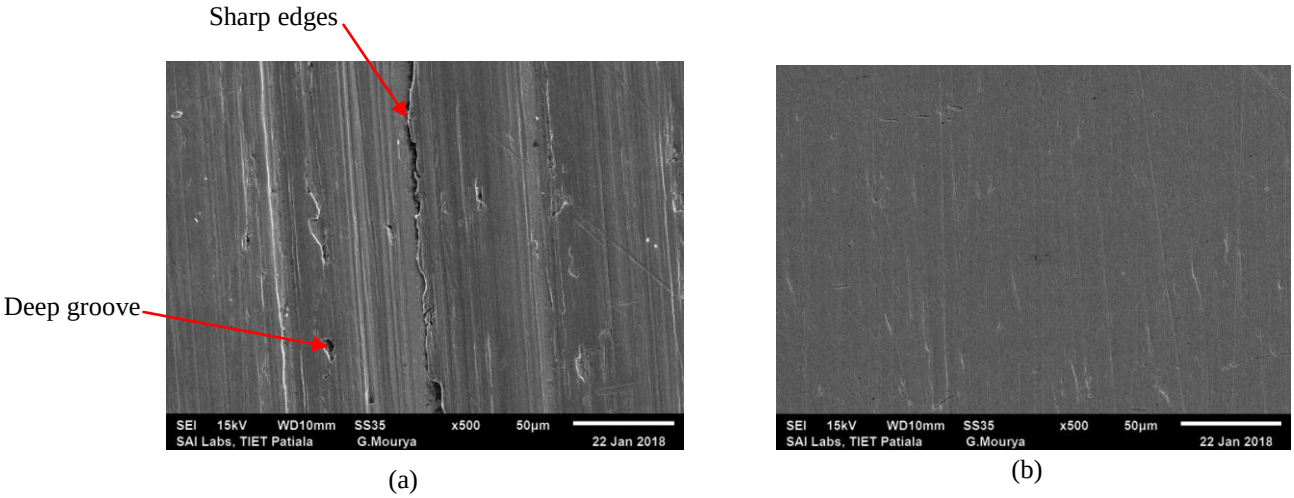

Fig. 4.20 Scanning electron microscopy images at 500X of (a) initial ground surface and (b) final finished surface after 120 minutes of finishing (at S= 20 %, C= 20 %, R= 500 RPM , Z= 70 cm/min and W= 2 mm).

From SEM images, the finishing surface textures by the present developed MR honing tool with the curved end magnetic surface has been observed. It can be clearly seen from the SEM images

that all the grinding marks and surface impurities over the inner surface of the cylindrical EN-31 workpiece have been removed to result in better-finished surface textures during the finishing performed by the present improved MR honing tool. The present developed magnetorheological (MR) honing process is useful for the significant internal finishing of the cylindrical workpieces after the traditional finishing processes to improve its functional applications. The present developed MR honing process can be used in aerospace, automobile and mechanical industry.

4.3 Conclusions

The following conclusions are drawn from the preliminary experimentations and parametric optimization of the magnetorheological honing process.

- On the inner surface of cylindrical mild steel workpiece, the surface roughness values R_a, R_q, and R_z get decreased by 76.28%, 76.67%, and 75.20%, respectively, with a magnetorheological honing tool having curved end magnetic surface in finishing time of 60 minutes. While in the case of MR honing tool with the flat end magnetic surface, these parameters get reduced by 47.97%, 46.24%, and 47.08% in the same finishing time of 60 minutes.
- The experimental results demonstrate that the improved design of MR honing tool with curved outer end magnetic surface has better process capability to finish the internal surface of the ferromagnetic cylindrical workpieces as compare to the initial designed MR honing tool having flat outer end magnetic surface in terms of reduced finishing time and better surface characteristics.
- The results obtained from the plan of experiments show that the percentage change in surface roughness R_a value was majorly contributed by the working gap followed by the tool rotating speed, the percentage concentration of SiC particles, the tool reciprocating speed and the percentage concentration of carbonyl iron particles.
- The optimum process parameters to finish the internal surface of the cylindrical ferromagnetic EN-31 steel workpiece were found as 20% volume concentration of SiC abrasive particles, 20% volume concentration of carbonyl iron particles, the rotating speed of tool as 500 RPM, the reciprocating speed of tool as 70 cm/min and the working gap of 2 mm.
- On the inner surface of ferromagnetic cylindrical EN-31steel workpiece, least surface roughness R_a value of 95 nm was achieved from the initial R_a value of 476 nm in 120 minutes

of finishing at optimum parameters with the MR honing tool having curved end magnetic surface.

- Finishing performed at different working gaps clearly demonstrate that the present developed MR honing tool with the curved end magnetic surface has flexibility for nano-finishing of the different size of the inner surface of the cylindrical workpieces.

CHAPTER 5

MATHEMATICAL MODELING OF SURFACE ROUGHNESS IN MAGNETORHEOLOGICAL HONING PROCESS

In order to predict functional performance of any particular finishing process, there is a need to theoretically analyze the material removal mechanism during its finishing operation. In this chapter, a mathematical model is developed for predicting the change in surface roughness while finishing the internal surface of ferromagnetic cylindrical workpieces with the present developed magnetorheological honing (MRH) process having tool with curved end magnetic surface. While finishing the internal surface of the ferromagnetic cylindrical workpieces, the effect of magnetic field is also induced in the working gap due to the effect of iron particles (present in the MR polishing fluid) and the ferromagnetic cylindrical workpiece. In the present work, a novel theoretical approach has been evolved to evaluate the magnitude and variation of magnetic flux density in the working gap by also considering the contribution of the effect of iron particles and ferromagnetic cylindrical workpiece. The mathematical modeling of change in surface roughness has been performed by considering the actual shape of abrasives as tetrahedron. The theoretical evaluation of magnetic normal force acting over the actual shape of tetrahedron abrasive particles has been performed due to the effect of total induced magnetic field in the working gap. The change in surface roughness value for different number of finishing cycles has been predicted with the help of the developed mathematical model. Considering the actual shape of abrasives as tetrahedron and calculating the total magnetic flux density induced in the working gap makes the developed mathematical model more practical in nature and unique for the present MRH process in finishing the ferromagnetic internal cylindrical surfaces as compared to the earlier other developed mathematical models in MR fluid based finishing processes with their different means of mechanism and applications.

5.1 Mechanism of material removal during surface finishing with the magnetorheological honing process

The present magnetorheological honing (MRH) process has been flourished for nano-finishing of the inner surface of the cylindrical workpieces (both non-ferromagnetic and ferromagnetic) with different internal diameters. The present MRH process constitutes of a MR honing tool having four radial polarized curved permanent magnet strips. These magnet strips are symmetrically

patterned about the central axis of the finishing tool at an angle of 90^0 from each other as shown in Fig. 5.1 (a). The schematic diagram of MRH tool used for finishing the different diametric sizes of the internal surface of the cylindrical workpieces is shown in Fig. 5.1 (a).

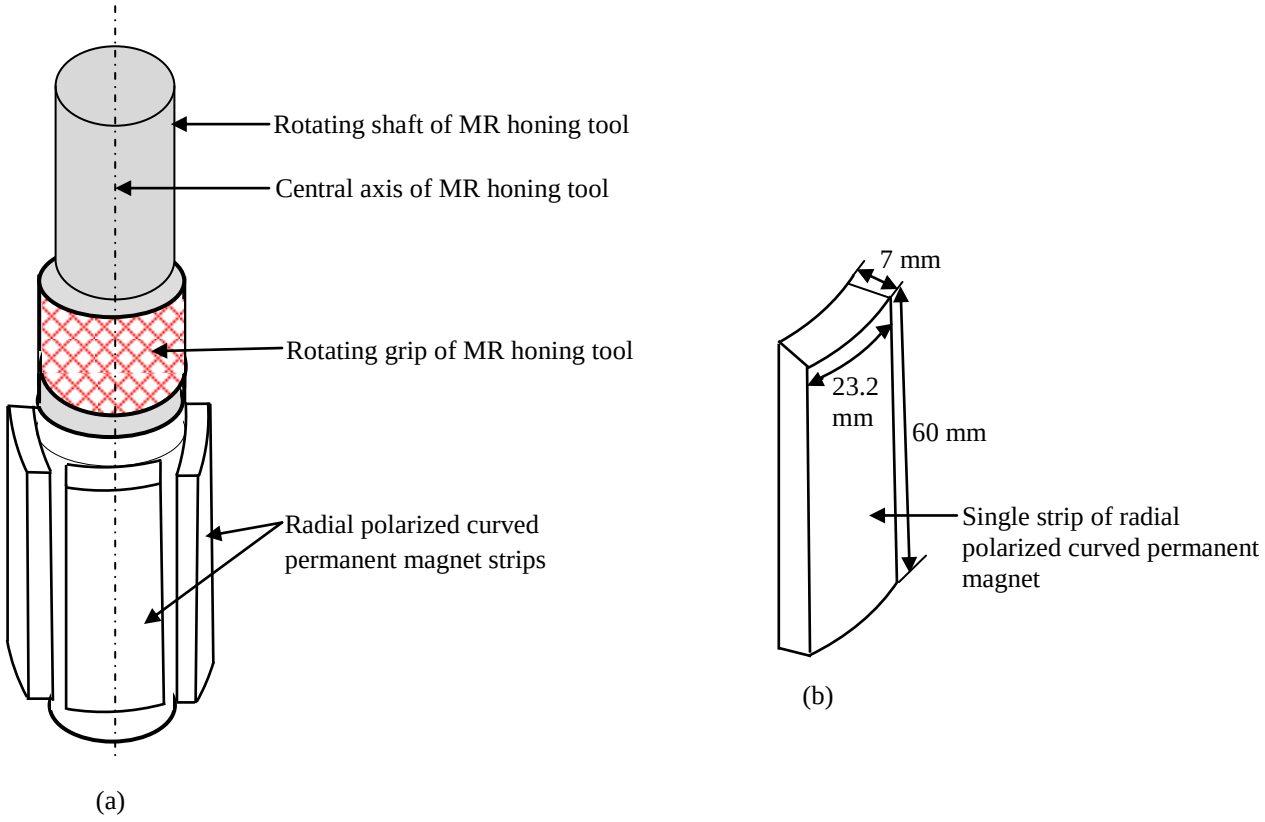

Fig. 5.1 (a) Schematic diagram of magnetorheological honing tool having curved permanent magnet strip over the outer periphery and (b) dimensions of single radial polarized curved magnet strip.

Each of the radial polarized curved permanent magnet strips has the thickness of 7 mm, arc length 23.2 mm and length of 60 mm as shown in Fig. 5.1 (b). The MRH tool has a unique rotating grip in it as shown in Fig. 5.1 (a). This rotating grip is used to move all the four permanent magnet strips, radially inwards or outwards simultaneously as per the requirement of the diametric size of the cylindrical inner surface to be finished. The MRH tool with the MR polishing fluid is rotated as well as reciprocated into the cylindrical component to finish its internal surface. When the MR polishing fluid is applied on the outer curved magnetic surfaces of the MRH tool, it becomes stiff due to the induction of magnetic field by the curved permanent magnetic strips. When the MRH tool with stiffened MR polishing fluid over its surface is inserted into the ferromagnetic cylindrical workpiece, the ferromagnetic workpiece gets

magnetized due to which the total magnitude of magnetic flux density in the working gap gets increased. The increased magnetic field in the working gap makes the MR polishing fluid stiffer. The iron particles make chains in the working gap due to the induced magnetic field. Because of the higher magnitude of magnetic flux density over the curved end surface of the permanent magnet strips, the magnetic iron particles attract towards the outer surface of the finishing tool. The magnetic force exerting over the iron particles due to the induced magnetic field attracts the iron particles towards the outer curved end surface of the permanent magnetic strips of the finishing tool. The non-magnetic tetrahedron shaped SiC abrasives present in the MR polishing fluid gets gripped in between the chains of iron particles and are pushed with levitation force towards the cylindrical component's internal surface as represented in Fig. 5.2 (a). Due to this levitation force, the SiC particles get embedded in between the peaks of surface roughness present over the cylindrical workpiece's internal surface with the action of indentation force (F_i) as represented in Fig. 5.2 (b). With the movement of MRH tool inside the cylindrical workpiece, gripped tetrahedron shaped SiC abrasives exhibits relative motion with the internal surface of the cylindrical component and removes the material from it by the shearing action. In this way, the developed MRH tool performs finishing on the internal surface of the cylindrical components. The abrasives which are present on the internal surface of cylindrical components and perform finishing are called active abrasives.

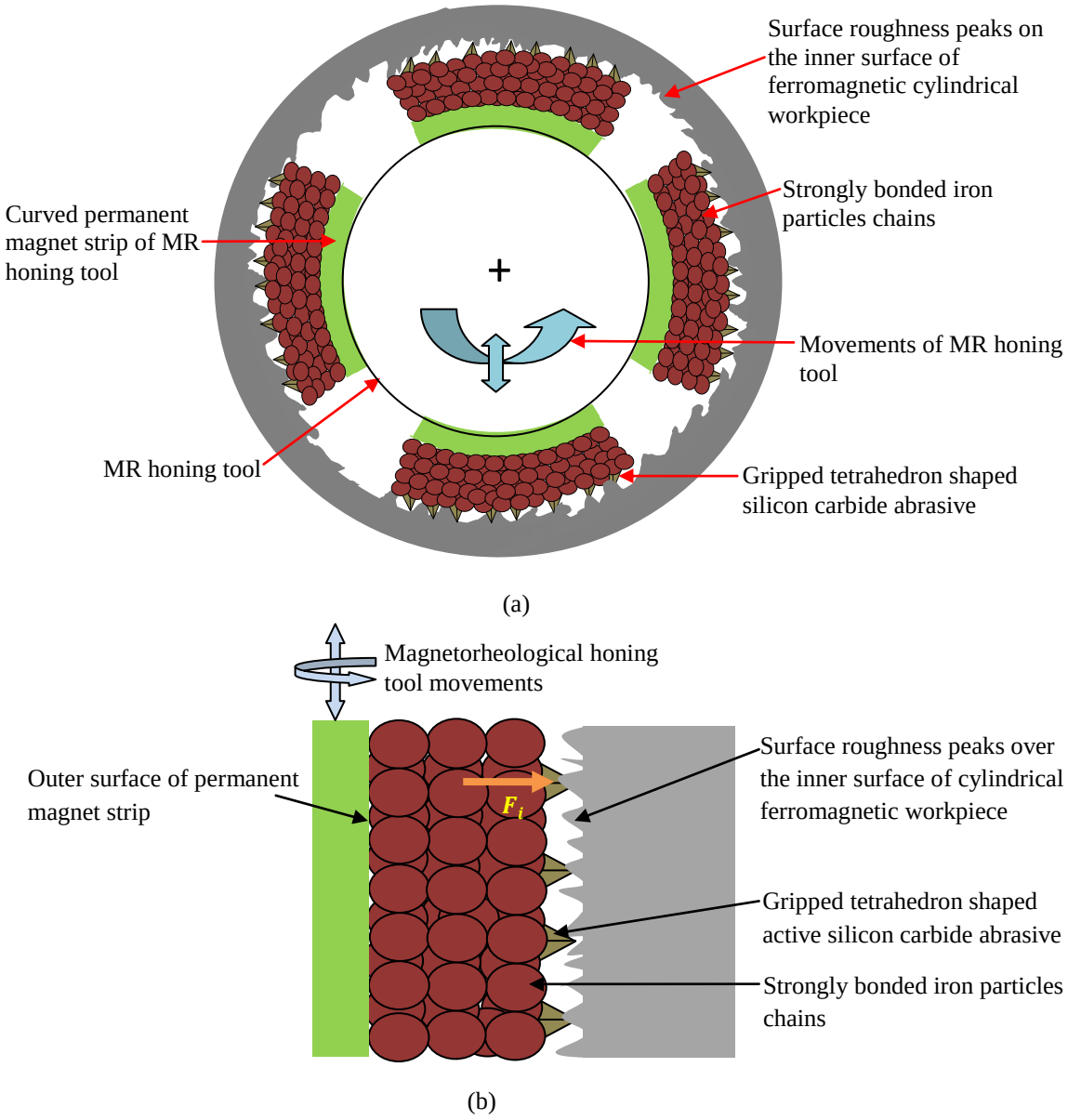

Fig. 5.2 (a) Schematic diagram of the magnetorheological honing process perform finishing over the inner surface of the ferromagnetic cylindrical workpiece and (b) enlarged cross-sectional front view shows the mechanism of surface finishing by the present developed process.

5.2 Mathematical modeling of surface roughness in the present magnetorheological honing (MRH) process

In the current work, an effort has been made to theoretically develop the mathematical model for calculating the magnitude of magnetic flux density in the working gap, indentation force exerting over tetrahedron shaped active SiC particles and decrease in surface roughness due to the removal of material while performed finishing by the present MRH process. For developing the

mathematical model in the MRH process, the certain assumptions have been taken into accounts which are given below:

- Dispersion of iron particles and shaped SiC abrasives is homogenous in the MR polishing fluid.
- Losses and leakages of the magnetic field have not been considered for the computation of normal force acting on the iron particles.
- The magnetic normal force acting over the active SiC abrasives is mainly responsible for their indentation into the roughness peaks present over the cylindrical workpiece internal surface.
- Silicon carbide abrasives are assumed as tetrahedron in shape with an edge length of 21.8 μm as per the ASTM and FEPA (Federation of European Producers of Abrasives) standards.
- Iron particles are assumed as spherical shaped with an average diameter of 15 μm.
- Interference of magnetic field in the MR polishing fluid region due to the positioning of four curved permanent magnet strips into the ferromagnetic cylindrical workpiece has not been considered.

There are various parameters on which the finishing performance of the present MRH process depends. Fig. 5.3 shows the fishbone diagram which shows the process parameters used in the present MRH process. Material from the internal surface of the cylindrical component is removed by the shearing action which is performed by the movement of abrasives on the cylindrical workpiece's inner surface. SiC abrasives are entangled in between the CIPs chains and are strongly gripped by the chains. As the CIPs chains strongly stick to the outer surface of the MR honing tool so they move with the movement of the MR honing tool. When the MR honing tool rotates and reciprocates inside the ferromagnetic cylindrical workpiece, there becomes a relative movement between the SiC abrasives and the inner surface of the cylindrical workpiece. The SiC abrasive particles pluck out material in micro-sized particles from the inner surface of the cylindrical workpiece. Strongly held abrasives by the iron particles chains indent into the cylindrical workpiece's inner surface and pluck out the material in the shape of tiny micro-sized particles with the movement of finishing tool. Here micro-sized particles mean that the sheared-out material (in the form of chips) by the SiC abrasive particles whose dimensions are in microns. The size of the microchip depends on the indentation of the micron size active abrasive particles on the workpiece surface during its finishing in various stages i.e. from the

initial ground surface to final nano-finishing. If it is an initial cutting from the ground rough surface then the chip size may predict in certain more microns size. But, when it is in the stage of nano-finishing, then the chip size may be predicted in very small micron sizes due to comparatively less indentation on the already finished surface.

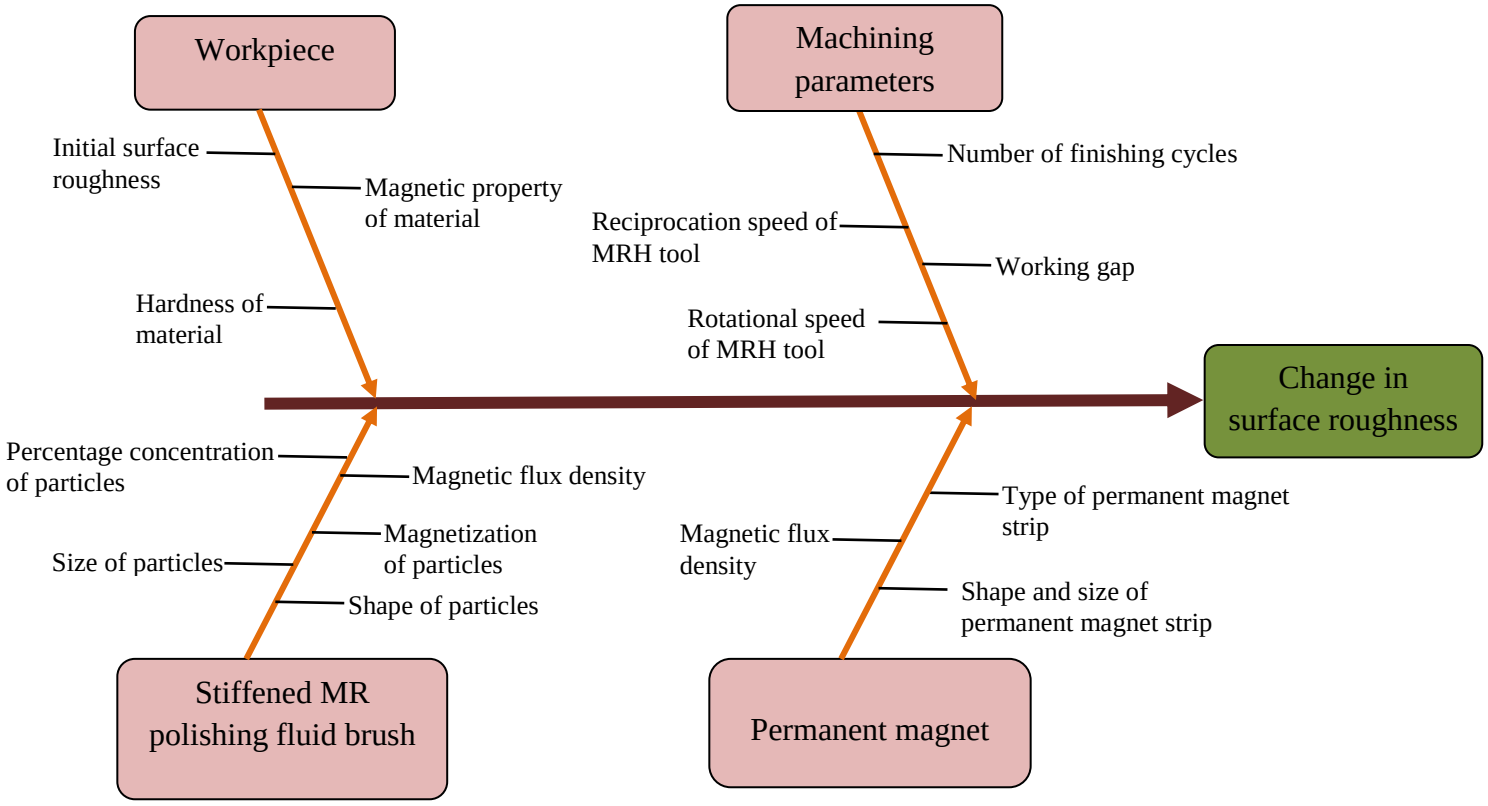

Fig. 5.3 Fishbone diagram exemplifying all the major parameters of the MRH process.

5.2.1 Calculation for number of active silicon carbide (SiC) abrasive particles present over the inner surface of cylindrical workpiece

The working gap in between the outer curved surface of the MR honing tool and the internal surface of the cylindrical workpiece is filled with the MR polishing fluid. The MR polishing fluid sticks over the outer curved surface of the four permanent magnet strips forming the sectors. When the outer end surface of the MRH tool with stuck MR polishing fluid is inserted into the ferromagnetic cylindrical workpiece to finish its internal surface, then the MR polishing fluid form an arc-like structure subtending an angle $(\theta_2^{'} - \theta_1^{'})$ over the outer curved end surface of the MRH tool magnetic strips in working gap as shown in Fig. 5.4 (a).

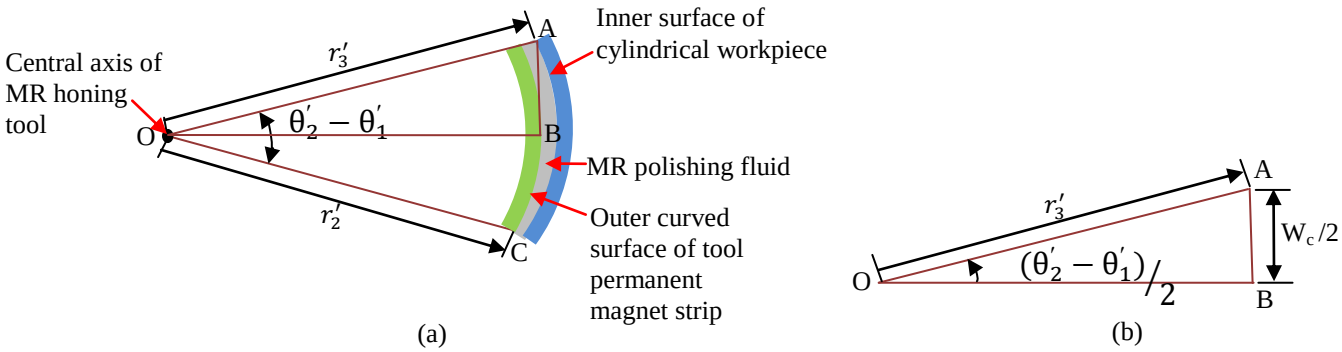

Fig. 5.4 (a) Sector formed by the MR polishing fluid over the tool outer curved end surface of the single permanent magnet strip in the MR honing process and (b) right-angle triangle formed by the MR polishing fluid over the tool outer curved end surface.

In Fig. 5.4 (a), r_2' is the radius of MR honing tool which is equal to 28.3 mm and r_3' is the inner radius of the ferromagnetic cylindrical workpiece over which finishing is performed and is equal to 31 mm for the present case. Considering the right angle triangle ΔAOB formed by the half of the sector as shown in Fig. 5.4 (b). The half of the angle subtended by the arc $(\frac{\theta_2'-\theta_1'}{2})$ can be calculated as given in Eq. (5.1).

$$\frac{(\theta_2'-\theta_1')}{2} = \sin^{-1}\left(\frac{w_c/2}{r_3'}\right) \tag{5.1}$$

where w_c is the total width of MR polishing fluid present on the solitary strip of the tool outer curved surface of the permanent magnet to finish the cylindrical workpiece's internal surface. Putting the values of w_c and r_3' for the present case of MRH process in Eq. (5.1), the value of $(\theta_2' - \theta_1')$ is calculated as given in Eqs. (5.2) and (5.3) subsequently.

$$\frac{(\theta_2'-\theta_1')}{2} = \sin^{-1}\left(\frac{12.3}{31}\right) \tag{5.2}$$

$$(\theta_2' - \theta_1') = 46.75^{\circ} \tag{5.3}$$

The MR polishing fluid sticks only over the tool curved end surface of the four permanent magnetic strips. So, when the MR honing tool moves inside the cylindrical workpiece, the stuck MR polishing fluid with the curved end surface of the four permanent magnetic strips perform finishing over the inner cylindrical surface. The internal surface area of cylindrical workpiece covered by the MR polishing fluid (A_{inner_single}), with the single strip of the curved permanent magnet which takes part in finishing, is evaluated using the Eq. (5.4).

$$A_{inner\_single} = \frac{2\pi r_3' h_w (\theta_2'-\theta_1')}{360} \tag{5.4}$$

Where h_w represent the height of cylindrical workpiece. Total inner surface area of cylindrical workpiece covered by the MR polishing fluid (A_{inner_total}), with the four strips of the curved permanent magnet which takes part in finishing, is calculated by Eq. (5.5).

$$A_{inner\_total} = 4 \times A_{inner\_single} = \frac{8\pi r_3' h_w(\theta_2' - \theta_1')}{360} \quad (5.5)$$

Number of active SiC particles (N_{AAP}) present over the ferromagnetic cylindrical workpiece's internal surface is evaluated by Eq. (5.6) (Singh *et* al., 2013).

$$N_{AAP} = \frac{\%\ volume\ of\ SiC\ particle \times A_{inner\_total} \times height\ of\ abrasive\ particle}{volume\ of\ single\ SiC\ abraive\ particle} \quad (5.6)$$

The volume of tetrahedron shaped single SiC particle present in MR polishing fluid is calculated by Eq. (5.7).

$$V_{SiC\_tetra} = \frac{a^3}{6\sqrt{2}} \quad (5.7)$$

where a is the edge length of SiC abrasive which is equal to 21.8 μm in the present case. The height of tetrahedron shaped single silicon carbide (SiC) abrasive can be calculated by Eq. (5.8).

$$h_{SiC\_tetra} = \sqrt{\frac{2}{3}}a \quad (5.8)$$

Number of active SiC particles per unit area (1mm×1mm) (N_a) present over the inner surface of the cylindrical workpiece can be evaluated by Eq. (5.9).

$$N_a = \frac{N_{AAP}}{A_{inner\_total}} \quad (5.9)$$

Using Eq. (5.6), the Eq. (5.9) can be further represented as Eq. (5.10).

$$N_a = \frac{\%\ volume\ of\ SiC\ particle \times height\ of\ abrasive\ particle}{volume\ of\ single\ SiC\ abraive\ particle} \quad (5.10)$$

The percentage concentration of SiC particles in MR polishing fluid is 20% in the present work. Using the Eqs. (5.7) and (5.8) in Eq. (5.10), the number of active SiC abrasives present per unit area (N_a) over the cylindrical workpiece's inner surface is calculated as given in Eq. (5.11).

$$N_a = 2915 / mm^2 \quad (5.11)$$

5.2.2 Computation of magnetic flux density distribution induced by the effect of magnetic tool, iron particles and ferromagnetic cylindrical workpiece in the present magnetorheological honing process

Finishing performance of the processes which make use of MR polishing fluid mainly depends on the distribution of magnetic flux density in the working gap. The bonding strength of MR polishing fluid present in the working gap depends on the magnitude of magnetic flux density

and its distribution in the working gap. If more stiff of the MR polishing fluid in the working gap, the better shear strength of MR polishing fluid can be found and it performs better finishing in MR fluid based finishing processes. In the present developed MRH process, the four radial polarized curved permanent magnet strips constituted the MR honing tool as shown in Fig. 5.1 (a), are used for internal surface finishing of the cylindrical workpieces with different diameters. The magnetic field is induced in the working gap due to which the MR polishing fluid becomes stiffen and performs finishing by its predetermined movements. In the present work, the magnetic field induced by the single curved radial polarized permanent magnet strip is analyzed for which a local XYZ coordinate system is considered as shown in Fig. 5.5 (a).

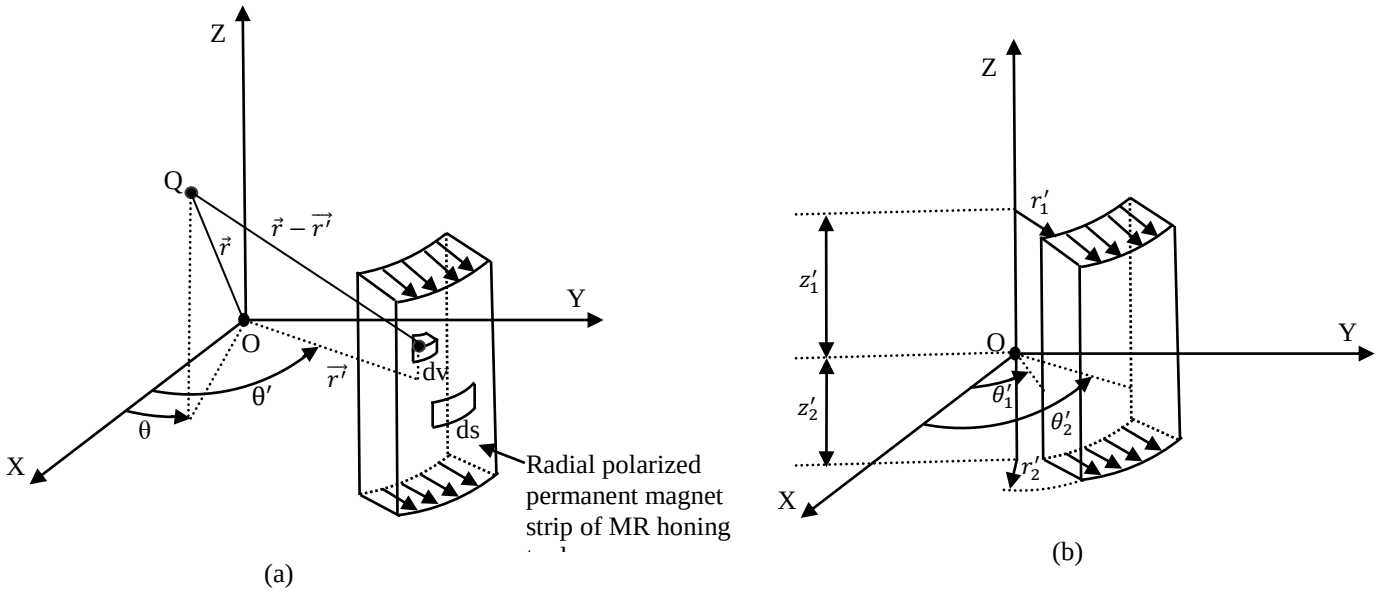

Fig. 5.5 (a) Evaluating magnetic field induced by volume and surface charge density on a point Q in cylindrical co-ordinate and (b) orientation of permanent magnet strip in the co-ordinate system for calculating the magnetic flux density.

The curved permanent magnet strip is considered in the three dimensional XYZ coordinate system as shown in Fig. 5.5 (a). The height of the magnet strip is considered along the Z-axis of the coordinate system. For calculating magnetic field due to single radial polarized curved permanent magnet strip, the dimensions of a magnet strip has been considered in the cylindrical co-ordinate i.e. r, θ, and z. The magnetic scalar potential Φ produced by the permanent magnet strip can be written by Eq. (5.12).

$$\vec{H} = -\vec{\nabla}.\Phi \tag{5.12}$$

An observation point Q is considered in the coordinate system as shown in Fig. 5.5 (a) to evaluate the induced magnetic field due to the considered permanent magnet strip. An infinitely

small element is considered in the curved permanent magnet strip with volume of dv and surface area of ds. This small element has surface charge density (σ_S) and volume charge density (σ_v). Magnetic field intensity (H) at point Q (present in the co-ordinate system) due to the considered small element is evaluated. Using electrostatic approach for Eq. (5.12), the magnetic field intensity produced by the permanent magnet strip at point Q can be expressed by Eq. (5.13) (Rakotoarison *et* al., 2007).

$$\overrightarrow{H_Q} = \frac{1}{4\pi\mu_0}.\left(\iint_S \frac{\sigma_s(\vec{r}-\vec{r'})}{\vec{r}-\vec{r'}|^3}\, ds + \iiint_v \frac{\sigma_v(\vec{r}-\vec{r'})}{|\vec{r}-\vec{r'}^3}\, dv\right) \tag{5.13}$$

where radii $\vec{r}$ and $\vec{r'}$ represents the position of Q (observation point) from the origin and extent of the field source enclosed by dv or ds from the origin respectively as shown in Fig. 5.5 (a). Orientation of permanent magnet strip in the co-ordinate system for calculating magnetic flux density is shown in Fig. 5.5 (b). Here $r_1^{'}$ and $r_2^{'}$ represents the inner and outer radii of curved magnet strip from the z-axis. $\theta_1^{'}$ and $\theta_2^{'}$ represents the start and end angle of the magnetic strip from the x-axis respectively. $z_1^{'}$ and $z_2^{'}$ represents the upper and lower half height of the magnet strip respectively from the origin as represented in Fig. 5.5 (b). The dimensional parameters of radial polarized magnets used in the present magnetorheological honing process are mentioned in Table 5.1.

Table 5.1 Dimensional parameters of radial polarized magnet strip used in the magnetorheological honing tool.

Symbols	Parameters	Values
$r_1^{'}$	Inner radius of permanent magnet strip	21.3 mm
$r_2^{'}$	Outer radius of permanent magnet strip	28.3 mm
$\theta_1^{'}$	Start angle of permanent magnet strip	-13π/100
$\theta_2^{'}$	End angle of permanent magnet strip	13π/100
$z_1^{'}$, $z_2^{'}$	Half height of permanent magnet strip	30 mm

Magnetic field at an arbitrary point (r, θ, z) in the cylindrical co-ordinate system from a radial polarized permanent magnet is due to the three components of the magnetic field. These components of magnetic field are in radial, axial and azimuthal direction. Three components of magnetic field intensity are found by summing up the all evaluated smaller magnitude of magnetic field intensity due to the presence of small element in all three directions. The radial

component of the magnetic field intensity at any point due to the single considered present radial polarized magnet strip (Fig. 5.5) can be expressed by Eq. (5.14) (Rakotoarison *et* al., 2007).

$$H_r(r,\theta,z) = \frac{J}{4\pi\mu_0}.\int_{\theta_1^{'}}^{\theta_2^{'}} \sum_{i=1}^{2}\sum_{j=1}^{2}(-1)^{i+j} dH_r(r,\theta,z,r_i^{'},\theta^{'},z_j^{'})\, d\theta^{'} \tag{5.14}$$

where dH_r can be written as in Eq. (5.15).

$$dH_r\left(r,\theta,z,r_i^{'},\theta^{'},z_j^{'}\right) = \frac{-r_i^{'}\left(z-z_j^{'}\right)\left(r-r_i^{'}\cos(\alpha)\right)}{\left[\left(r-r_i^{'}\cos(\alpha)\right)^2+\left(r_i^{'}\sin(\alpha)\right)^2\right].P(\alpha)} + \sin(\alpha)\tan^{-1}\left[\frac{\left(z-z_j^{'}\right)\left(r_i^{'}-r\cos(\alpha)\right)}{(r\sin(\alpha)).P(\alpha)}\right] - \cos(\alpha)\ln\left[P(\alpha)-\left(z-z_j^{'}\right)\right] \tag{5.15}$$

here $r, \theta\ and\ z$ represents the radius from the origin, angle from the x-axis and vertical distance from the X-Y plane respectively of the point where the magnetic field is required to be calculated. The two relations as expressed in Eqs. (5.16) and (5.17) are used in evaluating the three components of magnetic field intensity.

$$\alpha = \theta^{'} - \theta \qquad \text{with} \qquad \theta_1^{'} \leq \theta^{'} \leq \theta_2^{'} \tag{5.16}$$

$$P(\alpha) = \sqrt{\left(r - r_i^{'}\cos(\alpha)\right)^2 + (r_i^{'}\sin(\alpha))^2 + \left(z - z_j^{'}\right)^2} \tag{5.17}$$

here α is the difference between the angles $\theta^{'}$ and θ. The θ is the angle from the x-axis where magnetic field is required to find out and the $\theta^{'}$ is start or end angles (Fig. 5.5a). The magnetic field intensity at a point is evaluated by summing up the contribution of small-small elemental units present in the complete single permanent magnet strip. It is performed by adding up the several iterations corresponding to the different consecutive values of i and j which ranges from 1 to 2. Here $P(\alpha)$ defines distance between the points where magnetic field is required to find out and different small-small elemental units corresponding to the different consecutive values of i and j while summing the various iterations to calculate the magnetic field.

Similarly, the azimuthal component of the magnetic field intensity at a point due to the single considered present radial polarized magnet (Fig. 5.5) can be expressed by Eq. (5.18).

$$H_\theta(r,\theta,z) = \frac{J}{4\pi\mu_0}.\int_{\theta_1^{'}}^{\theta_2^{'}} \sum_{i=1}^{2}\sum_{j=1}^{2}(-1)^{i+j} dH_\theta(r,\theta,z,r_i^{'},\theta^{'},z_j^{'}) d\theta^{'} \tag{5.18}$$

where,

$$dH_\theta\left(r,\theta,z,r_i^{'},\theta^{'},z_j^{'}\right)=$$

$$\frac{-r_i^{'}(z-z_i^{'})(r_i^{'}\sin(\alpha))}{\left[(r-r_i^{'}\cos(\alpha))^2+(r_i^{'}\sin(\alpha))^2\right].P(\alpha)}-\cos(\alpha)\tan^{-1}\left[\frac{(z-z_i^{'})(r_i^{'}-r\cos(\alpha))}{(r\sin(\alpha)).P(\alpha)}\right]-\sin(\alpha)\ln\left[P(\alpha)-\left(z-z_i^{'}\right)\right] \quad (5.19)$$

Also, the axial component of the magnetic field intensity at a point due to the single considered present radial polarized magnet strip (Fig.5.5) can be expressed by Eq. (5.20).

$$H_z(r,\theta,z)=\frac{J}{4\pi\mu_0}.\int_{\theta_1^{'}}^{\theta_2^{'}}\sum_{i=1}^{2}\sum_{j=1}^{2}(-1)^{i+j}dH_z(r,\theta,z,r_i^{'},\theta^{'},z_j^{'})d\theta^{'} \quad (5.20)$$

where,

$$dH_z\left(r,\theta,z,r_i^{'},\theta^{'},z_j^{'}\right)=\frac{r_i^{'}}{P(\alpha)}-\ln\left[(r_i^{'}-r\cos(\alpha))+P(\alpha)\right]+\frac{1}{2}\ln[(r\sin(\alpha))^2+\left(z-z_i^{'}\right)^2] \quad (5.21)$$

In Eqs. (5.14), (5.18) and (5.20), *J* represents magnetic polarization of the permanent magnet and its value is taken as 1.519 Tesla for NdFeB permanent magnet in the present work (Rodewald *et* al., 2002). The magnitude of magnetic field intensity at an arbitrary point due to the single considered present radial polarized permanent magnet strip in the XYZ coordinate system is the resultant of all three components and can be calculated by Eq. (5.22).

$$H_0=\sqrt{H_r^2+H_\theta^2+H_z^2} \quad (5.22)$$

The magnetic flux density (B) at a particular point can be evaluated from the magnetic field intensity (H_0) using the relation as given in Eq. (5.23).

$$B_0=\mu_0 H_0 \quad (5.23)$$

here μ_0 represents the magnetic permeability of free space and is equivalent to $4\pi\times10^{-7}$ H/m. Eq. (5.23) gives the magnitude of magnetic flux density at a particular point in the co-ordinate system due to the single considered present radial polarized curved permanent magnet strip (Fig. 5.5). When MR honing tool with stiffened MR polishing fluid is inserted into the ferromagnetic cylindrical workpiece to finish its internal surface, the magnetic field in the working gap gets increased due to the magnetic effect of iron particles (present in MR polishing fluid) and the ferromagnetic cylindrical workpiece. Thus, total magnetic flux density (B) at any point in the working gap is the summation of magnetic flux density due to the single considered present radial polarized curved permanent magnet strip (B_0), also due to the effect of magnetic iron

particles and the ferromagnetic cylindrical workpiece. This total magnetic flux density (B) at any point in the working gap can be calculated by the Eq. (5.24).

$$B = B_0 + \mu_0\mu_{MR}M_{IP} + \mu_0\mu_{wrk}M_{wrk} \quad (5.24)$$

where μ_{MR} and μ_{wrk} represents the relative permeability of MR polishing fluid and ferromagnetic cylindrical steel workpiece, respectively. In the present work, values of μ_{MR} and μ_{wrk} are considered as 5 and 600 respectively (Singh *et* al., 2013). M_{IP} represents the magnetization of iron particles of MR polishing fluid in the working gap at that particular point where the iron particle is situated. The magnetization of iron particles of MR polishing fluid in the working gap is due to the induced magnetic flux density (B_0) from a radial polarized curved permanent magnet strip and also due to the effect of the ferromagnetic cylindrical workpiece. The value of M_{IP} is acquired from the M-B curve for the different iron particles at that particular point where the iron particle is situated in the working gap as represented in Fig. 5.6 (a).

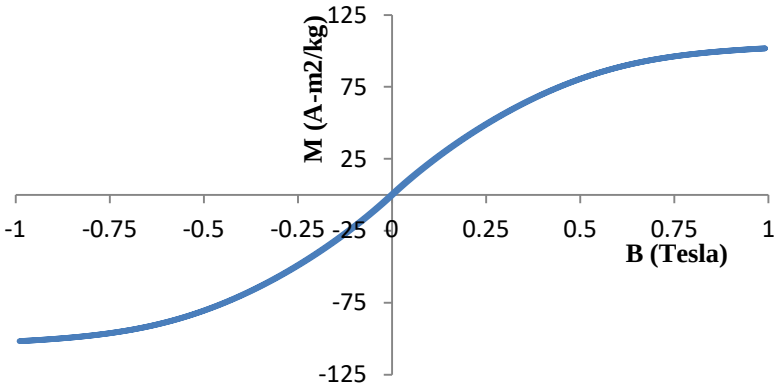

(a)

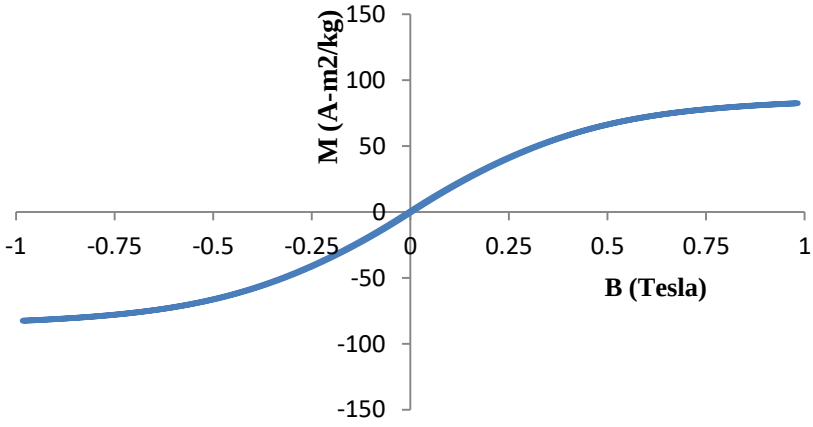

(b)

Fig. 5.6 M-B curve for (a) electrolytic iron particles and (b) ferromagnetic cylindrical steel.

M_{wrk} represent the magnetization of ferromagnetic cylindrical steel workpiece corresponding to the induced magnetic flux density (because of a curved permanent magnet strip and iron particles in working gap) at that particular point where the ferromagnetic workpiece is situated and its value is acquired from the M-B curve for ferromagnetic cylindrical steel as shown in Fig. 5.6 (b).

Using Eqs. (5.14) – (5.24) and the dimensional parameters of a radial polarized curved permanent magnet strip used in the present magnetorheological honing process as mentioned in Table 5.1, the magnitude of magnetic flux density has been calculated from the center of the curved permanent magnet strip in the MR polishing fluid region (working gap) towards the desired radial direction to get the magnetic indentation force on the cylindrical internal surface by considering θ=0 and z=0.

The theoretically evaluated distribution of magnitude of magnetic flux density in MR polishing fluid region (working gap) in the horizontal direction from the center of a curved permanent magnet strip towards the ferromagnetic cylindrical inner surface is calculated using the Eq. (5.24) and reported in Table 5.2. This calculated distribution of magnetic flux density values in working gap can be represented by the Eq. (5.25) having a best fitting curve of R^2=0.99.

$$B(r) = 369.72r^2 - 42.445r + 1.2151 \quad (5.25)$$

here *r* represents the distance from the outer surface of a curved permanent magnet strip to the ferromagnetic cylindrical component's inner surface in meters which is ranging from 0.0283m to 0.031m. The magnitude of magnetic flux density at different points in the working gap has also been measured experimentally with the help of digital gaussmeter and the results are reported in Table 5.2. Experimentally, a similar trend of decreasing the magnitude of magnetic flux density (B) (moving from tool's outer surface to the inner surface of the ferromagnetic cylindrical workpiece) is obtained as evaluated from the mathematical model (Table 5.2). The magnitude of magnetic flux density at different points in working gap evaluated from the mathematical model is in close agreement with the experimentally measured values of magnetic flux density at same points in working gap. Apart from evaluating the magnetic flux density variation in the MR polishing fluid region by the mathematical model and experimentally measured, the magnetic flux density variation has also been evaluated by performing finite element (FE) analysis in Maxwell Ansoft V13 software to validate the mathematical model.

Table 5.2 Magnitude of magnetic flux density in the MR polishing fluid region (working gap) and the magnetic normal force acting on iron particles present in the working gap.

Sr. No.	Distance from the central axis of MRH tool (m)	Magnitude of magnetic flux density B (Tesla) from theoretical mathematical model (Eq. (5.24))	Magnitude of magnetic flux density (Tesla) (measured experimentally)	Magnitude of magnetic flux density (Tesla) from finite element (FE) simulation performed in Maxwell Ansoft	Magnetic normal force acting on iron particle (F_I), $\times 10^{-8}$ (Newton) (Eq. (5.29))
1.	0.0283	0.31	0.32	0.51	1.94
2.	0.0289	0.30	0.31	0.49	1.87
3.	0.0293	0.29	0.31	0.48	1.82
4.	0.0299	0.28	0.29	0.47	1.72
5.	0.0303	0.27	0.28	0.46	1.61
6.	0.0310	0.25	0.26	0.44	1.52

The present developed magnetorheological honing tool with the presence of MR polishing fluid in working gap and the ferromagnetic cylindrical workpiece is modeled and numerically analyzed through FE with solution type of magnetostatic. The MR honing tool consisting of four curved permanent magnet strips made up of NdFeB (dimensions as mentioned in Table 5.1) with magnetic coercivity of 7.8 kA/cm (Rodewald *et* al., 2002), is modeled in Maxwell Ansoft V13 software. In the magnetostatically FE modeling, the relative permeability of MR polishing fluid is taken as 5 in the working gap of 2.7 mm along with the ferromagnetic cylindrical workpiece of relative permeability as 600 (Singh *et* al., 2013). The entire setup is insulated at the boundaries to avoid magnetic flux losses or leakages. The setup is simulated with solution type of magnetostatic. Ignorance of maximum surface deviation has been placed for initial mesh settings. Simulation has been performed with default settings of maximum normal deviation and maximum aspect ratio. The analysis of setup has been performed by keeping auto mesh generation with a percentage error of 1 and 10 numbers of passes. The distribution of magnetic flux density on the plane passing through the middle of cross-section of MR honing setup is evaluated from the FE analysis as shown in Fig. 5.7. From the Fig. 5.7, it can be observed that there is uniform distribution of magnetic flux density over the curved outer surface of the two permanent magnet strips as shown by the dotted line (A_1) in Fig. 5.7. On the other hand, the

magnitude of magnetic flux density decreased from the outer edges (A_2) to the middle over the curved surface (A_3) of the rest two magnetic strips as shown in Fig. 5.7.

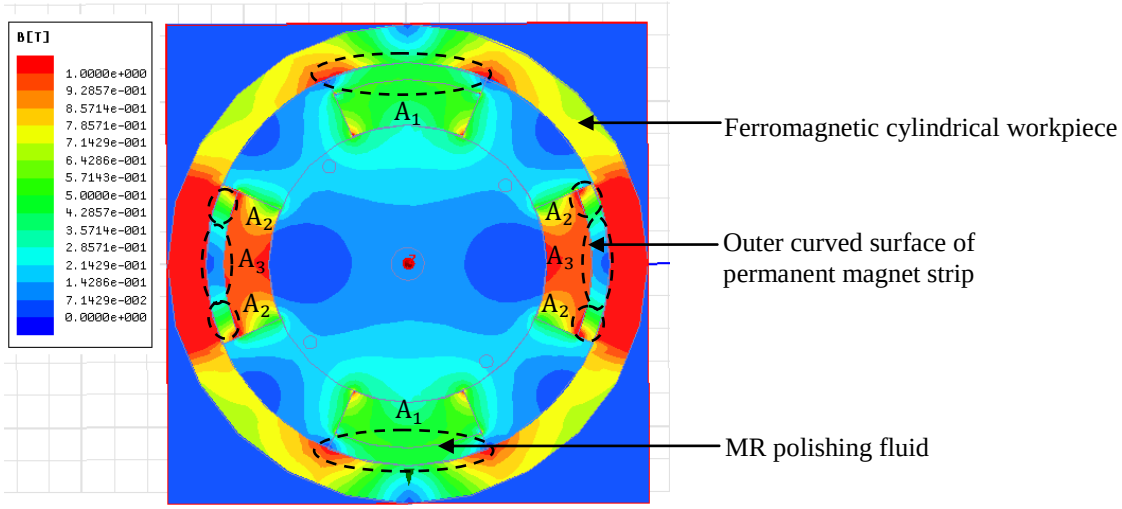

Fig. 5.7 Results obtained from the magnetostatic finite element analysis showing the distribution of magnetic flux density on the plane passing through the middle of cross-section of MR honing setup.

This variation in magnetic flux density over the curved surface of the two magnetic strips is occurring due to the interference of magnetic field in the working gap when the tool's four curved magnet strips are placed inside the ferromagnetic cylindrical workpiece. From the Fig. 5.7, it can be observed that over the outer curved surface of the two magnet strips having the interference of magnetic field lines, the higher magnetic flux density is present towards the start and end angle edges of the curved magnetic strips (A_2) and lower magnetic flux density towards the middle of the magnetic strips (A_3). To make the developed mathematical model more simpler and understandable, the average value of the magnitude of magnetic flux density distribution over the outer curved end surface of the permanent magnet strips (having interference of magnetic field lines) is assumed to be uniform. The formed CIPs chains get strong in the region where the higher magnitude of magnetic flux is present and get weak where the lower magnitude of magnetic flux density is present. The magnitude of magnetic flux density is higher in a certain region and lower in a certain region but the overall magnetic flux comes out to be an average value of the uniformly distributed magnitude of magnetic flux density. This distribution of magnetic flux density is considered as same as the average value of the uniformly distributed magnitude of magnetic flux density over the outer curved end surface of the other two magnetic strips where interference of magnetic field lines is almost negligible. So, mathematical model for

surface roughness in the present MR honing process has been developed based on the assumption as the uniform magnetic flux density induced from the curved end surface of all the four magnetic strips.

The two dimensional (2D) plot of the horizontal variation of the magnitude of magnetic flux density in MR polishing fluid region (working gap) from the centre of a single permanent magnet strip (having uniform distribution of magnetic flux density over its surface) is evaluated using the magnetostatic finite element analysis as shown in Fig. 5.8 (a). The magnitude of magnetic flux density at different points in the working gap is obtained from FE analysis and reported in Table 5.2. The variation in magnitude of magnetic flux density obtained from the FE analysis is also found decreasing as moving away from the outer curved surface of a magnetic strip to the ferromagnetic cylindrical workpiece's inner surface as similar to the trend as obtained from the mathematical modeling. The mathematically evaluated variation in magnetic flux density follows the same trend of negative slope as obtained through experimental measurement and FE analysis. Therefore, it confirms the consistency of the present developed mathematical model to calculate the magnetic flux density distribution in MR polishing fluid region (working gap). This is further helpful in calculating the indentation force acting over the active abrasives. The flow of magnetic flux lines in the MR honing tool along with the MR polishing fluid in working gap and the ferromagnetic cylindrical workpiece is also evaluated through the same FE analysis as represented in Fig. 5.8 (b).

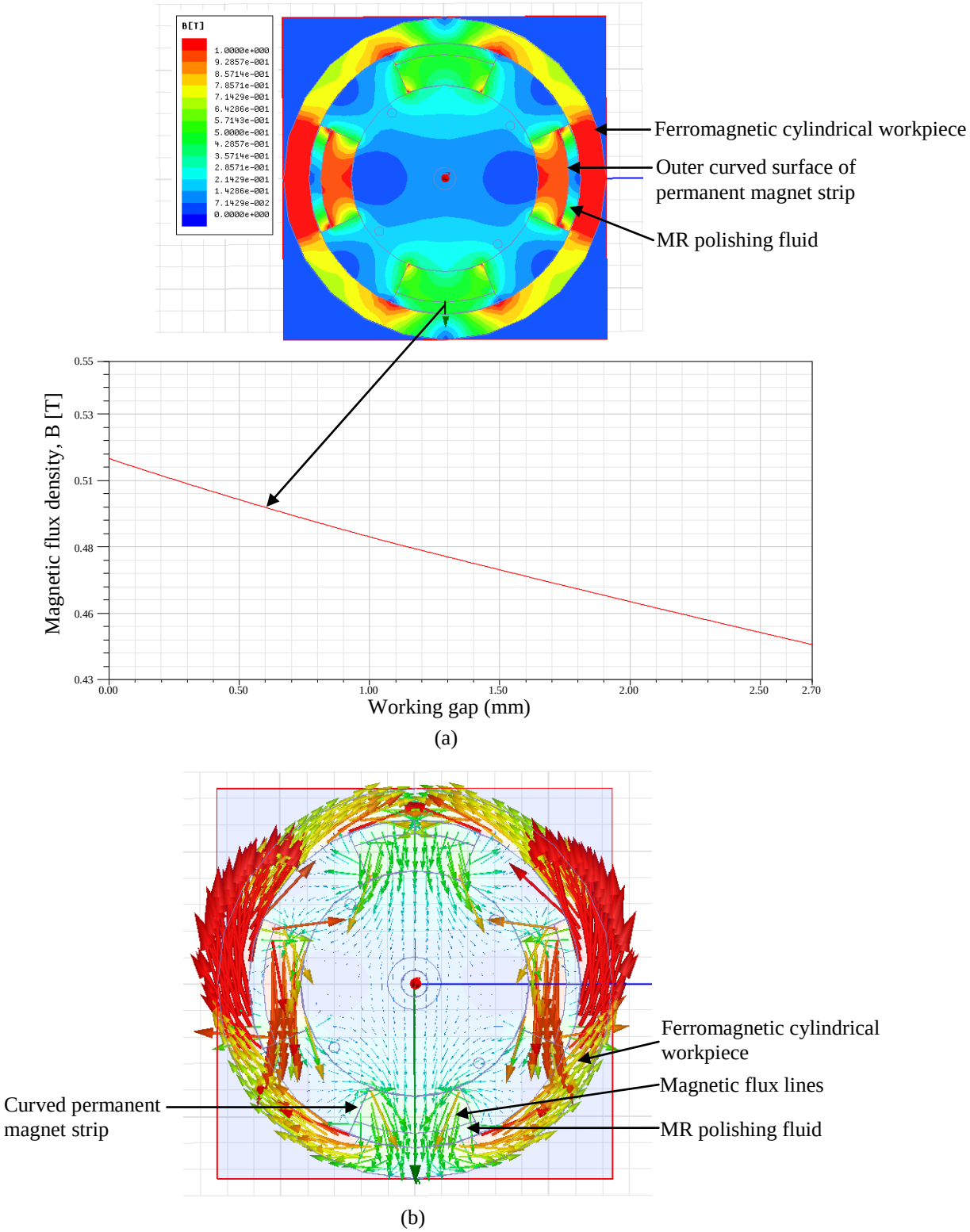

Fig. 5.8 Results obtained from the finite element analysis showing (a) 2D plot of variation in magnitude of magnetic flux density in the MR polishing fluid region (working gap) at the centre of a single curved permanent magnet strip having uniform magnetic flux density distribution over its outer surface and (b) direction of magnetic flux lines in the MR honing setup.

5.2.3 Computation of magnetic normal force exerted over the active silicon carbide (SiC) abrasive particle

While finishing is performed in the present magnetorheological honing process, magnetic iron particles get attracted towards the tool surface which in turn exerts levitation force over the abrasive particles towards the surface of the workpiece. This levitation force makes the abrasive particles indent into the cylindrical workpiece's surface. This magnetic levitation force is exerted by the micro-sized iron particles. Because of the induced magnetic field in the working gap, the iron particles present in working gap experience magnetic force (F_I) which make them to stick onto the magnetic external surface of the finishing tool. Magnitude of magnetic force acting over a single iron particle situated in the working gap (MR polishing fluid region) can be calculated by Eq. (5.26) (Stradling, 1993).

$$F_I = m_I \mu_0 \chi_m H \nabla H \tag{5.26}$$

here F_I is the magnitude of magnetic normal force in Newton exerting over single iron particle (present in the MR polishing fluid) due to the magnetic field, m_I is the mass of single iron particle in kg and can be calculated using size as average diameter of 15 μm, χ_m stands for the mass susceptibility of iron particle in m^3/kg, H stands for the magnetic field intensity in A/m and ∇H is the derivative of magnetic field intensity. Using the relation as stated in Eq. (5.23), the Eq. (5.26) can be rewritten as Eq. (5.27).

$$F_I = \frac{m_I \chi_m B \nabla B}{\mu_0} \tag{5.27}$$

Magnetic mass susceptibility (χ_m) of the iron particle can be evaluated by the relation as given in Eq. (5.28).

$$\chi_m = \frac{\mu_0 M_{IP}}{B} \tag{5.28}$$

here M_{IP} is the magnetization of an iron particle corresponding to the different magnitude of magnetic flux density, present at the point where the iron particle is located in the working gap and is obtained from the M-B curve for the iron powder as shown in Fig. 5.6 (a). Since the magnetic normal force exerting over the active SiC particle is in the radial direction i.e. towards the internal surface of the ferromagnetic cylindrical workpiece, so theoretically obtained variation in magnetic flux density in radial direction (Eq. (5.25)) is considered for calculating the magnetic normal force over the iron particles. So, the Eq. (5.27) can be written as the Eq. (5.29).

$$F_I = \frac{m_I \chi_m B(r) \frac{dB(r)}{dr}}{\mu_0} \tag{5.29}$$

here B (r) is magnetic flux density variation in the radial direction from the center of a curved permanent magnet strip in the working gap as evaluated by the theoretical mathematical modeling (Eq. (5.25)). $\frac{dB(r)}{dr}$ is the derivative of magnetic flux density variation (Eq. (5.25)) in the working gap and can be evaluated by (Eq. (5.30)).

$\frac{dB(r)}{dr}$ = 739.44r- 42.45 (5.30)

Using (Eq. (5.29)), the magnetic normal force acting over the iron particles present at different positions in the working gap have been calculated as reported in Table 5.2. With these calculated forces, the magnetic iron particles get attracted towards the external curved surface of a magnetic strip of the finishing tool and push back the active abrasive particles with levitation force towards the ferromagnetic cylindrical workpiece's internal surface. Due to the induced magnetization in the working gap, the iron particles form chains structure with the active abrasives over the cylindrical workpiece's internal surface as represented in Fig. 5.9 (a). It is assumed that the average of magnetic force acting on the different iron particles present at different positions in working gap results in levitation force which is completely exerted to the active silicon carbide (SiC) abrasive particle present over the inner surface of the cylindrical workpiece. This levitation force makes the active SiC abrasive particle to indent into the cylindrical workpiece's surface as shown in Fig. 5.9 (a). So, it is called the indentation force (F_i). The indentation force (F_i) acting over the active SiC abrasive particle calculated from the average of magnetic normal force (mentioned in Table 5.2) is given by Eq. (5.31).

$F_i = 1.75 \times 10^{-8}\ N$ (5.31)

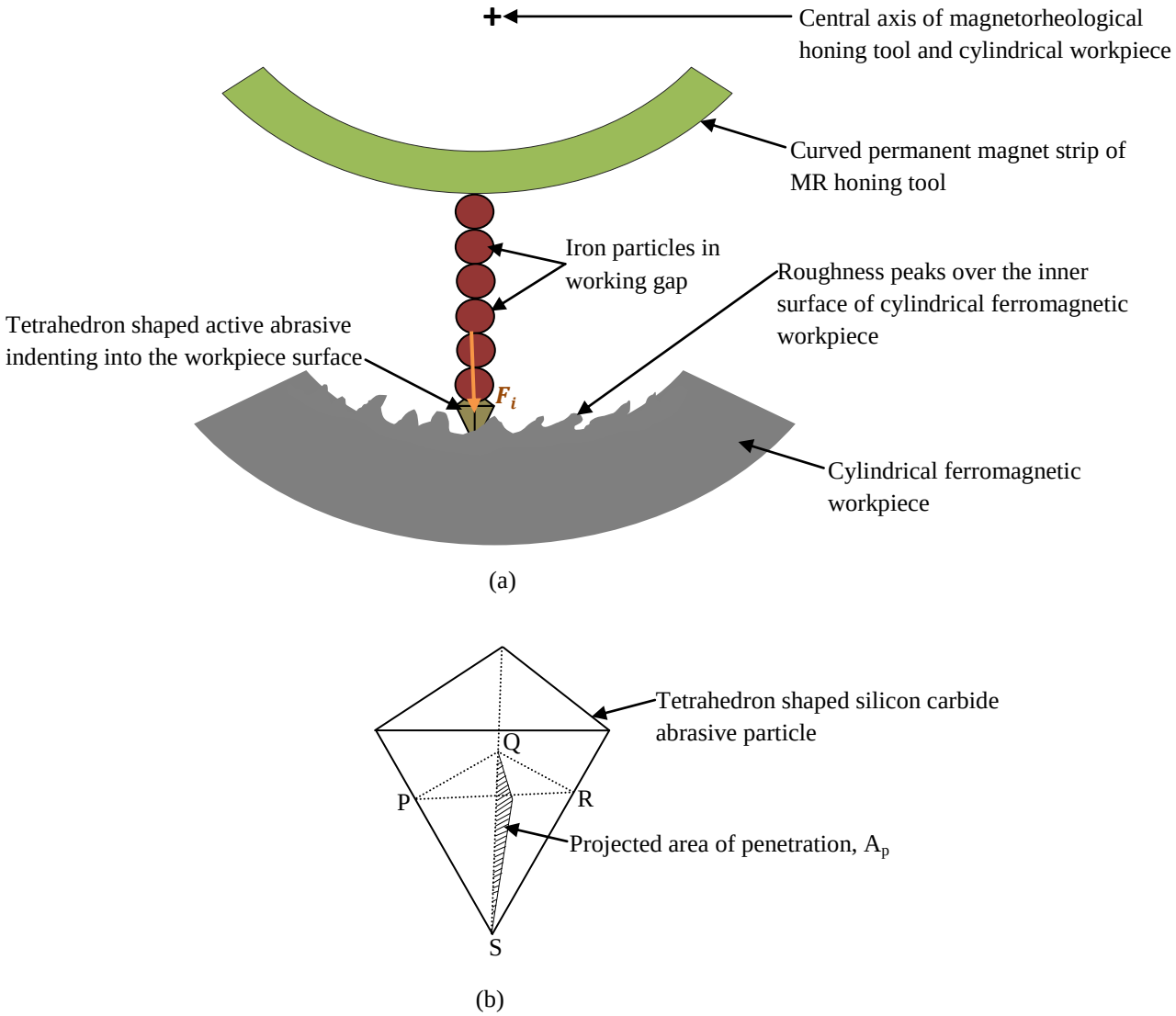

Fig. 5.9 (a) Enlarged view of working gap showing active abrasive indenting into the inner surface of the ferromagnetic cylindrical workpiece and (b) geometry of active abrasive showing the projected area of penetration.

5.2.4 Modeling of change in surface roughness during the present magnetorheological honing (MRH) process

Due to the indentation force acting over the active silicon carbide (SiC) abrasive particles, these active abrasives make nano-indentation into the cylindrical workpiece's internal surface as represented in Fig. 5.9 (a) for a single SiC abrasive particle. The performance of finishing by the present MRH process depends on the area of penetration of active abrasives into the roughness peaks present over the cylindrical workpiece's internal surface. The active abrasive indent into

the workpiece surface making the area of penetration (A_p) as shown in Fig. 5.9 (b) whose magnitude can be calculated by Eq. (5.32) (Mulik and Pandey, 2012).

$$A_p = \frac{3F_i}{4H_d} \tag{5.32}$$

where H_d is the hardness of cylindrical workpiece (mentioned in Table 5.3) in MPa which is measured experimentally.

Table 5.3 Parameters and conditions opted for mathematical modeling and experimentations.

Experimental parameters	Conditions
MRH tool rotating speed	400 RPM
MRH tool reciprocating speed	60 cm/min
Total finishing cycles	720
Cylindrical steel workpiece hardness	2842 MPa
Working gap	2.7 mm

The penetrated active abrasive which is gripped by the iron particles with the magnetic honing tool magnetic surface moves along with the movements of MR honing tool inside the cylindrical workpiece. With the simultaneous rotating as well as the reciprocating motion of MR honing tool, the active abrasives move in a helical path over the cylindrical workpiece's internal surface as represented in Fig. 5.10. This movement of penetrated active abrasive results in slashing out the surface roughness peaks and hence surface gets finished. Due to the magnetic field as induced by a curved permanent magnet strip, the magnetic iron particles get strongly stick over the outer tool surface and form strongly bonded chains in the working gap. The non-magnetic silicon carbide abrasives are pushed by the levitation force towards the inner surface of the ferromagnetic cylindrical workpiece due to the gradient of magnetic flux density (Fig. 5.8a) and are also strongly gripped by the iron particles chains. As the MR honing tool rotates and reciprocates inside the cylindrical workpiece, the formed iron particles chains with gripped abrasives move along with the movement of the finishing tool just like a brush.

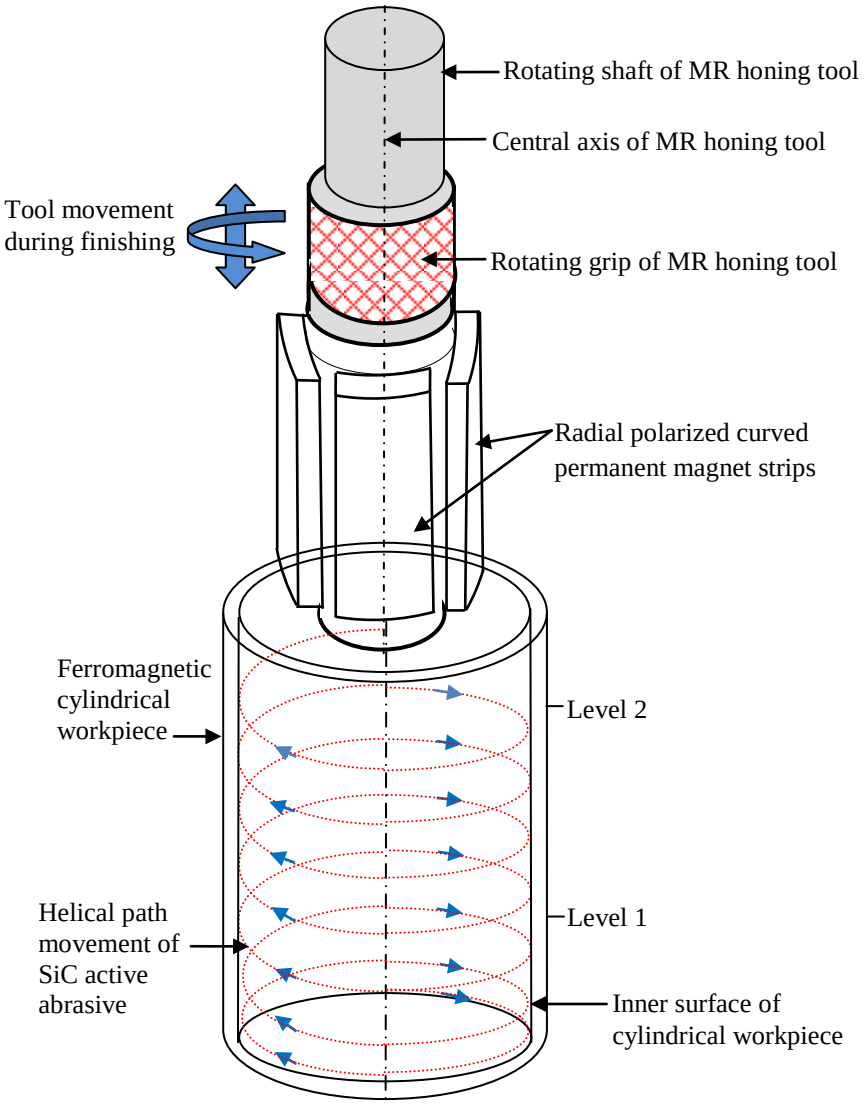

Fig. 5.10 Schematic diagram of helical path movement of the active abrasive over the inner surface of the ferromagnetic cylindrical workpiece.

So, rotating as well as the reciprocating speed of active abrasives has been considered same as that of respective rotating and reciprocating speed of MR honing tool. One complete movement of MR honing tool from bottom to top or vice-versa inside the cylindrical workpiece is considered as a finishing cycle. Length of the helical path (l_{hel}) covered by a single SiC active abrasive during a single finishing cycle of MR honing tool movement inside the cylindrical workpiece can be evaluated by Eq. (5.33).

$$l_{hel} = \left(\frac{V_a t_s}{\sin \emptyset}\right) \tag{5.33}$$

where V_a is the reciprocating velocity of the active SiC abrasive and $\emptyset$ is the helix angle made by the single SiC active abrasive during helical movement of MR honing tool inside the cylindrical workpiece. t_s is the time taken by the single active SiC particle to cover the complete height of

the cylindrical workpiece during a single cycle of MRH process which can be calculated by Eq. (5.34).

$$t_s = \left(\frac{h_w}{V_a}\right) \quad (5.34)$$

where h_w is the height of cylindrical workpiece and equal to 50 mm in the present work. Helix angle ($\emptyset$) made by the single SiC active abrasive during its movement on the inner surface the cylindrical workpiece can be calculated by Eq. (5.35).

$$\emptyset = \tan^{-1}\left(\frac{30V_a}{\pi r_{act} N_{act}}\right) \quad (5.35)$$

here r_{act} is the radial distance between central axis of the present magnetorheological (MR) honing tool and centre of active SiC abrasive particle which can be assumed as equal to inner radius of the cylindrical workpiece. N_{act} is the rotating speed of active abrasive as rotating over cylindrical workpiece's internal surface which is equal to the rotating speed of MR honing tool. It is considered that surface roughness peaks present over the cylindrical workpiece's internal surface are in shape of triangles as represented in Fig. 5.11 and are equally spread over the initial surface roughness value as R_a^0.

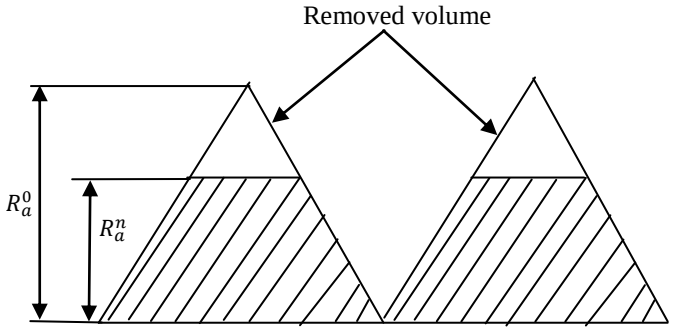

Fig. 5.11 Simplified surface roughness peaks geometry.

Active SiC abrasives move over the triangular peaks, erode out the material and perform the finishing. While moving over the triangular peaks of surface roughness, the actual length of contact (L_{act}) made by the single SiC active particle with the internal surface of the cylindrical workpiece is evaluated by Eq. (5.36) (Jain *et* al., 1999).

$$L_{act} = \left(1 - \frac{R_a^n}{R_a^0}\right) l_{hel} \quad (5.36)$$

where R_a^0 and R_a^n represents the initial surface roughness prior to experimentation and surface roughness value after n number of finishing cycles, respectively. The number of active abrasives (N_s) which performs finishing over the internal surface of cylindrical workpiece due to all four magnetic strips of the tool can be calculated by Eq. (5.37).

$$N_s = \left\{\frac{4(\theta_2^{'}-\theta_1^{'})2\pi r_3^{'} N_a l_{hel}}{360}\right\} \quad (5.37)$$

here N_a is the number of active abrasives per unit area (1mm×1mm) present over the internal surface of the cylindrical workpiece as calculated in Eq. (5.11). So, the volume of material removed in the nth cycle (V_n) of MR honing process can be evaluated by Eq. (5.38) (Jain *et* al., 1999).

$$V_n = A_p L_w N_s \quad (5.38)$$

here L_w is the working length traced by the active abrasives during the single cycle of MR honing (MRH) process. During the movement of MRH tool inside the cylindrical workpiece, the active abrasives present over the internal surface at the top of the cylindrical workpiece cover the zero distance. While active abrasives present over the internal surface at the bottom of the cylindrical workpiece cover the complete helical length. So, the working length traced by the active abrasives during the single cycle of MRH process is the mean of actual length covered by the active abrasives during the single cycle and is equal to $L_{act}/2$. Using this relation and Eqs. (5.36) and (5.37), the Eq. (5.38) can be expanded and written as Eq. (5.39).

$$V_n = \left\{\frac{A_p 4(\theta_2^{'}-\theta_1^{'})\pi r_3^{'} N_a l_{hel}^2}{360}.\left(1-\frac{R_a^n}{R_a^0}\right)\right\} \quad (5.39)$$

Also, the volume of material removal in nth cycle of MRH process can also be evaluated as equal to the actual length of contact made by the single SiC active abrasive particle with the inner surface of the cylindrical workpiece during a single cycle × inner circumference of cylindrical workpiece × height of surface roughness peak removed in the nth cycle and can be written as Eq. (5.40) (Jain *et* al., 1999).

$$V_n = \left\{\left(1-\frac{R_a^n}{R_a^0}\right) l_{hel}.(2\pi r_3^{'}).(R_a^{n-1}-R_a^n)\right\} \quad (5.40)$$

After comparing the Eqs. (5.39) and (5.40), the surface roughness value after n number of finishing cycles of the MRH process can be written as the Eq. (5.41).

$$R_a^n = R_a^{n-1} - \{\frac{2A_p(\theta_2^{'}-\theta_1^{'}) l_{hel} N_a}{360}\} \quad (5.41)$$

Here R_a^n and R_a^{n-1} represents surface roughness value over the internal surface of cylindrical workpiece after n and (n-1) number of finishing cycles, respectively. Thus, the surface roughness values (R_a) on the internal surface of cylindrical workpiece after n number of finishing cycles can be predicted using the Eq. (5.41). Using parameters and conditions as mentioned in Table

5.3, the mathematical modeling for surface roughness before experimentation in the present MR honing process has been performed for the initial surface roughness values (Table 5.4). Surface roughness values have been predicted theoretically after different number of finishing cycles as mentioned in Table 5.4.

5.3 Experimentation

For validation of the developed mathematical model for calculating the change in surface roughness values in the present magnetorheological honing (MRH) process, the experimentations were performed on the ferromagnetic cylindrical steel workpiece's internal surface. The experimentations were performed by the MRH tool with dimensional parameters as specified in Table 5.1. The working gap of 2.7 mm for MR polishing fluid is maintained in between the outer curved end surface of the magnetic finishing tool and the ferromagnetic cylindrical workpiece's internal surface. The MR polishing fluid composed of 20 % by volume electrolytic iron powder, 20 % by volume of silicon carbide abrasives and 60 % by volume of base fluid (composed of paraffin oil and AP3 grease) is utilized for experimentation. The photograph of the magnetorheological honing setup performing the finishing of the inner surface of ferromagnetic cylindrical workpiece is represented in Fig. 5.12. The conditions and parameters opted for experimentations are mentioned in Table 5.3. Surface roughness parameters were measured on the ferromagnetic cylindrical workpiece's internal surface with surface roughness tester make Mitutoyo Surftest SJ-400 with the cut-off length of 0.25 mm. Every time surface roughness parameter R_a value was measured at 8 separate locations over the cylindrical workpiece's inner surface. It was measured at two different levels along the height of the cylindrical workpiece as shown in Fig. 5.10.

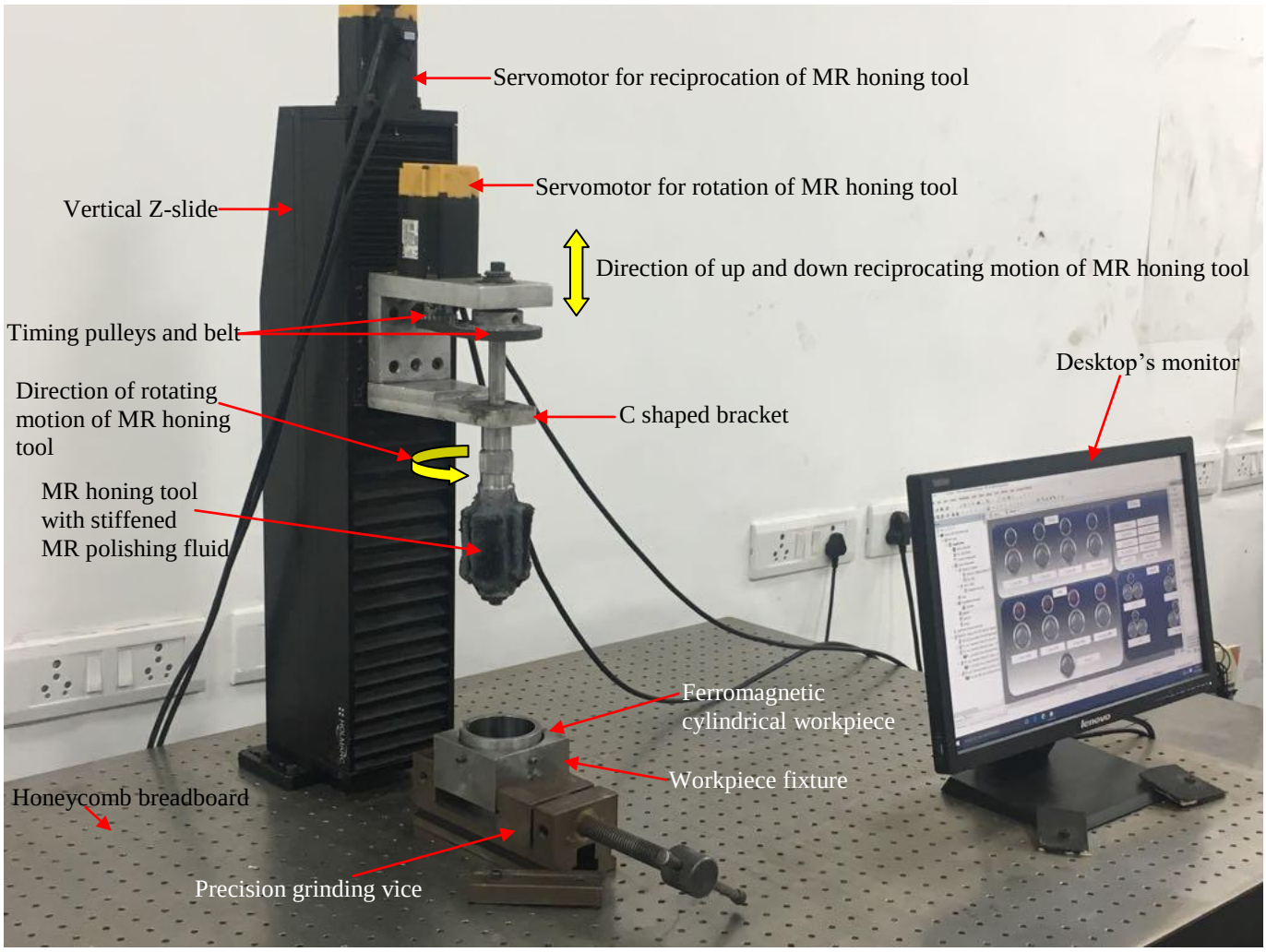

Fig. 5.12 Photograph of the magnetorheological honing setup performing the finishing of the inner surface of the ferromagnetic cylindrical workpiece.

On every single level, four measurements of R_a value were performed at equal distance on the cylindrical workpiece's inner periphery. Average of all the eight R_a values was performed after certain number of finishing cycles and compared with theoretically obtained surface roughness values as reported in Table 5.4.

Table 5.4 Comparison of theoretically calculated and experimental obtained surface roughness values for different number of finishing cycles.

Sr. No.	Number of finishing cycles	Finishing Cycle Time (Minutes)	Initial surface roughness value, R_a (µm)	Theoretically calculated final surface roughness value, R_a (µm)	Experimentally obtained average final surface roughness value, R_a (µm) (Eq. 5.41)	Percentage (%) error
1.	300	25	0.39	0.26	0.24	-8.06
2.	400	33.3	0.38	0.22	0.21	-4.76
3.	550	45.8	0.39	0.16	0.16	-3.08
4.	650	54.1	0.38	0.11	0.11	1.69
5.	720	60	0.39	0.09	0.09	1.03

Least value of surface roughness profile measured along a line at a particular point on the initial ground surface before finishing and after 720 numbers of finishing cycles is shown in Figs. 5.13 (a) and (b) respectively.

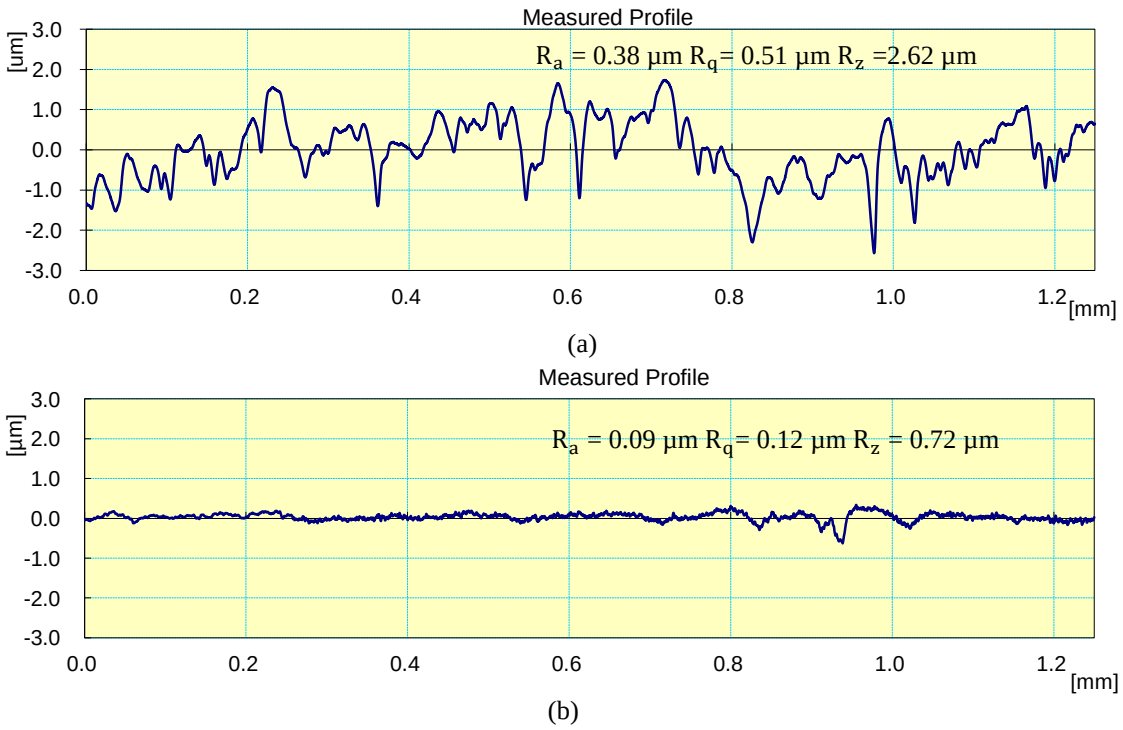

Fig. 5.13 Surface roughness contours over the inner surface of the cylindrical workpiece (a) ground surface before finishing and (b) finished surface after 720 numbers of finishing cycles (60 minutes of finishing) by the present MRH process.

To visualize the finishing accomplished by the present MR honing process, the scanning electron microscopy (SEM) analysis of the initial and finished surface after 720 number of finishing cycles was also performed. The SEM images of initial ground and final finishes surface are shown in Figs. 5.14 (a) and (b), respectively.

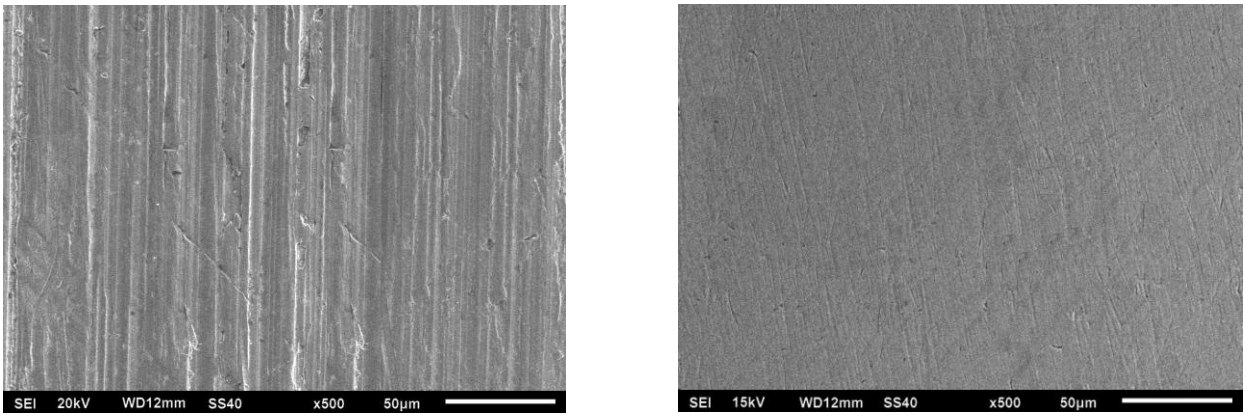

(a) (b)

Fig. 5.14 Scanning electron microscopy images at 500x (a) initial ground surface before finishing and (b) finished surface after 720 numbers of cycles (60 minutes of finishing) with the present MRH process.

5.4 Results and Discussion

A theoretical mathematical model has been developed to evaluate the magnitude and variation of magnetic flux density in the working gap. The model of induced magnetic flux density in the working gap is also included the contribution of effect of magnetic field induced by the iron particles of MR polishing fluid and the ferromagnetic cylindrical workpiece in the MR honing process. The theoretical evaluation of magnetic normal force acting over the actual shaped of tetrahedron abrasive particles (present in the working gap) due to the induced magnetic field in the working gap has been performed. The change in surface roughness value for different number of finishing cycles has also been predicted with the help of developed mathematical model. To verify the consistency of developed mathematical model for surface roughness in the present magnetorheological honing process, the validation of the model has been performed in two steps. The first half of the mathematical model i.e. calculation of magnetic flux density in the MR polishing fluid region (working gap) is validated with the results obtained from the finite element (FE) analysis using the Maxwell Ansoft V13 software and also with experimentally measured magnitude of magnetic flux density. Theoretical horizontal variation of magnetic flux

density (B) in the working gap of 2.7 mm from the finishing tool external curved permanent magnet strip surface at the centre is calculated with also including the contribution of the magnetic effect of the iron particles of MR polishing fluid in working gap and the ferromagnetic cylindrical workpiece as calculated by using Eqs. (5.14)-(5.24).The magnitude of magnetic flux density is evaluated as the maximum value of 0.310 T which is obtained over the external surface of the magnetic MR honing tool as reported in Table 5.2. The magnitude of magnetic flux density (B) is found decreasing as moving away from the outer finishing tool surface to the ferromagnetic cylindrical workpiece's internal surface. The least value of 0.254 T is obtained in the working gap at the point close to the ferromagnetic cylindrical workpiece's internal surface. Moreover, the magnetic flux density variation in working gap in horizontal direction is evaluated by performing finite element (FE) analysis in Maxwell Ansoft V13 software and also measured experimentally as reported in Table 5.2. The slope of magnetic flux density variation in the working gap (evaluated by FE analysis and measured experimentally) is found negative as similar to the trend as seen in mathematical model. Comparison of data as reported in Table 5.2 shows that horizontal distribution of magnitude of magnetic flux density in the MR polishing fluid region (working gap) computed from the mathematical model is in close agreement with experimentally measured values. This signifies the consistency in the developed mathematical model for evaluating the magnetic flux density in the working gap.

Another half of the mathematical model predicts the change in surface roughness value with different number of finishing cycles while performing finishing with the developed magnetorheological honing process. The mathematical model gives the disparity of magnetic flux density (B) in the MR polishing fluid region (Eq. (5.25)) which is helpful in predicting the magnitude of the magnetic normal force acting over the iron particles present in the working gap. The magnetic normal force acting over the iron particles make them stick to the external surface of the MR honing tool and give back repulsive levitation force to the silicon carbide (SiC) abrasive particles which indent them into the surface of the workpiece. Indentation force acting over the active abrasive (present over the cylindrical workpiece's internal surface) due to the iron particles has been evaluated mathematically (Eq. (5.31)). The magnitude of indentation force (F_i) acting over the active SiC particles is analogous to the magnitude and gradient of magnetic flux density in the MR polishing fluid region (Eq. (5.29)).

Abrasives get indent into the internal surface of the cylindrical workpiece and erode out the material from the surface by an amount proportional to the area of penetration (A_p). Increase in the exertion of indentation force acting over the active abrasives makes them indent deeper into the internal surface of the cylindrical workpiece. This resulted in increase in the area of penetration (Eq. 5.32). The increased area of penetration removes more material from the internal surface of the cylindrical workpiece with a single cycle of finishing (Eq. 5.38). Length of the helical path made by the single abrasive during the single finishing cycle depends on the rotating as well as the reciprocating speed of finishing tool (Eqs. (5.33) - (5.35)). The volume of material removed by the present MR honing process during a single finishing cycle also depends on the abrasive concentration present in the MR polishing fluid. The increased percentage concentration of abrasives results with the more material removal during finishing process (Eqs. (5.11), (5.37) and (5.38)). The change in surface roughness (R_a) values with different number of finishing cycles can be evaluated by Eq. (5.41). Experimentations have been performed over the internal surface of the ferromagnetic cylindrical workpiece to validate the developed mathematical model for different number of finishing cycles. With the parameters and conditions as mentioned in Table 5.3, the experimentations have been performed for different numbers of finishing cycles. The time required for performing one cycle of finishing in MR honing (MRH) process can be evaluated by Eq. (5.42).

$$\textit{Single-cycle time} = \frac{Reciprocating\ travel\ length}{Reciprocaing\ velocty\ of\ MRH\ tool} \tag{5.42}$$

The reciprocating travel length for each cycle in the present case is equal to workpiece height which is equal to 50 mm. The total number of finishing cycles performed during the MRH process can be evaluated by Eq. (5.43).

$$\textit{Total number of finishing cycles} = \frac{Process\ duration}{Single\ cycle\ time} \tag{5.43}$$

Theoretically evaluated change in surface roughness values obtained from the mathematical model is compared with changes observed during experimentation as reported in Table 5.4. The percentage error between the results obtained from theoretical mathematical model and experimentation is evaluated using Eq. (5.44).

Percentage error

$$= \frac{Experimental\ final\ surface\ roughness - Theoretical\ final\ surface\ roughness}{Experimental\ final\ surface\ roughness} \times 100 \tag{5.44}$$

As it can be observed from the Table 5.4 that percentage error between theoretical calculated and experimentally obtained surface roughness values is high and negative for initial few finishing cycles. This is due to the fact that while starting the experimentation from the initial ground surface, the reduction in surface roughness (R_a) values is too high. This is due to the sudden removal of loosely held roughness peaks of the inner ground surface of the cylindrical workpiece. Experimentally, the change in surface roughness (R_a) value gradually decreased with the increased number of finishing cycles due to difficulty in eroding out the material from flattened roughness peaks having high shear strength after removal of the sharp peaks. Percentage error between the theoretical predicted and the experimentally obtained final surface roughness (R_a) value after 720 finishing cycles is 1.03 as reported in Table 5.4. On further performing experimentation with increased number of finishing cycles, the significant reduction in surface roughness was not obtained. The reason behind this fact is that practically with a certain number of finishing cycles; almost all the sharp surface roughness peaks get eroded out and left with flattened surface roughness peaks. The flattened roughness peaks of the workpiece material possesses high shear strength due to which it became difficult for the stiffened MR polishing fluid to further erode out the material. Also, the abrasives with the size as used in the experimentation could not penetrate into the flattened peaks left over the finished workpiece's surface. It can also be observed from the Table 5.4 that percentage error between the theoretical predicted and experimental values of the final surface roughness increases with increasing the number of finishing cycles. The reason for this is that theoretical mathematical model predicts the final finished surface roughness value on the basis of the calculated projected area of penetration as calculated in Eq. (5.32). On the other hand experimentally, the projected area of penetration of active abrasive particles is usually decreased after a certain number of finishing cycles due to the high shear strength of the left out flattened area of the roughness peaks. Experimentally, after a certain limit of finishing cycles, further significant removal of material do not occur due to the non-penetration of abrasives into the workpiece's surface because of the high shear strength of the left out flattened surface of the roughness peaks. On the other hand, mathematical model predict the final surface roughness considering the area of penetration as calculated from Eq. (5.32) which get alters practically after a certain number of finishing cycles.

Scanning electron microscopy (SEM) images of the initial ground and finished surface after 720 numbers of finishing cycles are represented in Figs. 5.13(a) and 5.13(b), respectively. This

signifies that the significant finishing has been accomplished by the present developed MR honing tool over the ferromagnetic cylindrical workpiece's internal surface. Results obtained from the mathematical model are found in close relation with results obtained from the experimentations with least percentage error of 1.03 and a maximum of 8.06. This depicts the consistency of the developed mathematical model for predicting change in surface roughness values with various significant numbers of finishing cycles. The developed mathematical model helps in predicting the finishing performance of the present magnetorheological honing (MRH) process. It gives the relation of material removal in terms of surface roughness values with the various parameters like magnitude and gradient of magnetic flux density, percentage concentration of SiC abrasives, and rotating and reciprocating velocity of MRH tool. It details the in-sight mechanism of material removal in terms of change in surface roughness values during the MRH process. It can be used further to enhance the finishing performance of the developed finishing process and make it useful for industries dealing with the internal cylindrical surface finishing like cylindrical dies and molds industry, industries making cylindrical barrels for injection molding and cylindrical components used for flow of high purity liquid or gases etc.

5.5 Conclusions

The mathematical modeling for the change in surface roughness in the present magnetorheological (MR) honing process has been performed which draw the following conclusions.

- The developed mathematical model for the distribution of the induced magnetic flux density in working gap reveal the inclusion of magnetic effect also due to the iron particles of MR polishing fluid and the ferromagnetic cylindrical workpiece in the total induced magnetic flux density in the working gap.
- Distribution of magnetic flux density in the MR polishing fluid region (working gap) show the negative slope as moving away from the finishing tool's surface to the ferromagnetic cylindrical workpiece's inner surface which theoretically confirm the finishing capability of the developed process for the internal surface of the ferromagnetic cylindrical workpieces as relative motion possible between the gripped active abrasive particles and their inner surface.
- The magnitude of the indentation force acting over the active abrasive particle using the developed mathematical model for the distribution of the induced magnetic flux density in

working gap further predicts the removal of material in terms of change in surface roughness during finishing by the present MR honing process.

- Developed model for the change in surface roughness during the internal surface finishing of the ferromagnetic cylindrical workpiece using the present magnetorheological honing process signify the change in surface roughness depends on various parameters like magnitude and gradient of magnetic flux density in working gap, percentage volume concentration of abrasive particles in MR polishing fluid and rotating as well as reciprocating velocity of the MR honing tool.
- Results evaluated by the mathematical model of surface roughness values in the present magnetorheological honing process show the close agreement with results obtained from the experimentation as percentage error varied from 1.03 to 8.06.
- The developed mathematical model for present MR honing process can predict the change in surface roughness (R_a) value while performing internal surface finishing of the different industrial cylindrical components and it further helpful in increasing the operative functionality of the cylindrical products for industrial applications.

CHAPTER 6

CONCLUSIONS AND SCOPE OF FUTURE WORK

6.1 Conclusions

A new finishing tool based on magnetorheological fluid was designed and fabricated. The designed tool's capability has been successfully demonstrated for finishing the inner surface of the ferromagnetic cylindrical workpieces. The finishing tool's outer magnetic surface was made flexible to move radially inwards or outwards and can be adjusted as per the requirement of the internal surface diameter of the cylindrical workpieces to be finished. The process mechanism of the developed finishing tool was made similar to the conventional honing operation that is why the process was named as magnetorheological honing process. Results obtained in the present work confirm that the developed magnetorheological (MR) honing process is competent to nano-finish the inner surface of the cylindrical workpieces of different internal diameters. The mathematical model for change in surface roughness in present developed MR honing process details the in-sight mechanism of material removal for this newly developed process. Following conclusions have been drawn on the basis of results obtained from the present research work.

- The uniform magnetic flux density distribution on the improved design of the MR honing tool with curved end magnetic surface confirms the better finishing performance as compared to the initially designed flat end magnetic surface of the MR honing tool having the non-uniform magnetic flux density distribution.
- The improved design of the MR honing tool with curved end magnetic surface was found to have better finishing performance as it reduced the surface roughness parameters R_a, R_q, and R_z on the inner surface of cylindrical mild steel workpiece by 76.28%, 76.67%, and 75.20%, respectively in 60 minutes while the initially designed MR honing tool with flat end magnetic surface reduced the roughness parameters by 47.97%, 46.24%, and 47.08% respectively during the same finishing time of 60 minutes.
- The surface characteristics of the finished surface get improved better with the improved design of MR honing tool as compared to the finishing performed by the initially designed MR honing tool having flat end magnetic surface.
- The obtained quadratic response surface regression model reveals that the percentage change in surface roughness value majorly contributes by the process parameters such as the working

gap followed by the tool rotating speed, the percentage concentration of SiC abrasive particles, the tool reciprocating speed and the percentage concentration of carbonyl iron particles.

- The surface roughness Ra value gets reduced to 95 nm from the initial Ra value of 476 nm on the internal surface of the cylindrical EN-31 steel in 120 minutes of finishing with the present MR honing tool having curved end magnetic surface using optimum process parameters as 20% volume concentration of SiC abrasive particles, 20% volume concentration of carbonyl iron particles, the rotational speed of tool as 500 RPM, the reciprocation speed of tool ~~as~~ 70 cm/min and the working gap of 2 mm,
- Finishing performed at different working gaps confirms the flexibility of the present developed MR honing tool for nano-finishing of the inner surface of different sizes (internal diameters) of the different cylindrical workpieces.
- Significant enhancement in surface quality on the internal surface of the ferromagnetic EN-31 steel cylindrical workpiece as revealed by the scanning electron microscope (SEM) images confirm the usefulness of the present MR honing process in nano-finishing with better surface characteristics for the inner surface finishing of the EN-31 ferromagnetic cylindrical steel workpieces as commonly used in industries for manufacturing the punches and dies.
- The developed mathematical model for magnetic field demonstrates the distribution of the induced magnetic flux density in the working gap and also included the contribution of the magnetic effect of iron particles of MR polishing fluid and the ferromagnetic cylindrical workpiece.
- The mathematical model evaluated the distribution of magnetic flux density in the working gap with a negative slope as moving away from the finishing tool's surface to the ferromagnetic cylindrical workpiece's inner surface which theoretically confirm the finishing capability of the developed process for the internal surface of the ferromagnetic cylindrical workpieces as relative motion can possible between the gripped active abrasive particles and the ferromagnetic cylindrical inner surface.
- The developed theoretical model for the present magnetorheological honing process demonstrates the relation of change in surface roughness with various process parameters like magnitude and gradient of magnetic flux density in working gap, the percentage volume

concentration of abrasive particles in MR polishing fluid and rotating as well as the reciprocating velocity of the MR honing tool.

- The developed theoretical model of the surface roughness was found quite appropriate as the results evaluated by the mathematical model were found in close agreement with results obtained from the experimentation as error varied from 1.03 % to 8.06 %.
- The developed mathematical model for present MR honing process is useful to predict the change in surface roughness R_a value when the developed process is used for finishing the internal surface of the different cylindrical workpieces and is further helpful in increasing its operative functionality.
- The overall results reveal that the present developed MR honing process can be used for its extensive applications in industries for enhancing the functional capability of various ferromagnetic cylindrical components with different diametric sizes used in manufacturing industries like hydraulic cylinders, connecting rods, bearings, cylindrical molds and dies, cylindrical tubes for the flow of high purity liquids etc. and also for non-ferromagnetic components such as air bearings and pneumatic actuators etc.

6.2 Scope of future work

The recently developed MR honing tool has proved its capability to finish the inner surface of the different ferromagnetic cylindrical workpieces. Some of the scopes of future work by which efforts can be made to further enhance the finishing performance of the present developed MR honing process are listed as follows.

- An additional rotating motion can be provided to the workpiece to increase the relative motion between the abrasive particles and the inner surface of the cylindrical workpiece to further enhance the finishing performance of the developed tool.
- In the present work only the magnetostatic finite element analysis has been performed in Maxwell Ansoft V13 software for the developed MR honing process. To further analyze the variation of magnetic flux density during the finishing process, the dynamic analysis of the developed process can be performed in any suitable software like ANSYS.
- The accuracy of the developed mathematical model can further be enhanced by considering the effect of the interference of magnetic field induced in the working gap due to the placement of four curved permanent magnets in the ferromagnetic cylindrical workpiece.

- Further work and efforts can be performed to attain the dimensional and form accuracy over the inner surface of the cylindrical workpieces to make the process practically useful for industries.

REFERENCES

Ashtiani, M.; Hashemabadi, S.H.; Ghaffari, A. (2015) A review on the magnetorheological fluid preparation and stabilization. *Journal of Magnetism and Magnetic Materials* 374: 716-730.

ASTM E 11-09, November 2010.

Antony, L.V.M.; Reddy R. M. (2003) Processes for production of high-purity metal powders. *Journal of The Minerals, Metals & Materials Society* 71: 1949-2019.

Bagnoud, V.; Guardalben, M.J.; Puth, J.; Zuegel, J.D.; Mooney, T.; Dumas, P. (2005) High-energy, high-average-power laser with Nd:YLF rods corrected by magnetorheological finishing. *Applied Optics* 44(2): 282-288.

Balogun, V.A.; Mativenga, P.T. (2017) Specific energy based characterization of surface integrity in mechanical machining. *Procedia Manufacturing 7*:290-296.

Bedi, T.S.; Singh, A.K. (2016) Magnetorheological methods for nanofinishing- a review. *Particulate Science and Technology* 34(4):412–422.

Bedi, T.S.; Singh, A. K. (2017) Development of magnetorheological fluid based finishing process for finishing of ferromagnetic cylindrical workpiece. *Machining Science and Technology* 22(1):120-146.

Benardos, P.G.; Vosniakos, G.C. (2003) Predicting surface roughness in machining: a review. *International Journal of Machine Tools and Manufacture* 43:833-844.

Beyerer, J.; Puente Leon, F. (1997) Detection of defects in groove textures of honed surfaces. *International Journal of Machine Tools and Manufacture* 37(3):371–389.

Bossis, G.; Lacis, S.; Meunier, A.; Volkova, A. (2002) Magnetorheological fluids. *Journal of Magnetism and Magnetic Materials* 252:224-228.

Brecker, J.N.; Brown, R.; Matsuo, T.; Saito, K.; Sweeney, J.A.; Vansaun, J.B.; Shaw, M.C. (1969) Abrasive grain association on investigation of abrasive grain characteristics. 4th Annual Report. Carnegie Institute of Technology, Pittsburgh, Pennsylvania, USA.

Carlson, J.D.; Jolly, M.R. (2000) MR fluid, foam and elastomer devices. *Mechatronics* 10:555–569.

Chang, Y.P.; Hashimura, M.; Dornfeld, D.A. (2000) An investigation of material removal mechanisms in lapping with grain size transition. *Journal of Manufacturing Science and Engineering* 22(3):413-419.

Cheng, H.; Feng, Y.; Wang, T.; Dong, Z. (2010) Magnetorheological finishing of optical surface combined with symmetrical tool function. *Frontiers of Optoelectronics* 3(4): 408-412.

Das, M.; Jain, V.K.; Ghoshdastidar, P.S. (2008) Fluid flow analysis of magnetorheological abrasive flow finishing (MRAFF) process. *International Journal of Machine Tools and Manufacture* 48:415–426.

Das, M.; Jain, V.K.; Ghoshdastidar, P.S. (2010) Nano-finishing of stainless-steel tubes using rotational magnetorheological abrasive flow finishing process. *Machining Science and Technology* 14(3):365-389.

Das, M.; Jain, V.K.; Ghoshdastidar, P.S. (2011) The out-of-roundness of the internal surfaces of stainless steel tubes finished by the rotational–magnetorheological abrasive flow finishing process. *Materials and Manufacturing Processes* 26: 1073-1084.

Das, M.; Jain, V.K.; Ghoshdastidar, P.S. (2012) Nanofinishing of flat workpiece using rotational-magnetorheological abrasive flow finishing (R-MRAFF) process. *International Journal of Advanced Manufacturing Technology* 62(1):405–420.

Derringer, G.; Suich, R. (1980) Simultaneous optimization of several response variables. *Journal of Quality and Technology*. 12:214-219.

Dimkovski, Z.; Anderberg, C.; Rosen, B. G.; Ohlsson, R.; Thomas, T. R. (2009) Quantification of the cold worked material inside the deep honing grooves on cylinder liner surfaces and its effect on wear. *Wear* 267(12): 2235-2242.

Federation of European Producers of Abrasives, "Home and News From FEPA," http://www.fepa-abrasives.org.

Feng, Z.; Cheng, H.; Wang, Y.; Lei, S. (2005) Magnetorheological finishing of SiC aspheric mirrors. *Materials and Manufacturing Processes* 20(6): 917-931.

Fergani, O.; Shao, Y.; Lazoglu, I.; Liang, S.Y. (2014) Temperature effects on grinding residual stress. *Procedia CIRP* 14: 2– 6.

Ferreira, R.; Carou, D.; Lauro, C.H.; Davim, J.P. (2016) Surface roughness investigation in the hard turning of steel using ceramic tools. *Materials and Manufacturing Processes* 31 (5): 648–652.

Fox, M.; Agrawal, K.; Shinmura, T.; Komanduri, R. (1994) Magnetic abrasive finishing of rollers. *CIRP Annals* 43 (1):181-184.

Furst, E.M.; Gast, A.P. (2000) Micromechanics of magnetorheological suspensions. *Physics Revolution E* 61(6):6732–6739.

Genc, S.; Phule, P.P. (2002) Rheological properties of magnetorheological fluids. *Smart Materials and Structures* 11:140–146.

Gheisari, R.; Ghasemi, A.A.; Jafarkarimi, M.; Mohtaram, S. (2014) Experimental studies on the ultra-precision finishing of cylindrical surfaces using magnetorheological finishing process. *Production & Manufacturing Research* 2(1):550–557.

Golini, D.; Kordonski, W.I.; Dumas, P.; Hogan, S. (1999) Magnetorheological finishing (MRF) in commercial precision optics manufacturing. *Proceeding of SPIE Conference on Optical Manufacturing and Testing* 3782:80–91.

Gorana, V.V.; Jain, V.K.; Lal, G.K. (2004) Experimental investigation into cutting forces and active grain density during abrasive flow machining. *International Journal of Machine Tools and Manufacture* 44:201–211.

Gregory, R.D. (2006) Classical Mechanics, *1st edition; Cambridge University Press: Cambridge*, UK.

Gupte, P.S.; Wang, Y.; Miller, W.; Barber, G.C.; Yao, C.; Zhou, B.; Zou, Q. (2008) A study of torn and folded metal (TFM) on honed cylinder bore surfaces. *Tribology Transactions* 51:784–789.

Haeri, S.; Hashemabadi, S.H. (2008) Three dimensional CFD simulation and experimental study of power law fluid spreading on inclined plates. *International Communications Heat and Mass Transfer* 35:1041–1047.

Hoshino, T.; Kurata, Y.; Terasaki, Y.; Susa, K. (2001) Mechanism of polishing of SiO_2 film by CeO_2 particles. *Journal of Non-Crystalline Solids* 283:129–136.

Hong, K.P.; Cho, Y.K.; Shin, B.C.; Cho, M.W.; Choi, S.B.; Cho, W.S.; Jae, J.J. (2012) MR fluid polishing of Alumina reinforced zirconia ceramics using diamond abrasive for dental application. *Materials and Manufacturing Processes* 27: 1135-1138.

Huang, J.; Zhang, J.Q.; Liu, J.N. (2005) Effect of magnetic field on properties of MR fluid. *International Journal of Modern Physics*. B19: 597–601.

Jain, R.K.; Jain, V.K.; Dixit, P.M. (1999) Modeling of material removal and surface roughness in abrasive flow machining process. *International Journal of Machine Tools and Manufacture* 39: 1903–1923.

Jain, V.K. (2008) Abrasive-based nano-finishing techniques: An overview. *Machining Science and Technology* 12:257–294.

Jain, V.K. (2009) Magnetic field assisted abrasive based micro-/nanofinishing. *Journal of Materials Processing Technology* 209:6022–6038.

Jayswal, S.C.; Jain, V.K.; Dixit, P.M. (2005) Modeling and simulation of magnetic abrasive finishing process. *International Journal of Advanced Manufacturing Technology* 26 (5–6): 477–490.

Jha, S.; Jain, V.K. (2004) Design and development of the magnetorheological abrasive flow finishing (MRAFF) process. *International Journal of Machine Tools and Manufacture* 44:1019–1029.

Jha, S.; Jain, V.K. (2005) Nano-finishing techniques. In: Manufacturing and Nano-Technology, Editor: N.P. Mahalik, Springer Verlag, Heidelberg: 171–195.

Jha, S.; Jain, V.K. (2006) Modeling and simulation of surface roughness in magnetorheological abrasive flow finishing (MRAFF) process. *Wear* 261:856-866.

Jha, S.; Jain, V.K.; Komanduri, R. (2007) Effect of extrusion pressure and number of finishing cycles on surface roughness in magnetorheological abrasive flow finishing (MRAFF) process. *International Journal of Advanced Manufacturing Technology* 33: 725-729.

Jolly, M.R.; Bender, J.W.; Carlson, J.D. (1999) Properties and applications of commercial magnetorheological fluids. *Journal of Intelligent Material Systems and Structures* 10 (1):5-13.

Judal, K.B.; Yadava, V.; Pathak, D. (2013) Experimental investigation of vibration assisted cylindrical magnet abrasive finishing of aluminium workpiece. *Materials and Manufacturing Processes* 28: 1196-1202.

Kanaoka, M.; Liu, C.; Nomura, K.; Ando, M.; Takino, H.; Fukuda, Y. (2007) Figuring and smoothing capabilities of elastic emission machining for low-thermal-expansion glass optics. *Journal of Vacuum Science & Technology B, Nanotechnology and Microelectronics: Materials, Processing, Measurement, and Phenomena* 25: 2110-2113.

Khanna, O.P.; Lal, M. (2010) A text book of production technology. New Delhi, India: Dhanpat Rai publication.

Kim, J.D.; Kang, Y.H.; Bae, Y.H.; Lee, S.W. (1997) Development of a magnetic abrasive jet machining system for precision internal polishing of circular tubes. *Journal of Material Processing Technology* 71:384–393.

Komanduri, R.; Lucca, D.A.; Tani, Y. (1997) Technological advances in fine abrasive processes. *CIRP Annals – Manufacturing Technology* 46(2):545–596.

Kordonski, W.I.; Jacobs, S.D. (1996) Magnetorheological finishing. *International Journal of Modern Physics B* 10:2837–2848.

Kordonski, W.; Golini, D.; Dumas, P.; Jacobs, S. (1998) Magnetorheological suspension based finishing technology. *Proceeding of the SPIE* 3326:527–535.

Kordonski, W.I.; Golini, D. (1999) Fundamentals of magnetorheological fluid utilization in high precision finishing. *Journal of Intelligent Material Systems and Structures* 10(9):683–689.

Kordonski, W.I.; Gordokin, S.; Zhuravski, N. (2001) Static yield stress in magnetorheological fluid. *International Journal of Modern Physics B* 15(6–7):1078–1084.

Kordonski, W.I.; Shorey, A.B.; Tricard, M. (2004) Magnetorheological (MR) jet finishing technology. *Proceeding of ASME International Mechanical Engineering Congress* 13-19: 1-8.

Kordonski, W.I.; Shorey, A.B.; Tricard, M. (2006) Magnetorheological (MR) jet finishing technology. *Journal of Fluids Engineering*. 128(1): 20-26.

Kordonski, W.I.; Shorey, A. (2007) Magnetorheological (MR) jet finishing technology. *Journal of Intelligent Material Systems and structures* 18:1127–1130.

Lam, S.S.Y.; Smith, A.E. (1997) Process monitoring of abrasive flow machining using a neural network predictive model. *Industrial Engineering Research-Conference Proceedings* 477–82.

Lambropoulo, S.J.; Yang, F.; Jacob, S.D. (1996) Optical fabrication and testing. *Technical Digest Series (Optical Society of America, Washington DC)* 7:150–153.

Larsen-Bassea, J.; Liangb, H. (1999) Probable role of abrasion in chemo-mechanical polishing of tungsten. *Wear* 233–235: 647-654.

Lawrence, K.D.; Ramamoorthy, B. (2011) An accurate and robust method for the honing angle evaluation of cylinder liner surface using machine vision. *International Journal of Advanced Manufacturing Technology* 55: 611–621.

Lim, H.S.; Fatima, K.; Kumar, A.S.; Rahman, M. (2002) A fundamental study on the mechanism of electrolytic in-process dressing (ELID) grinding. *International Journal of Machine Tools and Manufacture* 42:935–43.

Loveless, T.R.; Williams, R.E.; Rajurkar, K.P. (1994) A study of the effects of abrasive-flow finishing on various machined surfaces. *Journal of Materials Processing Technology* 47: 133-151.

Martínez-Mateo, I. (2011) Surface damage of mould steel and its influence on surface roughness of injection moulded plastic parts. *18th International Conference on Wear of Materials* 271: 2512–2516.

Mazurek, I.; Roupec, J.; Klapka, M.; Strecker, Z. (2013) Load and rheometric unit for the test of magnetorheological fluid. *Meccanica* 48:631–641.

Michalski, J.; Pawlus, P. (1992) Description of honed cylinders surface topography. *International Journal of Machine Tools and Manufacture* 34(2): 199- 210.

Mohanty, H.K.; Mahapatra, M.M.; Kumar, P.; Biswas P.; Mandal, N.R. (2013) Predicting the effects of tool geometries on friction stirred aluminium welds using artificial neural network and fuzzy logic techniques. *International Journal of Manufacturing Research* 8(3): 296–312.

Mori, Y.; Yamauchi, K.; Endo, K.; Ide, T.; Toyota, H.; Nishizawa, K.; Hasegawa, M. (1990) Evaluation of elastic emission machined surface by scanning tunnelling microscopy. *Journal of Vacuum Science & Technology A: Vacuum, Surfaces, and Films* 8:621–624.

Montgomery, D.C. (2001) Design and analysis of experiments. 5th ed. New York: John Wiley & Sons Inc.

Mulik, R.S.; Pandey, P.M. (2012) Experimental investigations and modeling of finishing force and torque in ultrasonic assisted magnetic abrasive finishing. *Journal of Manufacturing Science and Engineering ASME* 134: 051008-1- 051008-12.

Obara, R.B.; Souza R.M.; Tomanik, E. (2017) Quantification of folded metal in cylinder bores through surface relocation. *Wear* 384–385:142–150.

Oh, S.; Seok, J. (2009) An integrated material removal model for silicon dioxide layers in chemical mechanical polishing processes. *Wear* 266: 839–849.

Pattnaik, S.; Karunakar, D.B.; Jha, P.K. (2012) Developments in investment casting process - A review. *Elsevier Journal of Materials Processing Technology* 212:2332 -2348.

Pawlus, P.; Cieslak, T.; Mathia, T. (2009) The study of cylinder liner plateau honing process. *Journal of Materials Processing Technology* 20: 6078-6086.

Pei, Z.J.; Billingsley, S.R.; Miura, S. (1999) Grinding induced subsurface cracks in silicon wafers. *International Journal of Machine Tools and Manufacture* 39(7): 1103-1116.

Premalatha, S.E.; Chokkalingam, R.; Mahendran, M. (2012) Magneto mechanical properties of iron based MR fluids. *American Journal of Polymer Science* 2 (4): 50–55.

Rajurkar, K.P.; Levy, G.; Malshe, A.; Sundaram, M.M.; McGeough, J.; Hu, X.; Resnick, R.; Desilva, A. (2006) Micro and nano machining by electro-physical and chemical processes. *Annals of the CIRP* 55: 643-666.

Rakotoarison, H.L.; Yonnet, J.P.; Delinchant, B. (2007) Using columbian approach for modeling scalar potential and magnetic field of a permanent magnet with radial polarization. *IEEE Transactions on Magnetics* 43(4): 1261-164.

Rhoades, L.J. (1988) Abrasive flow machining. *Manufacturing Engineering* 1:75–78.

Rodewald, W.; Wall, B.; Katter, M.; Uestuener, K. (2002) Top Nd-Fe-B magnets with greater than 56 MGOe energy density and 9.8 kOe Coercivity. *IEEE Transactions on Magnetics* 38(5): 2955-2957.

Ruben, H.J. (1987) In Advances in surface treatments, ed. A. Niku-Lari, 5:239. Oxford, United Kingdom: Pergamon Press.

Sabri, L.; Mansori, M.E. (2009) Process variability in honing of cylinder liner with vitrified bonded diamond tools. *Surface and Coatings Technology* 204: 1046-1050.

Sabri, L.; Mezghani, S.; Mansori, M.E.; Zahouani, H. (2011) Multiscale study of finish-honing process in mass production of cylinder liner. *Wear* 271:509-513.

Sadiq, A.; Shunmugam, M.S. (2009) Investigation into magnetorheological abrasive honing (MRAH). *International Journal of Machine Tools and Manufacture* 49:554–560.

Sadiq, A.; Shunmugam, M.S. (2010) A novel method to improve finish on non-magnetic surface in magnetorheological abrasive honing process. *Tribology International* 43:1122–1126.

Saraeian, P.; Mehr, H.S.; Moradi, B.; Tavakoli, H.; Alrahmani, O.K. (2016) Study of magnetic abrasive finishing for AISI321 stainless steel. *Materials and Manufacturing Processes* 31:2023–2029.

Saraswathamma, K.; Jha, S.; Rao, P.V. (2015) Experimental investigation into ball end magnetorheological finishing of silicon. *Precision Engineering* 42:218–223.

Seok, J.; Lee, S.O.; Jang, K.; Min, B.; Lee, S.J. (2009) Tribological properties of a magnetorheological (MR) fluid in a finishing process. *Tribology Transactions* 52(4):460-469.

Shaji, S.; Radhakrishnan, V. (2003) Analysis of process parameters in surface grinding with graphite as lubricant based on the Taguchi method. *Journal of Materials Processing Technology* 141:51–59.

Shinmura, T.; Takazawa, K.; Hatano, E.; Matsunaga, M. (1990) Study on magnetic abrasive finishing. *Annals of CIRP* 39(1):325–328.

Shorey, A.B.; Jacobs, S.D.; Kordonski, W.I.; Gans. R.F. (2001) Experiments and observations regarding mechanism of glass removal in magnetorheological finishing. *Applied Optics* 40(1):20–33.

Sidpara, A.; Das, M.; Jain, V.K. (2009) Rheological characterization of magnetorheological finishing fluid. *Materials and Manufacturing Processes* 24(2):1467–1478.

Sidpara, A.; Jain, V.K. (2011) Experimental investigations into forces during magnetorheological fluid based finishing process. *International Journal of Machine Tools and Manufacture* 51:358–362.

Sidpara, A.; Jain, V.K. (2012) Theoretical analysis of forces in magnetorheological fluid based finishing process. *International Journal of Mechanical Sciences* 56:50–59.

Sidpara, A.; Jain, V.K. (2013) Analysis of forces on the freeform surface in magnetorheological fluid based finishing process. *International Journal of Machine Tools and Manufacture* 69:1–10.

Singh, A.K.; Jha, S.; Pandey, P.M. (2011) Design and development of nanofinishing process for 3D surfaces using ball end MR finishing tool. *International Journal of Machine Tools and Manufacture* 51:142–151.

Singh, A.K.; Jha, S.; Pandey, P.M. (2013) Mechanism of material removal in ball end magnetorheological finishing process. *Wear* 302:1180–1191.

Singh, A.K.; Jha, S.; Pandey, P.M. (2012) Nanofinishing of a typical 3D ferromagnetic workpiece using a ball end magnetorheological finishing process. *International Journal of Machine tools and Manufacture* 63:21–31.

Singh, D.K.; Jain, V.K.; Raghuram, V. (2004) Parametric study of magnetic abrasive finishing process. *Journal of Materials Processing Technology* 149:22–29.

Singh, G.; Singh, A.K.; Garg, P. (2017) Development of magnetorheological finishing process for external cylindrical surfaces. *Materials and Manufacturing Processes* 32(5):581–588.

Spencer, A.; Almqvist, A.; Larsson, R. (2011) A numerical model to investigate the effect of honing angle on the hydrodynamic lubrication between a combustion engine piston ring and cylinder liner. *Proceedings of the Institution of Mechanical Engineers, Part J: Journal of Engineering Tribology* 225(7): 683-689.

Stradling, A.W. (1993) The physics of open-gradient dry magnetic separation. *International Journal of Mineral Processing* 39: 19–29.

Tricard, M.; Kordonski, W.I.; Shorey, A.B.; Evans, C. (2006) Magnetorheological jet finishing of conformal, freeform and steep concave optics. *CIRP Annals–Manufacturing Technology* 55(1):309–312.

Umehara, N.; Kirtane, T.; Gerlick, R.; Jain, V.K.; Komanduri, R. (2006) A new apparatus for finishing large size large batch silicon nitride (Si_3N_4) balls for hybrid bearing applications by magnetic float polishing (MFP). *International Journal of Machine Tools and Manufacture* 46:151–169.

Verma, G.C.; Kala, P.; Pandey, P.M. (2017) Experimental investigations into internal magnetic abrasive finishing of pipes. *International Journal of Advanced Manufacturing Technology* 88(5):1657–1668.

Vicente, V.J.; Klingenberg, D.J.; Hidalgo-Alvarez, R. (2011) Magnetorheological fluids: a review. *Soft Matter* 7:3701–3710.

Wang, Y.; Hu, D. (2005) Study on the inner surface finishing of tubing by magnetic abrasive finishing. *International Journal of Machine Tools & Manufacture* 45:43–49.

Yamaguchi, H.; Shinmura, T. (1999) Study of the surface modification resulting from an internal magnetic abrasive finishing process. *Wear* 225–229:246–255.

Yamaguchi, H.; Shinmura, T. (2004) Internal finishing process for alumina ceramic components by a magnetic field assisted finishing process. *Precision Engineering* 28:135–142.

Yamaguchi, H.; Shinmura, T.; Ikeda, R. (2007) Study of internal finishing of austenite stainless steel capillary tubes by magnetic abrasive finishing. *Journal of Manufacturing Science and Engineering* 129:885–892.

Yamauchi, K.; Yamamura, K.; Mimura, H.; Sano, Y.; Saito, A.; Souvorov, A.; Yabashi, M.; Tamasaku, K.; Ishikawa, T.; Mori, Y. (2002) Nearly diffraction- limited line focusing of

a hard x-ray beam with a elliptically figures mirror. *Journal of Synchrotron Radiation* 9:313–316.

Yin, S.; Shinmura, T. (2004) Vertical-assisted magnetic abrasive finishing and deburring for magnesium alloy. *International Journal of Machine Tools and Manufacture* 44:1297–1303.

Zantye, P.B.; Kumar, A.; Sikder, A.K. (2004) Chemical mechanical planarization for micro-electronics applications. *Material Science and Technology* 45:189–220.

LIST OF PUBLICATIONS AND PATENT

SCI Journals:

1. **Grover, V.**; Singh, A.K. (2017) A novel magnetorheological honing process for nano-finishing of variable cylindrical internal surfaces. *Materials and Manufacturing Processes* 32(5): 573-580.
   Status: ***Online published***
   Publisher: Taylor and Francis
   Impact factor: 2.669

2. **Grover, V.**; Singh, A.K. (2018) Improved magnetorheological honing process for nano-finishing of variable cylindrical internal surfaces. *Materials and Manufacturing Processes* 33 (11):1177-1187.
   Status: ***Online published***
   Publisher: Taylor and Francis
   Impact factor: 2.669

3. **Grover, V**.; Singh, A.K. (2018) Modeling of surface roughness in a new magnetorheological honing process for internal finishing of cylindrical workpieces, *International Journal of Mechanical Sciences* 144: 679-695.
   *Status: O****nline published***
   Publisher: Elsevier
   Impact factor: 3.570

4. **Grover, V.**; Singh, A.K. (2018) Analysis of particles in magnetorheological polishing fluid for finishing of ferromagnetic cylindrical workpiece. *Particulate Science and Technology* 36(7): 799-807.
   Status: ***Online published***
   Publisher: Taylor and Francis
   Impact factor: 1.081

5. **Grover, V.**; Singh, A.K. (2019) Modeling of surface roughness in the magnetorheological cylindrical finishing process. *Proceedings of the Institution of Mechanical Engineers, Part E: Journal of Process Mechanical Engineering* 233 (1): 104-117.
   Status: ***Online Published***
   Publisher: Sage
   Impact factor: 1.211

6. **Grover, V.**, Singh, A.K. (2019) Improved design of magnetorheological honing tool based on finite element analysis and experimental examination of its performance, *International Journal of Advanced Manufacturing Technology* 100 (5-8): 1067-1080.
   Status: ***Online Published***
   Publisher: Springer
   Impact factor: 2.601

7. **Grover, V.**; Singh, A.K. (2019) Parametric Optimization of a Newly Developed Magnetorheological Honing Process for Internal Finishing of Cylindrical Workpieces, *Indian Journal of Engineering and Materials Sciences*.
   Status: ***Communicated***
   Publisher: Niscair
   Impact factor: 0.543

International Conferences:

1. **Grover, V.**; Singh, A.K. (2016) Improved design of Magnetorheological Honing Tool using Finite Element Analysis. 6th International & 27th All India Manufacturing Technology, Design and Research Conference (AIMTDR-2016), December 16th-18th, 2016, held at College of Engineering, Pune. pp. 1773–1777.
   Status: ***Published***

Patent filed:

1. Singh, A.K.; **Grover, V.**; Bedi, T.S.; Chawla, N. (2015) A computer based magnetorheological honing process.
   Filed No.: 924/DEL/2015